Signals and factors required for mRNA localization during *Drosophila* oogenesis

Suzanne McDermott

Thesis presented for the degree of Doctor of Philosophy

The University of Edinburgh
2009

ABSTRACT

The intracellular localization of messenger RNA (mRNA) coupled with localized translation is a widespread strategy used to restrict protein function to specific regions of a cell. The subcellular destination of a localized mRNA is thought to depend upon the recognition of *cis*-acting RNA localization signals by *trans*-acting factors and the localization machinery. *gurken* mRNA localization and localized translation at the dorso-anterior corner of the *Drosophila* oocyte is essential for axial patterning of the embryo. Dorso-anterior localization requires the *gurken* localization signal, and *trans*-acting factors that have been identified by genetic approaches. However, the key features of the RNA signal, and the full complement of factors that are required for specific localization are not known. It has been hypothesized that the *gurken* localization signal contains consensus motifs for dorso-anterior localization, as the *I* Factor retrotransposon RNA also localizes to this region and contains a localization signal of similar predicted secondary structure. We are using Nuclear Magnetic Resonance (NMR) Spectroscopy to identify and compare RNA sequence and structural motifs in the two localization signals, and have shown that both structures contain common features that may represent key motifs required for dorso-anterior localization.

The *trans*-acting factors that can interact with the *gurken* localization signal were investigated in this work using a biochemical approach. RNA affinity chromatography identified a number of proteins that have a role in the localization and localized translation of a variety of mRNAs in *Drosophila* and other organisms, in addition to factors previously shown to be important for dorso-anterior *gurken* localization and translation. These included Hephaestus and CG17838, which were chosen for further study due to the roles of their vertebrate homologues, PTB and SYNCRIP respectively, in neuronal mRNA localization. Both Hephaestus and CG17838 accumulate at the posterior of the oocyte, in a similar manner to localized *oskar* mRNA, and can associate with *gurken* and *oskar*. Furthermore, CG17838 can interact with the known *gurken trans*-acting factors, Squid and Hrb27C. Analysis of *hephaestus* mutants suggests that Hephaestus has multiple roles within the

Drosophila oocyte including the maintenance of Gurken protein at the dorso-anterior in later stages of oogenesis. Previous studies have shown that this phenotype results from defects in processing or secretion of Gurken, although it is unclear how this relates to the interaction of Heph and *grk* mRNA.

CG17838 is essential for adult viability, and preliminary studies of *CG17838* germline clones suggest that CG17838 has a role in *gurken* localization or localized translation. Furthermore, *CG17838* mutant adult flies have a behavioural phenotype indicative of a defect in synaptic transmission, although further work is needed to assess if this is due to a conserved role for CG17838 in the regulation of localized mRNAs at the synpase. A growing number of proteins have been shown to be associated with both neuronal and maternal localized mRNAs, and the work presented in this thesis is consistent with the concept that core, conserved proteins are involved in the regulation of a number of localized mRNAs in different tissues and in different organisms. The conservation of a number of the *trans*-acting factors required for mRNA localization also means that the study of these factors during *Drosophila* oogenesis can lead to a greater understanding of how the process can go awry in human disease. This may be particularly important for understanding certain disorders of the nervous system, such as Fragile X syndrome and Spinal Muscular Atrophy (SMA).

DECLARATION

I hereby declare that this thesis is my own work and the experiments described in the following pages were performed by myself, unless otherwise stated. The experiments were carried out in the Wellcome Trust Centre for Cell Biology, University of Edinburgh, and the Department of Biochemistry, University of Oxford. This thesis has not been submitted for any other degree or professional qualification.

Suzanne McDermott
April 2009

ACKNOWLEDGEMENTS

I would like to thank my supervisor, Ilan Davis, for his enthusiastic support, encouragement and help over the last four years. Many thanks are also due to David Finnegan who gave me a bench and allowed me to take over his office in Edinburgh, and who was the source of great advice and scientific discussions. I am also indebted to our collaborators Juri Rappsilber and Peter Lukavsky for mass spectrometry and NMR expertise, Anne Ephrussi who provided flystocks and reagents that have been invaluable in for this work, and also to the Wellcome Trust for funding.

I am extremely grateful to all members of the Davis and Finnegan labs, past and present, who made the lab such a stimulating and also fun place to work. Special thanks go to Carine Meignin for her work with me on SYNCRIP, allowing me to present her results in this thesis, genetics help and also the many bike and surf chats. Thanks to Hille for showing me the ropes in my rotation and convincing me to stay, Vero for teaching me to inject and initial project ideas, Graeme for perseverance with NMR and tip racking, Tim for great discussions and also making sure I wasn't homeless in Oxford, Russell for help with computers, Richard for help with microscopes and Ana Maria for making sure I had everything I needed for the final few months and who made sure that the move to Oxford went smoothly. Thanks also to the Bird lab for biochemistry advice, equipment and cakes.

Finally, I would like my family for their support and also thank Pete for his endless patience and support throughout the PhD and whilst writing up.

LIST OF ABBREVIATIONS

AAA	ATPase associated with a variety of cellular activities
A-P	Anterior-Posterior
ATP	Adenosine triphosphate
bcd	*bicoid*
BLE	*bicoid* localization element
BRE	Bruno response element
cDNA	Complementary DNA
CPE	Cytoplasmic polyadenylation element
CPEB	CPE-binding protein
DEAE	Diethylaminoethyl
DFS	Dominant female sterile
DGC	*Drosophila* gene collection
DGRC	*Drosophila* genomics resource centre
DNA	Deoxyribonucleic acid
ds	Double stranded
DTE	Dendritic targeting element
D-V	Dorsal-Ventral
EGTA	Etylene glycol tetraacetic acid
EJC	Exon junction complex
ER	Endoplasmic reticulum
FLP	Flippase
FRAP	Fluorescence recovery after photobleaching
FRT	FLP-recognition target sequence
GFP	Green fluorescent protein
GLS	*gurken* localization signal
grk	*gurken*
GRNA chromatography	GST-RNA affinity chromatography
hb	*hunchback*
HCV	Hepatitis C virus
Hcph	Hephaestus
hnRNP	Heterogeneous nuclear ribonucleoprotein
HRP	Horseradish peroxidase
ILS	*I* Factor localization signal
IP	Immunoprecipitation
IRES	Internal ribosome entry site

kb	Kilobase
kDa	Kilodalton
MBP	Myelin Basic Protein
miRNA	microRNA
mM	millimolar
mRNA	messenger RNA
MTOC	Microtubule organizing centre
NLS	Nuclear localization signal
nM	nanomolar
NMR	Nuclear Magnetic Resonance
nos	*nanos*
NRE	Nanos response element
osk	*oskar*
PAGE	Polyacrylamide gel electrophoresis
PCR	Polymerase chain reaction
PTB	Polypyrimidine tract-binding protein
RGG box	Arginine-Glycine-Glycine box
RISC	RNA induced silencing complex
RNA	Ribonucleic acid
RNase	Ribonuclease
RNP	Ribonucleoprotein
rpm	Revolutions per minute
RRM	RNA Recognition Motif
RT	Reverse transcriptase
RTE	RNA trafficking element
SMA	Spinal Muscular Atrophy
snRNP	Small nuclear ribonucleoprotein
SYNCRIP	Synaptotagmin-binding, cytoplasmic, RNA-interacting protein
Syt	Synaptotagmin
tER	transitional ER
μM	micromolar
UTR	Untranslated region
UV	Ultraviolet

TABLE OF CONTENTS

FIGURES AND TABLES

Figures

Tables

INTRODUCTION

mRNA localization

The intracellular localization of messenger RNA (mRNA) is a widespread, evolutionarily ancient strategy used to spatially restrict protein function to specific regions of a cell (Bashirullah *et al.*, 1998; Martin and Ephrussi, 2009; Palacios and St. Johnston, 2001; St Johnston, 2005). Historically, intracellular protein localization was thought to occur mainly by sorting according to cellular destination signals within the protein itself. This view was challenged by the demonstration that maternal *β-actin* mRNA accumulates in the myoplasm of ascidian eggs (Jeffery *et al.*, 1983). Since then, a variety of mRNAs have been shown to localize in a wide range of cell types (Bashirullah *et al.*, 1998; Czaplinski and Singer, 2006; Kloc *et al.*, 2002; St Johnston, 2005) and in most cases the subcellular distribution of the protein is entirely dependent upon the localization of the transcript (Broadus *et al.*, 1998; Knoblich *et al.*, 1999; Li *et al.*, 1997; Shepard *et al.*, 2003). The best-studied examples of localized mRNAs involve transcripts whose protein products play diverse, but highly specialized roles in specific regions of polarized cells.

The biological roles of mRNA localization

Regulation of cell polarity and directed cell migration

Epithelial cells are highly polarized with separate apical and baso-lateral membrane compartments, each with a unique composition of lipids and proteins. This polarity is essential for cell function, cell and tissue morphogenesis and control of proliferation, and is regulated by the localization of highly conserved protein 'polarity' complexes to the two membrane domains. The mRNAs encoding two key polarity regulators, Stardust and Crumbs (both components of the apical Crumbs/Stardust/PATJ complex) are localized apically (Horne-Badovinac and Bilder, 2008; Li *et al.*, 2008), contributing to the establishment of cell polarity. In motile chicken embryo

fibroblasts, *β-actin* mRNA localization, coupled with localized translation, targets actin filaments to the leading edge (Sundell and Singer, 1990), where it is essential for cell polarization and directed cell migration (Kislauskis *et al.*, 1997). Neurons are amongst the most highly polarized of cell-types, typically containing a long filamentous axon and multiple dendrites that differ from one another morphologically and functionally. In part, this compartmentalization is maintained by the segregation of a number of transcripts to either axons or dendrites in developing neurons. For example, the localization of *tau* and *MAP2* mRNAs to axons and dendrites respectively may contribute to differential cytoskeletal organisation in the two neuronal domains (Aronov *et al.*, 2001).

Rapid response to local environmental cues and stimuli

Local translation of localized mRNAs is important in both developing and mature neurons. During neuronal development, axonal growth cones are guided by local environmental guidance cues as they navigate toward their synaptic partners. Axonally targeted mRNAs are translated in response to such cues, allowing for rapid, local synthesis of cytoskeletal regulators, for example, *RhoA* (Wu *et al.*, 2006), *β-actin* (Leung *et al.*, 2006; Zhang *et al.*, 2001) and *MAP1b* (Antar *et al.*, 2006) mRNAs. This allows the growth cone to turn toward or turn away from attractive or repulsive guidance cues respectively. In mature neurons, many, up to hundreds, of mRNAs are dendritically enriched (Eberwine *et al.*, 2002; Martin and Zukin, 2006). The regulated translation of post-synaptically localized mRNAs, such as *CaMKIIα*, *Arc*, *MAP2* and *β-actin*, allows each of the many synapses made by a particular neuron to alter its structure and function during synaptic plasticity, and may produce long-lasting changes in synaptic strength (reviewed in Dahm *et al.*, 2007; Sanchez-Carbente and DesGroseillers, 2008; Sossin and DesGroseillers, 2006; Steward and Schuman, 2001). mRNA localization is therefore thought to be very important for the plastic changes at synapses that underlie memory and learning.

Exclusion of a protein from regions of the cell

In oligodendrocytes, the mRNA encoding myelin basic protein (MBP) is transported into the distal processes (the 'myelin compartment') that generate myelin sheets to surround neuronal axons (Ainger *et al.*, 1997; Carson *et al.*, 1997; Trapp *et al.*, 1987). MBP associates with membranes to cause their compaction and is translated in the myelin compartment where it is incorporated into the myelin sheath. If the protein were to be translated in the cell body, then it could potentially interact with the wrong membranes, which would inhibit movement to the periphery and also interfere with cell function.

Segregation of cell fate and embryonic polarity determinants

mRNA localization can specify cell identity by the partitioning of cell fate determinants into one daughter cell in asymmetric cell division. This is vital in budding yeast, *Saccharomyces cerevisiae*, where the mRNA encoding the transcriptional repressor, ASH1 is localized to the bud tip of a dividing cell. This results in the sequestration of localized *ASH1* mRNA within the daughter cell, thereby ensuring that the mother and daughter cells have distinct mating types (Bobola *et al.*, 1996). Localized RNAs have also been shown to act as cell fate determinants in the asymmetric division of *Drosophila* neuroblasts, where *prospero* mRNA is localized to the basal cortex and determines ganglion mother cell fate following cell division (Broadus *et al.*, 1998).

Many of the best-characterized localized mRNAs are found in oocytes and early embryos (Bashirullah *et al.*, 1998). mRNA localization, coupled to translational regulation means that developmental gene expression can occur in a defined spatial and temporal manner, important when an asymmetric organism must be established from a single egg in a precisely timed series of events (Colegrove-Otero *et al.*, 2005; Johnstone and Lasko, 2001). In a number of examples, the primary axis of the organism is defined by the localization of cytoplasmic determinants in the egg. By targeting the protein to its site of function, but restricting its expression elsewhere,

precise patterning of the embryo can be achieved. This can be, for example by creating morphogen gradients, specifying cell lineages, or by controlling the direction of important signalling events. Examples include maternal *Vg1* (a signalling molecule of the TGF-β family) mRNA localization to the vegetal hemisphere of *Xenopus* oocytes (Melton, 1987; Yisraeli and Melton, 1988; Yisraeli *et al.*, 1990), where it later plays a role in mesoderm induction (Dale *et al.*, 1993; Thomsen and Melton, 1993). However, most evidence for the function of RNA localization in development comes from the *Drosophila* oocyte (Palacios and St. Johnston, 2001), where mRNA localization pathways play a central role in embryonic axis determination (St Johnston and Nüsslein-Volhard, 1992). Here, the localization of maternal mRNAs, such as *bicoid* (*bcd*), *oskar* (*osk*), *gurken* (*grk*) and *nanos* (*nos*), to specific regions of the oocyte is crucial for anterior-posterior (A-P) and dorso-ventral (D-V) patterning of the embryo.

Roles other than targeting protein synthesis

One thing which all the roles discussed have in common is the targeting of protein synthesis and function to a particular region of the cell. In a number of cases, localized RNAs may have roles other than the targeting of protein function, including structural roles. The *Xenopus* short interspersed repeat transcripts (*Xlsirts*) localize to the vegetal pole of the *Xenopus* oocyte (Kloc *et al.*, 1993). These are a family of noncoding and coding RNAs defined by the presence of a specific repeated sequence that acts as a vegetal localization element (Zearfoss *et al.*, 2003). There is evidence that the *Xlsirts* and another vegetally localized coding mRNA, *VegT* mRNA function in the anchoring of other localized RNAs at the vegetal pole (Kloc *et al.*, 2005). This is due to their integration into, and function in the organization of the cytoskeleton at the vegetal cortex in *Xenopus* oocytes. In a further example, genetic studies of the *osk* gene in *Drosophila* have shown that protein null alleles give only a subset of the phenotypes exhibited by RNA null alleles (Jenny *et al.*, 2006), suggesting that *osk* mRNA has functions other than in the synthesis of Osk protein.

The above examples illustrate how a number of localized mRNAs can play highly specialized roles at their final subcellular destination. However, more recent studies suggest that mRNA localization, coupled with localized translation is a much more prevalent mechanism for the regulation of gene expression than was previously thought. Past estimates for the percentage of localized mRNAs in early *Drosophila* development have ranged from one to ten percent (Dubowy and Macdonald, 1998; Tomancak *et al.*, 2002). A recent, high-throughput *in situ* hybridization screen of over 2000 genes expressed in the *Drosophila* early embryo, representing approximately 25% of the genome, showed that 71% of the mRNAs were distributed in spatially restricted patterns (Lécuyer *et al.*, 2007). It must be remembered that this study screened only a quarter of the genome in a distinct developmental window unique to insects, when the syncytial blastoderm embryo is undergoing cellularization. Although the number of localized transcripts could reflect a high demand for localization events peculiar to the conversion from a syncytial to a cellular environment, the percentage of localized transcripts, as well as the number of different localization patterns observed in this study, suggests that mRNA localization and regulated translation may be a means of regulating the majority of cellular functions rather than being restricted to the specialized biological processes described previously.

Why localize mRNAs?

The reasons for localizing mRNA rather than directly localizing protein have been touched upon in the discussion of the biological role of mRNA localization. Because one mRNA molecule can serve as a template for multiple rounds of translation, localizing mRNA rather than protein to the site where the protein is needed is much more economical in the cell. In addition, where there is a special requirement for high local levels of proteins that act as determinants to induce specific cell fates, or where the protein could be toxic in other regions of the cell, the synthesis of the protein must be restricted to defined cytoplasmic positions. mRNA localization targets the protein to the correct region of the cell, and also prevents its expression elsewhere, where it may be deleterious. mRNA localization also allows for local

control of protein, and therefore gene expression, meaning a cell can respond rapidly to a local requirement for the protein.

Mechanisms of mRNA localization

Studies in a number of diverse systems and species have shown that there are several potential mechanisms by which mRNA can be localized (Kloc *et al.*, 2002; Palacios and St Johnston, 2001; St Johnston, 2005). The models include localized synthesis and vectorial export of mRNA from a specific region of the nucleus, general degradation and selective protection at the site of localization, diffusion and specific anchoring at the site of localization or active transport along the cytoskeleton using molecular motors. Indeed, a combination of mechanisms may be used to localize different RNAs.

Local synthesis

Localized transcription followed by directional export from the nucleus is a simple, elegant way of localizing a transcript to a particular region. However, biological examples of this mechanism are rare. One example comes from mammalian multinucleate syncytial myofibres. The postsynaptic apparatus in myofibres is characterized by the accumulation of a number of membrane and cytoskeletal proteins. A number of mechanisms exist to ensure the precise localization and supply of these proteins, one of which is the localized transcription of the mRNAs encoding some of these components. mRNAs encoding several key synaptic proteins, such as the δ- and ε-acetylcholine receptor (Brenner *et al.*, 1990; Simon *et al.*, 1992) are transcribed preferentially in the nuclei that underlie the neuromuscular junctions, concentrating the mRNAs near the synapses where the corresponding proteins are required. This local transcriptional control involves the activation of synaptic expression by the nerve-derived signal agrin and the trophic factor neuregulin, and the concomitant repression of expression in extrasynaptic nuclei by electrical activity (reviewed in Schaeffer *et al.*, 2001 and Chakkalakal and Jasmin, 2003).

General degradation and local protection

Initially uniformly distributed transcripts may be degraded throughout most of the cytoplasm while being protected from degradation at the localization site. This mechanism has been shown to restrict several mRNAs to the posterior pole plasm of the *Drosophila* egg. Only 4% of *nos* mRNA is localized in the pole plasm of the newly laid egg, whilst the majority of the mRNA is distributed throughout the cytoplasm. The localized mRNA is stable, whilst the unlocalized mRNA is subject both to translational repression and to rapid degradation (Bashirullah *et al.*, 1999; Dahanukar and Wharton, 1996; Gavis *et al.*, 1996; Smibert *et al.*, 1996). The interaction of Smaug with the *nos* 3'UTR is responsible for translational repression and recruitment of the CCR4/NOT deadenylase, triggering deadenylation and degradation of the transcript (Zaessinger *et al.*, 2006). *hsp83* mRNA is also restricted to the pole plasm in this manner (Ding *et al.*, 1993). This posterior enrichment requires two *cis*-acting elements in the 3'UTR of the transcript (Bashirullah *et al.*, 1999). One is a degradation element that targets unlocalized RNA for destruction through the binding of Smaug (Semotok *et al.*, 2005; Semotok *et al.*, 2008), whilst the other is a protection element that stabilizes the localized RNA at the posterior.

Diffusion and anchoring

Transcripts may diffuse throughout the cytoplasm, but be trapped and anchored at the localization site, gradually becoming concentrated at this site. mRNAs localized in the *Drosophila* pole plasm, including *nos* mRNA, again provide an example of this, highlighting how multiple mechanisms can act in order to localize an mRNA. *nanos*, *cyclin B*, *germ cell-less* mRNAs are concentrated at the posterior of the *Drosophila* oocyte late in oogenesis. Cytoplasmic streaming in the oocyte facilitates the diffusion of these RNAs toward the posterior where they are anchored by components of the pole plasm, the formation of which depends upon the earlier localization and translation of *osk* mRNA at the posterior (Ephrussi and Lehmann, 1992; Forrest and Gavis, 2003; Jongens *et al.*, 1992; Nakamura *et al.*, 1996; Raff *et al.*, 1990; Wang *et al.*, 1994). Similarly, during the cleavage divisions of *Xenopus*

early embryogenesis, *cyclin B1* is localized to the mitotic spindle. Trapping of the mRNA is most likely mediated by an interaction between the CPE (Cytoplasmic Polyadenylation Element) within the transcript, and CPEB (CPE-binding protein) that decorates the spindle (Groisman *et al.*, 2000).

Active transport

Transport of mRNA by molecular motors along cytoskeletal filaments has been implicated as the major localization mechanism in most cell types. In principle, this represents a more efficient way of moving an mRNA cargo through the viscous environment of the cell cytoplasm as opposed to protection from degradation or diffusion followed by anchoring. mRNAs can be transported along actin by myosin motors or along microtubules by the two major superfamilies of microtubule motor proteins, Kinesins and Dyneins.

Molecular motors

Molecular motors are nanomachines that are able to convert chemical energy to mechanical work and take directional steps through repeated cycles of association and dissociation along cytoskeletal tracks. Movement results from force generation by conformational changes induced in the motor domain by ATP hydrolysis. Motors are widely used to traffic organelles, vesicles, pathogens and macromolecules and this will be a discussion of the cytoplasmic motors implicated in intracellular trafficking and transport events. However, molecular motors also have many other specialized functions, including axonemal Dyneins required for ciliary or flagellar beating (Gibbons, 1981; Porter, 1996; Woolley, 2000), Myosins responsible for the generation of contractile force in muscle, and mitotic roles for Kinesins and Dynein in chromosome and spindle motility (Hook and Vallee, 2006; Maney *et al.*, 2000; Wittmann *et al.*, 2001).

Cytoplasmic Dynein

Cytoplasmic Dynein is the major motor for minus-end directed transport along microtubules. It is a large and complex motor protein (1.2 MDa) composed of two identical heavy chains (each of which possess motor activity) (Nishiura *et al.*, 2004; Reck-Peterson *et al.*, 2006), two intermediate chains, and additional light intermediate and light chains (King, 2000a; Pfister *et al.*, 2006). The light and intermediate chains are involved in the assembly of the entire Dynein complex and in cargo recognition. Dynein heavy chain is a member of the AAA family of ATPases, and consists of a large globular motor 'head' domain, a coiled-coil extension (the stalk) that interacts with the microtubule in an ATP-dependent manner, and an extended tail domain (the 'stem') that dimerizes with a second heavy chain and also binds to the light and intermediate subunits (Burgess and Knight, 2004; Sakato and King, 2004; Samso *et al.*, 1998). The structure of the motor 'head' domain derives from the assembly of six AAA units (AAA1-6) into a hexameric ring (Roberts *et al.*, 2009). Despite the presence of ATP binding/hydrolysis motifs in the first four AAA units, hydrolysis of ATP at a single site (AAA1) is necessary and sufficient to drive motility along the microtubule (Kon *et al.*, 2004; Takahashi *et al.*, 2004). However, the AAA ring must be intact for proper functioning of the motor, and the other sites may play regulatory roles (reviewed in Numata *et al.*, 2008; Silvanovich *et al.*, 2003). The ATP hydrolysis cycle in AAA1 is coupled via conformational changes to changes in microtubule binding affinity at the tip of the stalk, which allows the heavy chain to step along the microtubule (Carter *et al.*, 2008; Gibbons *et al.*, 2007). Coordination of the two heavy chains is thought to allow Dynein to 'walk' in a hand-over-hand fashion (Gennerich and Vale 2009).

Most Dynein-mediated functions require an additional accessory complex known as Dynactin, which has roles in both cargo binding and motor processivity (Holleran *et al.*, 1998; King, 2000b; Schroer, 2004). Dynactin is composed of eleven subunits, including p150/Glued, p50/Dynamitin and Arp1. p150/Glued can bind to Dynein intermediate chain and to microtubules, and it is thought that these interactions can stabilise the attachment of Dynein to microtubules, or maintain Dynein in close

proximity to microtubules (Karki and Holzbaur, 1995). p50/Dynamitin is crucial for the structure of Dynactin (Eckley *et al.*, 1999), and overexpression of Dynamitin has been used to impair or abolish the function of Dynein in several studies (Burkhardt *et al.*, 1997; Wilkie and Davis. 2001). The Arp1 subunit assembles to form an actin-like filament at the base of the complex, and is thought to interact with membranous and kinetochore cargoes (Holleran *et al.*, 1996; Saffery *et al.*, 2000).

Cytoplasmic Dynein is required for the transport of a wide range of cargoes. The transport of vesicles from the endoplasmic reticulum (ER) to the Golgi is dependent on the Dynein-Dynactin complex, and disruption of Dynein function results in fragmentation of the Golgi. Dynein is also required for the minus end directed transport of many other organelles including endosomes, lysosomes, phagosomes and mitochondria (Caviston and Holzbaur, 2006). In neurons, Dynein is involved in the transport of a variety of axonal and dendritic vesicles and organelles. Axons have unipolar microtubules where the plus ends point in the direction of the synapse, and Dynein is responsible for retrograde movement from the synapse back to the cell body (Vallee *et al.*, 1989) Other Dynein cargoes include aggregating melanosomes in Xenopus melanophores (Aspengren *et al.*, 2009; Gross *et al.*, 2002) and lipid droplets in *Drosophila* embryos (Gross *et al.*, 2000). A variety of macromolecules, including proteins such as the neuronal intermediate-filament vimentin (Clarke and Allan, 2002) and RNAs, are also transported by Dynein. This is illustrated by the role of Dynein in the transport of pathogens such as herpes virus (Döhner *et al.*, 2002). The intracellular transport of HIV genomic RNA (vRNA) and viral proteins, and also viral production are dependent on Dynein motor function and endosomal membranes (Lehmann *et al.*, 2009).

Dynein transports a number of localized mRNAs toward the minus ends of microtubules (Tekotte and Davis, 2002). *wingless* and pair-rule transcripts localize to the apical cytoplasm above the nuclei in the *Drosophila* syncytial blastoderm embryo (Davis and Ish-Horowicz, 1991; Simmonds *et al.*, 2001). The use of genetics, inhibitors and high-resolution imaging has shown that this movement requires microtubules (nucleated from an apical microtubule organizing centre or MTOC) and

Dynein-Dynactin (Wilkie and Davis, 2001), as well as the Dynein cofactors Egalitarian (Egl) and Bicaudal-D (BicD) (Bullock and Ish-Horowicz, 2001). Egl and BicD bind dynein light chain and dynactin components respectively (Hoogenraad *et al.*, 2001; Navarro *et al.*, 2004; Short *et al.*, 2002). Similarly, the apical localization of the cell polarity regulators Stardust and Crumbs in epithelial cells has been shown to be dependent upon microtubules and Dynein (Horne-Badovinac and Bilder, 2008; Li *et al.*, 2008), as has the localization of *inscuteable* mRNA to the apical cortex of *Drosophila* embryonic neuroblasts (Hughes *et al.*, 2004). Experiments in which Dynein is inactivated indicate that *bcd* mRNA is transported in a Dynein-dependent manner to microtubule minus ends at the anterior of the *Drosophila* oocyte (Duncan and Warrior, 2002; Januschke *et al.*, 2002; Pokrywka and Stephenson, 1991; Weil *et al.*, 2006). Live imaging of fluorescently tagged *bcd* mRNA has further revealed that, although a portion of *bcd* mRNA is localized to the anterior during mid-oogenesis, the bulk of mRNA is localized and maintained at the anterior later in oogenesis. This is a dynamic process involving continuous active transport of *bcd* by Dynein on anterior microtubules (Weil *et al.*, 2006). The Dynein-dependent localization of *grk* mRNA during *Drosophila* oogenesis will be discussed separately.

Kinesins

Kinesins and Kinesin related proteins are an extended superfamily of proteins that share a homologous motor domain that can bind to the microtubule in an ATP-sensitive manner (for review of Kinesin family protein structure and function see Caviston and Holzbaur, 2006; Hirokawa, 1998; Hirokawa and Takemura, 2005; Miki *et al.*, 2005; Vale *et al.*, 2003). There is, however, considerable variation in the accessory subunits and cargo binding domains. In many of the Kinesins, this conserved motor domain is necessary and sufficient for motor function. The major Kinesin families involved in intracellular trafficking and transport processes are the Kinesin-1, -2 and -3 families. Kinesin-1 and most of the motors in the Kinesin superfamily move unidirectionally toward the plus end of the microtubule. However, minus end-directed Kinesins do also contribute to intracellular trafficking events, such as the minus end-directed transport of early endosomes.

Kinesin-1 (also referred to as Conventional Kinesin/KIF5) is composed of two heavy chains (KHC) and two light chains (KLC). Each KHC contains the motor domain, a long coiled-coil stalk interrupted by a central hinge and a globular tail domain. The accessory KLC binds to the KHC tail domain and both KLCs and KHC tail domains can bind cargoes. In various cell types, Kinesin-1 associates with the ER, Golgi (with cargo moving out from the Golgi to the plasma membrane), mitochondria, endosomes, lysosomes and intermediate filaments (Caviston and Holzbaur, 2006). Vaccinia virus virions that have been enveloped by membrane at the Golgi or late endosomes are transported to the cell periphery by Kinesin-1 (Rietdorf *et al.*, 2001; Ward and Moss, 2004). Other cargoes include plus end directed dispering melanosomes in *Xenopus* melanophores (Aspengren *et al.*, 2009) and lipid droplets in *Drosophila* embryos (Shubeita *et al.*, 2008). Just as Dynein is the major motor for retrograde movement in axons, Kinesin-1 is the major anterograde motor for vesicles and organelles such as mitochondria. Interestingly, genetically interfering with Kinesin-1 function inhibits both anterograde and retrograde transport. The same is also seen in Dynein mutants and in both cases, axonal swellings are observed in which both anterograde and retrograde cargoes accumulate (Martin *et al.*, 1999; Pilling *et al.*, 2006). It therefore seems that Dynein and Kinesin-1 are interdependent for axonal transport. Kinesin-1 is also required for the dendritic transport of proteins including AMPA glutamate (Hirokawa and Takemura, 2005).

The Kinesin-2 (also known as KIF3/Kinesin II) family consists of heterotrimeric complexes, composed of a heterodimer of motor-containing proteins responsible for force generation, the tails of which bind a third protein, known as Kinesin associated protein (KAP). KAP, which shares some similarity with KLC, is thought to interact with cargo. Members of the Kinesin-2 family transport membranous and vesicular cargo including late endosomes (Caviston and Holabaur, 2006) and N-cadherin and β-catenin-containing vesicles in mouse neural progenitor cells (Hirokawa and Takemura, 2005; Teng *et al.*, 2005). Kinesin-2 is also required for axonal transport of choline acetyltransferase in *Drosophila* (Ray *et al.*, 1999) and the adenomatous polyposis colon protein (APC) in tissue culture cells (Jimbo *et al.*, 2002).

Kinesin-3 (KIF1/Unc104) Kinesins are predomianantly monomeric (Okada *et al.*, 1995). This is in contrast to other Kinesins, which are oligomeric. However, when concentrated in solution or on membranes, Unc104/KIF1 can dimerize via coiled-coil regions adjacent to the motor domain, and dimerization allows the motor to move processively along microtubules like conventional Kinesin (Tomishige *et al.*, 2002). The Unc104 motor was initially discovered in a mutant screen in *C. elegans*, where null mutations cause paralysis due to a failure to transport synaptic vesicles in the axons of motor neurons (Hall and Hedgecock, 1991). It has since been shown that the mouse orthologues, KIF1A and KIF1B, are also required for the transport of synaptic vesicle precursors from the cell body to the presynaptic terminal (Yonekawa *et al.*, 1998).

Kinesin family members transport a number of localized mRNAs toward the plus ends of microtubules (Tekotte and Davis, 2002). *osk* mRNA in the *Drosophila* oocyte is localized to the posterior pole of the oocyte in a process that is dependent upon microtubules (Clark *et al.*, 1994) and Kinesin-1. Null alleles of *Khc* cause a phenotype in which *osk* RNA localizes around the anterior and lateral cortex of the oocyte (Brendza *et al.*, 2000; Cha *et al.*, 2002). Live imaging of fluorescently-tagged *osk* mRNA in *Khc* and *Dhc* mutant *Drosophila* oocytes has recently shown that Kinesin-1 mediates plus end directed movement of *osk* mRNA (Zimyanin *et al.*, 2008). Indeed, this study also showed that *osk* is not transported in a highly directed fashion toward the posterior by Kinesin-1, but that the mRNA moves in all directions with a slight posterior bias. This bias is sufficient for localization and arises from a weak bias in the orientation of microtubule plus ends toward the posterior of the oocyte.

Kinesin has also been implicated in the localization of *MBP* and *CamKIIα* mRNA into the myelinating processes of oligodendrocytes and the dendrites of neurons respectively. Antisense oligonucleotides directed against KHC can block the localization of injected *MBP* mRNA (Carson *et al.*, 1997), whilst a dominant-negative KIF5 mutant reduces the distance that *CamKIIα* mRNA can be found from the cell body. Furthermore, *CamKIIα* and another dendritically localized mRNA,

Arc, were shown to be in a complex purified using the tail of KIF5 (Kanai *et al.*, 2004). Interaction with multiple isoforms of Kinesin, specifically Kinesin-1 and Kinesin-2, is observed in the case of *Vg1* mRNA. Blocking the function of Kinesin-1 and Kinesin-2 by the injection of antibodies, or the expression of mutant Kinesins in *Xenopus* oocytes disrupts *Vg1* mRNA localization (Betley *et al.*, 2002; Messitt *et al.*, 2008). Furthermore, Kinesin-1 and Kinesin-2 have non-redundant functions in *Vg1* localization, and it is thought that they operate together to coordinate the transport of *Vg1* mRNA along a subpopulation of microtubules to the vegetal pole of the *Xenopus* oocyte.

Myosin

Members of the type-V Myosin (MyoV/Unconventional Myosin) family are widely used for intracellular transport along actin filaments (Reck-Peterson *et al.*, 2000; Vale, 2003). MyoV can be divided into four major structural domains. The motor domain contains the actin-binding site and ATP binding site, followed by an extended lever arm that is stabilized by binding calmodulin, or related light chains. The lever arm amplifies conformational changes on ATP hydrolysis. A coiled-coil rod region is responsible for dimerization of the molecule, and at the C terminus is a globular tail that binds adapter proteins that link MyoV to cargo. In metazoans, MyoV has been implicated in transport of various organelles on actin tracks (Vale, 2003), including ER movement in squid axoplasm and melanosome transport in *Xenopus* melanophores and mouse melanocytes (Aspengren *et al.*, 2009). The MyoV family has been widely studied in *S. cerevisiae*, where the motor Myo2p delivers secretory vacuoles and vesicles, mitochondria, Golgi and proteins such as Kar9 (required for anchoring microtubules to the bud tip) from the mother cell to the bud tip of a dividing cell (Reck-Peterson *et al.*, 2000).

One of the best-understood examples of active transport of mRNA is the MyoV motor, Myo4p, -mediated localization of *ASH1* mRNA along the actin cytoskeleton from the mother cell to the bud tip (Gonsalvez *et al.*, 2005; Müller *et al.*, 2007; Paquin and Chartrand, 2008). Microarray analysis has also identified a further 22

transcripts that are localized to the bud by the same machinery as *ASH1* (Shepard *et al.*, 2003).

Multiple motors move cargoes

In vitro studies with purified molecules have demonstrated that increasing the number of motors attached to a bead enhances motor processivity (Mallik *et al.*, 2005; Vershinin *et al.*, 2007). Electron microscopy, high-resolution tracking and motor stall force measurements indicate that teams of motors also operate during cargo transport *in vivo*. In *Drosophila*, lipid droplets are transported toward the plus end of microtubules into the interior of the syncytial blastoderm embryo. Both Dynein and Kinesin-1 are involved in the movement of these lipid droplets and it has been proposed that up to 4–6 Dyneins are active on individual droplets during minus-end-directed movement (Gross *et al.*, 2000). In addition, measurement of the stall forces for droplet motion powered by Kinesin-1 revealed that lipid droplets might also engage more than one molecule of Kinesin (Shubeita *et al.* 2008). In a further example, it is also thought that the highly processive movement of individual peroxisomes in cultured cells can be driven by as many as 11 Dyneins or Kinesins engaged at one time (Kural *et al.*, 2005). Visualization of localized mRNA in so-called transport particles by electron microscopy has also indicated that multiple motor molecules may be present in one RNA transport particle (Delanoue *et al.*, 2007).

Bidirectional movement of motor cargoes

Although some cargoes may be transported in a smoothly unidirectional manner through the cell, many move bidirectionally (reviewed in Welte, 2004). In these cases, runs in one direction are interrupted by pauses or processive movements in the opposite direction. It has been hypothesized that bidirectional motility enables motors to bypass obstacles within the cell and to correct errors in transport. Bidirectional motility is thought to result from the concurrent binding of oppositely oriented motors that are coordinately regulated. The regulatory mechanisms that

govern this coordination are not yet clear but might involve the direct coupling of motors, or coordination through accessory factors such as Dynactin. Among the many cargoes known to display this type of bidirectional motion are lipid droplets, mitochondria, pigment granules, peroxisomes and RNA transport particles. Both Dynein and Kinesin-1 are required for the bidirectional movement of FMR-containing RNA granules in thin processes formed by *Drosophila* S2 cells (Ling *et al.*, 2004). In oligodendrocytes, exogenous *MBP* RNA assembles into granules that move bidirectionally and colocalize with both Kinesin-1 and Dynein (Ainger *et al.*, 1997).

In some cases, bidirectional motility may be the result of the action of just one type of motor. In motility assays with multiple Dynein motors *in vitro,* Dynein moves exclusively to the minus ends. However, it has also been shown that highly purified Dynein/Dynactin complexes from mouse brain are capable of bidirectional transport to both plus and minus ends (Ross *et al.*, 2006). Moreover, apically localized mRNAs in the *Drosophila* syncytial blastoderm embryo are transported bidirectionally, and inhibition of Dynein suppresses movement in both directions (Bullock *et al.*, 2006). Plus end movement in this case is independent of Kinesin-1 and Kinesin-2. This suggests that Dynein itself, rather than the joint activities of Dynein and Kinesin is responsible for bidirectional movement of apical mRNAs. Dynactin has also been shown to be required for suppression of plus-end directed motion, thereby preventing basally directed movement in the embryo (Vendra *et al.*, 2007).

How does the transport machinery recognize mRNAs, and how is subcellular destination determined?

The destination of localized mRNAs is in part determined by *cis*-acting elements within the mRNA. It is thought that *trans*-acting factors recognize and interpret these elements, couple the mRNA cargo to the motor, and specify the destination of the mRNA. However, very little is known of the molecular mechanisms that govern this recognition and choice of destination, and the question of specificity remains a major question in the field.

Cis-acting elements

Cis-acting 'localization elements' (otherwise known as 'zipcodes' as they contain the cytoplasmic 'delivery address' for transport) have been identified through genetic and microinjection studies aimed at characterizing the minimal sequences that are necessary and sufficient for correct localization. Such studies have shown that localization elements are most commonly found in the 3'UTR of targeted mRNAs, but can also be located in the 5'UTR or coding regions (Serano and Rubin, 2003; Van De Bor *et al.*, 2005), and can vary in size from the 11-nucleotide RNA trafficking signal (RTE; also referred to as the A2RE motif) in the 3'UTR of *MBP* mRNA (Ainger *et al.*, 1997) to a 625-nucleotide region of the *bcd* 3'UTR (Macdonald and Struhl, 1988). Very few examples of 'consensus' localization sequences within mRNAs that can localize to the same subcellular destination have been identified.

A number of common themes have emerged from the study of localization sequences. Localization elements can be modular, with distinct elements directing different steps of localization, as is seen for *bcd* mRNA (Macdonald and Kerr, 1997). In this case, several elements (referred to as *bcd* localization elements, or BLEs) within the initially identified 625-nucleotide region are required for localization, and distinct elements direct distinct steps of transport (Macdonald and Kerr, 1997; Macdonald and Kerr, 1998; Macdonald *et al.*, 1993). The 50-nucleotide BLE1 was

shown to be specifically required for transport from the nurse cells of the *Drosophila* egg chamber to the oocyte. Additional BLEs are required for later steps of transport and for anchoring of the RNA at the anterior of the oocyte.

In a number of examples, the localization sequence has been predicted to form a stable secondary structure, which through mutagenesis experiments has been shown to be critical for localization. Mutations in BLEs that altered the primary sequence of the localization element whilst conserving the predicted secondary structure were shown to still allow *bcd* localization, suggesting that RNA structure, rather than primary sequence in this case, is critical (Ferrandon *et al.*, 1997). Localization element structure, and the hunt for consensus sequences and structure are explored further in Chapter 3.

Localization elements in some instances are also repeated and functionally redundant. For example, *nos* mRNA contains four different regions in its 3'UTR able to direct localization to the posterior of the *Drosophila* oocyte (Gavis *et al.*, 1996). Each signal is sufficient for localization, but functions more efficiently when present in multiple copies, or when combined with the other elements. Clustering of repeated, redundant elements is also observed within the short E2 and VM1 sequences of the 340-nucleotide *Vg1* localization element (VLE) in *Xenopus Vg1* mRNA (Lewis *et al.*, 2004), and in the four RNA stem loops (E1, E2A, E2B and E3) that target *ASH1* mRNA to the bud in *S. cerevisiae* (Chartrand *et al.*, 1999). It has been hypothesized that clustering of sequences facilitates the binding of *trans*-acting factors to the RNA, as well as the binding of factors that are required for localization but that do not bind the RNA directly.

Trans-acting factors

The ability to image localizing mRNAs in living cells has shown that the transport of RNA cargoes to their destination occurs in large ribonucleoprotein (RNP) particles, termed RNA transport granules (Ainger *et al.*, 1993; Bullock *et al.*, 2006; Ferrandon *et al.*, 1994; MacDougall *et al.*, 2003; Vendra *et al.*, 2007; Weil *et al.*, 2008; Wilkie and Davis, 2001; Zimyanin *et al.*, 2008). Within these particles, *trans*-acting factors bind the transported RNA directly, or indirectly by binding other proteins. These factors may play various roles, reflecting the multiple steps that are involved in transporting mRNAs to specific subcellular sites (Fig. 1.1). These roles include linking the RNA cargo to the motor, influencing motor activity, defining the specific cellular destination of a particular RNA, regulating the translation of the RNA whilst being transported, or anchoring the RNA once it has reached its final destination. Such factors may also be present as a result of earlier mRNA processing events, such as nuclear export or splicing, and also play further roles in localization. Furthermore, RNPs may be dynamic, and the specific constellation or arrangement of proteins within an RNP complex may change at different stages, ultimately specifying the fate of the RNA by influencing its structure and interactions with different factors (Dreyfuss *et al.*, 2002). Major questions remain about the biochemical nature of RNA transport granules, the proteins and RNAs that are present in them, what jobs these factors do and how they are organized both spatially and temporally.

RNA transport granules

The assembly of large RNA transport granules may be in part due to the assembly of oligomeric RNAs or RNPs, that can contain multiple, perhaps different, mRNAs and motors with the associated *trans*-acting factors. Oligomerization of RNAs within RNPs has been shown to be the case for *osk* mRNA, where intronless reporter mRNAs that contain only the *osk* 3'UTR can interact and 'hitch-hike' with endogenous *osk* mRNA to the posterior pole of the *Drosophila* oocyte (Hachet and Ephrussi, 2004). This 3'UTR-mediated oligomerization requires Hephaestus/PTB (discussed in chapter 5) and is needed for the translational repression of unlocalized

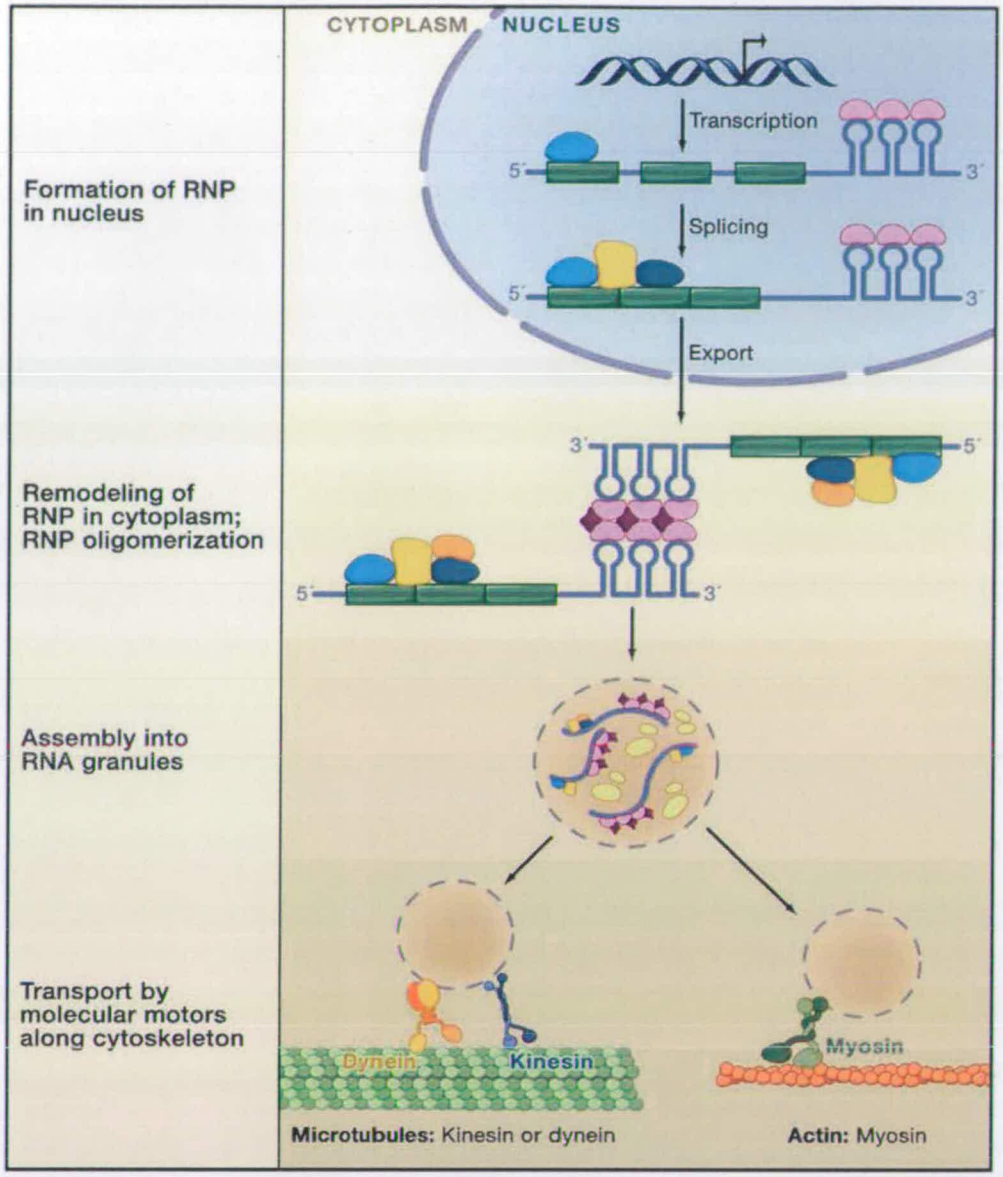

Figure 1.1 mRNA localization is a multi-step process (taken from Martin and Ephrussi, 2009). The pre-mRNA (exons in green; introns, 5' and 3'UTRs in grey) has *cis*-acting localization elements. These are usually in the 3'UTR and often form stem-loop structures. RNA-binding proteins (blue and purple) bind the pre-mRNA. In the nucleus, additional RNA-binding proteins (golden and dark blue) are added to form a ribonucleoprotein (RNP) complex. Following export into the cytoplasm, the RNP is remodeled as additional proteins (orange, dark purple) are added. In some cases, the RNP can form oligomers with other RNPs through protein-protein interactions. In the cytoplasm, RNPs are assembled into RNA granules that associate with motor proteins and are transported by cytoskeletal elements to their final destination.

osk mRNA (Besse *et al.*, 2009). This is consistent with the purification of large, translationally repressed particles that contain multiple *osk* transcripts and are assembled via RNA-protein and protein-protein interactions from *Drosophila* ovary extracts (Chekulaeva *et al.*, 2006). By using immunoelectron microscopy techniques, it has also been shown that *grk* mRNA, also in the *Drosophila* oocyte, is transported in particles that contain many individual RNA molecules assembled with numerous molecules of the Dynein motor and the *trans*-acting factor, Squid (Sqd) (Delanoue *et al.*, 2007).

Multiple different mRNAs can sometimes be targeted to the same subcellular destination by 'multiplexing' within the same RNA transport granules. It is has been shown, through simultaneous labeling of different mRNAs and proteins and tracking of single particles, that in *S. cerevisiae* the same Myo4p transport machinery localizes over 20 different mRNAs to the bud tip (Shepard *et al.*, 2003). A similar process of multiplexing is also used in neurons for the dendritic targeting of multiple mRNAs by the A2 pathway (Gao *et al.*, 2008). This pathway was initially identified as being responsible for *MBP* localization to the myelin compartment of oligodendrocytes (Ainger *et al.*, 1993), and has since been shown to target numerous exogenous (Shan *et al.*, 2003) and endogenous mRNAs to dendrites in neurons.

The identity of the *trans*-acting factors involved in mRNA localization has been studied through genetic screens for genes required for mRNA localization, and by the biochemical purification of RNA granules or affinity purification of proteins able to bind localization elements or motor proteins. A number of the principal factors are discussed below. Factors more specifically required for *grk* mRNA localization will be discussed separately.

Staufen

Staufen (Stau) was first identified in genetic screens searching for genes involved in pattern formation during *Drosophila* embryogenesis, and is required for the localization of *bcd* and *osk* mRNAs in the *Drosophila* oocyte (Frohnhöfer and Nüsslein-Volhard, 1987; St Johnston *et al.*, 1991). Stau has five distinct double-stranded RNA (dsRNA) binding domains (dsRBDs) of which dsRBDs1, 3 and 4 bind dsRNA *in vitro* without any specificity (Micklem *et al.*, 2000; St Johnston, 1992), indicating that additional proteins are required to achieve specificity. dsRBD2 and dsRBD5 were shown to have distinct roles in mRNA localization and translation of *osk* mRNA respectively (Micklem *et al.*, 2000). dsRBD5 has also been shown to direct the actin-dependent localization of *prospero* mRNA to the basal cortex of *Drosophila* neuroblasts (Schuldt *et al.*, 1998), indicating that distinct domains of Stau can mediate microtubule- and actin-based mRNA transport.

Stau colocalizes with *bcd* at the anterior of the oocyte, appearing at the same stage as when the bulk of *bcd* mRNA is localized and can bind *bcd* mRNA through the highly structured localization elements within the *bcd* 3'UTR (Ferrandon *et al.*, 1994; Ferrandon *et al.*, 1997). Stau is required for the later localization of *bcd*, and may also be required to anchor *bcd* on the transition from oogenesis to embryogenesis. Stau also localizes to the posterior pole of the *Drosophila* oocyte, in the same manner as *osk* mRNA (St Johnston *et al.*, 1991). Indeed, Stau and *osk* are interdependent for their localization (Ferrandon *et al.*, 1994), most likely through the interaction of Stau with the *osk* 3'UTR (Jenny *et al.*, 2006). The role of Stau in mRNA localization is evolutionarily conserved, and *Xenopus* Stau1 (XStau1) associates with *Vg1* mRNA and by expression of a dominant-negative form of the protein, has been shown to be required for its localization to the vegetal pole of the oocyte (Yoon and Mowry, 2004). Expression of both XStau1 and XStau2 peaks during mid-oogenesis when mRNA localization is taking place, and both proteins localize to the vegetal cortex (Allison *et al.*, 2004). Mammalian Stau1 and 2 are involved in the targeting of neuronal mRNAs to dendrites, and are purified with complexes containing localized neuronal mRNAs (Dûchaine *et al.*, 2002; Furic *et al.*,

2008; Tang *et al.*, 2001).

Nervous system *trans*-acting factors

As described above, Stau is required for neuronal mRNA localization, and a number of other factors have also been shown to be important for mRNA localization in the nervous system. FMRP (Fragile X Mental Retardation Protein) is an RNA binding protein that contains two hnRNP K homology (KH) domains and one RGG (arginine-glycine-glycine) RNA binding domain. Mutations in FMRP result in Fragile X syndrome, the most common form of X-linked mental retardation. FMRP can bind to a number of localized transcripts, including *MAP1b*, *PSD95* and its own mRNA, and has been shown to associate with Kinesin and to travel along microtubules (for review see Bassell and Warren, 2008). It is thought that FMRP plays a role in regulating the translation of its RNA targets, consistent with changes in several forms of synaptic plasticity in *Fmr1* null mice (Huber *et al.*, 2002; Nosyreva and Huber, 2006).

In oligodendrocytes, the identification of the 11-nucleotide RTE motif in the 3'UTR of *MBP* mRNA allowed the affinity purification of a protein specifically able to bind this sequence from rat brain (Hoek *et al.*, 1998). This protein was identified as hnRNP A2, which led to the RTE also being named the A2 recognition element, or A2RE. Together, the A2RE and recognition of this motif by hnRNP A2 result in targeting of numerous mRNAs by the A2 pathway.

Zipcode-binding proteins

Zipcode binding protein, or ZBP1, was first identified as a protein able to bind the zipcode of *β-actin* mRNA in chick embryo fibroblasts (Ross *et al.*, 1997). ZBP1 contains two RNA Recognition Motif (RRM) domains required for the localization of *β-actin*, and four KH domains that mediate binding to the zipcode, other *trans*-acting factors and to the actin cytoskeleton (Farina *et al.*, 2003). Orthologues of ZBP1 are present in *Xenopus* (Vera/Vg1RBP) (Deshler *et al.*, 1997; Deshler *et al.*,

1998), *Drosophila* (Imp) (Geng and Macdonald, 2006; Munro *et al.*, 2006) human and mouse, and all are implicated in mRNA localization in *Xenopus* oocytes, *Drosophila* oocytes and neurons (Boylan *et al.*, 2008) and mammalian fibroblasts and neurons (Zhang *et al.*, 2001) respectively. A further zipcode-binding protein, ZBP2, was more recently purified from chick embryo brain extract also through the ability to bind the *β-actin* zipcode. ZBP2 also contains KH domains and is a predominantly nuclear protein that influences *β-actin* mRNA localization in the cytoplasm by facilitating the binding of ZBP1 to the transcript (Pan *et al.*, 2007; Gu *et al.*, 2002). Orthologues have been shown to exist in *Xenopus* (VgRBP71) (Kroll *et al.*, 2002) and rat (MARTA1) (Rehbein *et al.*, 2000), and like ZBP1 orthologues these are also thought to be involved in mRNA localization. VgRBP71 is able to bind the *Vg1* localization element and is thought to activate translation, whilst MARTA1 (MAP2-RNA-trans-acting protein) binds with high affinity to the dendritic targeting element (DTE) of the *MAP2* transcript.

The She proteins

Genetic and biochemical analysis has identified a number of proteins able to bind the *ASH1* mRNA localization elements. Indeed, these proteins and their roles in mRNA localization are some of the best understood and characterized within the field. The RNA binding protein She2p is responsible for the recognition of bud-localized mRNAs, including *ASH1*, via its interaction with a conserved motif in the localization elements of these transcripts (Olivier *et al.*, 2005). She2p also interacts with the transport machinery, comprised of the type V myosin Myo4p, via the bridging protein She3p (Bohl *et al.*, 2000; Long *et al.*, 2000; Takizawa and Vale, 2000). Together, She2p, She3p and Myo4p form the 'locasome' that mediates trafficking of ASH1 mRNA along the actin cytoskeleton. During localization, *ASH1* mRNA is translationally repressed by the proteins Khd1p (Irie *et al.*, 2002) Loc1p and Puf6p (Gu *et al.*, 2004). Loc1p and Puf6p are predominantly nucleolar proteins that bind to She2p in the nucleus where She2p recruits these factors to the ASH1 mRNA, providing a further example of how nuclear events can influence cytoplasmic localization.

Nuclear history

Studies of a number of localized mRNAs suggest that cytoplasmic mRNA targeting can be initiated in the nucleus. Several *trans*-acting factors are nucleocytoplasmic shuttling proteins that associate with transcripts in the nucleus and subsequently direct mRNA targeting in the cytoplasm. *Trans*-acting factors involved in *osk* mRNA localization provide an example of this, and also of the dynamic nature of RNP assembly. Mago nashi (Mago) and Y14/Tsunagi are components of the nuclear exon-exon junction complex (EJC). The EJC proteins are deposited upstream of exon-exon junctions on mRNAs in a splicing-dependent manner and are thought to remain on the mRNA until the pioneer round of translation. These proteins, with Barentsz (Btz) (Van Eeden *et al.*, 2001) and eIF4III (Palacios *et al.*, 2004), are part of an *osk* localization complex (Hachet and Ephrussi, 2001; Mohr *et al.*, 2001; Newmark and Boswell, 1994). The involvement of the EJC suggests proteins assembled during splicing direct the cytoplasmic localization of *osk*. Indeed, splicing of the first intron is required for posterior localization (Hachet and Ephrussi, 2004). Since Btz is cytoplasmic and Mago, Y14 and eIF4III are nuclear, it has been suggested that assembly of the RNP occurs in a stepwise manner. EJC components have also been shown to be present in the dendrites of mammalian neurons, and eIF4AIII is associated with neuronal mRNA granules and dendritically localized mRNAs (Giorgi *et al.*, 2007; Glanzer *et al.*, 2005; Macchi *et al.*, 2003; Monshausen *et al.*, 2004).

Similarly, transcript recognition and formation of a specific RNP complex in the nucleus is an early event in *Vg1* mRNA localization in *Xenopus* oocytes. Vegetal pole localization of *Vg1* mRNA is directed in part by the *trans*-acting factors Vg1RBP60/hnRNPI/PTB (Cote *et al.*, 1999) and Vera/Vg1RBP (Deshler *et al.*, 1997). These factors bind to E2 and VM1 motifs in the VLE (Cote *et al.*, 1999; Deshler *et al.*, 1998; Kwon *et al.*, 2002), and mutations in the VLE that disrupt binding lead to mislocalization of the *Vg1* transcript. Immunoprecipitation of tagged Vg1RBP60/hnRNP I/PTB and Vera/Vg1RBP revealed that both proteins associate with *Vg1* mRNA in the nucleus as well as the cytoplasm and that the RNP is

remodelled following its export to the cytoplasm (Kress *et al.*, 2004). However, a strictly cytoplasmic form of the *Drosophila* orthologue of the nucleocytoplasmic shuttling protein VgRBP60/hnRNP I/PTB, Hephaestus (discussed further in Chapter 5), is able to repress *osk* translation throughout localization (Besse *et al.*, 2009), suggesting that nuclear function is not always required.

Translational regulation

For protein synthesis to be spatially restricted, translation of localizing mRNAs is silenced during transport, and activated once they reach their final destination. Translational regulation requires the presence of translational repressors that block translation at different steps, and that can be inactivated once translation is desirable. Several lines of evidence support this, including the accumulation of proteins encoded by localized mRNAs at the destination, the recruitment of translational repressors to transport RNPs (Chekulaeva *et al.*, 2006; Gu *et al.*, 2002; Nakamura *et al.*, 2004; Paquin *et al.*, 2007) the poor co-sedimentation of some localizing mRNAs in polysomal fractions (contain actively translated mRNA) (Chekulaeva *et al.*, 2006; Krichevsky and Kosik, 2001) and the presence of EJC components (thought to be removed from mRNAs only after the pioneer round of translation) in transport RNPs in a number of systems (Giorgi *et al.*, 2007; Hachet and Ephrussi, 2004).

In a number of examples, translation of the mRNA is directly linked to localization. Translational activation can be achieved by local proteins that compete for binding to translational repressors at the final destination. For example, Osk protein at the posterior of the *Drosophila* oocyte may interact with the translational repressor of *nos* mRNA, Smaug, acting to alleviate the translational repression of *nos* mRNA (Zaessinger *et al.*, 2006). Local post-translational modification of translational repressors at the final destination may also activate translation, as seen in the phosphorylation of ZBP1 by Src kinase once *β-actin* mRNA has been localized (Hüttelmaier *et al.*, 2005). Phosphorylation is restricted to sites of *β-actin* translation and decreases the binding affinity of ZBP1 for *β-actin*. In other examples, translational control is temporally regulated, and translation occurs later in response to specific cues, rather than directly following localization. This has been shown

extensively in neurons, where subsets of localized mRNAs are translated in dendrites following synaptic activation (for reviews see Bramham and Wells, 2007; Klann and Dever, 2004), or in developing axon growth cones in response to guidance cues (for review see Piper and Holt, 2004). In the *Drosophila* egg, *bcd* mRNA is translated at the anterior only upon egg activation (Sallés *et al.*, 1994; Surdej and Jacobs-Lorena, 1998).

Translational repressors can block translation at different steps and a number of localized mRNAs are regulated by multiple redundant mechanisms to ensure precise translational control. Mechanisms of translational repression include general 'masking' from the translational machinery by the formation of large RNP particles, as demonstrated for *osk* mRNA (Besse *et al.*, 2009; Chekulaeva *et al.*, 2006). A step frequently targeted by translational repressors is the association of the cap-binding protein eIF4E with the translation initiation factor eIF4G. Specific eIF4E-binding proteins (4E-BPs) are recruited to repressed mRNAs where they compete with eIF4G for eIF4E binding and block translation intiation (for review see Richter and Sonenberg, 2005). 4E-BPs include maskin protein, which acts on many maternal transcripts in *Xenopus* oocytes including *cyclin B1* and *c-mos* mRNAs (Stebbins-Boaz *et al.*, 1999), and may also repress translation of dendritically localized mRNAs in neurons (Huang *et al.*, 2002; Wu *et al.*, 1998). Maskin interacts with CPEB that in turn recognizes a uridine-rich CPE present in the 3′-UTR of selected mRNAs. *Drosophila* Cup is also a 4E-BP that acts to repress translation of *osk* and *grk* mRNAs through binding the RNA binding protein Bruno (Clouse *et al.*, 2008; Nakamura *et al.*, 2004).

Changes in poly(A) tail length are also correlated with the translational efficiency of a number of localized mRNAs. In general, those transcripts containing short poly(A) tails (~20 nucleotides) are translationally dormant, but upon cytoplasmic poly(A) elongation these transcripts are translationally activated by the recruitment of poly(A)-binding protein (PABP). Poly(A) tail length is regulated in a number of dendritically localized mRNAs, for example, synaptic stimulation results in polyadenylation and translation of the CPE-containing *CaMKIIα* mRNA at synapses

(Huang *et al.* 2002; Wells *et al.* 2001; Wu *et al.* 1998) through the action of CPEB as a positive regulator of translation. For *bcd* mRNA, elongation of the poly(A) tail has also been shown directly to be necessary for translation (Sallés *et al.*, 1994).

Translational control by non-coding RNAs and microRNAs

Proteins are not the only *trans*-acting factors that can repress translation of localized mRNAs. Non-coding RNAs have now been shown to play a role in translational repression. The small non-coding brain cytoplasmic 1 (BC1) RNA is expressed primarily in neurons. *In situ* hybridization studies of primary neuronal cultures have demonstrated that BC1 RNA is present throughout the cytoplasm from the soma to the distal processes of dendrites (Tiedge *et al.*, 1991). Recent work has shown that BC1 RNA dendritic transport requires a 65-nucleotide dendritic targeting element (DTE) (Muslimov *et al.*, 1997; Muslimov *et al.*, 2006), occurs in ribonucleoprotein (RNP) particles (Cheng *et al.*, 1996) that also contain PABP (Kondrashov *et al.*, 2005; Muddashetty *et al.*, 2002), and is mediated by microtubules and molecular motors (Cristofanilli *et al.*, 2006). BC1 operates as a general translational repressor and is able to block the formation of 48S translation initiation complexes by targeting the eIF4A translation initiation factor (Wang *et al.*, 2002). Specifically BC1 can uncouple the RNA unwinding activity of eIF4A from ATP hydrolysis, inhibiting the catalytic activity of eIF4A (Lin *et al.*, 2008). BC1 may also interact with FMRP (Zalfa *et al.*, 2005) and specific mRNAs, and complementary regions for BC1 have been found in *Arc*, *CamKIIα* and *MAP1b* mRNAs.

There is also a role for microRNA (miRNA)-mediated translational regulation in dendrites. In one study (Ashraf *et al.*, 2006), the translation of dendritically localized *Drosophila CaMKIIα* mRNA was shown to be regulated during olfactory learning. The involvement of small RNAs was suggested by the increase in *Drosophila CaMKIIα* protein in *dicer-2* mutant brains. The *CaMKIIα* 3'UTR was also found to contain two putative miRNA-binding sites, indicating that binding of miRNAs might function to repress translation. Importantly, the same study found that components of the RNA silencing machinery were also present at synapses and further found that

one of these proteins, encoding the RNA helicase Armitage, was degraded at the synapse during learning. As this study investigated the translation of transgenes containing or lacking the entire *CamKIIα* 3'UTR in wild-type, *dicer-2* and *armitage* mutant brains, direct roles for the predicted miRNA binding sites, or for Armitage in the regulation of *CamKIIα* translation were not demonstrated. However, these findings can be used to propose a model in which persistent generation of miRNAs is required to repress translation of *CamKIIα* and that neuronal activity leads to degradation of components of the RNA interference machinery such that translational repression is lifted. Interestingly, mutations in *armitage* also result in the premature accumulation of Osk protein during early *Drosophila* oogenesis, and it was hypothesized that RNA silencing is required for translational control of *osk* mRNA in the oocyte. However, further investigation has since shown that the premature translation of Osk in *armitage* mutants can be suppressed by mutations in genes encoding DNA damage checkpoint proteins (Klattenhoff *et al.*, 2007). Therefore, it is now thought that *armitage* mutations disrupt *osk* translational regulation through the activation of a DNA damage signaling pathway, and *osk* translational repression does not directly require RNA silencing involving Armitage. Armitage is required for the silencing of retrotransposons in the germline, and it is thought that loss of retrotransposon silencing could induce DNA double-strand breaks and therefore DNA damage signaling.

In other studies, (Schratt *et al.*, 2004, 2006) bioinformatics approaches were used to look for potential miRNA binding sites in a group of mRNAs that they had previously shown to be translated in cultured neurons in response to BDNF. This study found that the brain-specific miRNA miR-134 bound to sites in the 3'UTR of one of the mRNAs, encoding LimKinase 1 (LimK1), and that miR-134 represses translation of *LimK1* mRNA in dendrites. These findings are also consistent with miRNAs functioning to regulate translation at the synapse. Studies in non-neuronal cells have revealed that components of the RNA interference pathway and targets of miRNAs localize to "RNA processing bodies," or "P-bodies" (Liu *et al.*, 2005). The relationship between P-bodies and RNA granules in neurons and oocytes is now a widely studied question.

The nature of RNA transport granules

It has been proposed that maternal and neuronal RNA transport granules and anchoring structures are similar in composition, structure and function to each other and to RNA processing bodies (P bodies) and stress granules (Anderson and Kedersha, 2206; Kiebler and Bassell, 2006). P bodies were initially identified in different eukaryotic cell types as dynamic cytoplasmic sites for RNA degradation and storage of translationally repressed mRNAs (for review see Eulalio *et al.*, 2007). They are characterized by the presence of translational repressors as well as enzymes and cofactors that promote mRNA decay (including the decapping enzymes DCP-1 and -2 and the 5'-3'-exoribonuclease Xrn1/Pacman), and also by the lack of ribosomal proteins. Mammalian P bodies have since been found to contain mRNAs under miRNA regulation, as well as components of the RISC complex (for example the Ago proteins) required for miRNA action. Stress granules form in the cytoplasm of plant and mammalian cells following environmental stress, consisting of stalled ribosomal translation initiation complexes, mRNAs encoding most cellular proteins and translation initiation factors (Anderson and Kedersha, 2006).

Maternal and neuronal RNA granules have been shown to share a number of components. These include *Drosophila* Imp (an orthologue of Xenopus Vg1RBP and chicken ZBP1), Stau, FMRP, Barentsz, Cup, eIF4E and Me31B/Dhh1p. As the DEAD-box RNA helicase Me31B/Dhh1p is also a P body protein that inhibits translation and promotes decapping-mediated mRNA decay, it was hypothesized that there are similarities between maternal and neuronal RNA granules and P bodies, and that many RNA granules share a core composition and function (Barbee *et al.*, 2006; Kiebler and Bassell, 2006; Snee and Macdonald, 2009). Maternal and neuronal RNA granules were shown to contain two classic P body markers Xrn1/Pacman and DCP-1 in colocalization experiments and in some instances mRNAs localized to dendrites may be regulated by miRNAs (Ashraf *et al.*, 2006). Similarly, stress granules contain a number of RNA binding proteins involved in mRNA localization and localized translation, including Stau, FMRP and CPEB (Anderson and Kedersha, 2006). Together, these results suggest that there is a core complex and that this core

can be modified and elaborated upon in different biological contexts.

This idea has been challenged by studies in mammalian neurons that showed that neuronal localizing Stau-containing granules and P bodies are distinct structures that can transiently and dynamically interact in a process controlled by neuronal activity (Zeitelhofer *et al.*, 2008). Furthermore, there is a lack of colocalization between Xrn-1/Pacman and DCP-2 with *osk* mRNA in *Drosophila* oocytes (Lin *et al.*, 2008), although DCP-1 has been shown to be a component of the *osk* RNP, and is required for *osk* transport to the posterior pole of the *Drosophila* oocyte (Lin *et al.*, 2006). In conclusion, there are a number of cytoplasmic bodies within oocytes, neurons and other cells that are involved in the regulation of mRNA. Whether these are distinct bodies that can interact and 'swap' components, or whether these are all related and represent different assemblies of the same highly dynamic structure of core proteins that can be elaborated upon is still very much open to debate.

mRNA anchoring at the final destination

The role of the cytoskeleton in mRNA anchoring

In a number of examples, the actin cytoskeleton has been implicated in the tethering of the localized mRNA at the final destination. Examples include *β-actin* mRNA in fibroblasts (Farina *et al.*, 2003), *Arc* mRNA in veterbrate neurons (Huang *et al.*, 2007) and *ASH1* mRNA at the bud tip in *S. cerevisiae* (Beach *et al.*, 1999). In *Drosophila*, it is thought that cortical microfilaments could be involved in the retention of *osk* and *bcd* mRNAs at the posterior and anterior of the oocyte respectively. Genetic screens have identified two actin-binding proteins, Moesin and TropomyosinII (TmII) that are required for the localization of *osk* mRNA at the posterior of the oocyte (Erdelyi *et al.*, 1995; Jankovics *et al.*, 2002). Tropomyosin proteins are involved in actin-based motility in muscle, and associate with actin in nonmuscle cells. A P element allele of *Drosophila TmII* leads to mislocalization of *osk* to the anterior of the oocyte, although there is no evidence of a direct role for TmII in the anchoring of *osk* mRNA (Erdelyi *et al.*, 1995). Mutations in the

Drosophila moesin gene result in mislocalization of *osk* mRNA to a scattered distribution near the posterior pole of the oocyte and also in the detachment of the subcortical actin network from the cell membrane, suggesting that Moesin is required for both osk anchoring and for cross-linking of the actin network to the cell membrane (Jankovics *et al.*, 2002). The majority of *bcd* mRNA is localized to the anterior late in oogenesis, where it is maintained by a process of continual active transport by Dynein (Weil *et al.*, 2006; Weil *et al.*, 2008). Even later in oogenesis, this movement declines and the mRNA forms large, stationary foci at the anterior cortex. This stable cortical anchoring is sensitive to pharmacological disruption of the actin cytoskeleton.

Pharmacological disruption of the cortical actin cytoskeleton also disrupts *Vg1* mRNA anchoring at the vegetal cortex of the *Xenopus* oocyte (Alarcon and Elinson, 2001). Depletion of *Xlsirt* and *VegT* RNAs by antisense oligonucleotides also showed that these transcripts are required for the anchoring of *Vg1* mRNA through their structural role in the organization of the cytokeratin cytoskeleton (Kloc *et al.*, 2005).

The role of the motor in mRNA anchoring

Microtubules, and not actin, are required for the anchoring of apically localized mRNAs in the *Drosophila* blastoderm embryo (Delanoue and Davis, 2005). In a novel role for a molecular motor, Dynein colocalized with the apical mRNAs and injection of an inhibitory anti-Dynein antibody showed that Dynein is required for retaining the mRNA cargo in the apical cytoplasm. Here, Dynein acts as a static anchor and apical maintenance of the mRNA does not require Dynein motor activity (Delanoue and Davis, 2005). Similarly, Dynein is also required for the static anchoring of *grk* mRNA at the dorso-anterior of the *Drosophila* oocyte (Delanoue *et al.*, 2007).

The localization of *grk* mRNA

mRNA localization pathways play a central role in axis determination in *Drosophila* (St Johnston and Nüsslein-Volhard, 1992). Patterning of both the A-P and D-V axes are initiated by *grk* mRNA localization within the *Drosophila* oocyte. Given the importance of *grk* localization for *Drosophila* development, this will be used as a model for understanding the signals and *trans*-acting factors required for the localization of mRNAs. Before this can be discussed in greater detail, the process of *Drosophila* oogenesis must first be considered.

Drosophila oogenesis

A *Drosophila* ovary is composed of a cluster of 16-20 ovarioles, each of which contains a series of egg chambers that progressively increase in maturity in an anterior to posterior direction (King, 1970; Spradling, 1993) (Fig. 1.2). The egg chamber is the functional unit of oogenesis, and is the product of stem cell divisions at the very anterior tip of the ovariole in a region known as the germarium (Fig. 1.3).

The germarium

The germarium is divided into four regions that are defined by the developmental stage of the cyst. A germline stem cell (GSC) in region 1 divides asymmetrically to produce a cystoblast and a new GSC. The cystoblast then commences a pattern of cell division very different to that of the sister stem cell and undergoes precisely four mitotic divisions with incomplete cytokinesis. This results in a cyst of 16 germline cells that are interconnected by cytoplasmic bridges called ring canals. Once the 16-cell cyst has formed it moves into region 2a of the germarium. The topology of these mitotic divisions means that two cells have four ring canals (being connected to each other and to three other cells), two cells with three, four cells with two and eight cells with one ring canal. The cells with four ring canals are termed 'pro-oocytes' as one of these will always differentiate as the oocyte and enter meiosis by region 2b. The other 15 cells will begin to grow and differentiate as nurse cells, whose function

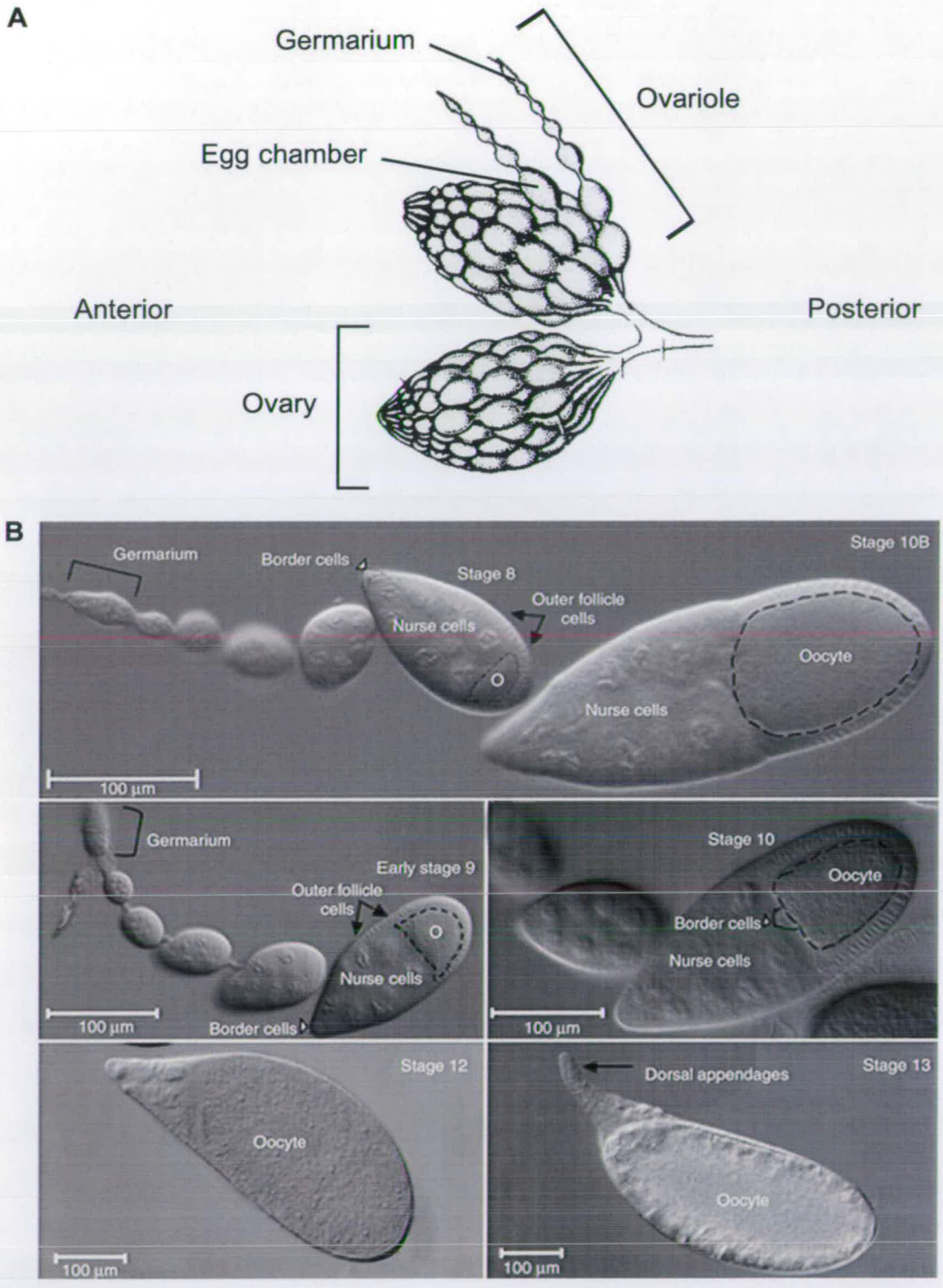

Figure 1.2 The *Drosophila* ovary and stages of oogenesis. (A) Schematic of the *Drosophila* ovaries (modified from King, 1970). Each ovary consists of 16-20 ovarioles, each of which contains a series of egg chambers that increase in maturity in an anterior to posterior direction. **(B)** Stages of egg chamber development, adapted from Prasad *et al.*, 2007. The oocyte (o) is outlined in stages 8-10, and the position of the border cells is indicated (arrowhead) where possible.

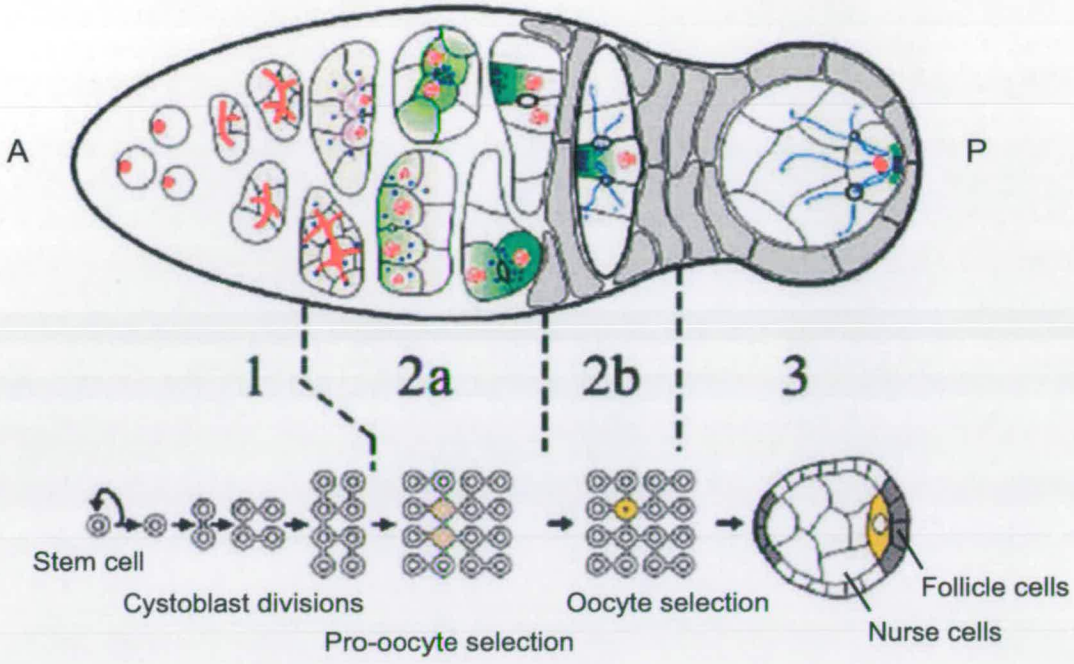

Figure 1.3 *Drosophila* early oogenesis and the germarium (adapted from Huynh and St Johnston, 2004). An egg chamber is made up of 16 germline cells surrounded by a single layer of follicle cells. The egg chambers are produced in the germarium, at the anterior of the ovariole. The germarium is divided into 4 developmental regions. The germline stem cells at the anterior tip of the germarium divide to produce cytoblasts, which divide four more times in region 1 to produce 16 cell germline cysts that are connected by ring canals and the fusome (red branched structure). In early region 2a, the synaptonemal complex (SC, red rings) forms along the chromosomes of the 2 cells with 4 ring canals (the pro-oocytes) as they enter meiosis. The SC then appears transiently in the 2 cells with 3 ring canals, before becoming restricted to the pro-oocytes in late region 2a. By region 2b, the oocyte has been selected, and is the only cell to remain in meiosis. In region 2a, cytoplasmic proteins, mRNAs, mitochondria (green), and the centrosomes (blue circles) progressively accumulate in the oocyte. The follicle cells (grey) also start to migrate and surround the germline cells. As the cyst moves down to region 3, the oocyte adheres strongly to the posterior follicle cells, resulting in its posterior position within the egg chamber. A, anterior; P, posterior.

during oogenesis is to synthesize and transport materials that are required for the growth and development of the oocyte. In addition, follicle cell stem cells in the germarium give rise to precursor follicle cells. These encapsulate the cyst in a somatic follicular epithelium and also separate individual cysts. Follicle cells later secrete the eggshell and also play an important role in establishing the future embryonic body axes through cell-cell communication with the germline.

Oocyte specification

The selection of the oocyte is the first 'symmetry-breaking' step in *Drosophila* development, and is therefore the first step in the establishment of the main body axes (for review see Huynh and St Johnston, 2004). The progress of oocyte specification can be followed by a number of markers. The synaptonemal complex, which marks cells in meiosis, appears first in the two pro-oocytes, then in additional cells, and finally is restricted to the oocyte (Carpenter, 1975; Hong *et al.*, 2003; Huynh and St Johnston, 2000; Page and Hawley, 2001). Other oocyte-specific proteins such as BicD, Egl, Btz and Cup and mRNAs such as *osk, BicD,* and *orb* also first concentrate in the pro-oocytes and finally concentrate in just the oocyte by the end of region 2a (Ephrussi *et al.*, 1991; Keyes and Spradling, 1997; Lantz *et al.*, 1994; Suter *et al.*, 1989; van Eeden *et al.*, 2001; Wharton and Struhl, 1989). The same is also true of the centrioles (Bolivar *et al.*, 2001) and of mitochondria (Cox and Spradling, 2003). Furthermore, microtubules are initially diffusely distributed throughout the cyst, and the minus ends are gradually restricted to the future oocyte (Bolivar *et al.*, 2001; Grieder *et al.*, 2000). Oocyte specification is a complex process, and there is evidence for three processes acting in parallel to restrict oocyte fate to one cell. Firstly, the future oocyte is labelled from the first stem cell division by a branched, membranous structure known as the fusome, and the future oocyte contains more fusome material than the fifteen neighbouring cells (de Cuevas and Spradling, 1998). This structure is made up of membranous vesicles kept together by high levels of cytoskeletal proteins including α-spectrin (de Cuevas *et al.*, 1996; Lin *et al.*, 1994), β-spectrin, ankyrin (de Cuevas *et al.*, 1996) and an adducin-like protein encoded by the *hu-li tai shao (hts)* gene (Lin *et al.*, 1994; Petrella *et al.*, 2007). The

fusome polarizes dynamic microtubules that are required, with Dynein and its associated proteins including Egl and BicD, for the localization of proteins and mRNAs into one cell (Bolivar *et al.*, 2001; Grieder *et al.*, 2000; Mach and Lehmann, 1997; McGrail and Hays, 1997; Navarro *et al.*, 2004; Ran *et al.*, 1994; Swan *et al.*, 1999; Theurkauf *et al.*, 1993). Secondly, the fusome also associates with acetylated, stable microtubules and with the Spectroplakin Short stop (Shot), and centrioles migrate along these microtubules in a process that also requires Dynein (Bolivar *et al.*, 2001; Roper and Brown, 2004). Thirdly, the fusome directs entry of the oocyte into meiosis in a process that requires Dynein, BicD and Egl, but is independent of microtubules (Bolivar *et al.*, 2001; Carpenter, 1994; Huynh and St Johnston, 2000).

Oocyte selection has taken place by the time the cyst reaches region 2b of the germarium. Beyond specification, a number of factors have been shown to be required for the maintenance of oocyte fate. For example, in *par-1* mutants, the oocyte de-differentiates to adopt the nurse cell fate (Cox *et al.*, 2001; Huynh *et al.*, 2001). In region 2b the cyst changes shape to become a one-cell thick disc spanning the width of the germarium, whilst a layer of somatic, epithelial follicle cells surround the cyst. The cyst then moves into region 3 of the germarium, also defined as stage 1 of oogenesis, where it rounds up to form a sphere in which the oocyte always lies at the posterior. The cyst now leaves the germarium and enters the vitellarium, where the egg chambers mature as they move posteriorly through the ovariole in 14 morphologically distinct phases (for a full description of each stage of oogenesis and the morphological changes see King, 1970; Spradling, 1993).

The vitellarium

Both the germline oocyte and nurse cells and the somatic follicle cells undergo morphological changes throughout oogenesis. The oocyte nucleus proceeds through meiotic prophase, forming a compact structure known as the karyosome. The nurse cell nuclei increase in size by multiple rounds of endoreplication and become highly polyploid. From stage 1-6, there is growth of both the nurse cells and oocyte. However, by stage 7, the oocyte increases in size relative to the nurse cells-by stage

10A it will occupy half of the egg chamber. This is due to a supply of nurse cell produced proteins, mRNAs and organelles moving into the oocyte via the ring canals. At stage 10B, this transport becomes rapid and nonselective, and is defined as dumping. The size of the oocyte also increases due to the uptake of yolk protein synthesised by the follicle cells from stage 8.

During oogenesis, distinct populations of follicle cells arise which vary in their function and in their pattern of migration (for review see Horne-Badovinac and Bilder, 2005; Wu *et al.*, 2008). Stalk cells and polar cells arise from the precursor cells that migrate between cysts. Stalk cells separate individual egg chambers, whilst polar cells reside at the anterior and posterior termini of egg chambers. Around stage 5, polar cells induce the epithelial follicle cells at the ends of the egg chamber to become terminal follicle cells as opposed to the mainbody follicle cells. The posterior terminal cells respond to signals from the oocyte in a *grk*-dependent process that ultimately establishes the embryonic body axes. At the beginning of stage 9, the anterior polar cells recruit 4-6 adjacent follicle cells to become border cells that delaminate from the epithelium and migrate posteriorly between the nurse cells. Concurrent with border cell migration, mainbody follicle cells migrate posteriorly to cover the oocyte. These cells become columnar and form a secretory epithelium that sequentially deposits the eggshell. Around 50 anterior terminal cells stretch flat to cover the nurse cells and are known as 'stretched cells'. At stage 10B a population of columnar follicle cells, known as centripetal cells, migrate inward at the oocyte-nurse cell boundary. These elongate apically over the oocyte surface and eventually form the operculum for larval exit at the anterior of the mature egg.

The most complex set of migrations form the dorsal appendages of the mature egg that are required for embryonic respiration. Two patches of dorso-anterior follicle cells are specified around stages 9-10 as a result of *grk*-dependent processes involved in axis specification. In each patch, two cell types, the floor cells and roof cells cooperate to form a tube that extends anteriorly. Chorion proteins are secreted into the lumen of each tube, and by stage 13, a flattened paddle is formed at the anterior (for review of eggshell patterning and morphogenesis see Berg, 2005). Also at the

anterior of the mature egg is a micropyle that is needed for sperm entry. Once egg maturation is complete, the nurse cells and follicle cells undergo apoptosis.

grk localization and axis determination in the *Drosophila* oocyte

grk encodes a TGF-α family member (Neuman-Silberberg and Schüpbach, 1993) that acts as a secreted oocyte ligand for the epidermal growth factor receptor, Torpedo (Top) (Schüpbach, 1987). RNA *in situ* hybridization (Neuman-Silberberg and Schüpbach, 1993), RNA injection (MacDougall *et al.*, 2003) and most recently fluorescent labelling of engodenous *grk* (Jaramillo *et al.*, 2008) have been used to follow *grk* mRNA localization during oogenesis and show that the pattern of *grk* localization changes during the progression of oogenesis (Fig. 1.4). These changes reflect the dual role of *grk* in axis specification, allowing for two rounds of signalling between the oocyte and specific sets of somatic follicle cells.

There has been some evidence of *grk* transcription in the oocyte nucleus (Saunders and Cohen, 1999), although it is now clear that *grk* mRNA is transported from the nurse cells into the oocyte (Clark *et al.*, 2007). In early oogenesis (stages 1-7) *grk* is transported into the oocyte and is localized in a posterior crescent between the nucleus and the overlying follicle cells (Neuman-Silberberg and Schüpbach, 1993). Local translation of *grk* and signalling to these adjacent terminal follicle cells by Grk results in the adoption of a posterior fate instead of the default anterior fate (Gonzalez-Reyes and St Johnston, 1998). The posterior follicle cells then signal back to the oocyte. Although the precise nature of this signalling event is unknown, members of the Salvaldor Warts Hippo (SWH) tumor-suppressor pathway (Meignin *et al.*, 2007; Polesello and Tapon, 2007) such as Merlin (MacDougall *et al.*, 2001) are required in the posterior follicle cells for the induction of axis specification in the oocyte. The final result of this signalling is the repolarization of the oocyte microtubule network. The MTOC appears to be at the posterior of the oocyte in stages 1-7, as indicated by a number of microtubule minus end markers (Clark *et al.*, 1994; Clark *et al.*, 1997; Theurkauf *et al.*, 1992). Following posterior Grk signalling, this MTOC disassembles and a diffuse anterior MTOC forms (Brendza *et al.*, 2000;

Clark *et al.*, 1997). The reorganization of the microtubule network is required for the migration of the oocyte nucleus to a dorso-anterior position (Gonzalez-Reyes *et al.*, 1995; Roth *et al.*, 1995). As the oocyte nucleus migrates to the anterior corner, *grk* transiently accumulates at the anterior margin of the oocyte in stage 8, finally localizing in a dorso-anterior perinuclear cap (Jaramillo *et al.*, 2008; MacDougall *et al.*, 2003; Neuman-Silberberg and Schüpbach, 1993) at stage 9. At this stage, local translation and the second Grk signal causes the overlying mainbody follicle cells to adopt a dorsal cell fate, allowing at a later stage for the correct specification and positioning of anterior and dorsal chorion structures, such as the dorsal appendages.

Microtubule polarity also determines the site of localization of *bcd* and *osk* transcripts which localize to the anterior and posterior of the oocyte respectively (Fig. 1.4). Anterior *bcd* localization is required for the formation of a morphogenetic gradient of Bcd protein in the early embryo for specification of the head and thorax (Berleth *et al.*, 1988; Driever and Nüsslein-Volhard, 1988). Similarly, *osk* localization at the posterior of the oocyte is required for the specification of the future germ cells and posterior structures (Ephrussi *et al.*, 1991; Kim-Ha *et al.*, 1991). Osk does not seem to play a direct role in determining cell fate in the embryo but recruits many other proteins and mRNAs to the posterior pole.

The mechanism of *grk* localization

The first evidence for active transport of *grk* RNA on cytoskeletal elements was the disruption of *grk* localization by overexpression of p50/Dynamitin (Januschke *et al.*, 2002; King and Schroer, 2000), supporting a role for Dynein in the localization of *grk*. An *in vivo* assay, consisting of the injection of fluorescently labelled RNAs directly into living egg chambers, developed by the Davis laboratory to allow real-time visualization of RNA movement, has shown that injected *grk* RNA localizes to the dorso-anterior corner of oocytes by active transport. These studies, in stage 8 and later oocytes, allowed the visualization of the assembly of injected *grk* RNA into discrete particles and the minus end directed movement of these particles along microtubules in two Dynein dependent steps (MacDougall *et al.*, 2003). The firs

***grk* mRNA localization**

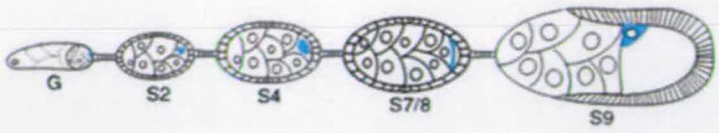

***osk* mRNA localization**

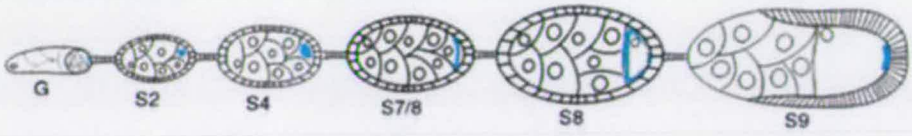

***bcd* mRNA localization**

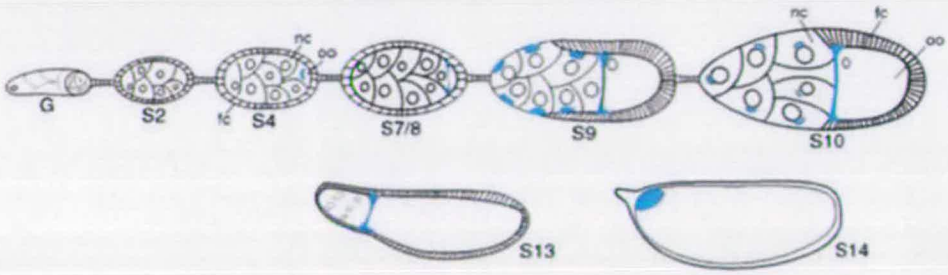

Figure 1.4 Schematic of the three mRNA localization pathways responsible for axis determination in *Drosophila* (modified from Lasko, 1999). mRNA is shown in blue. *bcd* mRNA localization to the anterior of the oocyte from stage 8 onwards is required for the formation of a morphogenetic gradient of Bcd protein in the early embryo for specification of the head and thorax. *osk* mRNA localization at the posterior of the oocyte from stage 9 onward is required for the specification of the future germ cells and posterior structures. *grk* mRNA localizes first at the posterior of the oocyte until around stage 7 of oogenesis, but by stage 9, *grk* has accumulated in a perinuclear cap at the dorso-anterior corner of the oocyte. Grk signalling at the posterior and at the dorso-anterior corner initiates patterning of both the anterior-posterior and dorsal-ventral axes. The numbers below each egg chamber refer to the stage of oogenesis. fc, follicle cells; nc, nurse cells; oo, oocyte.

step was through the interior of the oocyte from the posterior to the anterior, and the second, turning and moving toward the nucleus to the dorso-anterior cap. Each of these steps was thought to be mechanistically distinct, perhaps occurring on distinct arrays of microtubules. The same injection techniques were used to show that the transport of *grk* from the nurse cells to the oocyte is microtubule-, BicD- and Dynein-dependent, and that *grk* RNA recruits the Dynein-associated proteins Egl and BicD in the nurse cells (Clark *et al.*, 2007).

Labelling of endogenous *grk* has shown that posteriorly localized *grk* during early oogenesis and anteriorly localized *grk* in mid-oogenesis is dynamic, and that when Dynein is compromised, motility is reduced and localization disrupted (Jaramillo *et al.*, 2008). The dependence of *grk* mRNA localization on Dynein and microtubules is also consistent with the visualization of multiple molecules of *grk* mRNA in electron dense 'transport particles' within stage 9 oocytes by electron microscopy that also contain Dynein and the Dynein motor cofactors Egl and BicD (Delanoue *et al.*, 2007). These particles are found near microtubules and not in proximity to membrane bound organelles, suggesting that *grk* transport particles are the motor cargo, and that they are not hitchhiking on another membranous cargo. A screen of a phage display ovarian cDNA library for binding to *grk* 3'UTR has also suggested that the Dynein light chain DDLC1 can bind gurken mRNA (Rom *et al.*, 2007), which would be consistent with direct transport of *grk* by Dynein. Dynamic behaviour of *grk* subsides as oogenesis progresses reflecting the conversion of transport particles to static sponge bodies, where Dynein acts as a stable anchor for *grk* mRNA at the dorso-anterior cap.

grk has been shown to be anchored in large (up to 2.5 μm in size) cytoplasmic structures visible using electron microscopy of oocyte sections (Delanoue *et al.*, 2007). These structures were previously described as 'sponge bodies' due to their sponge-like appearance using electron microscopy and were found to contain RNA and Exuperentia (Exu), a protein implicated in *bcd* localization (Wilsch-Bräuninger *et al.*, 1997). Sponge bodies are present throughout the oocyte and nurse cell cytoplasm (the majority of *grk* mRNA is concentrated in sponge bodies at the dorso-

anterior corner of the oocyte), and consist of strands of electron-dense material interdigitated with cytoplasm and ER-like cisternae, often flanked by microtubules. Dynein is present in these sponge bodies and inhibitory antibody injection/analysis of Dynein mutants showed that Dynein is required for the structural integrity of these structures (Delanoue *et al.*, 2007).

Trans-acting factors required for *grk* localization

Female sterile genetic screens have identified a number of *trans*-acting factors required for *grk* mRNA localization in the *Drosophila* oocyte. Whilst some *grk* mislocalization phenotypes appear to be a result of cytoskeletal defects, such as those seen in *cappuccino (capu)* and *spire* (Manseau and Schüpbach, 1989), others play a more direct role in the localization of *grk*, including *squid* (*sqd*) and *K10*. Mutations in *sqd* and *K10* have the opposite effect on dorso-ventral polarity than those in *grk* or *top*, in that a gain of function dorsalization phenotype is observed (Kelley, 1993; Neuman-Silberberg and Schüpbach, 1993; Serano *et al.*, 1995; Wieschaus *et al.*, 1978). In *sqd* and *K10* egg chambers *grk* mRNA is mislocalized to the anterior of the oocyte, failing to complete localization to the dorso-anterior corner. The mislocalized mRNA is also ectopically translated, which results in ectopic Grk signalling around the entire circumference of the oocyte. This in turn, results in dorsal and ventral follicle cells adopting a dorsal fate, leading to the production of dorsal appendage around the entire circumference of the oocyte. Indeed, the name *sqd* derives from the squid-like appearance of the eggs.

Sqd functions in *grk* mRNA localization, anchoring and translational repression

Sqd, also known as Hrp40 (Matunis *et al.*, 1994; Matunis *et al.*, 1992a; Matunis *et al.*, 1992b), encodes an hnRNP whose homologues include vertebrate hnRNP A1/A2 and hnRNP D. hnRNPs are a large family of RNA binding proteins that are involved in all steps of RNA processing, including transcriptional regulation, splicing, 3'-end processing, nucleocytoplasmic transport, localization, translation and stability. Sqd contains two RNP consensus RNA Binding Domains (RBDs) and an M9

nucleocytoplasmic shuttling motif (Dreyfuss, 2002; Krecic and Swanson, 1999; Matunis *et al.*, 1992b).

Consistent with a role in *grk* localization, immuno-electron microscopy techniques have shown that Sqd is present in *grk* transport particles with Dhc, Egl and BicD (Delanoue *et al.*, 2007). Injection of *grk* RNA can also leads to an enrichment of Sqd at the dorso-anterior corner, indicating that Sqd is recruited to the dorso-anterior corner through its association with *grk* mRNA. UV cross-linking experiments have also shown that Sqd and *grk* mRNA can interact directly. Sqd is also required for the static anchoring of *grk* mRNA at the dorso-anterior corner, and is present in sponge bodies (Delanoue *et al.*, 2007). The inhibition of Sqd following the full localization and anchoring of injected *grk* RNA leads to the conversion of sponge bodies to transport particles and in *sqd* mutants, mislocalized *grk* mRNA at the anterior of the oocyte is also found in transport particles rather than sponge bodies. This is consistent with the results of FRAP experiments with both injected *grk* RNA (Delanoue *et al.*, 2007) and labelled endogenous *grk* mRNA (Jaramillo *et al.*, 2008) that show that mislocalized anterior *grk* mRNA in *sqd* mutants is in continual flux rather than statically anchored. Together, these experiments indicate that Sqd has a role in maintaining the integrity of anchoring structures, and may play a role in promoting and facilitating the reorganization of transport particles into sponge bodies.

The *sqd* gene is alternatively spliced to produce three protein isoforms, A, B and S. These proteins are identical over the majority of the protein, including the RBDs, and differ at the C terminus. Sqd A uses an alternative 3' exon to give a unique C terminus, where B and S differ in a strong consensus M9 shuttling motif present in Sqd S. All three isoforms contain a glycine-rich domain at the C-terminus. When the separate functions of each isoform were studied by rescue experiments in a *sqd* mutant background that lacks expression of all three isoforms in the germline, (Matunis *et al.*, 1994), Sqd A and S were shown to act together in the localization and translational control of *grk* (Norvell *et al.*, 1999). Sqd S could rescue the pattern of *grk* and Grk localization, whilst Sqd A, although showing little rescue of mRNA

localization, did rescue localization of Grk protein. Sqd B could rescue neither. Interestingly, Sqd B and S accumulate in oocyte and nurse cell nuclei, whilst Sqd A is cytoplasmic. The model proposed for Sqd action involves the association of Sqd S with *grk* to facilitate cytoplasmic localization, whereas Sqd A associates to facilitate translational regulation. Consistent with this is a recent study using germline genetic mosaics to ask whether Sqd functions in the oocyte or in the nurse cells of the egg chamber to regulate *grk* mRNA. This study showed that *grk* is translationally repressed during localization, and that this repression depends upon the function of Sqd A in the nurse cells (Caceres and Nilson, 2009).

The translational regulators, PABP and Cup can interact with each other and with Sqd both biochemically and genetically, providing further evidence for the role of Sqd as a translational regulator (Clouse *et al.*, 2008). *PABP* and *cup* mutants lay ventralized and dorsalized eggs respectively. Both *grk* mRNA and Grk protein are inefficiently localized in *cup* mutants indicating that Cup is required for translational repression of unlocalized *grk* mRNA. *cup* mutants enhance the dorsalization phenotype of weak *sqd* alleles, supporting a model wherein Cup functions with Sqd to mediate translational repression of *grk* mRNA. *PABP* mutants enhance the ventralization phenotype seen for both *grk* null heterozygotes and *encore* (*enc*) mutant homozygotes (here, *grk* is mislocalized to the anterior, but in contrast to the situation in *sqd* mutants, remains translationally repressed, Hawkins *et al.*, 1997), suggesting that PABP and Encore function together to activate translation of *grk* mRNA, working antagonistically to Cup and Sqd. This is further supported by the interaction of the two proteins in ovarian extracts (Clouse *et al.*, 2008), and the colocalization of Enc protein with grk mRNA at the dorso-anterior of the oocyte (Van Buskirk *et al.*, 2000).

An *in vitro* interaction has also been observed between Sqd and the translational repressor Bruno (Norvell *et al.*, 1999) and Bruno has also been shown to bind Cup (Nakamura *et al.*, 2004). Bruno represses Grk translation and binds to the *grk* 3'UTR through Bruno Response Elements (BREs) (Filardo and Ephrussi, 2003). A number of other proteins are also thought to be involved in the translational regulation of *grk*,

and these include the RNA helicase Vasa (Johnstone and Lasko, 2004; Tinker *et al.*, 1998; Tomancak *et al.*, 1998), (shown to be able to bind Bruno; Webster *et al.*, 1997) and Orb (Chang *et al.*, 2001).

The role of K10 in *grk* mRNA localization is less clear. K10 encodes a nuclear protein with helix-loop-helix domains, and is therefore predicted to interact with DNA (Cheung *et al.*, 1992; Prost *et al.*, 1988; Serano *et al.*, 1995). Interestingly, Sqd accumulation in the oocyte nucleus is abolished in *K10* mutants (Norvell *et al.*, 1999), suggesting that the defect in *grk* localization in these mutants might be due to a defect in Sqd S distribution. K10 and Sqd can physically interact (Norvell *et al.*, 1999) and FRAP experiments with labelled endogenous *grk* mRNA in K10 mutants show that mislocalized anterior *grk* mRNA in K10 mutants is dynamic rather than stably anchored, as is the case for the *sqd* mutant (Jaramillo *et al.*, 2008). This suggests a model in which K10 and Sqd S form a complex that is required for *grk* mRNA localization and anchoring.

Hrb27C (also known as Hrp48), also a member of the hnRNP family, has also been to shown to interact with Sqd (Goodrich *et al.*, 2004). Like *sqd* mutants, *hrb27C* mutants lay dorsalized eggs, and Hrb27C can directly bind to the *grk* 3'UTR. Hrb27C also interacts with Ovarian tumour (Otu) in coimmunoprecipitation experiments (Goodrich *et al.*, 2004), and a missense allele of *otu* shows *grk* localization and dorsalization defects (Goodrich *et al.*, 2004). The mutation lies in the tudor domain of Otu, an element present in proteins with putative RNA binding abilities. Furthermore, Hrb27C interacts with the translational repressor Glorund (Glo) and the splicing factor Half-pint (Hfp) (Kalifa *et al.*, 2009). It has been suggested that these proteins form a distinct complex to the Sqd/Hrb27C/Otu complex that functions in *grk* mRNA localization by regulating the alternative splicing of *otu*.

Imp is associated with both Sqd and Hrb27C, is able to bind to the *grk* 5'UTR, 5'coding region and the 3'UTR and is concentrated at the dorso-anterior corner of the oocyte. *Imp* mutants show that Imp does not have an essential role in *grk* mRNA

localization, but are able to suppress the dorsalization defect of *K10* mutants (Geng and Macdonald, 2006). Overexpression of *Imp* results in dorsalization of the eggshell, suggesting that Imp does contribute to *grk* mRNA localization and translational regulation, but that this role may be redundant. Dorsalization of eggshells laid by *Imp* overexpressing females is due to the mislocalization of *grk* mRNA and protein at the anterior in stage 9, although this improves slightly as oogenesis progresses. Therefore excess Imp and loss of Sqd or Hrb27C have the same effects on the patterning of the eggshell and on *grk* mRNA. It was suggested that this could be due to competition, either at the level of RNA binding, or later in the localization process (perhaps in sponge body formation) between Sqd and Hrb27C, and Imp.

Similarities between *grk* and *osk trans*-acting factors

Many of the factors described above are also involved in *osk* mRNA localization and translational regulation. Sqd (Norvell *et al.*, 2005), Hrb27C (Huynh *et al.*, 2004; Yano *et al.*, 2004) and possibly Imp (Munro *et al.*, 2006) regulate the efficient localization and translational regulation of *osk* in a similar manner as observed for *grk*. Indeed, Hrb27C has been shown to be essential for the formation of *osk* transport particles (Zimyanin *et al.*, 2008). Otu and Glo are also required for the localization of *osk* (Kalifa *et al.*, 2009; Tirronen *et al.*, 1995). Orb is required for the translational activation of both *grk* and *osk* mRNAs (Chang *et al.*, 2001; Christerson and McKearin, 1994), whilst Vasa is required for the accumulation of *osk* mRNA in the oocyte and for the translational activation of localized *grk* mRNA (Styhler *et al.*, 1998; Tomancak *et al.*, 1998). UAP56 is another RNA helicase that is required for both *osk* and *grk* mRNA localization (Meignin and Davis, 2008).

Previous studies have also shown that Bruno is also able to bind BREs in the *osk* 3'UTR, and mutations in these BREs reduce Bruno binding and result in ectopic Osk accumulation in the oocyte (Castagnetti *et al.*, 2000; Kim-Ha *et al.*, 1995). Bruno mediates translational repression via two mechanisms (Chekulaeva *et al.*, 2006). The first is the cap-independent packaging of *osk* into large silencing particles containing

multiple *osk* mRNA molecules, described earlier. The second is through the interaction of Bruno with Cup (Nakamura *et al.*, 2004). Cup is a 4E-BP that interacts with several factors known or thought to be associated with *osk* localization and translation, including Me31B (Nakamura *et al.*, 2001; Nakamura *et al.*, 2004). *osk* mRNA is prematurely translated in *cup* mutants (Nakamura *et al.*, 2004; Wilhelm *et al.*, 2003). It has been proposed that Cup binds directly to the cap-binding protein eIF4E, and interferes with the association of eIF4E and eIF4G, preventing translation initiation. Mutant flies where the Cup interaction with eIF4E is disrupted have ectopic Osk synthesis (Grk translation defects were not seen in this study, but different alleles were used than in Clouse *et al.*, 2008, where defects in Grk translation were observed). Therefore, a model can be proposed whereby Cup, Bruno, Sqd, Hrb27C, Otu and other factors are required for localization and translational repression. In this model, once the RNA is localized, translation is activated by the action of Orb and PABP (Fig. 1.5).

Together, these results suggest that the localization and particularly translation of *osk* and *grk* mRNAs are regulated by the same core components. The mRNAs are transported by different motors to different destinations, and these differences may be reflected in the elaboration of the RNP particles for each RNA, for example by the addition of the EJC components and perhaps other unknown factors for *osk*, and by as yet unidentified components for *grk*.

The *grk* Localization Signal (GLS)

Efforts to map the region of the *grk* transcript required for its localization have used transgenic fusions between *lacZ* and part of the genomic region of *grk*, as well as truncations of the *grk* cDNA. These studies showed that signals in the 5'UTR, open reading frame and 3'UTR were required for complete localization to the dorso-anterior corner and translational regulation of the grk transcript (Saunders and Cohen, 1999; Thio *et al.*, 2000). Sequences in the 5′ noncoding region were shown by these methods to allow for accumulation of the transcript within the oocyte in early stage egg chambers, while signals in the coding region and the 3′UTR were

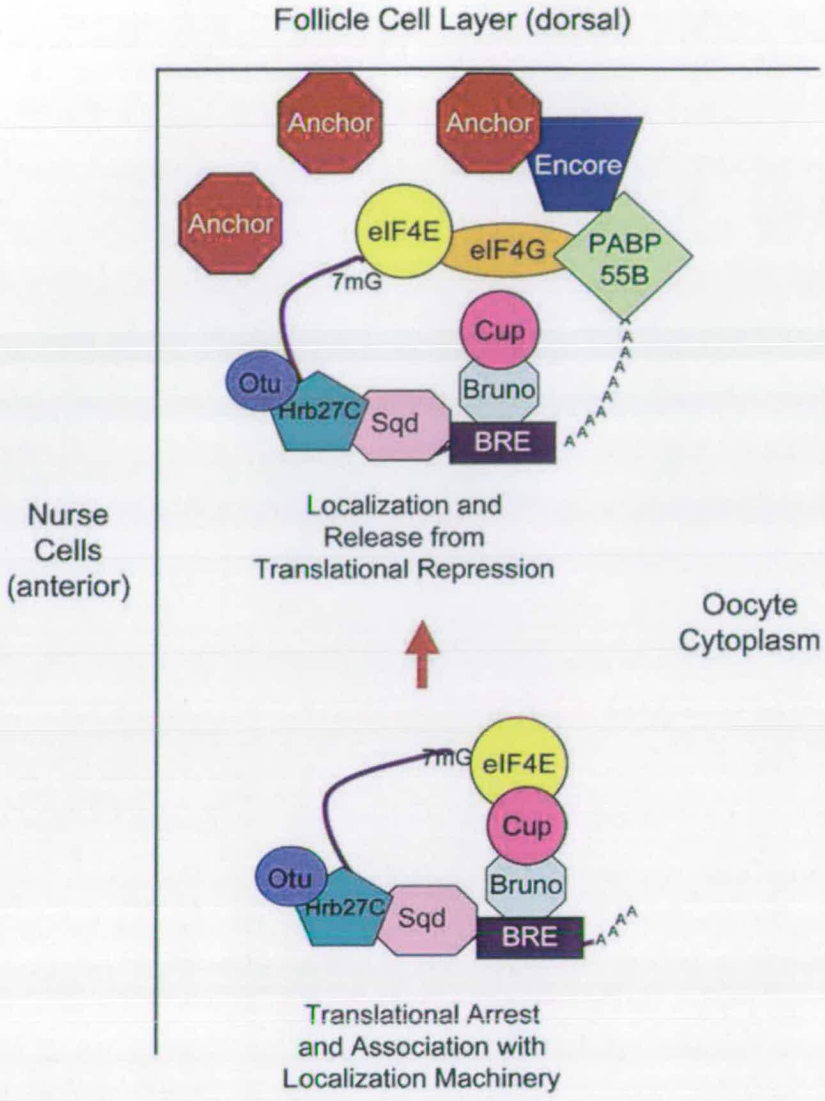

Figure 1.5 Model for the roles of Cup, Bruno, Sqd, Hrb27C, Otu, PABP and Enc in *grk* translational regulation (taken from Clouse *et al.*, 2008). During localization to the dorso-anterior corner, *grk* mRNA is translationally repressed by Cup, Bruno, Sqd, Hrb27C and Otu. PABP and Enc, and perhaps Orb act to mediate translational activation of *grk* once localization is complete. It is thought that the same factors are required for the translational repression of *osk* mRNA. Orb, and theoretically PABP are also required for translational activation of *osk*.

necessary for localization in mid to late stage egg chambers. More recent mapping of the *grk* localization signal by injection of fluorescently labelled portions of *grk* RNA into stage 8 or 9 oocytes revealed that a conserved 64-nucleotide RNA stem loop in the coding region is necessary and sufficient for localization of the transcript to the dorso-anterior corner (Van De Bor *et al.*, 2005). GLS RNA localizes in a Dynein and microtubule dependent manner, and moves in two steps as shown for full-length *grk*. Moreover, injected *grk* RNA lacking the GLS is not present in transport particles (Delanoue *et al.*, 2007). The GLS is discussed further in Chapter 3. Also included in this discussion is the localization element of the *I* Factor retrotransposon RNA.

The *I* Factor

The *I* Factor is a non-LTR retrotransposon, similar to the LINE1 (L1) elements of mammals (Fawcett *et al.*, 1986), that encodes two proteins, ORF1p and ORF2p. ORF1p is nucleic acid binding (Dawson *et al.*, 1997), whilst ORF2p contains domains with predicted endonuclease, reverse transcriptase and RNaseH activities (Fawcett *et al.*, 1986). *I* Factor transposition occurs at a high frequency in the germline of female progeny of a cross between 'inducer' males (contain full-length and potentially active *I* Factors in on their chromosomes) and 'reactive' females. Such female progeny are described as SF females (stérilité femelle), and manifest hybrid digenesis in that they have unusual characteristics, including greatly reduced fertility (Bucheton, 1990). Interestingly, the eggs laid by SF females have a ventralized phenotype, similar to *grk* mutants. Indeed, *I* Factor RNA has been detected in a cap adjacent to the oocyte nucleus at stages 8 and 9 and in an anterior ring (Seleme *et al.*, 2005), in a combination similar to *grk* and *bcd* mRNA localization. It is thought that as well as causing mislocalization of *grk* (thus leading to eggshell defects) (Van De Bor *et al.*, 2005), that perinuclear localization is important for the transposition process that is assumed to require entry of the RNA into the nucleus of the cell in which transposition takes place.

Using the *in vivo* injection assay, the signal for the localization to the cap was mapped to a 58-nucleotide RNA stem loop known as the *I* Factor localization signal,

or ILS (Van De Bor *et al.*, 2005). Secondary structure prediction using mfold (Zuker, 2003) predicts that the GLS and ILS have similar secondary structural elements and may represent a consensus structure for dorso-anterior localization (discussed further in Chapter 3). Furthermore, ILS RNA also localizes in two steps in a Dynein and microtubule dependent manner, and can compete with GLS and *grk* RNA for localization (Van De Bor *et al.*, 2005), suggesting that they can compete for *trans*-acting factors. Indeed, ILS RNA also remains at the anterior in *sqd* mutants, and fails to complete localization to the cap. Adjacent to the ILS is a second RNA stem-loop known as the A loop. RNA containing both the ILS and A loop moves more efficiently than RNA containing the ILS alone, but RNA containing the A loop alone is not sufficient for localization. The A loop is therefore not a localization signal but somehow promotes localization via the ILS (V. Van De Bor and E. Hartswood, unpublished data).

How is specificity defined?

With a number of localized mRNAs accumulating at different subcellular destinations, sometimes using the same molecular motor (both *bcd* and *grk* require Dynein for transport within the *Drosophila* oocyte), what determines which mRNA goes where? It is thought that specificity is determined by localization signals and the *trans*-acting factors that bind to these signals. A central question in the field is therefore how *cis*-acting sequences are interpreted by *trans*-acting factors, and how this recognition determines specific cellular destinations.

A simple view would be that transcripts that localize to a similar destination contain a conserved signal, and that the conserved localization signal defines a particular destination by binding to a particular complex of *trans*-acting factors. Such a model is supported by similarities in the perinuclear localization of *grk* and *I* Factor and between the GLS and ILS, which are hypothesized to represent a consensus signal for dorso-anterior cap localization. The composition of transport complexes that associate with different mRNAs may differ greatly when it is considered that the *Drosophila* genome encodes an estimated 500 RNA binding proteins (Lasko, 2000),

of which a number must be *trans*-acting factors for RNA localization during oogenesis. However, it has been shown already that *grk* and *osk* mRNAs require a number of common factors for localization and translational control, and Stau is required for the posterior targeting of *osk* and the anterior targeting of *bcd*. Furthermore, there is evidence that the same machinery, including Egl, BicD and Sqd, can drive localization of maternal RNAs, including *grk*, *bcd*, *nos*, *osk* and *K10* in the oocyte, as well as localization of apically localized transcripts in the embryo (Bullock and Ish-Horowicz, 2001; Lall *et al.*, 1999).

A more complex model than a specific RNA element binding a specific protein complex is therefore needed. A core complex of proteins may be able to recognize localized RNAs with different destinations. This is consistent with a motor complex containing Egl and BicD driving localization of maternal and apically localized transcripts in the embryo (Bullock and Ish-Horowicz, 2001). It is also consistent with the presence of many common factors required for *grk* and *osk* transport, and in maternal and neuronal RNA granules. It is then possible that distinct RNA binding proteins able to recognize different classes of localization element elaborate RNP complexes containing RNAs with different destinations. Alternatively, the same complex of proteins may have a different spatial organization on RNAs with different localization elements, although differences in the factors required for a number of localized mRNAs argue against this.

It has also been suggested that recruitment of different numbers of motors and regulatory proteins by different localization elements is important for specificity of destination. From studies in mammalian cells, it has been suggested that both RNAs containing a localization element and non-localized mRNAs can associate with motors and show directional movement (Fusco *et al.*, 2003). However, the presence of the localization element increased both the frequency and length of these directed movements. Similarly, in *Drosophila* embryos, *cis*-acting elements in apically localized mRNAs (with bidirectional motility as a result of Dynein activity) stimulate the frequency and duration of minus end directed movements. The duration of plus end movements was not altered by localization signals, suggesting that

localization elements do not simply regulate the rate of dissociation of transcripts from motors. Rather, in this case, the extent of minus end directed movement was correlated with the ability of the localization element to recruit Egl, BicD and Dynein. It has therefore been suggested that RNA localization elements bias directional movement by controlling the number of motor molecules incorporated into a transport RNP via the differential recruitment of the motor cofactors Egl and BicD, and producing a range of transcript distributions (Bullock *et al.*, 2006). In addition to *trans*-acting factors controlling the relative number of different motors within a transport complex, it is also possible that such factors can control the conformation or processivity of the motor, for example, it has been suggested that Stau is required for full Kinesin-1 activity in *osk* mRNA localization (Zimyanin *et al.*, 2008).

mRNAs that are localized to specific destinations may also be trafficked along specific cytoskeletal tracks within the cell. It has been suggested that *grk* mRNA moves to the dorso-anterior in two Dynein-dependent steps, and that each step requires a different population of microtubules (MacDougall *et al.*, 2003). It is also thought that *Vg1* mRNA is transported by Kinesin-1 and -2 to the vegetal pole of Xenopus oocytes on a subset of microtubules where the plus ends are oriented toward the vegetal pole (Messitt *et al.*, 2008). It is also possible that specific microtubule tracks are marked by specific post-translational modifications. The Kinesin-1 family member Kif5c preferentially binds to and trafficks on detyrosinated microtubules in live cells (Dunn *et al.*, 2008), whilst neurites enriched in acetylated microtubules selectively support Kinesin-mediated transport of the JNK regulator JIP-1 to axonal growth cones (Reed *et al.*, 2006).

Aims of this thesis

Given the central role of localization elements and *trans*-acting factors in the definition of specificity, the work in this thesis aims to define these in greater detail for *grk* mRNA localization. This moves towards a better understanding of the molecular mechanism underlying *grk* mRNA localization during *Drosophila* oogenesis, and also ultimately aims to answer more general questions regarding consensus localization elements and the arrangement of *trans*-acting factors on a localized RNA, and therefore specificity.

- **Chapter 3** Are the GLS and ILS consensus elements for dorso-anterior cap localization? Secondary structure prediction has shown that the GLS and ILS contain similar secondary structural elements. However, the structure and shape of folded RNA molecules is determined also by tertiary interactions that give rise to the biologically functional form of the RNA molecule. Knowledge of the tertiary structure of GLS and ILS RNA is therefore important for any study of the critical determinants of GLS and ILS activity. To this end, in collaboration with Dr Peter Lukavsky at the Laboratory of Molecular Biology, Cambridge, GLS and ILS RNA samples have been made for the assignment of high-resolution solution structures by nuclear magnetic resonance (NMR) spectroscopy. Graeme Ball, a post-doctoral researcher in the Davis lab, is assigning the RNA structures.

- **Chapter 4** What factors can bind to the GLS? GRNA affinity chromatography (Czaplinski *et al.*, 2005) has been used to purify the RNP that can form on RNA containing the GLS.

- **Chapters 5 and 6** Characterization of the roles of GRNA-identified proteins in *grk* mRNA localization. Two proteins, Hephaestus (chapter 5) and CG17838 (chapter 6) were identified as being able to specifically associate with GLS-containing RNA in affinity chromatography. Orthologues of both of these proteins have been implicated in the regulation of localized mRNAs in other organisms, and so the functions of these proteins in *Drosphila* oogenesis were

studied further. These studies suggest roles for Hephaestus and CG17838 in both *grk* and *osk* RNA localization, and also indicate that the roles of these proteins in mRNA localization may be conserved between different tissues (neurons and oocytes) and also across different organisms.

MATERIALS AND METHODS

Molecular Biology

Solutions and reagents

All solutions and buffers used were prepared as described in 'Molecular Cloning-A Laboratory Manual' (Sambrook *et al.*, 1989), unless otherwise stated. Phosphate buffered saline (PBS), Tris-EDTA (TE), Tris-acetate-EDTA (TAE), and Luria Betani (LB) media, were prepared and autoclaved by the Swann Building (University of Edinburgh) or Department of Biochemistry (University of Oxford) media kitchens. The media kitchens also prepared LB-agar plates. The composition of these buffers is given below:

Buffer	**Composition**
10 x PBS, pH 7.4	1.37 M NaCl, 27 mM KCl, 100 mM Na_2HPO_4, 20 mM KH_2PO_4
10 x TAE	0.4 M Tris base, 10 mM EDTA (pH 8.0), 1.2% (v/v) glacial acetic acid
TE	10 mM Tris-HCl (pH 7.5), 1 mM EDTA (pH 8.0)
LB	For 1 litre: 10 g Bacto tryptone (Difco), 5 g Bacto yeast extract, 5 g NaCl
LB-Agar	For 1 litre: 16 g Bacto tryptone (Difco), 10 g Bacto yeast extract, 5 g NaCl

Bacterial Strains

Routine Cloning

XL-1 Blue Competent Cells (Stratagene)

E. coli recA1 endA1 gyrA96 thi-1 hsdR17 supE44 relA1 lac [F' *proAB lacI*^{q}*ZΔM15* Tn*10* (Tet^{r})]

Protein Expression

BL21 Competent Cells (Stratagene)

E. coli B F^{-} *dcm ompT hsdS*(r_B^- m_B^-) *gal*

BL21-CodonPlus (DE3)-RIL (Stratagene)

E. coli B F^{-} *ompT hsdS*(r_B^- m_B^-) *dcm*$^{+}$ Tet^{r} *gal* λ(DE3) *endA metA::Tn5*(kan^{r}) Hte [*argU ileY leuW* Cam^{r}]

Propagation and preparation of plasmid DNA

For standard cloning and amplification, XL-1 Blue cells were transformed with plasmids using heat-shock. 100 µl cells were incubated with 1-50 ng of plasmid DNA or 20% of a ligation reaction for 30 min on ice. The cells were then heat-shocked at 42°C for 45 s. After a further 2 min on ice, 900 µl LB media was added and the cells allowed to recover for 1 h at 37°C. Cells were plated onto LB-agar plates containing the appropriate antibiotic for plasmid selection (100 µg/ml ampicillin and kanamycin; 50 µg/ml chloramphenicol) and grown overnight at 37°C. A single transformed colony was then chosen and grown in 5 ml LB containing the appropriate antibiotic for 12-16 h at 37°C. Depending on the downstream application and the amount of plasmid required the plasmid was then either isolated using the QIAprep Spin Miniprep Kit (Qiagen), or grown further and isolated using the QIAfilter Plasmid Midi or Maxi Kit (Qiagen). All kits were used according to the manufacturer's protocol.

DNA sequencing

Sequencing reactions were carried out in a final volume of 10 µl. Template DNA was added to 4 µl Big Dye Terminator v3.1 Cycle Sequencing Kit (Applied Biosystems) and 1.6 pmols of sequencing primer. The amounts of template DNA used were 50-100 ng for PCR products and 200-300 ng for plasmid DNA. The cycling programme for the sequencing reaction consisted of 25 cycles of: 30s, 96°C; 30 s, 50°C and 4 min, 60°C. The sequencing reactions were then analysed by the School of Biological Sciences Sequencing Service (SBSSS), University of Edinburgh (now known as The Gene Pool) or Geneservice, University of Oxford.

PCR

Standard PCR

Standard PCR reactions were performed in 50 µl using 50-100 ng template DNA, 1 x PCR buffer containing 15 mM $MgCl_2$ (Roche), 0.2 mM each dNTP (Roche), 0.3 µM each primer (forward and reverse), 2.5 U Taq DNA polymerase (Roche). The standard cycling programme consisted of 5 min, 94 °C, followed by 30 cycles of 20 s, 94 °C; 30 s, annealing 45-65°C (dependent on the T_m of the primers used) and elongation 30 s-2 min (dependent on the length of PCR product), 72°C. After a final 7 min extension at 72°C, reactions were held indefinitely at 4°C. Products were verified by agarose gel electrophoresis and if required, gel purified using the QIAquick gel extraction kit (Qiagen).

PCR to generate DNA templates for NMR RNA

DNA templates for the synthesis of RNA for NMR were constructed by PCR using overlapping primers (Appendix A.2.1). The template was constructed in a 50 µl reaction containing 0.2 mM each dNTP, 20 pmoles each primer, 2.6 U Expand High-Fidelity Taq Enzyme Mix (Roche) in the supplied buffer containing 15 mM $MgCl_2$. Annealing and extension of the overlapping primers was carried out with one cycle

of 5 min, 95 °C; 1 min, 65°C and 10 min, 72°C. The resulting double-stranded template was then amplified in a 100 µl PCR reaction containing 50 µl extension reaction, 100 pmoles each amplification primer (Appendix A.2.1), 0.2 mM each dNTP, 5.2 U Expand High-Fidelity Taq Enzyme Mix (Roche) in the supplied buffer containing 15 mM $MgCl_2$. The cycling programme consisted of 30 cycles of 1 min, 95°C; 1 min, 50°C and 45 s, 72°C. After a final 10 min extension at 72°C, reactions were held indefinitely at 4°C. The smaller templates for NMR RNA were purified on 10% TBE-acrylamide gels (Bio-Rad), and crushing and eluting the DNA bands into TE buffer.

Reverse transcriptase (RT)-PCR

Total RNA, or immunoprecipitated RNA (see RNA Immunoprecipitation) was used as a template for reverse transcription. RT was carried out using the Superscript III First-Strand Synthesis Supermix (Invitrogen) as described in the manufacturer's protocol. Either oligo$(dT)_{20}$ or random hexamers were used as primers for the RT reaction depending on the experiment. For cloning of CG17838-F, total RNA was reverse transcribed from oligo$(dT)_{20}$ primers, whilst for RNA immunoprecipitation experiments, random hexamers were used. Typically 10% of the RT reaction was then amplified by PCR as described above.

Gel electrophoresis

TAE-agarose gel electrophoresis

Samples were mixed with 1 x gel loading buffer (Bioline) and loaded onto 1% (unless otherwise stated) agarose gels (1 g agarose (agarose MP, Roche), 100 ml 1 x TAE) containing 0.5 µg/ml ethidium bromide. Electrophoresis was carried out in 1 x TAE running buffer at a constant voltage of 120 V, and nucleic acids were visualized using a UV transilluminator.

SDS-polyacrylamide gel electrophoresis (SDS-PAGE)

Recipes for stacking and resolving gels of a given percentage can be found in 'Molecular Cloning-A Laboratory Manual' (Sambrook *et al.*, 1989). NuPAGE Novex 4-12% Bis-Tris gels (Invitrogen) were also used. Briefly, samples were heated to 90°C in 2 x protein sample buffer (with reducing agent added prior to use) (Invitrogen) and loaded alongside a pre-stained standard (SeeBlue Plus2, Invitrogen) for gels to be used in western blotting or coomassie stained, or an unstained standard (Mark12, Invitrogen) for gels to be silver stained. Electrophoresis was carried out in Tris-glycine running buffer (25 mM Tris, 250 mM glycine, 0.1% SDS, to pH 8.3) or in 1 x NuPAGE MOPS electrophoresis buffer (Invitrogen) for pre-cast gels, at a constant voltage of 180 V-200 V. Separated proteins were visualized by staining in Coomassie Blue solution (0.5% Coomassie Blue R-250, 45% MeOH, 10% glacial acetic acid), followed by soaking in destain (45% MeOH, 10% glacial acetic acid), or by silver staining (SilverQuest kit, Invitrogen).

Antibodies

Antibodies and dilutions used for western blotting, immunofluorescence and immunoprecipitation are described in appendix A.1. All anti-peptide antibodies produced in this work were polyclonal antibodies raised and affinity purified by Eurogentec, using the 'Double X strategy'. The Double X Strategy involves the design of two peptides from the same antigen and immunising the animal hosts with both peptides at the same time.

anti-Hrb27C antibody production

Polyclonal antibodies were raised against Hrb27C by immunising rabbits with two peptides; 1: N-CRTGPGNSASKSGSEY-C and 2: N-EGASNYGAGPRSAYGNC-C, which correspond to nonconserved regions in the C-terminal Glycine-rich domain (Huynh *et al.*, 2004).

anti-CG17838 antibody production

Rabbits were immunised with two peptides; 1: N- QKADDRGDGERTEDYC-C and 2: N-TGQRKYGGPPPHWEGC-C, which correspond to a nonconserved and a partially conserved region in the N-terminus respectively.

The final bleeds taken from rabbits immunised with these two peptides were also affinity purified in lab. Filtered antiserum was incubated with CNBr-activated sepharose resin (GE Healthcare Life Sciences) that had been coupled to 5 mg of either peptide or to 5 mg GST-CG17838-F. The resin was washed with PBST (1x PBS + 0.05% Tween20) and anibodies eluted with 100 mM glycine (pH 2.5) into 2 M Tris-HCl pH 8.0.

Polyclonal anti-protein CG17838 antibodies were also raised by immunising guinea pigs with GST-CG17838-F that had been expressed in *E. coli* and purified using glutathione sepharose (GE Healthcare Life Sciences). As for the anti-peptide antibodies, the anti-protein antibodies were raised and affinity purified by Eurogentec and in lab.

Western Blotting

Following electrophoresis, proteins were transferred to nitrocellulose (Schleicher and Schuell), or to Polyvinylidene Fluoride (PVDF) (Bio-Rad) membranes using the XCell II Blot Module (Invitrogen) as per manufacturer's instructions. The membrane was blocked with 5% non-fat dry milk in 1 x TBS (50 mM Tris-HCl pH 7.5, 150 mM NaCl) + 0.5% Tween20 (TBST). Primary and secondary antibodies and dilutions are described in appendix A.1. The membrane was washed with TBST following incubation with primary and secondary antibodies. Chemiluminescent detection was carried out according to the manufacturer's protocol (ECL Plus Western Blotting Detection System, GE Healthcare Life Sciences) and the membrane exposed to film (Hyperfilm ECL, GE Healthcare Life Sciences). When required, membranes were stripped by incubation in stripping buffer (100 mM 2-

mercaptoethanol, 2% SDS, 62.5 mM Tris-HCl pH 6.7) for 30 min at 50°C, with occasional agitation. Membranes were then washed extensively at room temperature with TBST before blocking and re-probing.

In vitro transcription, labelling and purification of RNA

Preparation of templates for *in vitro* transcription

For standard transcription, 5-10 µg plasmid DNA was digested using the appropriate restriction enzyme (New England Biolabs) according to manufacturer's instructions. Digests were visualized by TAE-agarose electrophoresis and purified using the QIAquick PCR purification kit (Qiagen), or by phenol/chloroform extraction.

For transcription of NMR samples, the purified PCR DNA templates were digested with *Hind*III-*Eco*RI and inserted into pUC18 digested with the same enzymes. Following transformation and sequencing, a 2.5 L culture of cells was grown overnight at 37°C. Plasmid DNA was then isolated using the QIAfilter plasmid Giga Kit (Qiagen) and resuspended in HPLC-grade water to a concentration of 700 µg/ml. A typical yield from a 2.5 L culture was in the range of 6-12 mg. Plasmid was linearized with *Bbs*I (New England Biolabs) overnight at 37°C using 50 units (50 U) of enzyme per 700 µg plasmid DNA. The reaction mixture containing only fully linearised plasmid was used directly for the RNA transcription reaction without removal of the restriction enzyme.

Synthesis of fluorescently labelled RNAs

Fluorescently labelled and capped sense RNAs for injection into living oocytes were *in vitro* transcribed in 50 µl reactions. 1-2 µg linearized template DNA (*gurken* cDNA was a gift from T. Schüpbach) was added to 1 x transcription buffer (40 mM Tris-HCl, pH 8.0, 6 mM $MgCl_2$, 10 mM DTT and 2 mM spermidine) (Roche), 0.4 mM rATP, 0.4 mM rCTP, 0.36 mM UTP (Roche), 0.04 mM AlexaFluor 546- or 488-UTP (Molecular Probes), 0.12 mM rGTP, 0.3 mM 7mG(5')ppp(5')G cap analogue

(Ambion), 40 U RNasin RNase inhibitor (Promega) and 20 U T7, T3 or SP6 RNA polymerase (Roche), according to the promoter present in the template. The transcription reaction was incubated for 3 h at 37°C, after which the template DNA was digested with 2 U RQ1 RNase-free DNase (Promega) for 15 min at 37°C. Unincorporated nucleotides were removed using Sephadex G-50 RNA spin columns (Roche) according to the manufacturer's instructions. RNA was then precipitated by the addition of 1/5 volume 5 M NH_4OAc pH 5.2 and 2.5 volumes 100% EtOH. Following incubation at -20°C overnight/on dry ice for 1 h, the RNA was pelleted by centrifugation at 14000 rpm for 20 min at 4°C. The pellet was washed with 75% EtOH and resuspended in 5-10 µl DEPC-treated water depending on the size of the pellet. Final RNA concentration was typically 250-500 ng/µl.

Synthesis of DIG-labelled RNAs

Sense and anti-sense RNA probes were synthesised for RNA *in situ* hybridization in 10 µl reactions. 1 µg linearized template DNA (*gurken* cDNA was a gift from T. Schüpbach, *oskar* cDNA was a gift from A. Ephrussi and *hephaestus* cDNA was obtained from the DGC cDNA collection) was added to 1 x transcription buffer (Roche), 1 x DIG labelling mix and 20 U T7, T3 or SP6 RNA polymerase (Roche). The DIG RNA labelling mix (Roche; 10 x) contains 10 mM ATP, 10 mM CTP, 10 mM GTP, 6.5 mM UTP and 3.5 mM DIG-11-UTP, pH 7.5. The transcription reaction was incubated for 2 h at 37°C, after which template DNA was digested with 2 U RQ1 RNase-free DNase (Promega) for 7 min at 37°C. The RNA was visualized by TAE-agarose gel electrophoresis and used without any further purification for *in situ* hybridization. RNA probes were diluted in hybridisation buffer (50% formamide, 5xSSC, 0.1% Tween20, adjusted to pH 6.5 with HCl) at 1/500-1/1000 depending on the efficiency of the transcription reaction.

Synthesis of ^{32}P-labelled RNAs

^{32}P-RNA probes were prepared for use in UV cross-linking and EMSA reactions in a final volume of 20 µl. ORF16 and ORF16ΔGLS in p6xE2 (see GRNA chromatography) were linearized with *Spe*I, whilst hunchback (hb) and nanos (nos) templates were created by PCR from hb cDNA (a gift from B. Edgar) and nos cDNA (DGC *Drosophila* Gold Collection) (for primers see appendix A.2.5). 2 µg linearized template or 200 ng PCR DNA was added to a reaction mix consisting of 1 x transcription buffer (Roche), 5 mM rATP, 5 mM rCTP, 5 mM GTP, 0.5 mM UTP (Roche), 4.5 µl 800 Ci/mmol α-^{32}P-UTP (Perkin Elmer), 40 U RNasin RNase inhibitor (Promega), and 20 U T7, T3 or SP6 RNA polymerase. The reaction was incubated for 3 h at 37°C, after which template DNA was digested with RNase-free DNaseI (Promega). 1 µl of the reaction was taken prior to purification for calculation of ^{32}P incorporation.

Probes were gel purified using denaturing urea-PAGE. Briefly, probes were incubated for 3-5 min at 95°C in denaturing gel buffer (95% formamide, 0.025% xylene cyanol, 0.025% bromophenol blue, 0.5 mM EDTA and 0.025% SDS) in order to denature any secondary structure. The probes were then loaded onto a denaturing 5% acrylamide/8 M urea polyacrylamide gel which was ran until the bromophenol blue dye front reached the bottom of the gel. Following exposure to autoradiography film (BioMax MS; Kodak), the full-length probe was excised and eluted in gel elution buffer (0.5 M NH_4OAc, 1 mM EDTA and 0.1% SDS) overnight at 37°C. The probe was then concentrated using EtOH precipitation as described above and resuspended in 20 µl DEPC-treated water. Yield and specific activity was determined by measuring the Cerenkov radiation of pre- and post-purification samples in a Beckman LS3801 scintillation counter.

Preparation of RNA for NMR

Expression of T7 RNA polymerase for *in vitro* transcription

pT7-911 (a gift from J. Houseley) contains the sequence for bacteriophage T7 RNA polymerase with a N-terminal His_6 affinity tag. BL21 Competent Cells (Stratagene) were transformed with plasmid pT7-911 using standard procedures and transformants isolated by ampicillin selection. A 50 ml culture of cells was diluted in 1 L LB, grown at 30°C to an $O.D._{600}$ 0.6, and induced with 1 mM IPTG for 3 h. Cells were harvested by centrifugation at 6000 g for 20 min at 4°C. Cell pellets were resuspended in 25 ml lysis buffer (20 mM Tris pH 8.0, 200 mM NaCl, 1 mM imidazole, 10% glycerol, 0.1% Tween 20 and Complete EDTA-free protease inhibitor (Roche)). Cells were lysed by sonication and the lysate clarified by centrifugation at 26 000 g for 20 min at 4°C. Cleared lysate was bound to 5 ml packed volume Ni-NTA-agarose resin (Qiagen) that had previously been equilibriated with lysis buffer, and incubated with rocking at 4°C for 2 h. The resin was then washed with 16 column volumes lysis buffer, followed by 8 column volumes lysis buffer containing 10 mM imidazole. Elution was in lysis buffer containing 100 mM imidazole.

His_6-T7 containing fractions were diluted with dilution buffer (20 mM Tris pH 8.0, 10% glycerol, 0.1% Tween 20 and Complete EDTA-free protease inhibitor (Roche)), in order to reduce total salt concentration in the sample from 200 mM to 50 mM. Protein was then added to 10 ml packed volume SP sepharose (Sigma), previously equilibriated in the above dilution buffer containing 50 mM NaCl and loaded onto a column. The resin was washed with 16 column volumes dilution buffer containing 50 mM NaCl, followed by 8 column volumes dilution buffer containing 100 mM NaCl and a further 8 column volumes with dilution buffer containing 200 mM NaCl. Elution was in dilution buffer containing 500 mM NaCl. Protein concentration was determined using Bradford reagent and protein concentrated to 5 mg/ml in YM-30 Centriprep units. Glycerol was added to 50% and DTT added to 20 mM.

In vitro transcription of RNA for NMR

All procedures used HPLC-grade water and chemicals purchased from Sigma. The RNA yield from *in vitro* transcriptions was optimised for each individual DNA template in 25 µl trial reactions by varying the magnesium concentration from 4-52 mM. To prepare milligram quantities of RNA a large-scale 20 ml transcription reaction was performed (Lukavsky and Puglisi, 2004). The reaction mixture contained 6-12 mg linearized template DNA, 40 mM Tris-HCl pH 8.1, 1 mM spermidine (Sigma), 5mM DTT, 0.1% Triton-X 100, 4 mM each NTP (Sigma), 12-24 mM magnesium chloride and 1200 U/ml lab-prepared T7 RNA polymerase. After 1 h incubation at 37 °C, pyrophospate, which forms during the transcription reaction and can sequester Mg^{2+}, was pelleted by centrifugation. Additional magnesium chloride was then added, the amount depending on the size of the pyrophosphate pellet. The reaction was stopped after a further 1 h at 37°C by addition of EDTA to 50 mM. Transcribed RNAs were analysed by denaturing PAGE (8% and 8 M urea) and visualized by staining with 0.1% toluidine blue.

Ion-exchange chromatographic purification and concentration of *in vitro* transcribed RNA for NMR

A 15 ml HiTrap DEAE column (GE Healthcare Life Sciences) was equilibriated with five column volumes of 50 mM sodium phosphate buffer at pH 6.5 with 0.1 mM EDTA. The transcription reaction mixture was loaded onto the equilibriated DEAE column. Following elution with a gradient of 2 M NaCl, collecting 10 ml fractions, fractions were analysed by denaturing PAGE. RNA containing fractions were combined and concentrated to 1 ml in Centriprep centrifugal units (Amicon), washed five times with NMR buffer (10 mM sodium phosphate pH 6.0) and concentrated again to 1 ml. The final concentration step to the desired NMR concentration (1-2 mM) was performed in a 2 ml Centricon centrifugal unit (Amicon). As a general rule, for RNA oligonucleotides less than 30 nucleotides in length a MWCO of 3 kDa was used, whilst for larger constructs the MWCO was 10 kDa.

Biochemistry

GRNA Affinity Chromatography

Expression of GλH for GRNA affinity chromatography

pGλH (a gift from K. Czaplinski) contains the λ N protein RNA-binding peptide sequence (DAQTRRRERRAEKQAQWKAAN) cloned downstream of an N-terminal GST tag with a His_6 tag at the C-teminus. BL21-CodonPlus (DE3)-RIL (Stratagene) cells were used as expression required rare tRNAs. A 5 ml culture of cells transformed with pGλH was diluted into 2 L LB, grown at 30°C to an $O.D._{600}$ 0.4, and induced with 1 mM IPTG for 2 h. Cells were harvested by centrifugation at 6000 g for 20 min at 4°C. Cell pellets were resuspended in 15 ml lysis buffer (50 mM Tris pH 8.0, 500 mM NaCl, 5% glycerol and Complete EDTA-free protease inhibitor (Roche)) also containing 0.1% Triton-X 100 and 1 mM DTT. Cells were sonicated and the lysate clarified by centrifugation at 26 000 g for 20 min at 4°C. The lysate was added to 4 ml packed glutathione sepharose (GE Healthcare Life Sciences) equilibriated in lysis buffer and rotated at 4°C for 1 h. The glutathione sepharose was then washed with 15 column volumes lysis buffer containing 0.001% Triton X-100 and 1 mM DTT. Elution was in wash buffer containing 20 mM glutathione and the eluate was dialysed against lysis buffer to which Triton-X 100 was added to 0.001%. Protein concentration was determined using Bradford reagent. The protein sample was diluted to 1 mg/ml, made to 20 mM imidazole, and added to 2 ml Ni-NTA resin equilibriated in lysis buffer containing 0.001% Triton-X 100 and 20 mM imidazole. After rotating at 4°C for 1 h, the resin was washed with 10 column volumes of lysis buffer with 30 mM imidazole and eluted with lysis buffer containing 250 mM imidazole. Protein was dialysed against 50 mM Tris pH 8.0, 250 mM NaCl, 20% glycerol and 0.5 mM DTT. Protein concentration was determined using Bradford reagent and protein concentrated to 2.6 mg/ml using YM-10 Centriprep units (Amicon).

Preparation of RNA for GRNA chromatography

p6xE2 (a gift from K. Czaplinski) contains two tandem copies of the BoxB hairpin cloned downstream of six tandem copies of the Vg1 localisation element E2 motif which lie between *Hind*III and *Spe*I sites. ORF16, ORF16ΔGLS, Loc+ (contains the A loop and the ILS), Loc+ΔILS (contains the A loop and not the ILS) and ILS_{mut} sequences contained in pGEM-T were gifts from V. Van De Bor and E. Hartswood. ORF16, ORF16ΔGLS, A+ILS, A and ILS_{mut} sequences were amplified by PCR from the above plasmids using primers (Appendix A.2.2) that incorporated a *Hind*III site at the 5', and a *Spe*I site at the 3' end of the product, and sub-cloned into p6xE2 from which the E2 motifs had been digested. The resulting plasmids therefore contain the indicated sequence upstream of the BoxB hairpin. All plasmids were verified by sequencing. p6xE2 plasmids containing GLS and hb sequences were gifts from V. Van De Bor. Commercial large-scale T3 transcription kits (T3 Megascript Kit; Ambion) were used to transcribe RNA used in GRNA chromatography. RNA quality was determined by measuring $O.D._{260}$ and agarose gel electrophoresis.

Preparation of ovarian lysate for GRNA

Lysate was prepared as described in *Drosophila* protocols. Ovaries from 100 flies homogenized in 200 µl cold lysis buffer typically gave extracts of 10 mg/ml. Lysates were pre-cleared through an equivalent packed volume of glutathione sepharose equilibriated in GRNA buffer (50 mM Tris-HCl pH 7.5, 50 mM NaCl, 1.5 mM $MgSO_4$, 2 mM DTT, 0.05% NP-40, 10% glycerol and Complete EDTA-free protease inhibitor (Roche)).

Preparation of the RNA matrix for GRNA chromatography

The buffer used throughout is GRNA buffer. 50 µl of 1:1 glutathione sepharose resin in buffer was added to 26 µg of GλH protein and 200 pmol of the indicated RNA in a total volume of 400 µl. The RNA had previously been heated and snap-cooled. Resin, GλH protein and RNA were incubated at 4°C with shaking for 1 h. The

glutathione sepharose beads were collected by centrifugation (always 3000 rpm, 1 min) and the supernatant removed. RNA remaining in the supernatant was extracted by the addition of an equal volume of phenol/chloroform and EtOH precipitation. The quantity and quality of RNA in the supernatant was assessed by measurement of absorbance at 260 nm and by TAE-agarose gel electrophoresis.

Isolation of RNA binding proteins using GRNA chromatography

300 µl buffer and 200 µl pre-cleared ovary extract (containing approximately 2 mg protein), plus 0.1 mg/ml *E.coli* tRNA and 1 µg/ml heparin, were added to the RNA matrix and the mixture incubated at 4°C with shaking for 1 h. Beads were collected and washed end over end 3 times for 2.5 min with 500 µl buffer. After washing the supernatant was removed and total material eluted with 100 µl elution buffer (0.1% SDS, 2.5 mM Tris pH 6.8 and 5 mM DTT) at room temperature. Eluates were concentrated by TCA precipitation and analysed by SDS-PAGE and silver staining.

Mass Spectrometry

Eluates were separated by SDS-PAGE so that the GλH could be resolved and cut away from all other proteins. The remaining eluate was ran as short a distance as possible into the gel so that each lane could be excised in a minimum number of fractions. Processing of the gel, trypsin digestion, mass spectrometry and data analysis was carried out by Dr Juri Rappsilber, Wellcome Trust Centre for Cell Biology, University of Edinburgh.

Recombinant protein purification

GST-Sqd A, -Sqd S, -Sqd B, -GFP and GST

GST-Sqd A, GST-Sqd S and GST-Sqd B were expressed using plasmids (gifts from T. Schüpbach) that contain the full-length cDNAs cloned into pGex3. GST protein was expressed using pGex3, whilst GST-GFP was obtained from I. Stancheva. BL21 Competent Cells (Stratagene) were transformed with each plasmid, and protein expressed and purified as described for the GST-tag of GλH. Protein was dialysed against 50 mM Tris pH 8.0, 250 mM NaCl, 20% glycerol and 0.5 mM DTT, and concentration was determined using Bradford reagent.

GST-CG17838-F

To generate a GST fusion protein of CG17838-F, RT-PCR was performed on mRNA purified from ovaries taken from 50 Oregon-R females. The coding region was amplified using primers (Appendix A.2.3) that incorporated a *Bam*HI site at the 5', and an *Eco*RI site at the 3' end of the product, and sub-cloned into pGex3 that had been digested with the same enzymes. The resulting protein contained an N-terminal GST-tag. A 5 ml culture of BL21 Competent Cells transformed with plasmid was diluted into 2 L LB, grown at 30°C to an $O.D._{600}$ of 0.4, and induced with 0.1 mM IPTG for 2 h at 30°C. Cells were harvested by centrifugation at 6000 g for 20 min at 4°C. Cell pellets were resuspended in15 ml lysis buffer (50 mM Tris pH 8.0, 500 mM NaCl, 5% glycerol, Complete EDTA-free protease inhibitor (Roche) and pepstatin A (1.0 μg/ml; Sigma)) also containing 0.1% Triton-X 100 and 1 mM DTT. Protein was then purified as described for the GST-tagged proteins described above, the only differences being the use of double the volume of wash buffer and half the volume of glutathione sepharose resin.

GST-pulldown assay

^{35}S-labelled (Perkin Elmer) proteins were made using the TnT Quick Coupled Transcription/Translation System (Promega). CG17838-F template was prepared by PCR from the CG17838-F cDNA using a forward primer that contains the T7 promoter and Kozak sequence (Appendix A.2.3). Squid template was taken from the DGC *Drosophila* Gold Collection. Lysate containing labelled proteins was pre-cleared by incubation with equivalent packed volume of glutathione sepharose equilibriated in binding buffer (Tris-HCl pH 7.5, 150 mM NaCl, 0.05% NP-40, 5% glycerol and Complete EDTA-free protease inhibitor (Roche)). 50 µl 1:1 glutathione sepharose resin in buffer was incubated with 2 µg GST fusion protein in a total volume of 200 µl for 1 h at 4°C. The GST fusion protein-bound beads were collected by centrifugation and the supernatant removed. 25 µl pre-cleared lysate was added to the resin in 450 µl binding buffer. After incubation for 1 h at room temperature, the resin was washed four times with 500 µl binding buffer. The bound fraction was eluted by boiling in SDS-PAGE sample buffer, and analysed by SDS-PAGE followed by autoradiography.

Immunoprecipitation

Lysate was prepared as described in *Drosophila* protocols. Ovaries from 50 flies homogenized in 200 µl cold lysis buffer typically gave extracts of 5 mg/ml. Extracts prepared from 50 adult heads in 100 µl cold lysis buffer were also used where indicated for immunoprecipitation. In this case, either 1 mM $CaCl_2$ or 1 mM EGTA was added to the IP buffer as required. Lysates were pre-cleared through an equivalent packed volume of protein A- or protein G-sepharose (GE Healthcare Life Sciences) equilibriated in IP buffer (50 mM Tris-HCl pH 8.0, 150 mM NaCl, 0.5% NP-40, 10% glycerol and Complete EDTA-free protease inhibitor (Roche)). Antibodies and pre-immune sera were added to the pre-cleared lysates at the appropriate dilution (Appendix A.1) and incubated overnight at 4°C with mixing. 50 µl 1:1 protein A- or protein G-sepharose equilibriated in IP buffer and pre-blocked with 0.5% (final concentration) BSA was then added to each tube and the reaction

incubated for 4 h at 4°C with mixing. The beads were then rinsed once with cold IP buffer and washed four times for 5 min each at 4°C. After the final wash, as much of the supernatant as possible was removed, the beads were resuspended in 25µl protein sample buffer (Invitrogen), boiled for 5 min, spun at 900 g for 5 min, and the supernatant loaded onto a gel for SDS-PAGE and western blotting.

RNA binding assays

RNA Immunoprecipitation

Immunoprecipitation was carried out as described with the following modifications. 1 U/µl RNasin RNase inhibitor (Promega) or 50 ng/ml RNaseA/T1 (Ambion) were added where indicated in the incubation and the wash steps. To elute bound RNA, the beads were resuspended in 100 µl IP buffer with 0.1% SDS and 30 µg proteinase K (Roche), and incubated at 50°C for 30 min. Total and immunoprecipitated RNA was purified using Trizol (Invitrogen) extraction and precipitated by the addition of 1/5 volume 5 M NH_4OAc pH 5.2, 2.5 volumes 100% EtOH and glycogen (Roche). Following incubation at -20°C overnight, the RNA was pelleted by centrifugation at 14000 rpm for 20 min at 4°C. The pellet was washed with 75% EtOH and resuspended in DEPC-treated water. Following DNase (Promega) treatment, immunoprecipitated RNA and 10% total RNA was then used as a template for cDNA synthesis in combination with Superscript III (Invitrogen) RT and random hexamer primers (Invitrogen). 10% of the RT product was then PCR-amplified using specific primers (Appendix A.2.4).

Pulldown with poly(U)-sepharose

^{35}S-labelled proteins were prepared as described for GST-pulldown assays. Binding assays were performed using of poly(U)-sepharose 4B or sepharose 4B (GE Healthcare Life Sciences) equilibriated in binding buffer (as GST-pulldown buffer). 50 µl 1:1 resin in buffer was incubated with 15 µl lysate for 1-2 h at room temperature with or without homopolymer competitors (Sigma) in a total volume of

400 µl. The resin was then washed four times with 500 µl binding buffer. The bound fraction was eluted by boiling in SDS-PAGE sample buffer, and analysed by SDS-PAGE followed by autoradiography.

UV cross-linking analysis

Binding reactions were carried out in a final volume of 10 µl and set up in a 96-well microtitre plate. Recombinant protein at a concentration of 100-1000 nM was added to 50-100 kcpm ^{32}P-labelled RNA probes in IP buffer (immunoprecipitation protocol) with the addition of 0.1 mg/ml *E. coli* tRNA (Roche) and 1 mg/ml heparin (Sigma). Reactions were incubated for 15 min at room temperature. The reactions were cross-linked on ice at 999mJ in a Stratalinker 1800 UV cross-linker (Stratagene). Free and unprotected RNA was digested with 5 µl RNaseA (Sigma) at 37°C for 15-30 min. 15 µl 2 x protein sample buffer (Invitrogen) was added to each reaction, and samples analysed by SDS-PAGE followed by drying of the gel and autoradiography.

EMSA

Binding reactions were assembled as for UV cross-linking. Following incubation of protein and RNA probe, 2 µl 30% glycerol was added and 6 µl each reaction loaded onto a non-denaturing 5% acrylamide gel. Electrophoresis was carried out in 1 x Tris-borate-EDTA (TBE) buffer (89 mM Tris-borate, 2 mM EDTA) at a constant voltage of 200V for 3 h. Gels were dried and visualised by autoradiography.

Drosophila protocols

Flystocks

Strains were raised on standard cornmeal-agar medium at 18°C or 25°C. Oregon-R was used as the wild-type strain. For a comprehensive list of all fly stocks used, see appendix A.3 of this thesis.

Preparation of ovaries prior to oocyte injection

Flies were transferred to freshly yeasted bottles less than 12 hours after eclosion. The ovaries of 2-3 day old, well-fed females were dissected into oxygen-rich halocarbon oil (Series 95; KMZ chemicals) on coverslips (Thickness no. 1; BDH), which allowed culturing of egg chambers for up to two hours. Egg chambers were dissected out and the appropriate stages aligned so that multiple egg chambers could be injected during the experiment.

Microinjection of oocytes

Fluorescently labelled RNAs at concentrations of 250-500 ng/ul were injected into cultured oocytes using Eppendorff femtotip needles.

Dissection and fixation of *Drosophila* ovaries for staining

Flies were transferred to freshly yeasted bottles less than 12 hours after eclosion. The ovaries of 2-3 day old females were dissected in 1 x PBS and immediately transferred to 3.7% formaldehyde in 1 x PBS + 0.1% Tween20 (PBST) for 20 min. After fixation, ovaries were washed three times for 5 min in PBST. Following *in situ* hybridisation or incubation with antibodies for immunofluroescence, ovaries were stained with 1 μg/ml 4', 6-diamidino-2-phenylindole (DAPI) to label nuclei, and mounted in Vectashield (Vector laboratories).

RNA *in situ* hybridization of *Drosophila* ovaries

Prior to *in situ* hybridization fixed ovaries were stored in 100% methanol at -20°C. *In situ* hybridization with fluorescent tyramide detection was performed using standard methods (Tautz and Pfeifle, 1989) with previously described modifications (Wilkie and Davis, 1998; Wilkie *et al.*, 1999). Ovaries were re-hydrated by washing in 1:1 methanol:PBST, followed by PBST, post-fixed in 3.7% formaldehyde in PBST for 10 min and rinsed five times for 5 min in PBST to remove all traces of fix. Ovaries were then washed in 1:1 PBST:hybridization buffer (50% formamide, 5 x SSC, 0.1% Tween20, adjusted to pH 6.5 with HCl) for 10 min, followed by a further 10 min wash with hybridization buffer alone. Pre-hybridization was carried out for 1 h at 70°C in hybridization buffer with the addition of 100 µg/ml *E. coli* tRNA and 50 µg/ml heparin. DIG-labelled RNA probes were hybridized to ovaries overnight at 70°C. Following hybridization, ovaries were washed twice in hybridization buffer, and once in 1:1 PBST:hybridization buffer for 20 min each at 70°C. Ovaries were then transferred to room temperature and washed four times in PBST for 20 min. DIG-labelled probes were detected with sheep HRP-conjugated anti-DIG antibody (1:500; Roche) for 2 h at room temperature. Ovaries were then washed extensively in PBST. The HRP-coupled antibody was visualized by tyramide signal amplification (TSA). Ovaries were incubated with tyramide-Cyanine-3 or –Cyanine-5 in amplification buffer (1:50; Perkin Elmer). The reaction was allowed to proceed for 4 minutes before washing with PBST, DAPI staining and mounting in Vectashield.

Immunofluorescence with *Drosophila* ovaries

Following dissection and fixation, ovaries were blocked in 10% Normal Goat Serum (GE Healthcare Life Sciences) in 0.2% PBST (1 x PBS + 0.2% Tween20) for 2 h at room temperature or overnight at 4°C. Samples were then incubated with primary antibody in 2% PBST (1 x PBS + 2% Tween20) overnight at 4°C or for 2-4 h at room temperature if blocking had previously been carried out overnight (Appendix A.1 for details of antibodies and dilutions). This was followed by three 20 min washes with 0.2% PBST and incubation with Alexa-conjugated secondary antibodies

(see Appendix A.1) in 2% PBST (1:500; Molecular Probes) for 2 h at room temperature. Ovaries were also stained where appropriate with Alexa-conjugated phalloidin (20 nM; Molecular Probes) in order to label F-actin. Following incubation with secondary antibody, with or without phalloidin, the ovaries were washed for 20 min three more times with 0.2% PBST before staining with DAPI and mounting in Vectashield.

Eggshell preparation

For eggshell preparation, 2-3 day-old flies were allowed to lay eggs at 25°C on apple juice-agar plates. Freshly laid eggs were collected, washed in PBS, mounted in a 1:1 mixture of lactic acid:Hoyer's medium and incubated overnight at 65 °C. The slides were examined by dark-field microscopy.

Extraction of genomic DNA

10 adult flies were collected in an Eppendorf microcentrifuge tube and frozen at -70°C. Frozen flies were homogenized in 200 µl of a solution containing 0.1 M Tris-HCl, pH 7.5, 0.1 M EDTA, 0.1 M NaCl and 0.5% SDS. The homogenized mixture was incubated at 65°C for 30 min. 400 µl of 1:2.5 5M KOAc: 6M LiCl was then added and the sample left on ice for 10 minutes. Following centrifugation at 14000 rpm for 15 min, 350 µl isopropanol was added to the supernantant to precipitate the DNA. The sample was then centrifuged again at 14000 rpm for 15 min, the pellet washed with 75% ethanol, dried and resuspended in 50µl TE.

Total RNA extraction

Total RNA was isolated by Trizol extraction. Ovaries were dissected in PBS, transferred to 500 µl Trizol Reagent (Invitrogen) per 50 ovaries and homogenized. 0.2 ml chloroform (per 1 ml of Trizol) was added, the sample incubated for 3 min at room temperature and centrifuged at 12000 rpm for 15 min. The aqueous phase containing the RNA was taken and 0.5 ml isopropanol (per 1 ml Trizol initially used)

added in order to precipitate the RNA. The sample was incubated at room temperature for 10 min and centrifuged at 12000 rpm for 10 min at 4°C. The RNA pellet was then washed with 75% ethanol, dried and resuspended in DEPC-treated water.

Preparation of ovarian lysate

For preparation of fresh ovarian lysate, ovaries were dissected in cold PBS and flash frozen in liquid nitrogen. For every 100 ovaries, 200µl cold lysis buffer (20 mM Tris pH 8.0, 100 mM NaCl, 2 mM DTT, 10% glycerol and Complete EDTA-free protease inhibitor (Roche) was added. Once thawed, the ovaries were homogenized, NP-40 was added to a final concentration of 0.5%, and the extract incubated for 5 min. Dissection, homogenization and incubation were all carried out on ice. The lysate was centrifuged at 900 g for 5 min at 4°C. The supernatant was transferred to a new tube and the protein concentration determined using Bradford reagent. The lysate was then either frozen in liquid nitrogen and stored at -70°C, or used directly.

Preparation of adult head lysate

Head lysate was prepared as described for ovarian lysate except that either 1 mM $CaCl_2$ or 1 mM EGTA was added to the lysis buffer, and that the lysate was centrifuged at 20 000 g for 20 min.

Microscopy

Imaging was performed on a widefield DeltaVision microscope (Applied Precision, Olympus IX70 and with a Roper Coolsnap HQ). The majority of images were acquired with a 20x/0.75 NA objective and then deconvolved using softWoRx (Applied Precision) (Davis, 2000; Parton and Davis, 2006) in order to re-assign out-of-focus light to the point of origin.

THE STUDY OF GLS AND ILS STRUCTURE USING NMR SPECTROSCOPY

Introduction

A major question in the field of mRNA localization is that of specificity. How is the destination of a localized RNA determined, and how are distinct RNA molecules sorted to numerous subcellular destinations using only a limited number of mechanisms? In the general case of motor-dependent localization, it is thought that specific *trans*-acting factors, or a certain arrangement of factors can bind to and interpret signals within the RNA, and it is this interaction that drives the association of RNA with motors and also determines destination.

Studies of many localized RNAs have revealed the presence of *cis*-acting RNA localization elements that are necessary and sufficient for correct localization. The minimal sequences required for localization of *gurken* and *I* Factor transcripts to the dorso-anterior of the oocyte were mapped using *in vivo* injection of fluorescently labelled RNA (Van De Bor *et al.*, 2005). The GLS is a conserved, 64-nucleotide RNA hairpin found within the 5' of the *gurken* coding region, whilst the ILS is a 58-nucleotide hairpin in the second open reading frame of the *I* Factor. The GLS and ILS localization signals defined by this assay share only 34% sequence identity and no common primary sequence motifs (Fig. 3.1A). Moreover, BLAST searches in the *Drosophila* sequence databases using the GLS sequence failed to find the ILS and *vice versa*. However, the mfold (Zuker, 2003) RNA structure program predicts that they contain similar secondary structural elements (a hairpin loop with two internal loops and a bulge) (Fig. 3.1B). This predicted structural similarity has led to the hypothesis that these elements represent a consensus structure for localization to the dorso-anterior cap in the oocyte.

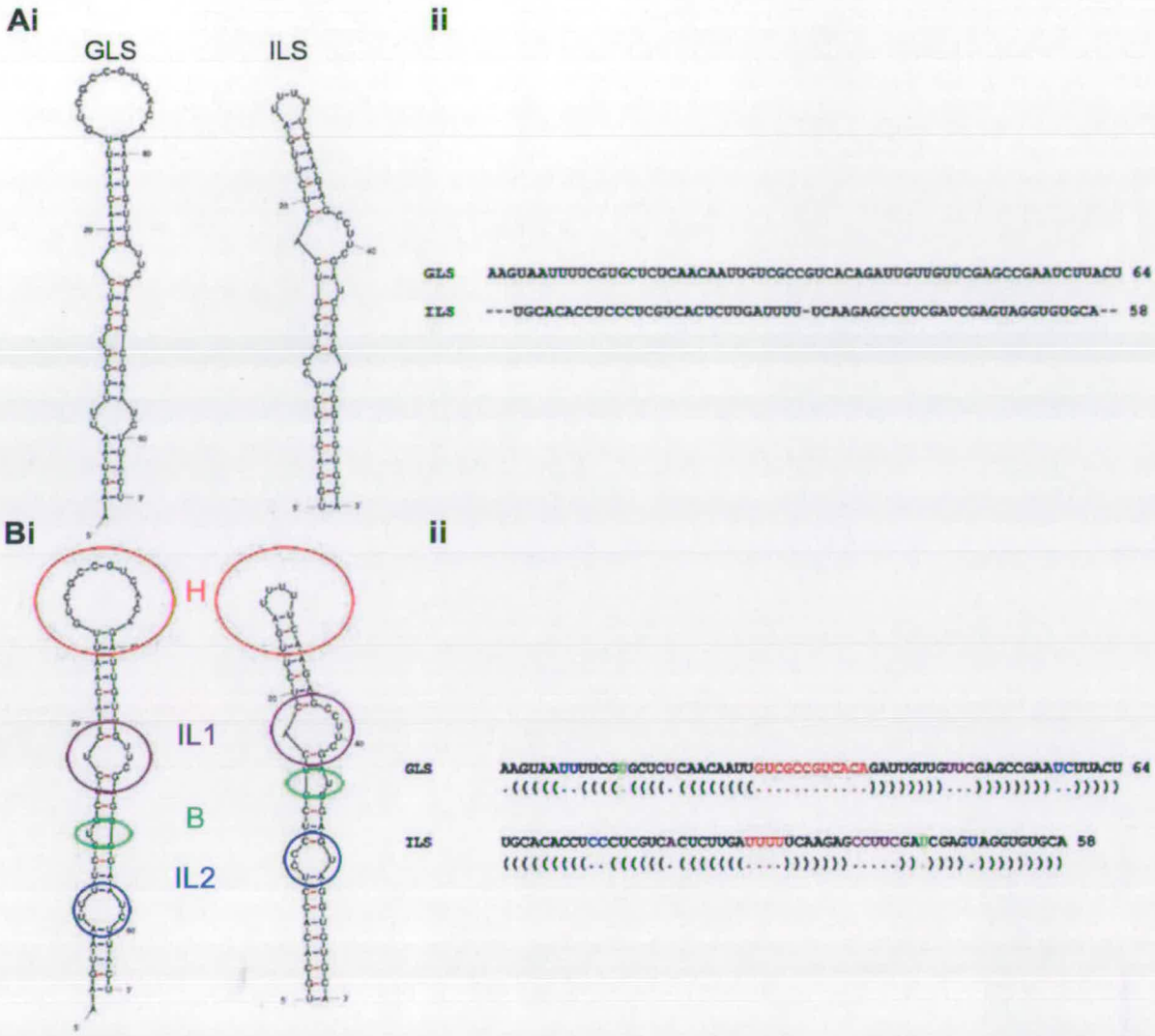

Figure 3.1 The GLS and ILS may represent a consensus structure required for localization to the dorso-anterior cap. (A) The GLS and ILS hairpins share little primary sequence identity. **i** Minimum free energy secondary structures of the GLS and ILS as predicted by mfold. **ii** The GLS and ILS have limited sequence identity. **(B) i** Secondary structure prediction by mfold reveals that the GLS and ILS contain similar secondary structural elements, a hairpin loop (H-red), a first internal loop (IL1-purple), a bulge (B-green), and a second internal loop (IL2-blue). **ii** 'Bracket notation' representation of the secondary structures of the GLS and ILS, showing the shared secondary structural elements using the colours described above. A base pair between base i and j is represented by a '(' at position i and a ')' at position j, unpaired bases are represented by dots.

Comparison of the localization elements of mRNAs that localize to the same destination has not led to the identification of very many consensus localization sequences or structures. Primary sequence comparison of the *Vg1* localization element (VLE) in two *Xenopus* species revealed two 5-6-nucleotide sequences, referred to as E2 and VM1 motifs (Lewis *et al.*, 2004). The VLE contains multiple, clustered copies of these motifs, and it has since been observed that the localization element of *VegT* mRNA has a cluster of E2 motifs essential for vegetal localization (Kwon *et al.*, 2002). In this case, the same *trans*-acting factor, necessary for localization, can bind these motifs in the *Vg1* and *VegT* LEs. Further searches with a motif found within the E2 sequence led to the identification of similar motifs in most known vegetally localized mRNAs, and resulted in the identification of new localized mRNAs (Betley *et al.*, 2002).

The above comparison was based on primary sequence, and consensus secondary structures have proved harder to find. Recently however, an algorithm named RNApromo (Rabani *et al.*, 2008) has been able to predict structural elements within sets of mRNAs with common localization patterns. A motif common to apically localized mRNAs within the embryo (Lécuyer *et al.*, 2007) such as *K10, runt* and *wingless,* and a motif found in dendritically localized mRNAs within mouse neurons (Zhong *et al.*, 2006) have been identified and predicted to be important for apical localization and dendritic targeting respectively. In a second example, very relevant to this work, the predicted secondary structures of the GLS and ILS have been used successfully by a bioinformatics method known as 'RNA2DSearch' to search the *Drosophila* genome for related localization signals in transposable elements (Hamilton *et al.*, 2009). Two transposons (*G2* and *Jockey*) were found to contain GLS/ILS-like RNA stem-loops. Furthermore, these stem-loops were required for the dynein-dependent localization of the transposon transcripts to the anterior and dorso-anterior of the *Drosophila* oocyte. The study described above therefore adds weight to the hypothesis that the secondary structures of the GLS and ILS represent a consensus structure for dorso-anterior localization, and in a broader sense, adds credence to the concept that shared consensus localization elements target mRNAs to common subcellular destinations.

When considering the possibility that the GLS and ILS contain a consensus for dorso-anterior localization in the oocyte, it must be remembered that the architecture of RNA is also shaped by specific tertiary interactions that can give rise to more complex structures than those predicted by programs such as mfold. RNA has multiple functions including the decoding and transfer of genetic information (messenger RNA, transfer RNA, small nuclear RNAs), regulation of gene expression (riboswitches and micro RNAs) and catalysis (ribozymes, ribosomal RNA, small nuclear RNAs). This functional versatility of RNA is dependent upon the variety of complex structures formed by secondary (helices containing, loops and bulges) and tertiary interactions (for example, kissing hairpin loops, coaxial stacking of helices and ribose zippers). It must also be remembered that programs such as mfold (Zuker, 2003) predict RNA secondary structure by free energy minimization i.e. folding the RNA into the structure with the minimum free energy (Mathews and Turner, 2006). These programs are limited in that they do not take into account the full range of possible base pairs and cannot predict certain motifs such as pseudoknots.

The determination of the three-dimensional structures of the GLS and ILS is therefore needed if we are to identify the sequences and/or structures that are required for specific localization to the dorso-anterior cap. X-ray crystallography has allowed the determination of the structures of several large and complex RNAs. Structures of the ribosomal RNAs and proteins, with bound mRNA and tRNAs are notable examples (Korostelev *et al.*, 2006; Selmer *et al.*, 2006; Yusupov *et al.*, 2001; Yusupova *et al.*, 2001). Others include group I introns (Adams *et al.*, 2004a; Adams *et al.*, 2004b; Golden *et al.*, 2005; Guo *et al.*, 2004) and riboswitches complexed with metabolites (Batey *et al.*, 2004; Montange and Batey 2006). However, the conformational flexibility of RNA can provide an obstacle to crystallization, which investigators have overcome by the co-crystallization of RNA with proteins. Concomitant with this is a loss of information about the different conformations RNA molecules can adopt. NMR spectroscopy offers a tool for studying the structure and dynamics of RNA in solution, and also interactions with ligands such as other proteins, nucleic acids, ions and solvent molecules.

Historically, NMR has been used to study relatively small RNA molecules. This is largely due to difficulties in resonance assignment. As RNA is composed of four chemically similar nucleotides, and the predominant secondary structure is the A form helix, many nucleotides experience a similar chemical environment. This results in resonance overlap, reducing the amount of information that can be obtained from spectra. Combined with aggregation problems caused by the high concentration of RNA required in an NMR sample, this can make structure determination difficult.

This difficulty is reflected in the sizes of RNA structures deposited in the Nucleic Acid Database (http://ndbserver.rutgers.edu). Of 287 NMR structures containing only RNA molecules, 19 are 40-nucleotides/15 kDa and over. Of these, only three are 60-nucleotides/20 kDa and over. The vast majority of RNA NMR structures are of extended secondary structures of less than 15 kDa. This is because in many cases, larger RNAs are dissected into smaller thermodynamically stable subdomains, such as helices and loops. However, three recent NMR structures have demonstrated that it is possible to solve structures of higher molecular mass by NMR (Davis *et al.*, 2005; D'Souza *et al.*, 2004; Lukavsky *et al.*, 2003). The sizes of the RNAs in these studies range from the 75-nucleotide/25 kDa HCV IRES domain II (Lukavsky *et al.*, 2003) to the 101-nucleotide/35 kDa core encapsidation signal of Moloney Murine Leukaemia Virus (MMLV) (D'Souza *et al.*, 2004).

Aims of this chapter

Despite the difficulties described above, the aim of the work presented in this chapter was to study the GLS and ILS by NMR spectroscopy. This was in order to be able to better test the hypothesis that the GLS and ILS represent a consensus structure for localization to the dorso-anterior cap in the *Drosophila* oocyte. It was decided that NMR would be the superior method to use, as firstly, the proteins that can associate with the GLS and ILS were unknown when this work began and so the RNA would be difficult to crystallize, and secondly, X-ray crystallography results in the loss of conformational information.

This chapter describes the preparation of GLS and ILS RNA samples for study by NMR. Dr Graeme Ball, a postdoctoral researcher in the Davis lab, who has specialized in NMR for his PhD, carried out all NMR spectroscopy and the structure assignment. The work described here was also carried out in collaboration with Dr Peter Lukavsky at the Laboratory of Molecular Biology, Cambridge. The patterns of base-pairing and preliminary solution structures of GLS and ILS RNAs are presented, and common sequences/structures discussed.

Results

Preparation of GLS and ILS RNA NMR samples

By NMR standards, the GLS and ILS are large RNAs (Lukavsky and Puglisi, 2005; Tzakos *et al.*, 2006). For this reason we chose to work with M1 and I3. These are truncated forms of the GLS and ILS respectively, both lacking the second internal loop of the parent hairpin (Fig. 3.2A, B). M1 is 49-nucleotides in length, whilst I3 is 37-nucleotides long. Fluorescently labelled M1 and I3 still localize when injected into stage 8/9 oocytes, albeit with lower efficiencies than the full length GLS and ILS RNAs (V. Van De Bor, unpublished).

Structure determination by NMR demands milligram quantities of unlabelled and isotopically ^{13}C and/or ^{15}N-labelled RNA. These samples can be efficiently prepared by *in vitro* transcription from DNA templates using T7 RNA polymerase (Milligan *et al.*, 1987; Puglisi and Wyatt, 1995). M1 and I3 DNA templates were prepared for *in vitro* transcription by insertion of the corresponding DNA coding sequence, plus the T7 promoter site and flanking restriction sites into the high copy number plasmid pUC18. Fragments were designed as shown (Lukavsky and Puglisi, 2004; Fig. 3.3A) and were prepared by PCR. Initially, overlapping primers were used to create a PCR template (Fig. 3.3B), which was then amplified using a forward primer corresponding to the *Hind*III site/T7 promoter, and a reverse primer corresponding to the *Bbs*I/*Eco*RI sites (Fig. 3.3C). Purified plasmid DNA was linearized and used directly in *in vitro* transcription reactions. As commercially available T7 RNA polymerase can be expensive for large-scale RNA synthesis, recombinant, histidine-tagged T7 RNA polymerase was also prepared and purified using plasmid pT7-911Q (Abramochkin and Shrader, 1995; Ichetovkin, 1997).

The magnesium chloride concentration required for the *in vitro* transcription reactions was optimized for each DNA template in order to maximise the yield of RNA obtained. Small-scale transcription reactions with magnesium concentrations

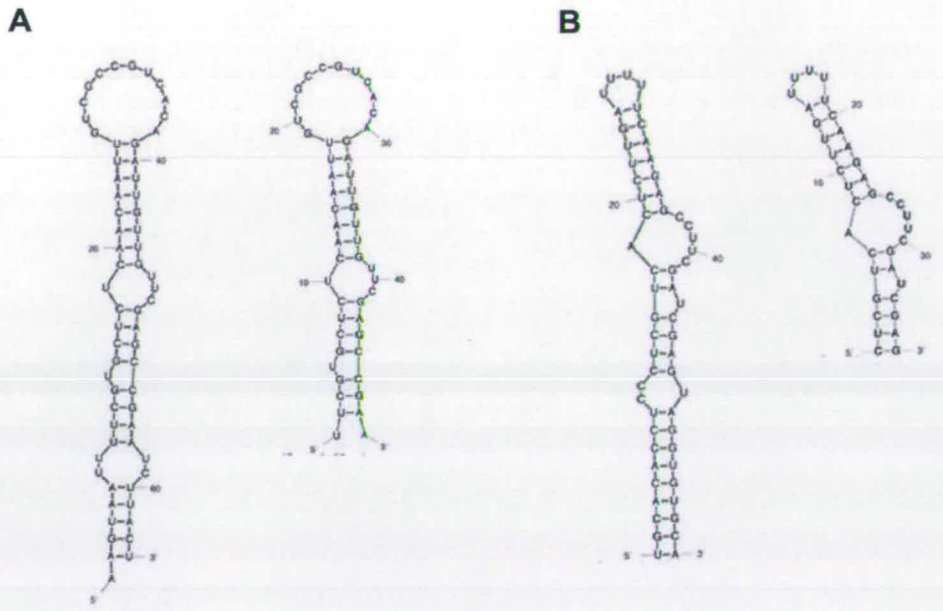

Figure 3.2 Secondary structure prediction of **(A)** GLS and M1, a truncated GLS lacking the second internal loop and **(B)** ILS and I3, a truncated ILS also lacking the second internal loop.

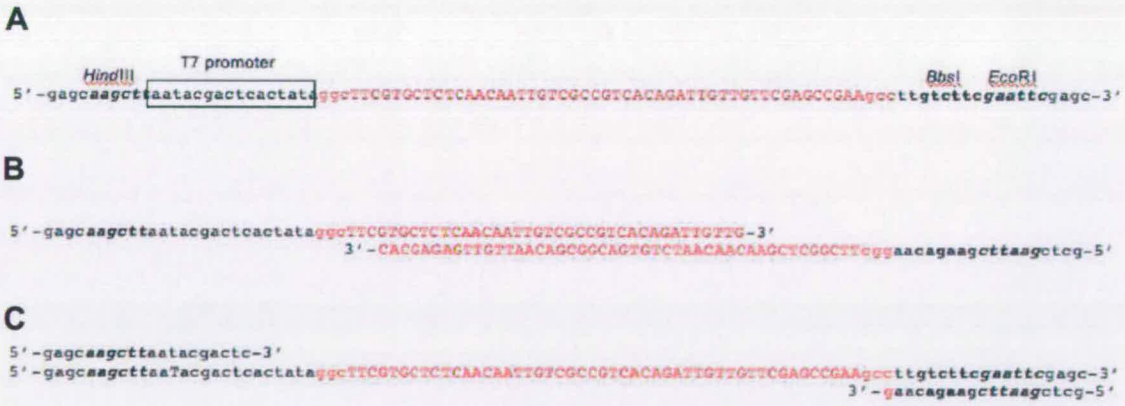

Figure 3.3 Sequence, design and PCR construction of DNA templates for *in vitro* transcription. (A) Design of plasmid DNA template for *in vitro* transcription of M1. Transcribed sequence is highlighted in red; restriction sites are bold. **(B)** PCR strategy using overlapping primers and **(C)** subsequent amplification for construction of DNA template for *in vitro* transcription of M1.

ranging from 8 to 56 mM were carried out, and RNA yield assessed using denaturing PAGE and staining with toluidine blue (Fig. 3.4A).

To prepare milligram quantities of RNA, *in vitro* transcription reactions were carried out in a final volume of 20 ml. During transcription there is an accumulation of pyrophosphate. This can sequester magnesium and so inhibit the rate of transcription. To overcome this, and therefore maximise RNA yield, the pyrophosphate precipitate was spun down following 1 h incubation. Additional magnesium chloride was added and the transcription reaction continued for a further hour.

RNAs synthesized by *in vitro* transcription are usually heterogeneous at the 3' end, due to either premature termination, or the addition of one or more non-coded nucleotides to yield longer transcripts (Milligan *et al.*, 1987). These longer transcripts with extra non-coded nucleotides will be referred to collectively as N+1 transcripts. Purification of the desired full-length RNA product is commonly achieved by preparative denaturing PAGE, followed by elution from the gel (Wyatt *et al.*, 1991). PAGE has also been combined with the use of self-cleaving ribozymes and DNAzymes (Cheong *et al.*, 2004; Schürer et al., 2002; Shields *et al.*, 1999) in order to purify to single nucleotide resolution. Although denaturing PAGE allows the purification of medium and longer length RNAs, such as M1 and I3, the gel purification protocol suffers from a number of disadvantages. Incomplete polymerization or partial hydrolysis of the gel result in water-soluble acrylamide oligomers that can bind to the desired RNA product and cannot be completely removed (Lukavsky and Puglisi, 2004). This leads to an increase in the molecular size of the RNA and reduces the information that can be gained from an NMR experiment. In addition, any purification protocol involving the precipitation of RNA, especially larger RNAs, can lead to the formation of aggregates (Lukavsky and Puglisi, 2004).

Anion exchange chromatography has been used to purify homogeneous length shorter-sized RNAs to single nucleotide resolution (Anderson *et al.*, 1996; Wincott *et al.*, 1995). To avoid the disadvantages of denaturing PAGE, diethylaminoethyl

(DEAE) anion exchange chromatography was used to purify M1 and I3 RNAs. Although this did not result in exclusion of N+1 transcripts, it is possible to take this into account in the NMR assignment (P. Lukavsky, unpublished). This protocol can yield RNA for NMR studies very rapidly. The transcription reactions were applied to an equilibrated DEAE column and eluted with a gradient of 2M NaCl. A typical elution profile is shown (Fig. 3.4B). Two major peaks are observed, the first corresponding to plasmid DNA, and the second to the RNA product (Fig. 3.4B, C). Fractions were analysed by denaturing PAGE (Fig. 3.4D) and by measuring OD at 260 nm. The fractions containing the correct product were then combined, concentrated and exchanged into the appropriate NMR buffer. Analytical gel filtration was further used to look at the final samples (Fig. 3.4E).

For M1, multiple species of molecule were observed following denaturing gel electrophoresis. This was thought to be due to incomplete denaturation of multimers of these RNAs during electrophoresis. It was hypothesised that multimers could form by association of the unpaired bases in the GC-rich hairpin loop of M1. The final M1 RNA sample eluted as a single peak during gel filtration. As a larger RNA was present in a small amount following denaturing PAGE, assumed to be due to incomplete denaturation, it was thought that this single gel filtration peak represented this larger multimer formed by the RNA under nondenaturing conditions. Following purification of I3 (Fig. 3.5A), a single band was observed following denaturing gel electrophoresis (Fig. 3.5B). The final sample also eluted as a single peak following gel filtration (Fig. 3.5C).

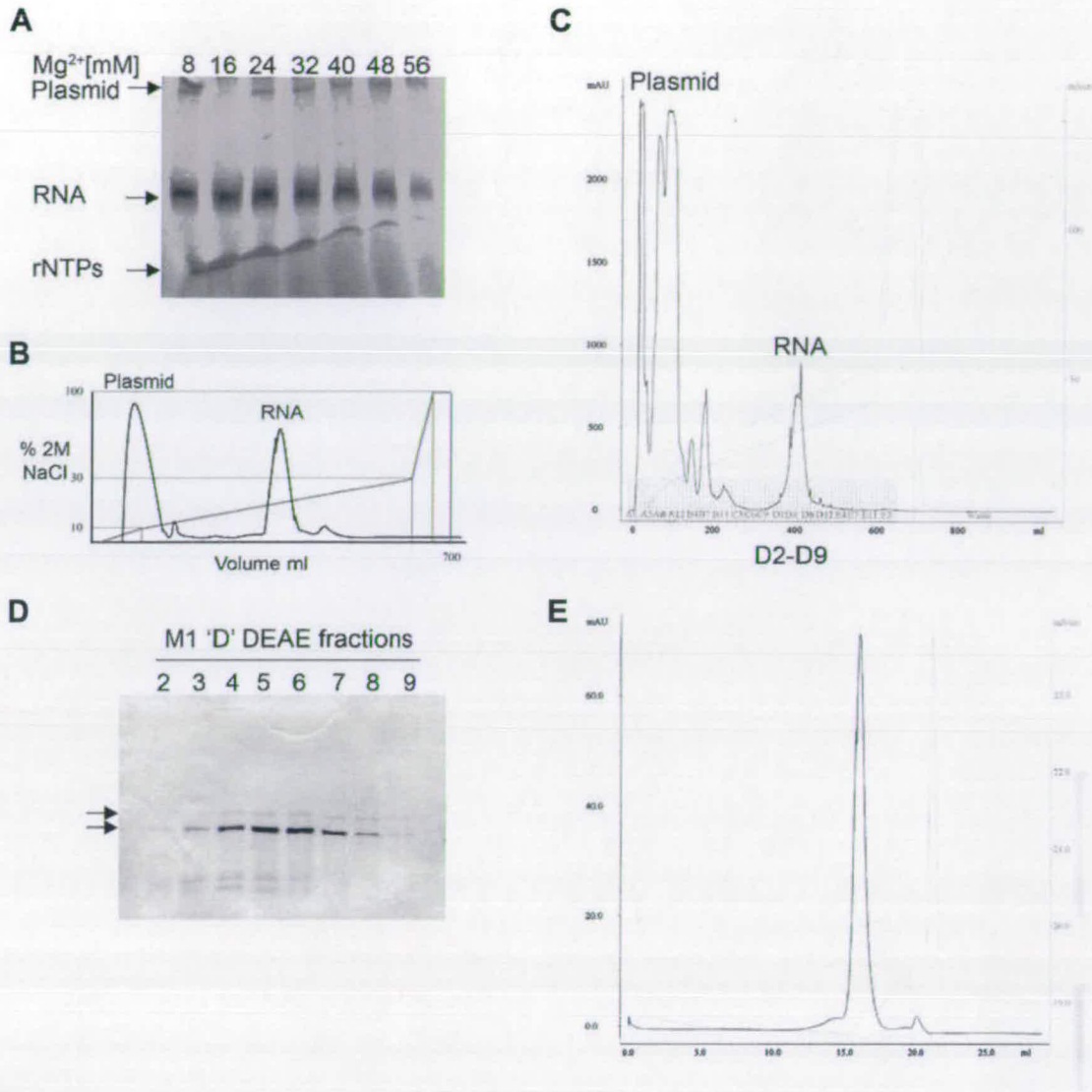

Figure 3.4 Transcription and preparation of M1 for NMR. (A) Denaturing PAGE analysis of RNA yield from small scale *in vitro* transcription reactions at different magnesium concentrations. RNA, plasmid DNA and rNTPs were visualized by staining with toluidine blue. **(B)** RNA purification by DEAE anion exchange chromatography. A typical elution profile shows two major peaks, the first containing plasmid DNA, and the second containing the RNA. **(C)** Purification of a large scale M1 transcription reaction by DEAE chromatography. The RNA was eluted in fractions D2 to D9. **(D)** Denaturing PAGE analysis of M1 DEAE chromatography fractions. Arrowheads indicate multiple species of molecule. It is thought that the higher band represents a multimer that was not completely denatured in during electrophoresis. **(E)** Analytical gel filtration of purified and concentrated M1 RNA.

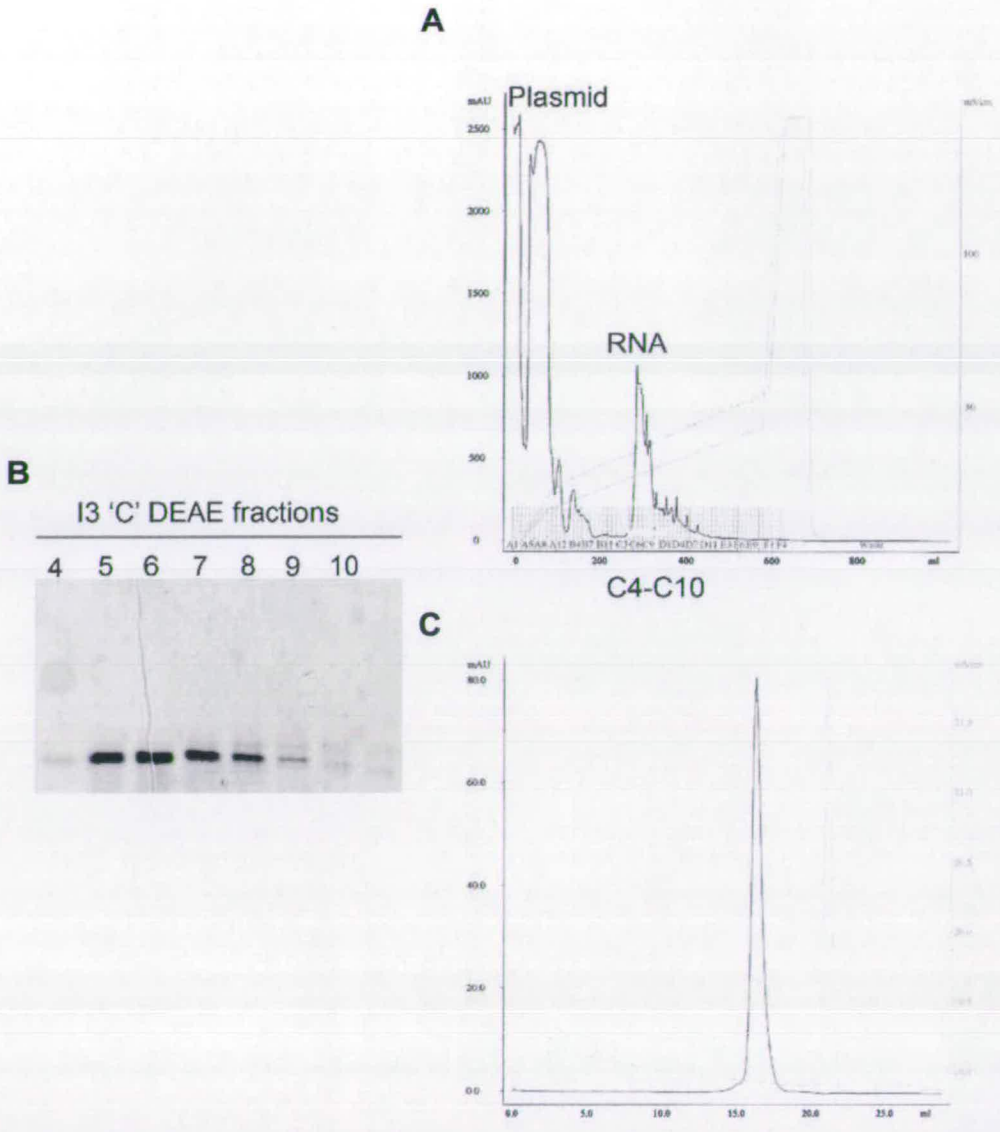

Figure 3.5 Transcription and preparation of I3 for NMR (A) Purification of a large-scale I3 transcription reaction by DEAE chromatography. The RNA was eluted in fractions C4 to C10. **(B)** Denaturing PAGE analysis of I3 DEAE chromatography fractions. **(C)** Analytical gel filtration of purified and concentrated I3 RNA.

Introduction of a UUCG tetraloop

It was thought that multimerization of M1 could be taking place through the GC-rich hairpin loop. In order to reduce aggregation and improve folding, the loop of M1 was replaced with a UUCG tetraloop. RNA tetraloops, i.e. RNA loops containing four nucleotides, occur frequently in biologically active RNAs. Indeed, they are the most common type of loop in ribosomal RNAs (Woese *et al.*, 1990). The majority of tetraloops belong to three main families, UNCG, GNRA and CUUG (N=U, C, G; R=G, A). They are all characterized by a very high thermodynamic stability and melting temperature, whilst among these three classes the UUCG tetraloop is the most stable (Antao et al., 1991). A number of X-ray and NMR structures exist for the UUCG tetraloop (Allain and Varani, 1995; Cheong *et al.*, 1990; Ennifar *et al.*, 2000) that show a non-canonical base pair between U1 and G4. The two central nucleotides are unpaired, but form stacking and hydrogen bond interactions with the outer two nucleotides. It is this network of interactions that stabilizes the structure. Tetraloops carry out a variety of functions, one of which is to direct the correct folding of complex RNA structures (Tuerk *et al.*, 1988; Uhlenbeck 1990). This has been exploited experimentally to reduce aggregation and stabilize RNA secondary structure for structure determination (D'Souza *et al.*, 2004). Therefore this strategy was also engaged for the M1 RNA.

The ability of tetraloop containing GLS RNA to localize in the oocyte was tested using the *in vivo* injection assay. Tetraloop containing ILS was also tested by this assay for purposes of comparison. In both cases, replacement of the hairpin loop with a tetraloop was not predicted to affect secondary structure (Fig. 3.6A, D). The results show that the wild-type GLS localized to the dorso-anterior cap in stage 8 or 9 oocytes (Fig. 3.6B, Table 3.1), whereas GLS with the hairpin loop replaced by a UUCG tetraloop became evenly distributed throughout the oocyte (Fig. 3.6C, Table 3.1). This shows that the GLS hairpin loop is absolutely required for dorso-anterior localization. Conversely, the wild type ILS and ILS RNA containing the tetraloop both localize to the dorso-anterior cap (Fig. 3.6E, F, Table 3.1). This has implications for the assessment of what the determinants of dorso-anterior localization are and

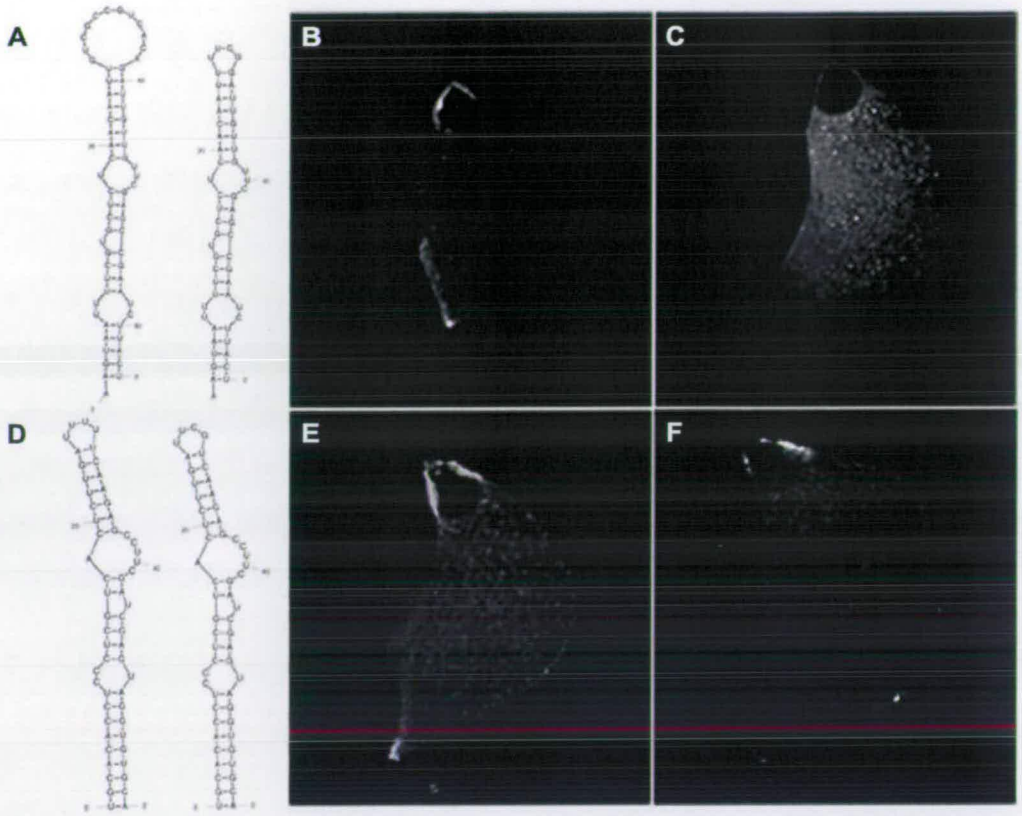

Figure 3.6 Replacement of the hairpin loop with a UUCG tetraloop abolishes GLS localization to the cap, whilst localization of the ILS is not affected (A and D) Replacement of the GLS and ILS hairpin loops with a UUCG tetraloop does not affect the predicted secondary structures. **(B)** Fluorescently labelled GLS RNA localizes to the dorso-anterior cap. **(C)** Replacement of the GLS hairpin loop with a tetraloop prevents localization to the dorso-anterior cap. **(E)** Fluorescently labelled ILS RNA localizes to the dorso-anterior cap. **(F)** Replacement of the ILS hairpin loop with a tetraloop does not affect dorso-anterior localization.

also for deciding which RNA to make for NMR. The tetraloop M1 was predicted to be non-functional and therefore was not pursued in NMR studies. It was also noted that tetraloop I3 gave a good spectrum and could also be used for NMR.

TABLE 3.1 *in vivo* injection assay for localization of GLS, tetraloop GLS, ILS and tetraloop ILS to the dorso-anterior cap in stage 8/9 oocytes.

RNA	n injected	n localized dorso-anterior cap
GLS	21	20
GLS tetraloop	25	0
ILS	20	19
ILS tetraloop	22	20

Dissection of M1 and I3 into stable secondary structure elements

Unambiguous assignment of the chemical shifts obtained with full-length M1 (without tetraloop replacement) and I3 was not possible. This was due to overlap of proton resonances. This is not surprising when it is considered that M1 and I3 are still relatively large RNA molecules consisting of four nucleotides, each with at least ten protons, in similar chemical environments. Dissection of the RNA into thermodynamically stable secondary structural elements, such as helices and loops, can surmount the problem of overlap. The pattern of chemical shifts of the subdomains can be compared to those of the full-length RNA to ensure that the fragments maintain the same conformation in or out of the context of the full RNA. This method, used to determine the structure of the 77-nucleotide HCV IRES domain II (Lukavsky *et al.*, 2003), combines the data obtained from both the full RNA and the fragments to define both local structures and global conformation to calculate the final structure.

Adopting this method, M1 (without using tetraloop replacement as this did not localize) (Fig. 3.7A) and I3 (Fig. 3.7B) were each separated into two fragments, stem and loop. A UUCG tetraloop was added in order to close the top of the stem portion. The ability of these isolated fragments to form the same secondary structure as in the full-length molecule was assessed using mfold. The wild type M1 loop fragment proved difficult to make, purify and obtain usable spectra for. This was due to difficulties in folding the loop to form hairpin monomers, flexibility, and lack of structure (as is the case with the full length M1). The loop fragment of I3 was made, but has not been studied yet. However, it was possible to prepare unlabeled and labeled samples for the stem portions of both M1 and I3, and these have been used to define both the base-pairing patterns and the structures of the stems. For I3, the combination of a labelled stem sample and an unlabelled full-length tetraloop I3 sample was sufficient to define the structure of the stem portion and also predict the base pairing for the full-length molecule.

Base-pairing patterns are as predicted by mfold

In NMR studies, proton resonances contain valuable information about the base pairing in an RNA molecule, including both standard Watson-Crick type base pairing and non-canonical base pairs. Signals can only be observed when the protons are protected from exchange with the solvent water, and are therefore involved in hydrogen bonding i.e. involved in base pairing. Furthermore, the chemical shifts of these base-paired protons are in one particular region of the spectrum. By counting the number of proton resonances in this region, it is essentially possible to count the number of base-pairs (Fürtig et al., 2003). The base-pairing pattern for M1 (Fig. 3.8A) and I3 stems (Fig. 3.8Bi), and also full-length tetraloop I3 (Fig. 3.8Bii), by NMR are as predicted by mfold, each containing a bulged U and an internal loop of unpaired nucleotides (corresponding to IL1 Fig. 3.1). All paired nucleotides form standard Watson-Crick type base pairs.

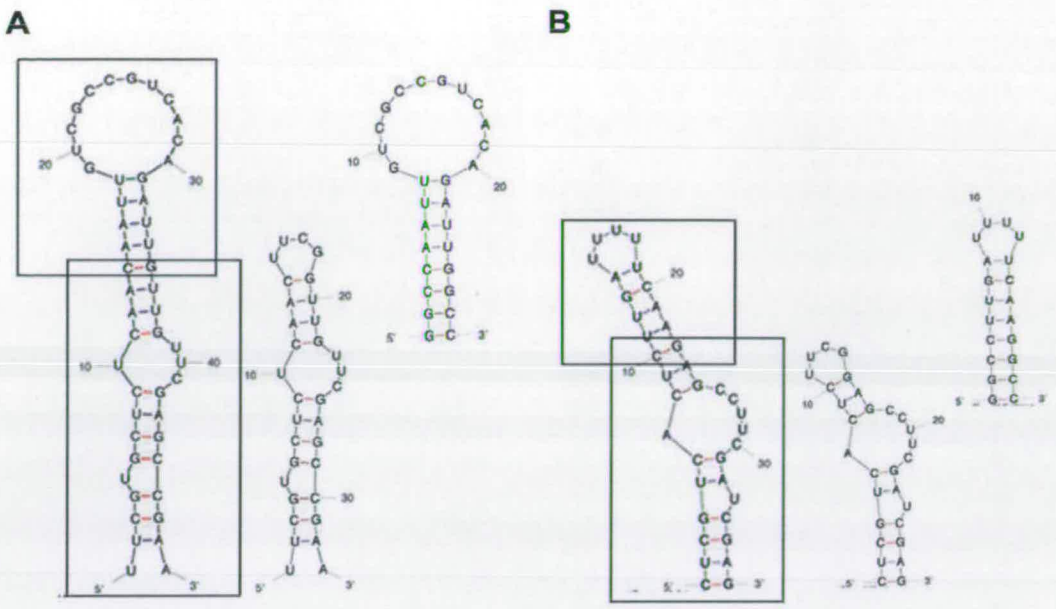

Figure 3.7 Separation of (A) M1 and (B) I3 into stem and loop fragments. The fragments are predicted to form the same secondary structures as in the full-length secondary structure predictions.

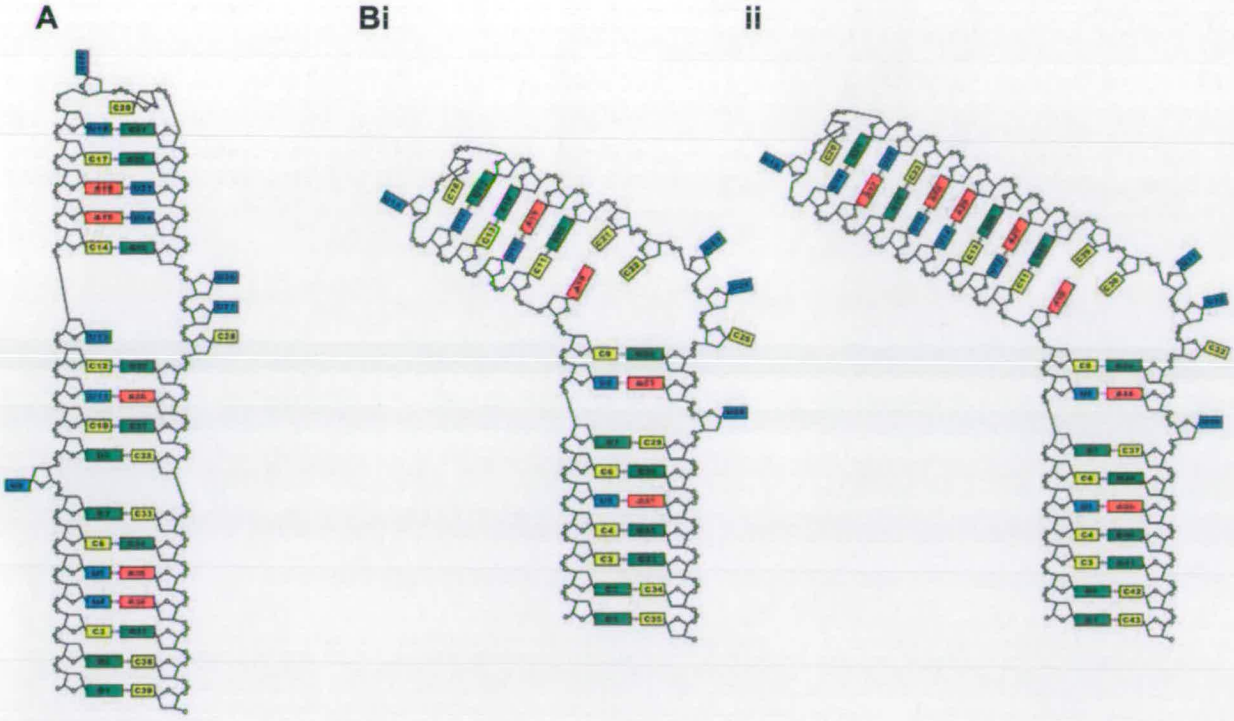

Figure 3.8 The base-pairing pattern of the stem fragments of M1, I3, and full-length tetraloop I3, are as predicted by mfold. Schematic representation of the base-pairing and secondary structure of **(A)** the stem fragment of M1 RNA, **(Bi)** the stem fragment of I3 RNA and **(Bii)** the full-length tetraloop I3.

Structures of M1 and I3 stem fragments

M1 stem (Fig. 3.9) forms an extended helical structure. The single stranded nucleotides U26, U27, C28 and U13 form an asymmetric internal loop, separating the helical region into two, and introducing a very slight bend. U26, U27 and C28 are flipped out of the structure, whilst U13 is not. Unpaired U8 is bulged out of the lower helix.

I3 stem (Fig. 3.10) forms a bent helical structure. The single-stranded nucleotides A10, C21, C22, U23, U24 and C25 create an asymmetric internal loop, which introduces a bend between the lower and upper helical regions. U23, U24 and C25 are flipped out of the structure, whilst A10, C21 and C22 are not. Unpaired U28 is bulged out of the lower helix.

In both cases, helical regions are thought to be A form, although this is not definitively known until the structures of the hairpin loops, and the overall structures of M1 and I3 are known. The overall shape of the two stems looks superficially different. The I3 stem has a greater kink, and the M1 stem is more extended. However, the common structure of the internal loop and of the bulged U highlights two important features that could be important for the shared function of the two localization elements.

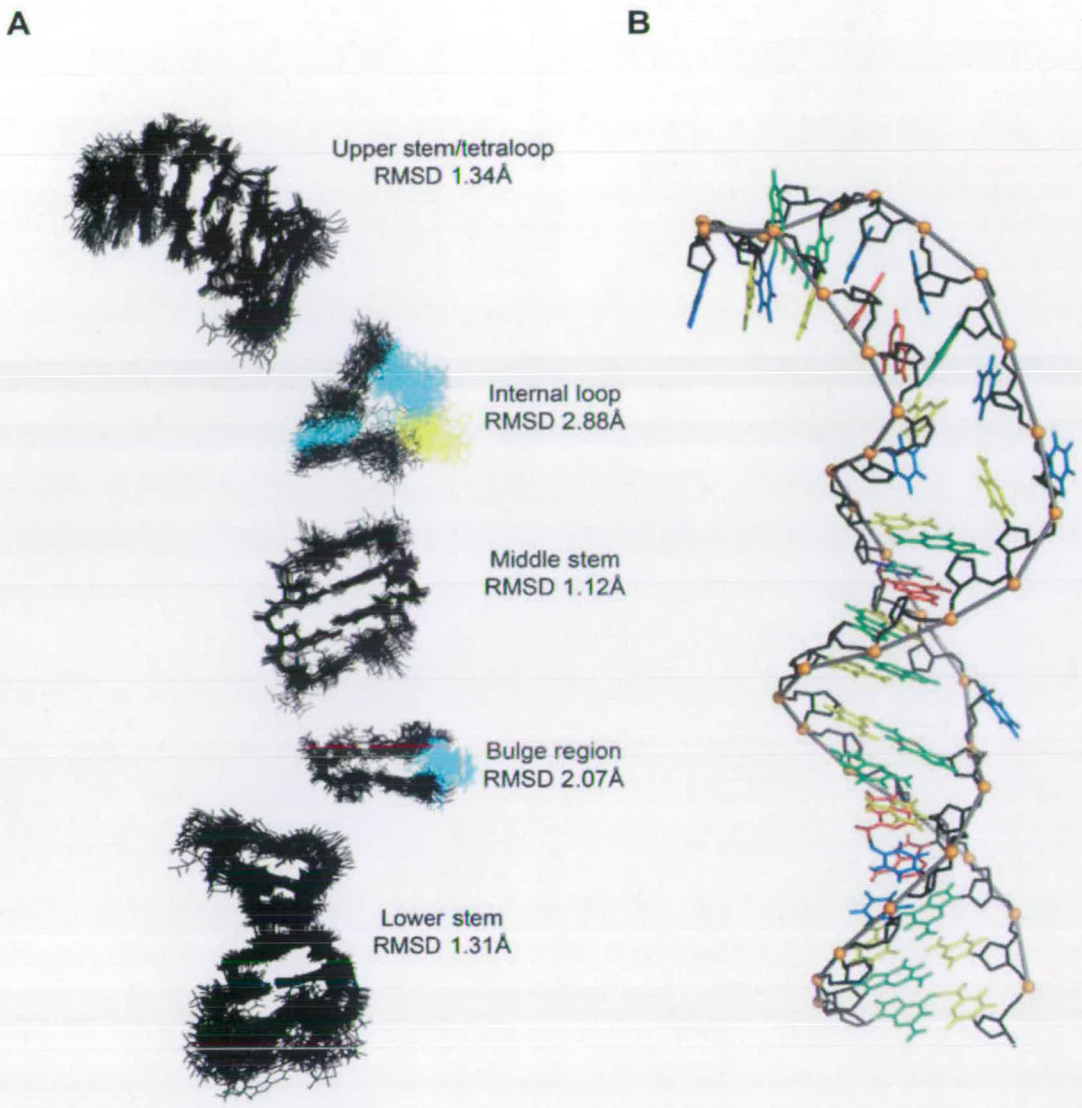

Figure 3.9 Structure of the M1 stem. (A) Superposition of the lowest energy 28 of 100 structures for separated secondary structural elements of the M1 stem. The asymmetric internal loop and bulged U are highlighted. **(B)** The lowest energy structure of the M1 stem.

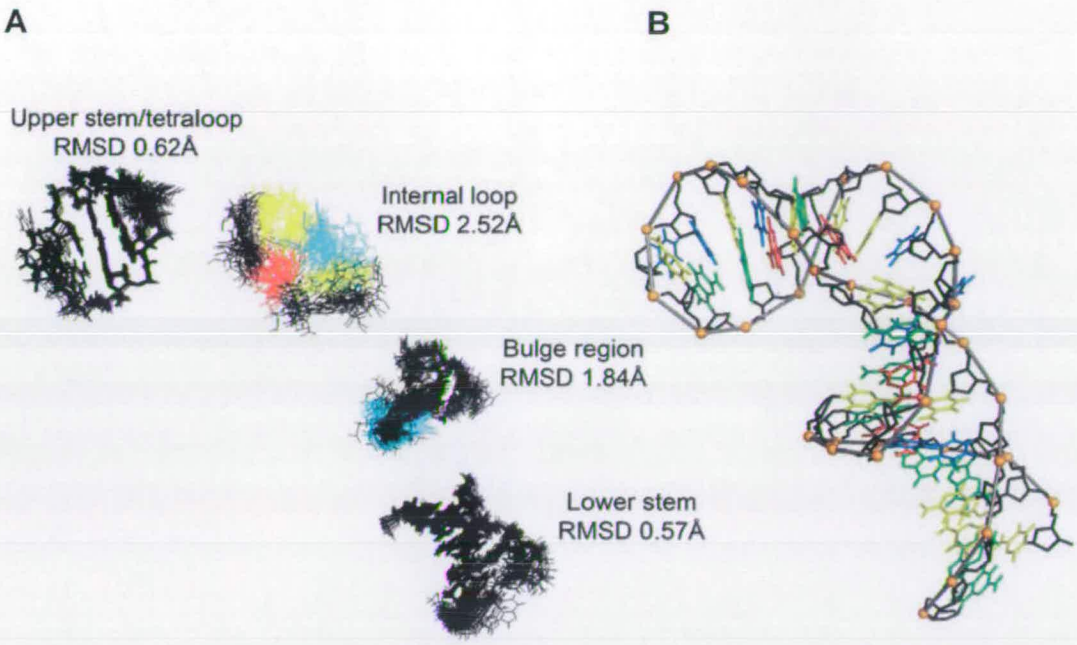

Figure 3.10 Structure of the I3 stem. (A) Superposition of the lowest energy 25 of 100 structures for separated secondary structural elements of the I3 stem. **(B)** The lowest energy structure of the I3 stem.

Discussion

NMR spectroscopy has been used successfully to define the base-pairing patterns and preliminary partial solution structures of functional, truncated GLS and ILS hairpins, M1 and I3. However, we were unable to prepare and study the full-length structures of the GLS and ILS. Furthermore, the solution structures of only the stem portions of truncated GLS and ILS were obtained by NMR spectroscopy. The hairpin loop of the GLS was shown to be essential for dorso-anterior localization, but was not amenable to study by NMR. Without the full structure of the hairpin loops, it is not possible to state with confidence that the structure obtained for the stem portions is that which occurs in the full GLS or ILS, or also what form the RNA helix takes in the GLS and ILS.

Using this approach we were able to confirm that the base-pairing pattern for both stems and for full-length tetraloop I3 (where a tetraloop replaces the hairpin loop are as predicted by mfold. All paired nucleotides form canonical Watson-Crick type base pairs, and the predicted nucleotides form bulges and loops. However, so far this approach has not yielded any new information regarding the structures of the GLS and ILS that was not already predicted by mfold, and the helical secondary structure of the stem portions of the localization elements is not observed to form a complex tertiary structure. However, it must be remembered that the structures presented here are not the complete localization elements, and it is possible that tertiary interactions may occur in full-length GLS and ILS. Differences were observed in the overall shape of the stem structures of M1 and I3. Despite this, the solution structures of the M1 and I3 stems have confirmed the mfold prediction that two features are common to the structures of the GLS and ILS. The exposure of UUC nucleotides in the first internal loop, and also the bulged U in both structures suggests that these features could be important for dorso-anterior localization.

The requirement for the first internal loop and bulge in dorso-anterior localization

Although the primary sequence of the first internal loop differs between the GLS and ILS, it can be seen from the structures of the M1 and I3 stems that in both cases, the same three nucleotides, UUC (U26, U27, C28 in M1 and U23, U24, C25 in I3), are flipped out of the structure. The importance of these three nucleotides in the first internal loop is further highlighted by GLS mutagenesis studies (V. Van De Bor, unpublished) where removing the internal loop completely prevents localization. Changing the identity of the remaining U in the asymmetric first internal loop, U13, or removing this nucleotide does not perturb localization. However, replacing this U with GAA so that the internal loop is replaced with a base-paired stem prevents localization. It would therefore seem that it is the UUC of the first internal loop that is important for localization, and that these nucleotides need to be single stranded. This is also supported by preliminary ILS mutagenesis studies (V. Van De Bor, unpublished), in which deletion of the two U residues in the UUC also abolishes localization. In contrast, despite the conservation of the bulged U of the GLS amongst the putative GLS sequences of different *Drosophilids,* (Fig. 3.11A) this residue, U8 of the GLS, can be removed or the identity changed and localization retained, arguing against a role for this nucleotide in dorso-anterior localization.

It is unclear as to whether it is the specific identity of the UUC nucleotides, or the structure created by them that is important for localization. When the putative GLS sequences of a range of *Drosophila* species are compared, most have the UUC sequence (Fig. 3.11A). However, *D. virilis grk* RNA (which can localize to the dorso-anterior cap in *D. melanogaster* oocytes; Van De Bor *et al.*, 2005) contains a loop with the same secondary structure, but in place of the UUC sequence is CGC. This suggests that it is the structure or the spacing that these three nucleotides form that is important for localization, rather than the actual sequence. Further evidence that this may be the case comes from RNA2DSearch (Hamilton *et al.*, 2009). Two transposable elements, *G2* and *Jockey*, were found to contain GLS/ILS-like hairpins (G2LS and JLS respectively) that could localize to the cap when injected into

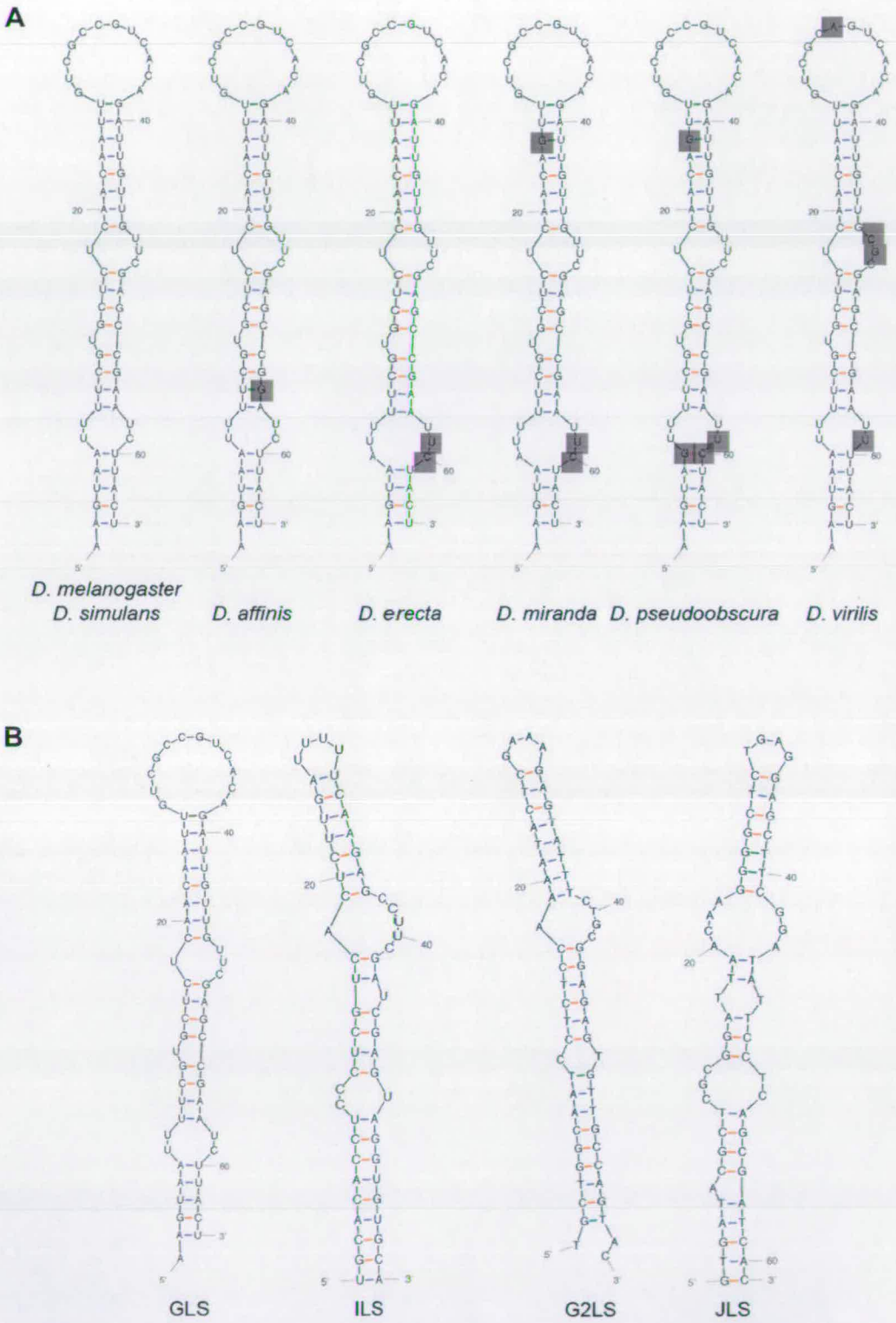

Figure 3.11 (A) Predicted GLS secondary structure from the different *Drosophilids*. Nucleotides that differ from *D. melanogaster* are shown in grey. **(B)** Predicted secondary structures of the G2 and Jockey localization signals (G2LS and JLS respectively).

oocytes. Both of these hairpins contain an internal loop in a similar position to the first internal loop of the GLS and ILS, but the sequences are different from each other, and from the GLS and ILS (Fig. 3.11B).

Tetraloops and the importance of the hairpin loop in dorso-anterior localization

It was hoped that replacement of the hairpin loops of M1 with a UUCG tetraloop would reduce multimerization. However, tetraloop GLS does not localize to the cap, and so was not prepared for NMR. ILS tetraloop, in contrast, does localize and I3 tetraloop RNA can be prepared for NMR. This experiment also highlights features important for localization and also illustrates how mutagenesis experiments can be used in conjunction with NMR structure determination to identify what is required for localization.

In the case of the tetraloop GLS, abolition of localization can mean that structure and/or specific nucleotides within the wild type hairpin loop are required for localization. For the ILS, the UUUU hairpin loop can be replaced by a UUCG tetraloop, and localization is not affected. A UUUU tetraloop is predicted to have a different structure to a UUCG tetraloop. UUCG forms a very stable loop (Antao *et al.*, 1991; Tuerk, 1988), whereas the UUUU loop is very flexible, forming a number of conformations that differ mainly in their base stacking (Koplin *et al.*, 2005). This indicates that the sequence and structure of the ILS hairpin loop can be changed and localization is not affected. However, preliminary ILS mutatgenesis experiments suggest that replacement of the UUUU loop with an even less stable (Groebe and Uhlenbeck, 1988) CCCC loop abolishes localization. This leaves the possibilities that either a solvent exposed U in the loop (which both the UUUU and UUCG loops have) is required or that a loop of any sequence with a certain level of stability is required in terms of the spacing/structure it provides, and the CCCC loop is not stable enough.

An alternative explanation is that a different part of the ILS plays the role provided by the hairpin loop in the GLS. This has been shown to be the case for the RNAs

recognised by the human spliceosomal protein U1A. This protein recognises the same sequence in a different structural context in two RNA molecules, hairpin II of U1 snRNA, and the 3'UTR of its own pre-mRNA (Jovine *et al.*, 1996; Tang and Nilsson, 1999). It may also be the case that although the GLS and ILS do share a common feature in the first internal loop, the two signals may be recognized in different ways by diverse *trans*-acting factors, and that they do not represent consensus elements for dorso-anterior localization.

Future experiments

Further mutagenesis experiments are therefore needed to study the role of the hairpin loop and the first internal loop in the GLS and ILS in order to determine whether these elements are part of a consensus for dorso-anterior cap localization. The absolute requirement for these elements as well as the relative importance of sequence and structure for localization can be tested in this way. In mutagenesis experiments specific nucleotides or a number of nucleotides can be replaced with others to specifically change sequence and conserve structure, or to change both sequence and structure. Alternatively, non-nucleotide mimetics such as polyethylene glycol can be used to replace nucleotides without changing sequence, to look at the importance of the spacing provided by specific nucleotides in a structure.

It is also hoped that refinement of the key determinants of dorso-anterior localization by NMR and mutagenesis can be used to refine programs such as RNA2DSearch, improving genome-wide searches for RNA secondary structures similar to known localization elements. Programs that can predict three-dimensional structure using sequence information, such as the MC-Fold and MC-Sym (Macromolecular Conformations by SYMbolic programming) pipeline are now also becoming available (Parisien and Major, 2008). Constraints supplied by the known NMR structures may also improve the prediction of the three-dimensional structures of new localization elements, such as the G2LS and the JLS.

Improvements to NMR sample preparation and studies

The large size of M1 and I3 RNAs in terms of NMR, enhance the problem of resonance overlap encountered when studying RNA by NMR. Resonance overlap can be reduced in a number of ways. Fragmentation of the RNA into smaller stable subdomains, used in the structure determination of the 77-nucleotide, 25kDa HCV IRES domain II (Lukavsky *et al.*, 2003), was employed here to reduce complexity. Fragmentation does raise the question that the chosen subdomains do not maintain the same conformation in and out of the context of the full RNA. In the case of M1, it has not been possible to make the full-length RNA, or the loop fragment (full and fragmented tetraloop I3 has been made and can be used), so this question cannot be answered at the present time.

Multimerization through the GC-rich M1 hairpin loop hindered the study of this RNA. Replacing this loop with a tetraloop meant that the RNA did not localize to the dorso-anterior cap, and so the tetraloop M1 was not used. The hairpin loop is also unstructured and flexible, and so is not easy to study by NMR. Mutagenesis will be used to search for loop variants that can still localize but where multimerization is reduced, and where NMR is possible. These loop variants can then be fragmented, and the fragments and full length RNAs used in structure determination. It must also be considered that multimerization of the GLS is functionally relevant and required for GLS localization within the oocyte. There is a precedent for this in that RNA-RNA interactions are also thought to be important for *bicoid* localization, where dimerization of *bicoid* between specific hairpin loop structures is essential for the binding of Staufen (Ferrandon *et al.*, 1997).

The structures of some of the largest RNAs studied by NMR have been determined not by fragmentation, but by selective and segmental labelling techniques, providing alternative methods for reducing resonance overlap. Nucleotide specific isotopic labelling was used to aid resonance assignment for the 101-nucleotide core encapsidation signal of Moloney Murine Leukaemia Virus (MMLV) (D'Souza *et al.*, 2004), and the 30kDa GAAA tetraloop-receptor complex (Davis *et al.*, 2005).

Segmental labelling (differential labelling of different segments of RNA and ligation to create the full length RNA) has also been used to determine the structure of the 77-nucleotide dendritic targeting element (DTE) of BC1 RNA (Tzakos *et al.*, 2006), and has made the 313-nucleotide, 100kDa HCV IRES accessible to NMR measurements (Kim *et al.*, 2002). It is possible that these techniques could be applied to assigning the structures of the GLS and ILS.

Finally, an alternative approach such as X-ray crystallography could be considered if proteins able to bind the GLS and ILS were identified and crystallized with the RNA. This would dramatically increase the size of structure that could be determined, meaning that the full-length GLS and ILS could be studied. Furthermore, addition of potential binding partners to an NMR sample can be used to study changes in conformation upon protein binding. The next chapter describes the purification of GLS-interacting proteins, using a method known as GRNA chromatography.

BIOCHEMICAL IDENTIFICATION OF *GRK TRANS*-ACTING FACTORS

Introduction

Localized mRNAs are organized into and transported in large RNP particles containing many RNAs and proteins. The first evidence that this was the case resulted from a study of *MBP* mRNA localization in live oligodendrocytes (Ainger *et al.*, 1993). Here, it was shown that injected exogenous MBP mRNA appeared as intracellular granules of uniform size, around 300 nm in diameter. Indeed, most studies of mRNA localization in living cells, either with labelled injected RNA or tagged endogenous mRNA, rely on the formation of RNP particles that can be visualized using the light microscope (Bullock *et al.*, 2006; Ferrandon *et al.*, 1994; Macdougall *et al.*, 2003; Vendra *et al.*, 2007; Weil *et al.*, 2008; Wilkie and Davis, 2001; Zimyanin *et al.*, 2008). RNA transport particles have also been visualized by electron microscopy. Nonmembrane-bound electron-dense particles that vary in size between 70-600 nm have been shown to be present in the *Drosophila* oocyte and found to contain multiple *grk* mRNA molecules and proteins including Dynein, BicD, Egl and Sqd (Delanoue *et al.*, 2007).

The idea that localized mRNAs assemble into large particles is further supported by the purification of large granules containing localized mRNAs from brain extracts. Sedimentation experiments have identified dense particles 150-1000 nm in diameter (Elvira *et al.*, 2006; Krichevsky and Kosik, 2001), whilst large RNP particles (up to 1000S) have been purified using the C-terminal domain of Kinesin KIF5 (Kanai *et al.*, 2004). Transport RNPs are thought to contain many proteins that are involved in the multiple steps of mRNA localization, such as recognition, transport, translational regulation and anchoring of the localized transcript. However, although a number of protein components that can associate with localized mRNAs, or are required for mRNA localization have been identified (for *grk*, see table 4.1), many questions

remain about the biochemical nature of transport RNPs, the proteins that are present in them, what jobs these proteins do and how they are organized.

Genetic studies have identified a number of *trans*-acting factors required for mRNA localization in various systems. *Drosophila* is an excellent model system in which to do such studies, as defects in mRNA localization lead to patterning defects in the egg and embryo. A number of genetic screens, carried out over the last 30 years have identified factors required for *bcd* and *osk* mRNA localization in the oocyte. These include Stau, Mago, Exuperentia (Exu) and Swallow (Swa) (Berleth, 1988; Boswell *et al.*, 1991; Frohnhöfer and Nüsslein-Volhard, 1987; Kim-Ha *et al.*, 1991; Schüpbach and Wieschaus, 1986; Schüpbach and Wieschaus, 1989; St Johnston *et al.*, 1991; St Johnston and Nüsslein-Volhard, 1992). Similarly, genetic screens for dorso-ventral defects in eggs and embryos have identified a number of factors required for *grk* localization and signaling, including Sqd and K10 (Kelley, 1993; Manseau and Schüpbach, 1989; Schüpbach, 1987; Schüpbach and Wieschaus, 1991; Wieschaus, 1978) (table 4.1). Essential genes that also play a role in mRNA localization were identified in more recent genetic screens that made use of the FLP-dominant female sterile (DFS) technique (Martin *et al.*, 2003) to screen for mutants that disrupt the localization of GFP-Stau. In this way, the ESCRT II complex, previously shown to be required for endosomal protein sorting, was shown to be required for *bcd* mRNA localization (Irion and St Johnston, 2007).

TABLE 4.1 *Trans*-acting factors previously identified as being required for *grk* mRNA localization/translational regulation/anchoring.

Factor	Role	Interactions	Source
Dynein	Transport/anchoring	Dynein light chain (DLC) can interact with *grk* 3'UTR Dynein present in transport particles and sponge bodies	Delanoue *et al.*, 2007; Januschke *et al.*, 2002; Jaramillo *et al.*, 2008; Macdougall *et al.*, 2003; Rom *et al.*, 2007
BicD	Transport	Present in transport particles and sponge bodies Interacts with Dynactin components	Clark *et al.*, 2007; Delanoue *et al.*, 2007; Hoogenraad *et al.*, 2001; Short *et al.*, 2002
Egl	Transport	Present in transport particles and sponge bodies Interacts with DLC	Clark et al., 2007; Delanoue et al., 2007; Mach and Lehmann, 1997; Navarro et al., 2004
Sqd	Localization/translational repression/anchoring	UV cross-links to *grk* 3'UTR, GLS, 5'UTR, and also an RNA lacking the GLS (ORF16ΔGLS) Interacts with Hrb27C, Imp, PABP, Cup, K10 and Bruno Present in transport particles and sponge bodies	Cáceres and Nilson, 2008; Delanoue *et al.*, 2007; Jaramillo *et al.*, 2008; Jennifer Goodrich and Trudi Schüpbach, unpublished data; Kelley, 1993; Norvell *et al.*, 1999
Hrb27C	Localization/translational repression	UV cross-links to *grk* 3'UTR Interacts with Sqd, Imp, Otu, PABP and Cup Present in sponge bodies	Delanoue *et al.*, 2007; Goodrich *et al.*, 2004
Imp	Localization/translational regulation. May compete with Sqd and Hrb27C	Highest affinity binding to *grk* 5'UTR and 5' of coding sequence Interacts with Sqd and Hrb27C	Geng and Macdonald, 2006
Otu	Localization/potentially translational repression	Interacts with Hrb27C	Goodrich *et al.*, 2004
K10	Potentially localization/translational repression/anchoring	Interacts with Sqd	Jaramillo *et al.*, 2008; Norvell *et al.*, 1999; Wieschaus, 1978
Bruno	Translational repression	UV cross-links to *grk* 3'UTR Interacts with Sqd and Vasa	Filardo and Ephrussi, 2003; Webster *et al.*, 1997
PABP	Translational activation	Interacts with Sqd, Hrb27C and Cup	Clouse *et al.*, 2008
Cup	Localization/translational repression	Interacts with Sqd, Hrb27C and PABP	Clouse *et al.*, 2008
Encore	Localization/translation	Interacts with PABP	Hawkins *et al.*, 1997

TABLE 4.1 (continued) *Trans*-acting factors previously identified as being required for *grk* mRNA localization/translational regulation/anchoring.

Vasa	Translational activation	Interacts with Bruno	Styhler *et al.*, 1998; Tomancak *et al.*, 1998 Webster *et al.*, 1997
Orb	Localization and translation activation		Chang *et al.*, 2001; Christerson and McKearin, 1994
UAP56	Localization		Meignin and Davis, 2008

Despite the identification of several factors by genetics, the actual functions of a number of these proteins, such as Exu, Swa and K10 in mRNA localization have remained unclear. Factors such as Capu and Spire have also since been shown to have indirect roles in mRNA localization via the organization of the cytoskeleton within the oocyte (Dahlgaard *et al.*, 2007). Genetic approaches may also fail to identify direct-acting localization factors due to the potential for redundancy among proteins that are in the same localization complex or due to factors having inessential roles in localization. For example, mutation of *Imp* does not substantially alter *grk* expression and localization, but does partially suppress a *grk* misexpression phenotype. This suggests that Imp does contribute to *grk* regulation but may act redundantly and may not have an essential role. Consistent with this, overexpression of Imp disrupts *grk* mRNA localization (Geng and Macdonald, 2006). Similarly, mutants lacking *Imp* localize and translate *osk* normally, but mutation of Imp binding sites within the *osk* transcript prevents *osk* translation and anchoring (Munro *et al.*, 2006). This indicates that a 'factor X' is also required to act through Imp binding sites for *osk* regulation. In the case of Hrb27C, differences in the alleles examined have meant that a gene has been shown to be required for *grk* mRNA localization or not in different studies (Goodrich *et al.*, 2004; Huynh *et al.*, 2004; Yano *et al.*, 2004).

Due to the above reasons, an alternative and complementary approach is also needed to obtain a more detailed picture of the components of transport RNPs. Potential *trans*-acting factors have been identified using biochemical approaches, and when coupled with subsequent genetic/functional analysis, these have isolated a number of novel factors. UV cross-linking analysis was originally used to identify proteins that could associate directly with localization element RNA. Experiments with *Xenopus* oocyte extract showed that the VLE is the binding site for at least 6 different oocyte proteins (Mowry, 1996) subsequently shown to include Vera/Vg1RBP (Deshler *et al.*, 1998), VgRBP60 (Cote *et al.*, 1999) and VgRBP71 (Kolev and Huber, 2003). Two proteins, Exl (Macdonald *et al.*, 1995) and BSF (Mancebo *et al.*, 2001), able to bind regions required for localization in the *bcd* 3'UTR were also identified in this way. However, a caveat of UV cross-linking is that factors that are part of a complex through protein-protein interactions rather than direct contact with the RNA will not

be identified. Gel retardation of an RNA corresponding to a *bcd* localization element (IV/V domain) able to direct normal patterns of localization during oogenesis, combined with fractionation, further identified a large ovarian protein complex containing at least three RNA binding proteins, Smooth (Sm; related to VgRBP60), Modulo (Mod), Swa, PABP and Nod (a member of the Kinesin family of motor proteins (Arn *et al.*, 2003). Subsequent UV cross-linking experiments showed that only Mod in this complex directly associated with the RNA and *mod* mutants displayed mislocalized *bcd* mRNA.

Affinity purification using localization element RNA or proteins known to be important for localization has also been used as a method to purify complexes of proteins that could be components of localization RNPs. In density gradient centrifugation, GFP-Exu purified with a large RNase sensitive complex and subsequent co-immunoprecipitation showed that this complex contained several other proteins including Yps, and also *osk* mRNA (Wilhelm *et al.*, 2000), whilst a two-step tandem RNA affinity purification (TRAP) with an individual *nos* localization element was used to isolate the hnRNP M homologue Rumpelstiltskin (Rump) (Jain and Gavis, 2008). As stated previously, the C-terminal domain of Kinesin KIF5 was used to purify a large granule in mouse brain extracts. 42 proteins were identified in this granule with mRNAs for *CamKIIα* and *Arc*. The major proteins identified included factors already known to be important for dendritic transport such as FMRP and Stau, and colocalized with Kinesin-associated granules in dendrites. Such approaches have therefore been very successful in identifying known and novel components of transport RNPs.

In order to identify *trans*-acting factors required for *grk* localization and translational regulation other than those already isolated and characterized through genetic methods (table 4.1), I have taken a biochemical approach using the affinity of factors for GLS-containing RNA. Potentially interesting factors are then analyzed further genetically (Chapters 5 and 6) to look at function in mRNA localization. Factors able to bind to RNA containing the GLS could potentially be components of *grk* transport particles or sponge body anchoring structures, as *grk* lacking the GLS is not

incorporated into these structures (Delanoue *et al.*, 2007). The GLS is also sufficient for localization in the oocyte following injection, meaning it must be able to recruit all the factors necessary for *grk* localization in the oocyte cytoplasm (Van De Bor *et al.*, 2005).

An affinity chromatography approach known as GRNA chromatography, originally developed to examine localization RNP formation on the vegetal localization element (VLE) of *Vg1* mRNA (Czaplinski *et al.*, 2005), was adapted for use with *Drosophila* ovarian extract. This method was previously used successfully to identify the hnRNP D family protein 40LoVe as a specific VLE binding protein, and was also used in *Drosophila* ovary translation extracts (at the same time as this work was being completed) to show that Bruno, Cup and Me31B associate with BRE RNA in *osk* translation silencing particles (Chekulaeva *et al.*, 2006). By using such an approach it is possible to understand *grk* localization and translational regulation in greater molecular detail and isolate novel factors not previously identified via genetic screens. It is also possible to answer deeper questions regarding the proteins required for mRNA localization as a whole, including whether other factors associated with *osk* regulation also interact with *grk*, and whether there is a core complex of factors required for mRNA localization in oocytes, and also between oocytes and other tissues such as the nervous system.

Aims of this chapter

- To use GRNA chromatography to isolate components of the *grk* transport RNP that can be studied further using genetic techniques, and so obtain greater insight into the requirements for and the regulation of *grk* localization in the *Drosophila* oocyte.
- To compare the identified factors with factors known to be required for the localization of other mRNAs in the literature, and to ask whether some of the same factors are required across localized mRNAs.

Results

A 21 amino acid peptide of the λ phage N antiterminator protein (λ peptide) binds specifically to the BoxB sequence of the N utilization site of λ phage RNA with a K_d of approximately 5.2 nM (Cilley and Williamson, 1997). Glutathione sepharose was converted into an RNA affinity matrix (Czaplinski *et al.*, 2005) through binding GST-λ peptide fusion protein (GSTλ) that in turn is bound to two tandem copies of the BoxB RNA hairpin (Fig. 4.1) fused to the RNA of interest. For the identification of factors specifically able to bind the GLS, GRNA resins were prepared using ORF16, ORF16ΔGLS, GLS, or as a negative control, non-localizing hb RNA (Fig. 4.2A). ORF16 RNA consists of the GLS surrounded by 211 nucleotides spanning the 3' of the 5'UTR into the 5' of the *grk* open reading frame. ORF16ΔGLS is the same sequence, but lacks the GLS. GRNA resins with the different RNAs were assembled and the supernatant collected for assessment of RNA loading onto the column. This was done by measurement of OD at 260 nm and by denaturing agarose gel electrophoresis (Fig. 4.2B). By absorbance measurements, between 59 and 82% of RNA loaded actually bound to the column (GLS, 81.6%; ORF16, 69.1%; ORF16ΔGLS, 67.8%; hb, 59.6%). The same GRNA resins were then incubated in *Drosophila* ovary lysate, followed by washing and elution of all bound proteins (Fig. 4.3A). Total lanes were then analyzed by mass spectrometry (in collaboration with Juri Rappsilber). For this, eluates were separated again by SDS-PAGE for a short distance, just long enough to be able to separate and remove GSTλ as shown (Fig. 4.3B). A caveat of this current protocol is that only proteins that migrate slower than GSTλ during electrophoresis are analyzed. Work is ongoing to change the conditions so that GSTλ is not eluted from the resin with the RNA and RNA-associating proteins. This may also eventually allow eluates to be analyzed by mass spectrometry without the need for SDS-PAGE, reducing the loss of sample during these steps.

The results of two independent experiments are shown in table 4.2 (for full tables of all proteins see appendix A.4). A number of proteins did specifically associate with the GLS, including Glorund (Glo), a factor shown to bind the translational control

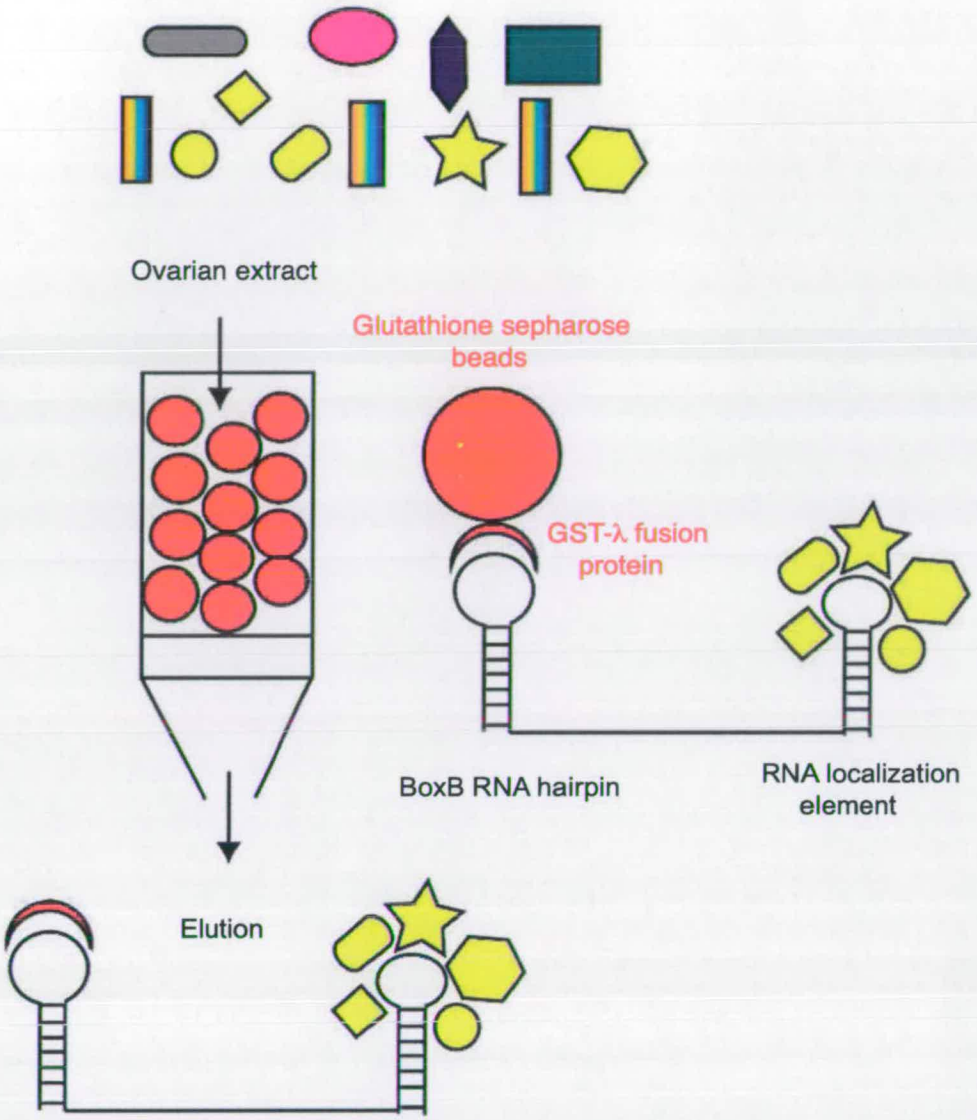

Figure 4.1 Illustration of the GRNA chromatography method. The λ peptide/BoxB interaction is used to make an RNA affinity matrix. GST-λ peptide fusion protein interacts with the BoxB RNA hairpin fused to the RNA of interest and to glutathione sepharose beads. This forms the GRNA resin, on which proteins that interact with the RNA of interest can be isolated.

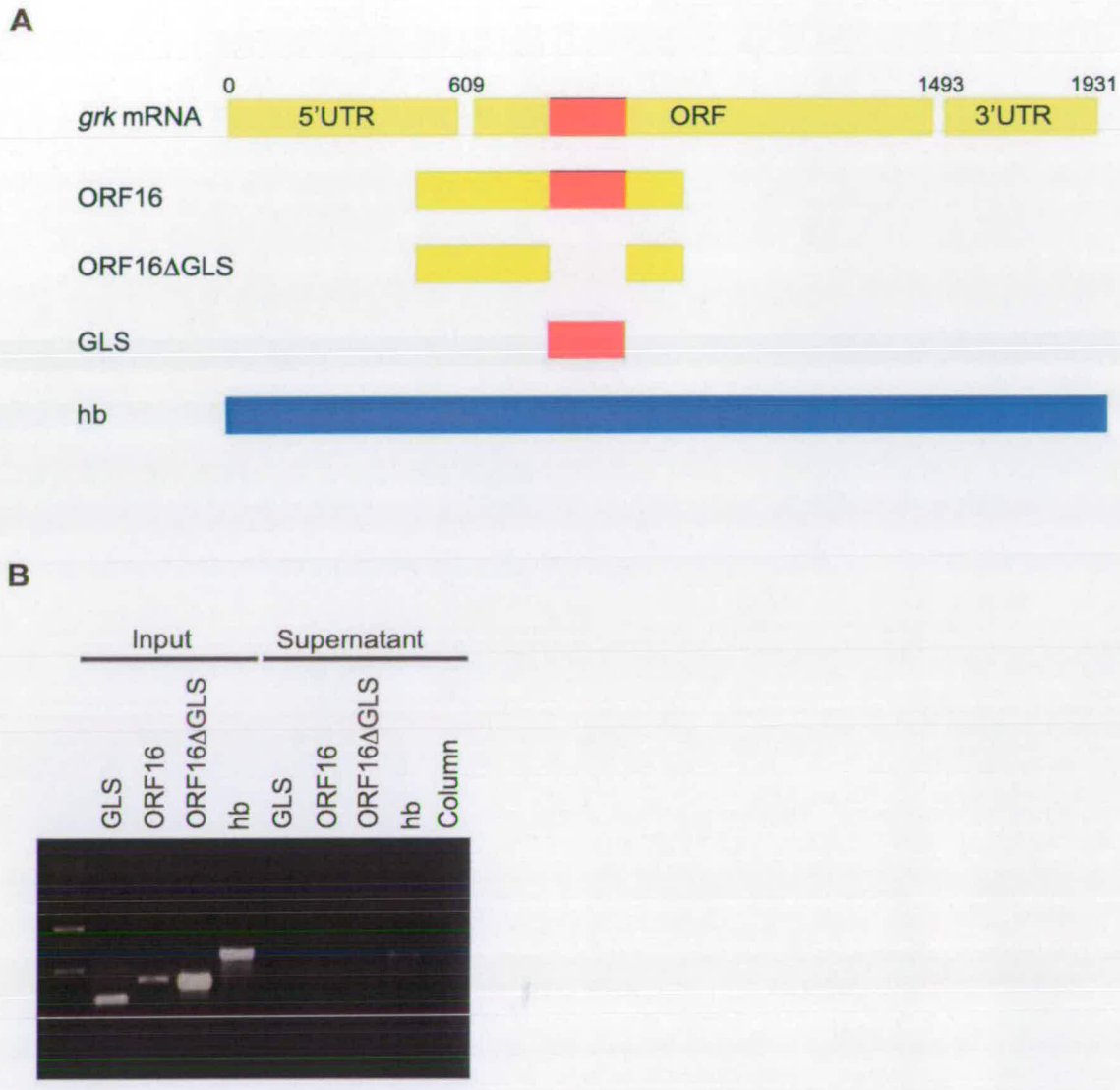

Figure 4.2 Preparation of GRNA resins for the isolation of *grk* and GLS binding proteins. (A) GRNA resins were made with the following RNAs: ORF16, GLS plus surrounding 211 nucleotides; ORF16ΔGLS, ORF16 lacking GLS; GLS alone; hb, hunchback as non-localizing RNA control. **(B)** Loading of RNA onto the GRNA column was assessed by denaturing agarose gel electrophoresis.

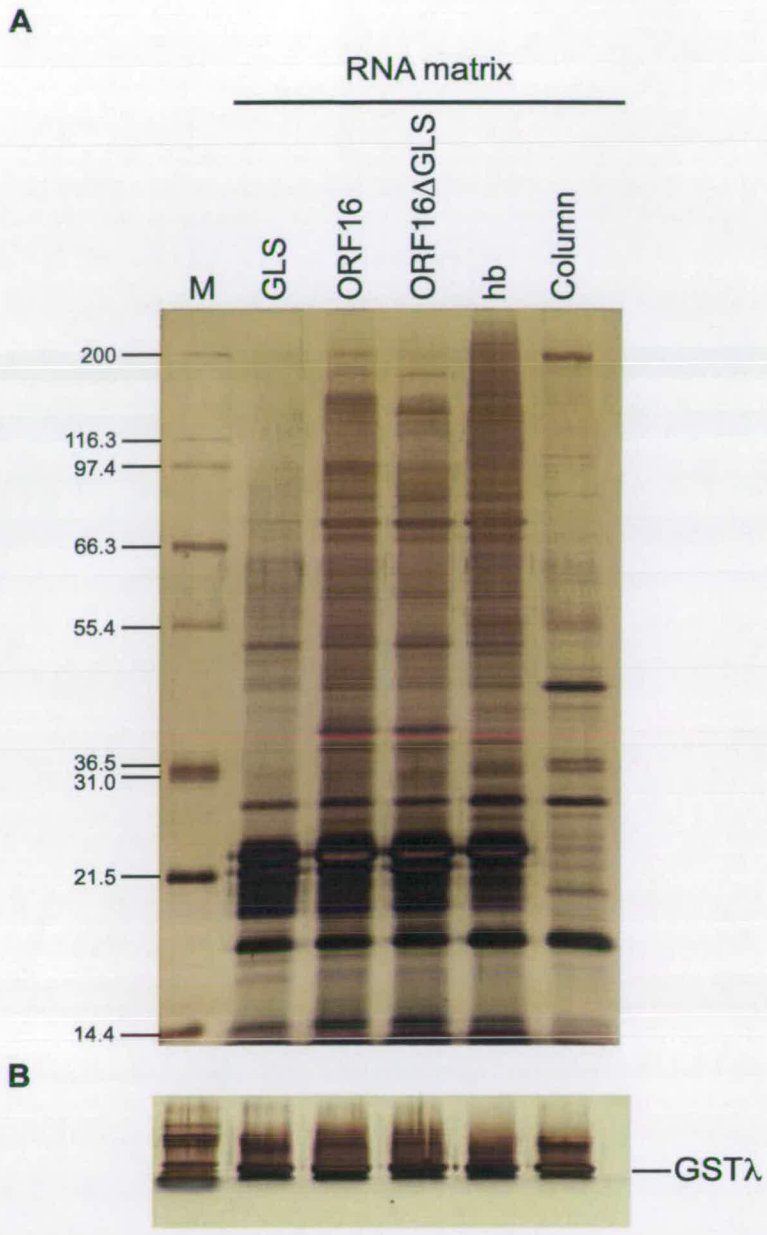

Figure 4.3 GRNA can be used to identify *grk* and GLS binding proteins. (A) A silver-stained 10% SDS-PAGE gel of total eluate from GLS RNA (lane 2), ORF16 RNA (lane 3), ORF16ΔGLS RNA (lane 4), hb RNA (lane 5) and column alone (lane 6) GRNA resins. Lane 1 (M) contains molecular weight markers with the sizes indicated to the left. **(B)** All proteins above GSTλ in each lane were taken for identification of protein mixtures by mass spectrometry. The GSTλ protein is indicated.

element (TCE) of *nos* mRNA. The ability of the TCE to repress translation *in vivo* reflects its ability to bind Glorund (Kalifa *et al.*, 2006). However, apart from Me31B, Eflα and PABP, there was no overlap in the proteins able to recognize the GLS and ORF16. As the GLS is able to recruit *trans*-acting factors necessary and sufficient for localization in the cytoplasm of the oocyte following injection, it was expected that a higher number of proteins would associate with the GLS, including for example Sqd (which can bind the GLS in cross-linking experiments). It was thought that the shorter GLS did not fold correctly leading to a number of proteins failing to recognize the RNA. All further analysis therefore used the ORF16/ORF16ΔGLS comparison to look at GLS-interacting proteins.

Proteins that could specifically associate with ORF16 RNA were identified by subtracting the proteins able to associate with ORF16ΔGLS and hb RNAs from the proteins able to associate with ORF16. In this way proteins only able to bind in the presence of the GLS (either directly through the GLS, or through surrounding regions that adopt the correct structure only when the GLS is present) were isolated. Candidate proteins found to associate with ORF16 only (or with both ORF16 and GLS) in the initial experiment were Me31B, Sqd, Dpl, Bicaudal C (BicC), Hrb27C, Eflα, Deadhead (Dhd), Exu, CG5205, Rigor mortis (Rig), PABP, CG17838, Fibirallin (Fib), CG6745, Hephaestus (Heph) and a small number of ribosomal proteins. A repeat of the experiment produced additional candidates. There was some overlap between proteins identified and Me31B, Sqd, Eflα, Exu, PABP, CG17838 and Heph bound only ORF16 in the repeat. The additional candidates were Upf1, Argonaute 2 (Ago2), NXF1, UAP56, Transcription-associated protein 1 (TRA1) and Piwi. The purification of different sets of ORF16 interacting proteins in different experiments could be due to fluctuations in non-specific binding of proteins to the RNA, and it is highly likely that some candidates are binding non-specifically and do not interact with *grk* mRNA *in vivo*.

Comparison of the factors known to be required for *grk* regulation (table 4.1) with the factors identified by GRNA (table 4.2) reveals that a number of known proteins, such as Sqd, Imp, Hrb27C, PABP and UAP56 were isolated, indicating that the

experiment successfully identified *grk trans*-acting factors. However, other known factors such as Bruno, Cup and Otu were not isolated by GRNA. Dynein heavy chain was identified as able to associate with ORF16, ORF16ΔGLS and hb, but the lack of other Dynein motor components, and accessory factors such as BicD and Egl is striking. This could be due to the conditions used for the GRNA binding reaction and wash steps-perhaps the factors that have been isolated are the factors that can associate with GLS-containing RNA with the greatest affinity. RNP complexes are also dynamic complexes, and it is likely that the components of these complexes change as localization proceeds. This approach takes no account of different stages of oogenesis and localization and so proteins required at certain stages may not be isolated. A number of proteins (for example regulators of translation) may also bind elsewhere within the *grk* transcript and will not have been detected by the ORF16 GRNA experiment. For example the BREs required for Bruno binding reside within *grk* 3'UTR.

hb was used as the non-localizing RNA control. However, it is possible that proteins required for *grk* regulation could also bind *hb*. For example, Mod associated with all RNAs, but has been shown to be required for *bcd* mRNA localization in the *Drosophila* oocyte. Vasa also associated with all RNAs. Trailer hitch (Tral) associated with ORF16, ORF16ΔGLS and hb, but could also be interesting due to its function with Me31B in FMRP-mediated translational repression (Barbee *et al.*, 2006), discussed later in this chapter.

TABLE 4.2 GRNA results. The proteins able to associate with ORF16 are listed in black. Y indicates whether a given ORF16-interacting protein could also associate with GLS, ORF16ΔGLS or hb RNA. (y) indicates that only one peptide from the given protein was identified in the GRNA experiment. The results of a second, repeat experiment are highlighted in blue. The repeat column indicates whether a protein was able to specifically associate with ORF16 in the repeat experiment. A blue Y in other columns indicates whether a given protein could also associate with other RNAs. Where the protein name is in blue, this protein was identified only in the repeat experiment. For a full list of proteins for both experiments see Appendix A4.

Accession number	Protein name	Molecular function	GLS	ORF16ΔGLS	hb	Repeat-ORF16
S06602	Modulo	RNA, DNA, protein binding	Y	Y	Y	
AAN10728	Me31B	ATP-dependent RNA helicase; RNA binding	Y			Y
Q8IGE9_DROME	Growl	RNA binding; ATP binding	Y	Y	Y	
Q8IR99_DROME	Imp	mRNA binding				
VJFF1	Vitellogenin I precursor	structural molecule; catalytic activity		Y	Y	Y
A25876	Vitellogenin III precursor	structural molecule; catalytic activity	Y	Y	Y	Y
Q9VTZ0_DROME	Trailer hitch (Tral)	unknown		Y	Y	
S26759	Protein on ecdysone puffs (pep)	DNA binding; ssRNA binding; Zn ion binding		Y		
XUFF1	Glutathione S transferase D1	Glutathione transferase activity	Y	Y		
SQD_DROME	Squid (Sqd)	mRNA binding				Y
Q7KR17_DROME	Dodeca satellite binding protein 1 (Dp1)	ssDNA binding; satellite DNA binding; mRNA binding				
Q24009_DROME	Bicaudal C (BicC)	RNA binding; protein binding				
AAL28590	Vitellogenin II precursor	structural molecule; catalytic activity		Y	Y	Y
RB27C_DROME	Hrb27C	ssDNA binding; mRNA binding			Y	Y
EF1A1_DROME	Ef1alpha48D (Ef1α)	translation elongation factor activity; GTPase activity; GTP binding	Y			Y
S02160	DNA topoisomerase Top2	DNA binding; DNA topoisomerase activity; mRNA binding; satellite DNA binding			Y	
Q95RE4_DROME	Ypsilon schachtel (Yps)	DNA binding; mRNA binding		Y	Y	
AAF57901	Glutathione S transferase S1	glutathione transferase activity	Y	Y	Y	
S47867	Thioredoxin-like protein Deadhead (Dhd)	disulfide oxidoreductase activity				
Q3KN45_DROME	Hsc70-4	ATPase activity; ATP binding; unfolded protein binding; chaperone binding	Y	Y	Y	
AAF57429	Exuperentia (Exu)	sugar binding	(y)			Y
Q9VF56_DROME	CG5205	RNA helicase activity; ATP-dependent helicase activity; nucleic acid binding; ATP binding				

Q541C2_DROME	GAPDH2	glyceraldehyde-3-phosphate dehydrogenase activity; NAD binding		Y	Y	
AAF57440	Rigor mortis (Rig)	ligand-dependent nuclear receptor transcription coactivator activity; protein binding				
S30887	Polyadenylate-binding protein (PABP)	poly(A) binding; protein binding; mRNA binding;	(y) Y			Y
RS3A_DROME	40S ribosomal protein S3a	structural constituent of ribosome	Y	Y	Y	
Q5BIL1_DROME	RpL14	structural constituent of ribosome				
A4V364_DROME	CG17838	mRNA binding				Y
Q9W1V3	Fibirallin (Fib)	mRNA binding				
Q9V3W7_DROME	SF2	mRNA binding; protein binding			Y	
Q9VSK9_DROME	CG6745	pseudouridine synthase activity; RNA binding				
Q9W1B9_DROME	RpL12	structural constituent of ribosome	Y		Y	
S35620	Ribosomal protein S3.e	structural constituent of ribosome		Y		
Q95WY3_DROME	Nucleolar KKE/D repeat protein Nop56	unknown		Y		
Q3T7F7_DROME	Polypyrimidine tract binding protein (PTB)-Hephaestus (Heph)	poly-pyrimidine tract binding; mRNA binding				Y
HHFF83	Heat shock protein 83	ATPase activity, coupled; ATP binding; unfolded protein binding	Y	Y	Y	Y
RS19A_DROME	RpS19	structural constituent of ribosome	Y			
RENT1_DROME	Regulator of nonsense transcripts I homologue (Upf1)	helicase activity				Y
AGO2_DROME	Argonaute 2 (Ago2) protein	protein binding; siRNA binding; translation initiation factor activity; endoribonuclease activity				Y
NXF1_DROME	Nuclear RNA export factor 1 (Protein tip-associating) (Protein small bristles) (DmNXF1)	mRNA export from nucleus; adult behavior; long-term memory; poly(A)+ mRNA export from nucleus				Y
VASA_DROME	ATP-dependent RNA helicase Vasa	RNA helicase activity; ATP-dependent helicase activity; RNA binding; protein binding; ATP binding	Y	Y	Y	Y
UAP56_DROME	ATP-dependent RNA helicase WM6 (DEAD box protein UAP56) (HEL/UAP56)	RNA helicase activity; RNA splicing factor activity, transesterification mechanism; ATP-dependent RNA helicase activity; ATP binding; nucleic acid binding				Y
DYHC_DROME	Dynein heavy chain, cytosolic (DHC64C)	ATPase activity, coupled; microtubule motor activity; motor activity; ATP binding; cysteine-type endopeptidase activity	Y	Y	(y)	Y
TRA1_DROME	Transcription-associated protein 1 (dTRA1)	transcription regulator activity; protein kinase activity; binding; phosphotransferase activity				Y
PIWI_DROME	Piwi	RNA binding; mRNA binding; protein binding	Y			Y

TABLE 4.2 (continued) GRNA results.

Proteins specific to GLS only

Accession number	Protein name	Molecular function
Q9VGH5_DROME	Glorund	mRNA binding
SMD2_DROME	SmD2	unknown
Q95RG1_DROME	RpS9	structural constituent of ribosome
S08118	Histone His2Av	DNA binding
NH2L1_DROME	Hoi-polloi	mRNA binding
AAF52576	CG18591	RNA splicing factor activity, transesterification mechanism

I have also used GRNA chromatography to isolate proteins specifically able to associate with the ILS in order to answer more specific questions about the machinery that transports *grk* and *I* Factor mRNA to the dorso-anterior corner. These questions include whether the GLS and ILS are recognized by the same factors and use the same machinery, other than dynein and microtubules, to localize to the dorso-anterior, or whether there subtle differences in the proteins able to associate with the GLS and ILS. In addition, the experiment was also designed to identify factors able to associate with the A loop, and so perhaps explain how the A loop promotes ILS localization.

For identification of factors specifically able to bind the ILS and the A loop, GRNA resins were prepared using A+ILS, AΔILS, and A+ILS$_{mut}$ (Fig. 4.4A). ORF16, ORF16ΔGLS and hb were also used as previously described. A+ILS consists of the ILS and the adjacent A loop within 150 nucleotides of surrounding sequence. AΔILS is the same sequence lacking the ILS, whilst A+ILS$_{mut}$ is the same sequence as A+ILS containing two nucleotide substitutions in the upper stem of the ILS. These mutations have previously been shown to disrupt base-pairing within this stem and to disrupt localization of injected ILS within the oocyte (V. Van De Bor, unpublished). Once again, loading of RNA onto the resin was assessed by measurement of the OD_{260} and by agarose gel electrophoresis (Fig. 4.4B). 65% to 79% of RNA loaded bound to the resin (ORF16, 65.3%; ORF16ΔGLS, 69.6%; A+ILS, 70.3%; AΔILS, 79.9%; A+ILS$_{mut}$, 72.2%; hb, 66.1%). Again, total lanes were submitted for analysis by mass spectrometry (Fig. 4.4C). However, this is still in progress and we are still awaiting the results of this analysis. It is anticipated that the protein composition of the *I* Factor and *grk* RNP complexes are very similar, but could be subtly different. An important difference is that localization of the endogenous *I* Factor during transposition requires ORF1 protein (Seleme *et al.*, 1999), and may require factors that will import the RNA into the oocyte nucleus once localization is complete, a step that is missing in the case of *grk*.

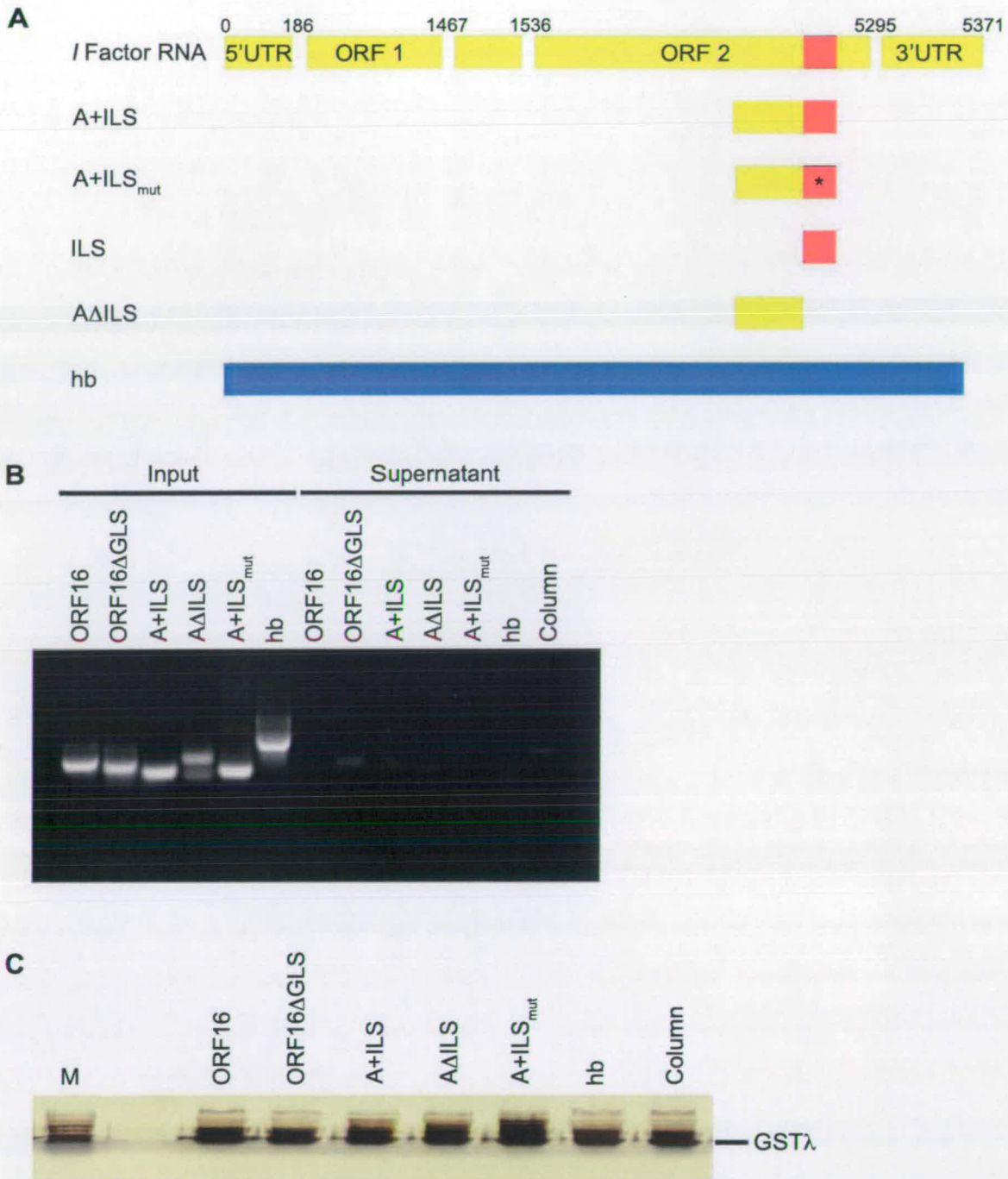

Figure 4.4 Preparation of GRNA resins for the isolation of *I* Factor and ILS binding proteins. (A) GRNA resins were made with the following RNAs: ORF16, ORF16ΔGLS, hb and column as previously described; A+ILS, the ILS plus the adjacent A loop within surrounding sequence; AΔILS, A+ILS lacking the ILS; $A+ILS_{mut}$, A+ILS which carries mutations in the upper stem of the ILS that disrupt localization (V. Van De Bor, unpublished). **(B)** Loading of RNA onto the GRNA column assessed by agarose gel electrophoresis. **(C)** Preparation of final eluate from each resin for mass spectrometry.

Discussion

GRNA has been used as a screen for transport/anchoring components able to associate either with GLS-containing RNA, or with other proteins that can directly contact the RNA throughout oogenesis. In this way, a number of known and candidate *grk trans*-acting factors were successfully identified. As discussed previously, it is likely that some candidates are binding non-specifically in this screen and do not interact with *grk* mRNA *in vivo*. It is not possible to conclude which factors are specific components of the *grk* RNP until further experiments, such as study of the expression pattern of the candidate proteins, and also mutant analysis during oogenesis, are carried out.

There are a number of factors that are more difficult to envisage as binding specifically as a result of what is already known about these proteins and their functions. For example, Piwi is a member of the Argonaute protein family that associates with a class of small RNAs known as piRNAs. The piRNA pathway is functional only in the germline and acts to suppress transposable element activity by guiding the cleavage of sense and antisense transposable element transcripts (Obbard and Finnegan, 2008). As it is difficult to conceive how Piwi could act in *grk* localization given what is currently known, it is possible that Piwi is binding non-specifically to the double-stranded RNA that is added to the GRNA binding reaction. Other examples also include dTRA1 as a component of a chromatin remodeling complex required for DNA repair (Kusch *et al.*, 2004), Rig as a nuclear receptor interacting protein required for a proper ecdysone respone during larval development (Gates *et al.*, 2004), and Fibrillarin as a component of a small nucleolar ribonucleoprotein (snoRNP) particle that localizes to the Cajal body in the nucleolus and is thought to participate in the first step of pre-rRNA processing (Gautier *et al.*, 1997).

Validation of the GRNA experiment

The isolation of factors known to be directly required for *grk* localization, translational regulation and anchoring (Sqd, Hrb27C, Imp, PABP, UAP56) validates the use of this approach to identify components of the *grk* RNP. Sqd is required for localization, translational repression and anchoring, and is present in transport particles and sponge bodies within the oocyte. UV cross-linking in ovarian extracts has shown that Sqd can directly contact most parts of the *grk* mRNA, including the GLS, 5'UTR, 3'UTR and coding regions beyond the GLS (Cáceres and Nilson, 2008; Delanoue *et al.*, 2007; Jaramillo *et al.*, 2008; Kelley, 1993; Norvell *et al.*, 1999; Jennifer Goodrich and Trudi Schüpbach, unpublished data). In UV cross-linking therefore, the GLS is not essential for Sqd binding, although in this experiment, Sqd associates only with ORF16 RNA containing the GLS and not with ORF16ΔGLS or hb RNA. The conditions used in the cross-linking and GRNA binding reactions were not considerably different. Differences in the specificity of protein binding in UV cross-linking and GRNA have also been seen previously, where Vera/Vg1RBP, VgRBP60 and XStau1 and 2 bound the VLE and also the non-localizing control in *Xenopus* extract GRNA (Czaplinski *et al.*, 2005). This suggests that the ability of a protein to cross-link RNA does not necessarily correlate with the ability to specifically associate with the RNA, and also indicates that GRNA is more widely useful in purifying complex RNPs.

Hrb27C, Imp, PABP and UAP56 also specifically bound ORF16 RNA (although Hrb27C bound ORF16ΔGLS in the repeat). Hrb27C and Imp are required for *grk* localization and translational repression, and Hrb27C is present in sponge bodies (Delanoue *et al.*, 2007; Geng and Macdonald, 2006; Goodrich *et al.*, 2004). Both proteins coimmunoprecipitate with Sqd and this is consistent with the purification of all three proteins with ORF16 in GRNA. Hrb27C can directly interact with the *grk* 3'UTR, although interaction with other parts of *grk* mRNA has never been tested, whilst Imp binds with highest affinity to the 5' of the coding region. This region overlaps with the ORF16 RNA used in this experiment, and so specific association of Imp with ORF16 RNA in GRNA is consistent with previous binding experiments.

PABP is required to activate translation of *grk* mRNA (Clouse *et al.*, 2008) and can also interact with Sqd, again consistent with the GRNA result. Further interactions of PABP with factors identified here, or other localized mRNAs have also been described in other systems. PABP was purified as part of a complex able to bind the *bcd* IV/V domain (Arn *et al.*, 2003). It can bind the dendritic targeting element of *vasopressin* mRNA where it is involved in regulation of translation, stability and transport in dendrites (Mohr *et al.*, 2001a; Mohr *et al.*, 2001b). With Imp, PABP is involved in the translational repression of its own mRNA (Patel *et al.*, 2005). PABP can also bind the non-coding RNA BC200 (BC1) in dendritic RNA granules (Muddashetty *et al.*, 2002).

UAP56 is a DExH/D-box RNA helicase that has been shown by genetics and by *in vivo* injection experiments to be required in the oocyte cytoplasm for *grk* RNA localization (Meignin and Davis, 2007). In the oocyte cytoplasm UAP56 is thought to act as a remodelling factor for dynamic transport RNPs. The role of UAP56 in cytoplasmic RNA localization is in addition to its well-studied function in nuclear export. In *Drosophila*, UAP56 is essential for the export of both spliced and intronless mRNAs (Gatfield *et al.*, 2001; Meignin and Davis, 2007), providing a link between nuclear export and mRNA localization. UAP56 therefore most likely remains on *grk* mRNA following export.

Novel factors specifically associating with ORF16

In addition to factors known to important for the localization of *grk*, and that associate with *grk,* additional factors were also identified. These include factors required for the regulation of other localized mRNAs in *Drosophila* oogenesis and also in other systems, as well as novel proteins not previously shown to interact with localized mRNAs.

Regulation of other localized mRNAs-Exu, Ef1α, Heph, CG17838

exu was first identified in genetic screens for mutants affecting *bcd* mRNA localization. In *exu* mutants, *bcd* localization is affected throughout oogenesis and early embryogenesis. The mRNA fails to localize specifically at the anterior and is dispersed throughout the oocyte cytoplasm (Berleth *et al.*, 1988; St Johnston *et al.*, 1989). Exu protein contains no known domains, with the exception of a region with weak homology to an RNA-binding motif (Macdonald *et al.*, 1991; Marcey *et al.*, 1991). However, this domain is dispensable for the *bcd* mRNA localization function of Exu (Wang and Hazelrigg, 1994). By electron microscopy, Exu is detected in sponge bodies in the oocyte and in the nurse cells where Exu is thought to associate with *bcd* mRNA (Wilsch-Bräuninger *et al.*, 1997). A series of RNA injection experiments has also led to the hypothesis that, in the nurse cells, Exu promotes the recruitment of anterior-targeting factors to *bcd* mRNA. This recruitment is thought to render the mRNA competent for the transport to the anterior margin of the oocyte (Cha *et al.*, 2001). Exu was also shown to be a component of a large, RNase-sensitive complex that contains several other proteins including Yps, and also *osk* mRNA (Wilhelm *et al.*, 2000). Defects consistent with mislocalization of *grk* mRNA are not observed in *exu* mutants. However, the presence of Exu in sponge bodies and RNA transport particles in the oocyte, and the requirement for Exu for *bcd* localization suggests that Exu could be a component of the *grk* transport RNP.

The conventional role of the translation factor Ef1α is to bind and transport aminoacyl-tRNA to the A site of the ribosome in a GTP-dependent mechanism. However, Ef1α may have additional functions beyond translation, and for example can bind actin and microtubule bundles and may regulate cytoskeletal dynamics (Liu *et al.*, 1996; Murray *et al.*, 1996). A number of studies have suggested that Ef1α is a component of localized RNPs. The protein is found in the mRNA particles that are transported within oligodendrocytes (Barbarese *et al.*, 1995; Carson *et al.*, 1997). In neuronal processes, localized mRNA granules colocalize with Ef1α (Bannai *et al.*, 2004; Bassell *et al.*, 1998; Knowles *et al.*, 1996). The protein was also isolated as part of the large RNA granule able to associate with KIF5 in mouse brain extracts

(Kanai *et al.*, 2004), and was shown to localize to transported mRNA granules in dendrites. It is unclear exactly what function Ef1α has in neuronal RNA granules and whether it is required for localized translation as would be expected. Indeed, work in chick embryo fibroblasts has indicated that Ef1α is involved in anchoring localized *β-actin* mRNA via its ability to bind the actin cytoskeleton (Liu *et al.*, 2002). The association of Ef1α with localized neuronal mRNAs, and its function in anchoring *β-actin* mRNA in fibroblasts indicates that it is a very good candidate to be a component of the *grk* RNP, functioning in either translation, or interacting with the cytoskeleton, for example in RNA anchoring.

Heph is the *Drosophila* orthologue of mammalian polypyrimidine tract-binding protein (PTB) and *Xenopus* VgRBP60. Heph was recently described as being required for proper *osk* mRNA localization and translational repression (Besse *et al.*, 2009) by promoting the formation of high order RNP particles containing multiple molecules of *osk*. This is highly supportive of Heph being a component of the *grk* transport RNP, and of a function for Heph in *grk* localization/translational regulation. The function of Heph/PTB is described in greater detail in Chapter 5.

CG17838 is the *Drosophila* orthologue of mammalian SYNCRIP (Chapter 6). Like Ef1α, SYNCRIP has previously been shown to be a component of RNA granules localized to dendrites (Bannai *et al.*, 2004; Duning *et al.*, 2007; Kanai *et al.*, 2004) and is also a P body component (Moser *et al.*, 2007). Purification of SYNCRIP associating proteins reveals that SYNCRIP is present in complexes containing proteins that are the orthologues of many presented here as binding specifically to ORF16 RNA. These include Imp, PABP, hnRNPA1/A2, DEAD-box RNA helicases, PTB and Ef1α. The functions and interactions of SYNCRIP and CG17838 are presented in more detail in Chapter 6 of this work. However, it is very clear that CG17838, in association with a number of proteins also identified in this work, could be required for the regulation of *grk*.

Translational regulation-Me31B and BicC

Me31B is part of an evolutionarily conserved DEAD-box RNA helicase family that includes human RCK/p54, *Xenopus* Xp54 and *S. cerevisiae* Dhh1p, and is a P body protein that inhibits translation and promotes decapping-mediated mRNA decay. It is also present in both neuronal and maternal RNA granules in Drosophila and other systems. *Drosophila* Me31B is detected as cytoplasmic particles in the nurse cells, is transported into the oocyte throughout oogenesis, and is also a component of sponge bodies. Oocyte localizing mRNAs including *osk*, *bcd* and *nos* are present in these particles, as are Exu and Yps, and in egg chambers lacking *me31B osk* mRNA is prematurely translated in early oogenesis (Nakamura *et al.*, 2001). Me31B interacts with Exu, Yps, Bruno, Cup and eIF4E (Nakamura *et al.*, 2001; Nakamura *et al.*, 2004), and the ability of Me31B to associate with GLS-containing mRNA and Exu in GRNA is consistent with a role for Bruno, Cup, Exu and Me31B in both *osk* and *grk* translational regulation during localization.

In *Drosophila* neurons, Me31B is present within Stau, FMRP and *CamKIIα* mRNA-containing granules, and co-immunoprecipitates with the P body component Tral and dFMR1 from adult head extracts, (Tral did associate with ORF16 RNA, but also with ORF16ΔGLS and hb in GRNA experiments, and so was discounted in the original analysis), and all three proteins are required for FMRP-mediated translational repression and dendrite morphogenesis (Barbee *et al.*, 2006).

BicC can also interact with Me31B, Tral, Cup and PABP (Kugler *et al.*, 2009). Like Me31B, BicC (which is a KH-type RNA binding protein) is required for translational repression of *osk* mRNA (Saffman *et al.*, 1998) and is also a sponge body component in oocytes (Snee and Macdonald, 2009), consistent with BicC being a potential *trans*-acting factor of the *grk* transport RNP. BicC can also act antagonistically to Orb and negatively regulate expression of its own mRNA and other targets by recruitment of the CCR4/NOT deadenylase complex (Chicoine *et al.*, 2007). The localization pattern of *grk* mRNA in *BicC* mutant oocytes is slightly disrupted so that the mRNA remains between the anterior cortex and the oocyte nucleus rather than in

a cap structure (Kugler *et al.*, 2009; Snee and Macdonald, 2009), and Grk signalling is also impaired. However the defect in *grk* localization is currently thought to be indirectly due to effects of the mutant on the cytoskeleton, whilst the main cause of impaired Grk signalling appears to be mainly due to a defect in secretion leading to ectopic accumulation of Grk protein in the oocyte.

Other forms of RNA regulation-Ago2, Upf1, NXF1

The Argonaute (Ago) proteins are essential components of the RNA induced silencing complex (RISC) that drives RNA silencing. There are two major mechanisms of RNA silencing, resulting in either degradation or translational repression of RNAs, and both activities localize to P bodies (Liu *et al.*, 2005; Sen *et al.*, 2005). Double-stranded siRNAs are recognized and unwound by RISC. One strand of siRNA is bound by Ago2, and this ribonucleic acid complex selects and cleaves the complementary region in the target mRNA. This cleavage results in gene silencing. miRNPs can affect gene expression by inhibiting translation. In this process, miRNAs are bound Argonaute proteins, and incorporated into RISC-like complexes in a manner similar to siRNAs. However, miRNAs do not form perfect base-pairs with their target mRNA and do not usually elicit cleavage of the target. In *Drosophila* it was thought that Ago2 and another Argonaute protein, Ago1 had independent roles in siRNA- and miRNA-induced silencing respectively (Okamura *et al.*, 2004). However, it has since been shown that the roles of Ago2 and Ago1 can overlap (Meyer *et al.*, 2006), and a number of endogenous miRNAs bind to Ago2 *in vivo* (Kawamura *et al.*, 2008). Both Ago2 and Ago1 can repress translation using different mechanisms. Ago1-RISC primarily promotes deadenylation, whilst Ago2 blocks the eIF4E-eIF4G interaction to disrupt translational initiation at the cap (Iwasaki *et al.*, 2009).

A link between Ago2 and localized RNA comes from studies of neuronal RNA granules, where Ago2 has been shown to colocalize with Stau and FMRP in dendritic RNA granules (Barbee *et al.*, 2006), and to interact with FMRP (Ishizuka *et al.*, 2002; Jin *et al.*, 2004). It is therefore possible that Ago2 may function in the oocyte

to repress translation of localized mRNAs in conjunction with small RNAs. In the oocyte Ago2 is found in very small cytoplasmic particles rather than in any defined structures such as sponge bodies (Reich *et al.*, 2009). However, Ago2 is recruited to the dorso-anterior corner of the oocyte upon injection of *grk* mRNA (J. Soetaert, unpublished), and the 3'UTR of *grk* is predicted to contain a number of miRNA target sites in the miRBASE database (http://microrna.sanger.ac.uk/targets/v5).

Nonsense-mediated decay (NMD) is a process that degrades mRNAs containing PTCs (premature translation termination codons) (Brogna and Wen, 2009). The NMD pathway is primarily driven by the RNA helicase Upf1, where activation of the helicase activity is believed to induce remodelling of the targeted RNA and associated proteins. Remodelling is then thought to promote association with mRNA decay factors and drive rapid decay. Upf1 can transit through P bodies in mammals and yeast, and like Ago2 and Me31B, colocalizes with Stau and FRMP in *Drosophila* dendritic RNA granules (Barbee *et al.*, 2006). One model for PTC recognition in NMD invokes the idea that a PTC should be upstream of an exon-exon junction (and therefore upstream of an intron). The EJC is deposited upstream of exon-exon junctions by the spliceosome, and can interact with and act as a binding platform for NMD factors, leading to recruitment and activation of Upf1 (Brogna and Wen, 2009). Although EJC components direct the cytoplasmic localization of *osk* mRNA in the oocyte (Hachet and Ephrussi, 2001; Mohr *et al.*, 2001; Newmark and Boswell, 1994; Palacios *et al.*, 2004; van Eeden *et al.*, 2001) and are also present in the dendrites of mammalian neurons (Glanzer *et al.*, 2005; Macchi *et al.*, 2003; Monshausen *et al.*, 2004), it is difficult to conceive how Upf1 could be recruited to non-spliced ORF16 in the GRNA experiment. However, in addition to functioning in NMD, Upf1 can also act as a general translational repressor (Muhlrad and Parker, 1999; Sheth and Parker, 2006) and can physically interact with Stau (Kim *et al.*, 2005). It is therefore thought that Upf1 might work in neuronal granules, in conjunction with Stau to repress translation of localized mRNAs, and it is possible that Upf1 could act as a translational repressor in the oocyte.

NXF1, like UAP56, is essential for nuclear export of mRNA (Herold *et al.*, 2001; Wilkie *et al.*, 2001). Indeed, the two proteins are thought to bind sequentially to mRNA in order to promote export. UAP56 is thought to bind mRNA co-transcriptionally where it can recruit NXF1 via adaptor proteins that include the EJC component REF1 (Gatfield and Izaurralde, 2002). It is therefore tempting to speculate that like UAP56, NXF1 also remains on *grk* mRNA and functions in cytoplasmic RNA localization. However, a partial loss of function of NXF1 does not result in the dorso-ventral defects observed in *uap56* mutants (Meignin and Davis, 2007; Wilkie *et al.*, 2001). This could mean that NXF1 was identified in the GRNA experiment only via its interaction with UAP56, and is not part of the *grk* RNP. Alternatively, NXF1 could be a component of the *grk* RNP, remaining with the mRNA following export, but plays a non-essential redundant role, or no role at all in *grk* localization.

Ribosomal proteins

Ribosomal proteins were observed to associate specifically with ORF16. However, the identity of the specific ribosomal proteins shown to associate with ORF16 varied from experiment to experiment. Imaging of sponge bodies and transport particles by electron microscopy also shows these structures to be devoid of ribosomes (Delanoue *et al.*, 2007). Ribosomal proteins were therefore not considered any further.

Other proteins

A number of other proteins that do not have obvious links to mRNA localization were also identified, as were a number of unknown *Drosophila* proteins. These include Dp1 and CG5205. Dp1 was originally shown to be a single stranded DNA binding protein required for chromosome condensation and segregation. It has multiple KH domains and so can also bind RNA (Huertas *et al.*, 2004). More recently is has been shown that Dp1 is part of a complex also containing Hrb27C and PABP that can enhance the translation of *hsp83* mRNA through binding a *cis*-acting

element in the *hsp83* 3'UTR (Nelson *et al.*, 2007). CG5205 is predicted to encode a DExH/D-box RNA helicase with 45% identity to *S. cerevisiae* SLH1. SLH1 is thought to block the translation of non-poly(A) mRNAs by an effect on eIF5B, and therefore on 60S ribosomal subunit joining (Searfoss *et al.*, 2001).

Proteins able to specifically associate with ORF16 are also present in the *osk* RNP, and in neuronal granules and P bodies

The proteins identified here as candidate *grk* RNP factors add to the list of factors common to the regulation of *grk* and *osk* mRNAs. Both Heph/PTB and Me31B are required for *osk* localization and/or translational regulation, and Exu-containing granules also contain *osk*. A number of factors (or orthologues of the factors) have also been shown to interact with, or be required for localization of other mRNAs both in *Drosophila* and other organisms (table 4.3). This is especially true of factors involved in neuronal RNA localization, adding to the similarities between maternal and neuronal RNA granules. It would be interesting to repeat this experiment with brain extracts, such as adult head and larval brain, in order to test whether the same proteins also recognize the GLS in the nervous system. Table 4.3 also illustrates the similarities in components of transport RNA granules, sponge bodies and P bodies. Several of the protein candidates have been shown to be components of the same complexes functioning in multiple forms of RNA regulation including localization in multiple systems. These proteins have been highlighted in red in table 4.3. Together, these results suggest that core conserved complexes of proteins are involved in the regulation of localized mRNAs in different tissues and different organisms.

There are ways by which the GRNA technique could be improved. GRNA could be made into a two-step purification protocol through the addition of a second tag to the RNA such as the streptavidin aptamer or StreptoTag (Bachler *et al.*, 1999). Purification could also be carried out from transgenic flies carrying tagged mRNAs. This method would allow the purification of complexes that have formed *in vivo*.

However, in this work GRNA has been used successfully to identify candidate components of the *grk* transport RNP. There is a precedent for a number of the isolated proteins to be part of the *grk* localization complex with functions in localization, translational control or anchoring. This experiment does not reveal any information regarding the organization of the proteins on the RNA, and further experiments are required to identify which proteins directly contact the RNA, and which proteins are members of the complex through protein-protein interactions. The ultimate aim of such experiments would be to understand the necessary factors and their organization to an extent that process of mRNA localization could be reconstituted *in vitro* and the basis of specificity understood. Chapters 5 and 6 of this thesis focus on two candidate factors, Heph and the novel *Drosophila* protein CG17838, and study their roles in the regulation of localized mRNAs and their interactions with localized mRNAs and known *trans*-acting factors. These factors were chosen due to the roles of their orthologues (PTB/VgRBP60 and SYNCRIP respectively) in mRNA localization and translational regulation in *Xenopus* oogenesis and in neurons.

TABLE 4.3 Proteins that can associate specifically with ORF16 are also present in maternal and neuronal RNA granules and P bodies. Interactors highlighted in red are proteins, or orthologues of proteins identified in this study. This is to illustrate how the same proteins may interact in multiple forms of RNA regulation, including localization, in multiple systems. Where a protein is known to directly contact an RNA, this is also listed in interactors.

ORF16 associating protein	Localized mRNAs	RNA granules	Interactors	Source
Sqd	*grk, osk*	*grk* transport particles Sponge bodies	*grk* mRNA *osk* mRNA Hrb27C Imp PABP Cup K10 Bruno	Clouse *et al.*, 2008; Delanoue *et al.*, 2007; Norvell *et al.*, 1999; Norvell *et al.*, 2005
Hrb27C	*grk, osk*	Sponge bodies	*grk* mRNA *osk* mRNA Sqd	Delanoue *et al.*, 2007; Goodrich *et al.*, 2004; Huynh *et al.*, 2004; Yano *et al.*, 2004
Imp	*grk, osk* *Vg1* (Vg1RBP) *β-actin* (IMP1, ZBP1)	Rapid transport in germline and in neuronal particles	*grk* mRNA *osk* mRNA *Vg1* mRNA (Vg1RBP) *β-actin* mRNA (IMP1, ZBP1) Sqd Hrb27C	Boylan *et al.*, 2008; Geng and Macdonald, 2006; Munro *et al.*, 2006
PABP	*grk, bcd* *vasopressin* BC200 (BC1)	Dendritic RNA granules	BC200 (BC1) RNA *Vasopressin* mRNA Sqd Imp	Arn *et al.*, 2003; Clouse *et al.*, 2008; Mohr *et al.*, 2001a; Mohr *et al.*, 2001b; Muddashetty *et al.*, 2002; Patel *et al.*, 2005
UAP56	*grk, osk, bcd*		NXF1	Gatfield and Izaurralde, 2002; Meignin and Davis, 2007
Exu	*bcd, osk*	Sponge bodies	*osk* mRNA Yps	Berleth *et al.*, 1988; Cha *et al.*, 2001; St Johnston *et al.*, 1989; Wilhelm *et al.*, 2000; Wilsch-Bräuninger *et al.*, 1997

TABLE 4.3 (continued) Proteins that can associate specifically with ORF16 are also present in maternal and neuronal RNA granules and P bodies.

Ef1α	colocalizes with localized neuronal mRNAs including *IP$_3$R, CaMKIIα* and *Arc* *β-actin*	Neuronal RNA granules (dendrites and oligodendrocytes)	*β-actin* mRNA KIF5 associating neuronal complex including SYNCRIP, Stau, FMRP, DEAD-box helicases	Bannai *et al.*, 2004; Barbarese *et al.*, 1995; Bassell *et al.*, 1998; Carson *et al.*, 1997; Kanai *et al.*, 2004; Knowles *et al.*, 1996; Liu *et al.*, 2002
CG17838	colocalizes with localized neuronal mRNAs including *IP$_3$R, CaMKIIα* and *Arc* (SYNCRIP) BC200 (BC1) (SYNCRIP)	Neuronal RNA granules P bodies	BC200 (BC1) and PABP PTB and hnRNPA1 (viral RNA) PABP (RNA stability) KIF5 associating neuronal complex including Ef1α, Stau, FMRP, DEAD-box helicases In human cells forms a complex with Imp, hnRNPs, PABP, DEAD-box helicases	Bannai *et al.*, 2004; Choi *et al.*, 2004; Duning *et al.*, 2007; Kanai *et al.*, 2004; Moser *et al.*, 2007
Me31B	*osk* colocalizes in granules with *osk, bcd, nos, CaMKIIα*	P bodies Sponge bodies Neuronal RNA granules	Exu Yps Bruno Cup eIF4E Tral Stau FMRP	Barbee *et al.*, 2006; Nakamura *et al.*, 2001; Nakamura *et al.*, 2004
BicC	*osk, grk*	Sponge bodies	Me31B PABP Cup Tral	Chicoine *et al.*, 2007; Kugler *et al.*, 2009; Saffman *et al.*, 1998; Snee and Macdonald, 2009; Wilhelm *et al.*, 2005

TABLE 4.3 (continued) Proteins that can associate specifically with ORF16 are also present in maternal and neuronal RNA granules and P bodies.

Heph/PTB	*osk* *Vg1* (VgRBP60) *β-actin* (PTB) at growing neurite terminals	*osk* RNP complexes	*osk* mRNA *Vg1* mRNA (VgRBP60)	Besse *et al.*, 2009; Cote *et al.*, 1999; Ma *et al.*, 2007
Ago2	*grk* colocalizes with localized neuronal mRNAs including *CaMKIIα*	Neuronal RNA granules P bodies	FMRP	Barbee *et al.*, 2006; Ishizuka *et al.*, 2002; Jin *et al.*, 2004; J. Soetaert, unpublished
Upf1	colocalizes with localized neuronal mRNAs including *CaMKIIα*	Neuronal RNA granules P bodies	Stau	Barbee *et al.*, 2006; Kim *et al.*, 2005

THE FUNCTIONS OF HEPHAESTUS DURING *DROSOPHILA* OOGENESIS

Introduction

Drosophila Hephaestus (Heph) was identified in Chapter 4 as one of a number of proteins able to bind specifically to GLS-containing RNA. It was therefore hypothesized that Heph could be a component of a *grk* RNP at one or a number of stages of oogenesis and play a role in *grk,* and possibly other mRNAs, localization, localized translation or anchoring in the oocyte. This hypothesis is supported by functions for the mammalian and *Xenopus* orthologues of Heph, PTB and VgRBP60, in mRNA localization and localized translation in *Xenopus* oocytes and in neurons. Although the role of *Drosophila* Heph has been studied during spermatogenesis (Davis *et al.*, 2002; Robida and Singh, 2003; Schulz *et al.*, 2004) and adult wing development (Dansereau *et al.*, 2002), very little was known regarding the function of the protein in oogenesis when this work began.

Heph and its orthologues

The *heph* locus is contained within 140 kb of genomic sequence on chromosome 3 at 100D-100E (Fig. 5.1A). Alternative splicing is predicted to result in a number of *heph* transcripts. Examination of genomic sequence indicates that *heph* is a single gene, and has no paralogues in *Drosophila* (Adams *et al.*, 2000). There are at least three predicted Heph protein variants, the foremost being isoforms A, B and C (Fig. 5.1B). Isoform A includes an N-terminal glutamine-rich (Q-rich) domain, and both isoforms A and B include a bipartite nuclear localization signal (NLS). Heph belongs to the hnRNP family of RNA binding proteins, and all predicted isoforms contain four RNA Recognition Motifs (RRM 1-4).

Heph is the *Drosophila* orthologue of polypyrimidine tract-binding protein (PTB), sharing over 50% amino acid identity and 60% similarity with vertebrate forms of

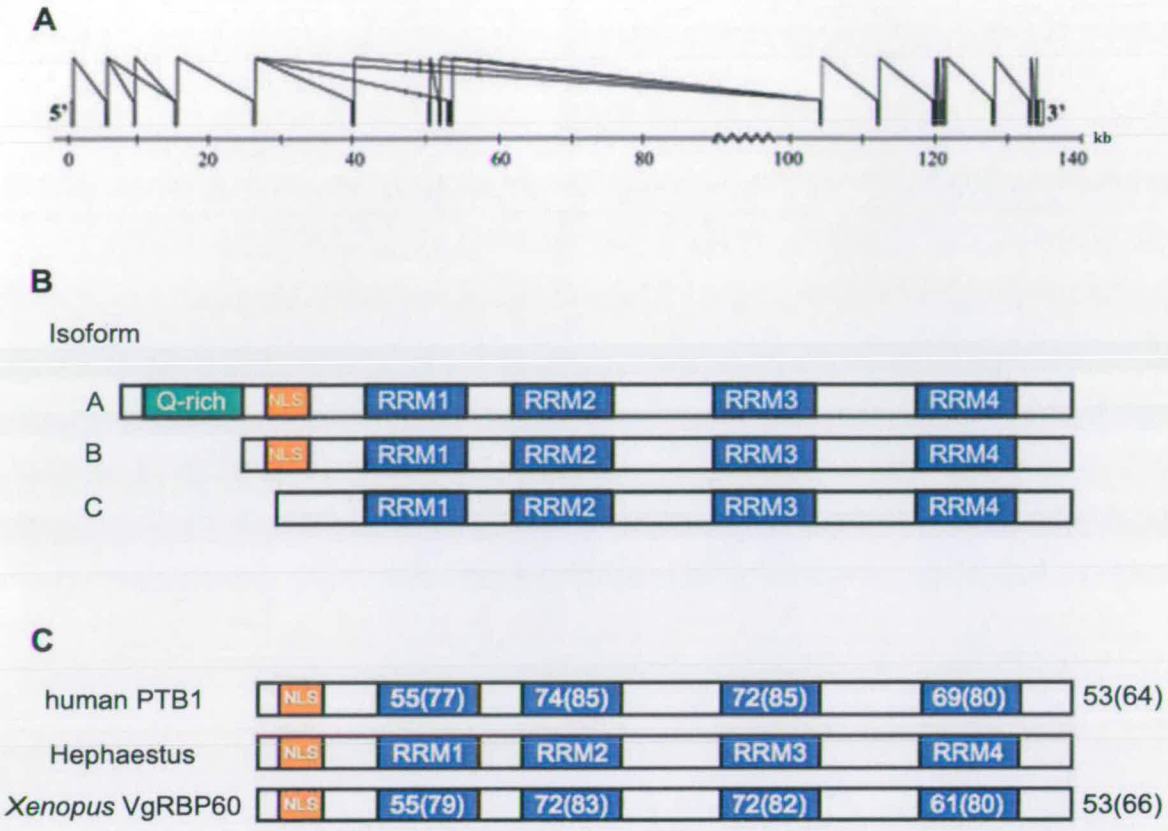

Figure 5.1 The *heph* locus (A) The *heph* locus is contained within 140 kb of genomic sequence on chromosome 3 at 100D-100E (adapted from Dansereau *et al.*, 2002). Black bars represent exons, and the lines joining different exons represent the pattern of alternative splicing. Alternative splicing is predicted to produce a number of transcripts. **(B)** It is predicted that alternative splicing produces at least three protein variants: isoforms A and B include a bipartite nuclear localization signal (NLS). Only isoform A includes an N-terminal glutamine-rich domain (Q-rich). **(C)** Heph is the *Drosophila* orthologue of vertebrate polypyrimidine tract binding protein (PTB) (*Xenopus* VgRBP60). Percent amino acid identity is indicated and, in brackets, percent similarity.

PTB (mammalian PTB/hnRNPI and *Xenopus* VgRBP60). The percent amino acid identity increases up to over 70% within the RRM domains (Dansereau *et al.*, 2002; Davis *et al.*, 2002) (Fig. 5.1C). PTB also has four RRM domains and an N terminal extension containing both nuclear localization and export signals (Li and Yen, 2002; Oh *et al.*, 1998; Perez *et al.*, 1997; Romanelli *et al.*, 1997), accounting for both nuclear and cytoplasmic functions for this protein. RRMs 3 and 4 are joined by a highly flexible linker and interact extensively to form a compact globular structure, whilst the structure of the overall protein is elongated (Conte *et al.*, 2000; Petoukhov *et al.*, 2006; Simpson *et al.*, 2004). PTB is monomeric in solution, but may be able to oligomerize through the central part of the protein (Oh *et al.*, 1998; Perez *et al.*, 1997a).

There are three main mammalian PTB isoforms, PTB1, 2 and 4 (Ghetti *et al.*, 1992; Gil *et al.*, 1991). PTB2 and PTB4 contain 19 or 26 additional amino acids respectively between RRM 2 and RRM 3 as a result of the inclusion of PTB exon 9, which has two alternative 3' splice sites. A fourth isoform lacking RRM 1 and RRM 2 has been reported in T lymphocytes (Hamilton *et al.*, 2003). Unlike the *Drosophila* genome, mammals have related genes that are expressed in a tissue specific manner and that encode proteins with 70-80% homology to PTB. nPTB (neural PTB) is expressed in adult brain, muscle and testis, and as with PTB, alternative splicing can give rise to a number of isoforms (Ashiya and Grabowski, 1997; Markovtsov *et al.*, 2000; Polydorides *et al.*, 2000). ROD1 (regulator of differentiation 1) is expressed only in haematopoietic cells (Yamamoto *et al.*, 1999). A fourth paralogue, smPTB (smooth muscle PTB), is restricted to smooth muscle cells of rodents (Gooding *et al.*, 2003). The number of splice isoforms and tissue-specific variants allows PTB to have varying activity in different cell types and on different substrates. Indeed, it has been shown that the alternatively spliced isoforms of PTB have distinct activities in regulating the splicing and translation of certain substrates (Wollerton *et al.*, 2001). The individual isoforms and paralogues of PTB have no direct relationship with particular predicted Heph isoforms.

The function of Heph

heph was first identified in a genetic screen for loci required for spermatogenesis (Castrillon *et al.*, 1993). The original male sterile P-element-induced allele, *ms(3)heph*^{2}, causes the loss of an abundant male-specific transcript (Robida and Singh, 2003). *heph*^{2} homozygous males show an enlarged tip of the testis where cysts of elongated spermatids accumulate. The mutant also lacks fully individualized motile sperms, leading to the conclusion that loss of *heph* affects spermatid differentiation. In addition, overexpression of *heph* from EP lines or from a *UAS-heph* cDNA under the control of a germline *nos-Gal4* driver, causes the loss of early germ cells (Schulz *et al.*, 2004). When the animals were shifted to a lower temperature, testes with a small number of germ cells were occasionally observed, suggesting that *heph* also plays a role in the transition from the spermatogonia to spermatocyte differentiation program.

A study of the expression pattern of *heph* by *in situ* hybridization (Davis *et al.*, 2002) supports a role for *heph* in spermatogenesis. *heph* is expressed in the testis, specifically found in primary spermatocytes. In the ovaries, *heph* is expressed in the nurse cells of stage 10 egg chambers. *heph* is also uniformly distributed in the freshly laid embryo, showing that the mRNA is maternally supplied. Expression in the embryonic mesoderm and later in the developing central nervous system (CNS) also suggests that *heph* could potentially function in muscle and neuronal development. Finally, *heph* was detected in the developing eye and wing imaginal discs. Further work has since shown that *heph* plays a role in wing development by acting through the Notch pathway (Dansereau *et al.*, 2002). *heph* alleles were shown to cause wing defects in genetic mosaic animals. Somatic clones lacking *heph* express Notch target genes, induce ectopic wing margin in adjacent wild-type tissue, inhibit wing-vein formation and have increased levels of Notch intracellular domain (NICD). *Delta* is epistatic to *heph* indicating that *heph* is required to attenuate Notch activity following activation by Delta in the wing. By looking at the diverse functions of Heph orthologues, which range from regulation of alternative splicing, mRNA localization, and perhaps even transcriptional activation (Rustighi *et al.*, 2002), it is possible to

predict multiple roles for the protein in mRNA regulation during oogenesis, including a role in mRNA localization and localized translation.

The functions of PTB

PTB was first purified as a protein that binds to the 15-20-nucleotide pyrimidine-rich sequence, the polypyrimidine tract, which typically precedes the 3' splice site of higher eukaryotic pre-mRNA introns (Garcia-Blanco *et al.*, 1989). SELEX (systematic evolution of ligands by exponential enrichment) experiments have also shown that PTB binds specifically to pyrimidine-rich stretches, with a preference for UCUU stretches (Perez *et al.*, 1997b; Singh *et al.*, 1995). However, the dissociation constants for the interaction of PTB with these sequences are relatively high when compared with those for the interaction with physiological target sequence elements (Conte *et al.*, 2000; Perez *et al.*, 1997b) and a strict consensus sequence for PTB has yet to be identified.

NMR structures of individual RRMs in association with RNA suggest that high affinity binding by PTB is the result of multiple RRM/RNA complexes. Each RRM within PTB can bind one RNA molecule and has its own slightly different consensus RNA binding sequence (Auweter *et al.*, 2007; Oberstrass *et al.*, 2005). The arrangement and interaction of RRM 3 and 4 with each other and with RNA has also led to the model that PTB binding can result in RNA looping (Oberstrass *et al.*, 2005). Such restructuring of the RNA substrate, in addition to sequence specific binding of the RNA, is thought to be crucial in enabling PTB to carry out its many functions in the cell (Liu *et al.*, 2002; Mitchell *et al.*, 2003; Oberstrass *et al.*, 2005). PTB is thought to be an RNA chaperone, and by the binding and remodelling of RNA can promote or inhibit the binding of other factors. In this way, PTB is able to act as a positive or negative regulator of a number of forms of RNA metabolism, including alternative splicing, RNA 3'-end processing and stability, translation and localization.

Regulation of alternative splicing

Alternative splicing is a process by which multiple mRNAs are synthesized from a single primary transcript, allowing for the synthesis of a diverse set of proteins and involving the combinatorial use of alternative 5' splice sites, 3' splice sites, introns and exons. As mentioned previously, PTB was first purified as a polypyrimidine tract binding protein (Garcia-Blanco *et al.*, 1989). Subsequent work has shown that PTB can bind pyrimidine-rich elements and thereby mediate splicing repression of nearby splice sites in a long list of alternatively spliced pre-mRNAs, including the α- and β-tropomyosin, α-actinin (Perez *et al.*, 1997b; Southby *et al.*, 1999; Waites *et al.*, 1992), *c-src* and γ2 $GABA_A$ receptor pre-mRNAs. In all of the cases above, repression of a splice site by PTB results in tissue-specific patterns of splicing. In a simple model, it is thought that PTB mediates splice site repression by the overlap of PTB binding sites with binding sites for splicing factors such as U2AF, U2snRNP, or with enhancer sequences, blocking exon definition and spliceosome assembly. However, the presence of multiple PTB binding sites, sites more distant from splice signals, and downstream as well as upstream of repressed exons argues for a more complicated model, perhaps invoking the ability of PTB to loop out essential RNA elements.

The case of the calcitonin/calcitonin gene related peptide (CT/CGRP) gene also reveals that PTB can positively regulate exon inclusion by binding to a polypyrimidine splicing enhancer (Lou *et al.*, 1999). However, binding to the enhancer is also required for polyadenylation of the exon-including RNA, implying that the positive effect on splicing efficiency may be due to another function of PTB, that of 3'-end processing.

3'-end processing and mRNA stability

A second role for PTB in RNA processing has been identified through its recognition of polyadenylation signals. Polyadenylation signals are comprised of an AAUAAA sequence 20-30 nt upstream of the cleavage site to which the poly(A) tail is added. The polyadenylation signal is recognised by cleavage polyadenylation stimulating factor (CPSF) in an interaction that is enhanced by the binding of cleavage stimulatory factor (CstF) to pyrimidine-rich downstream sequence elements (DSEs). PTB is thought to compete with CstF for binding to the DSE, thereby inhibiting 3' cleavage and polyadenylation (Castelo-Branco *et al.*, 2004). Pyrimidine-rich upstream sequence elements (USEs) may also be present and required for full activity of the polyadenylation signal. In the case of the C2 complement gene, the USE has been shown to bind PTB, which in this instance is required for efficient polyadenylation (Castelo-Branco *et al.*, 2004). These examples suggest that PTB has a modulatory function in mRNA 3'-end processing, operating to control the overall levels of mRNA synthesized in the cell. In addition to regulating 3'-end formation, PTB can also control mRNA levels by influencing mRNA stability. PTB can bind to a polypyrimidine-rich sequence in the 3'UTR of insulin mRNA in a glucose-dependent manner. It is thought that this masks destabilizing elements in the 3'UTR increasing the stability of this mRNA in pancreatic β-cells (Fred *et al.*, 2006).

Translational control

Translation initiation of eukaryotic mRNAs is mostly mediated by the m^7Gppp cap structure at the 5' end of an mRNA that is recognised by the translation initiation factor complex. However, the genomic RNA of the *Picornaviridae* (a large family of viruses that includes poliovirus and human rhino virus) lacks a cap structure. In this case, translation is initiated from highly structured internal ribosome entry sites (IRESs). Efficient initiation from IRESs requires cellular components known as IRES *trans*-acting factors (ITAFs) as well as the canonical translation initiation factors. PTB has been shown to be an ITAF, required in internal ribosome entry by a number of picornaviral IRESs (Belsham and Jackson, 2000; Song et al., 2005). PTB

may also regulate the translation of hepatitis C virus (HCV) by binding to an IRES and also to multiple sites within the RNA (Ali and Siddiqui, 1995; Anwar *et al.*, 2000), and is also thought to be required for the replication of this virus (Aizaki *et al.*, 2006; Chang and Luo, 2006).

Cellular RNAs can also contain IRESs, and under conditions that inhibit cap-dependent translation (for example cell stress, apoptosis and viral infection) the expression of certain proteins is maintained by IRES-dependent translation (Spriggs *et al.*, 2005; Spriggs *et al.*, 2008) (examples include the BAG-1 (Bcl-2-associated athanogene 1; Pickering *et al.*, 2004). Most of the cellular IRESs studied require PTB for function, and in many cases it has been shown that PTB plays a role in the recruitment of the ribosome. PTB can also bind to other regions within cellular RNAs such as *Bip* (Kim *et al.*, 2000), where it can inhibit IRES-dependent translation, demonstrating that PTB can also be a negative regulator of cap-independent translation.

mRNA localization and localized translation

Of particular relevance to this work, PTB has been shown to play a role in RNA transport and the regulation of localized translation in a number of model systems. Transport of *Vg1* mRNA to the vegetal pole of the *Xenopus* oocyte is dependent on the recognition of short, reiterated sequence motifs in the *Vg1* localization element (VLE) that provide binding sites for *trans*-acting factors. The *Xenopus* orthologue of PTB, VgRBP60, interacts directly with VM1 motifs within the VLE (Cote *et al.*, 1999), whilst another protein, Vg1RBP/Vera, binds VM1 motifs as well as E2 motifs in the VLE. Both proteins have essential roles in *Vg1* mRNA localization. More specifically, it has been shown that VgRBP60/PTB is required for a critical remodelling step in which an initially indirect Vg1RBP-VLE interaction in the nucleus is switched to a direct interaction in the cytoplasm (Lewis *et al.*, 2008).

In the nervous system, localization of mRNA, such as *β-actin,* is known to be required for neurite growth. In neuronal cells, PTB is phosphorylated in response to activation of the PKA pathway, which results in accumulation of PTB at growing neurite terminals. Here, it is thought that PTB is required for neurite growth and for the localization of *β-actin* mRNA transcripts to neurite terminals (Ma *et al.*, 2007).

Aims of this chapter

The general aim of the work described in this chapter was to study the function of Heph in mRNA localization and localized translation in the oocyte, with particular regard to *grk* mRNA, by asking the following questions:

- What is the expression pattern of Heph during oogenesis and embryogenesis?
- Does Heph interact with localized mRNAs in the germline?
- Does the distribution/levels of localized transcripts and the proteins they encode change in *heph* mutants?

Results

The expression pattern of *heph* mRNA during oogenesis

To investigate how Heph might function in the context of a polarized oocyte, the spatial distribution of *heph* mRNA and protein within developing wild-type egg chambers was analysed by fluorescence *in situ* hybridization (FISH) and by immunostaining. Previously, Davis *et al.* (2002) reported the expression pattern of *heph* in stage 10 egg chambers using a traditional HRP detection system. Here, *heph* mRNA is highly expressed in the nurse cells, and is uniformly expressed in the newly deposited embryo, indicating that *heph* is a maternally contributed transcript. However, this previous study did not examine the expression of *heph* mRNA in earlier egg chambers when important RNA localization events are taking place.

This work is consistent with the previous study in that *heph* is strongly expressed in stage 10 egg chambers. *heph* is only weakly expressed in younger egg chambers (Fig. 5.2C, D). Distinct foci of *heph*, which may correspond to nascent transcripts, were detected in nurse cell nuclei and throughout the cytoplasm of the nurse cells at stage 10 (Fig. 5.2A, B). The ability to possibly detect nascent transcripts may be due to the large size of the *heph* gene, and therefore of the unspliced nascent transcript following transcription. Confirmation of the identity of these foci could be obtained by *in situ* hybridisation using a probe for an intron within the *heph* gene, where the intron probe would give the same expression pattern as the antisense probe.

Also consistent with Davis *et al.* (2002), *heph* expression becomes patterned in the developing CNS in late stage embryos. FISH on mixed stages of embryo revealed that *heph* is expressed in a subset of cells of the CNS stages 13-16 (Fig. 5.3A). Visualization at a higher magnification showed that *heph* RNA is asymmetrically localized within these cells (Fig. 5.3B).

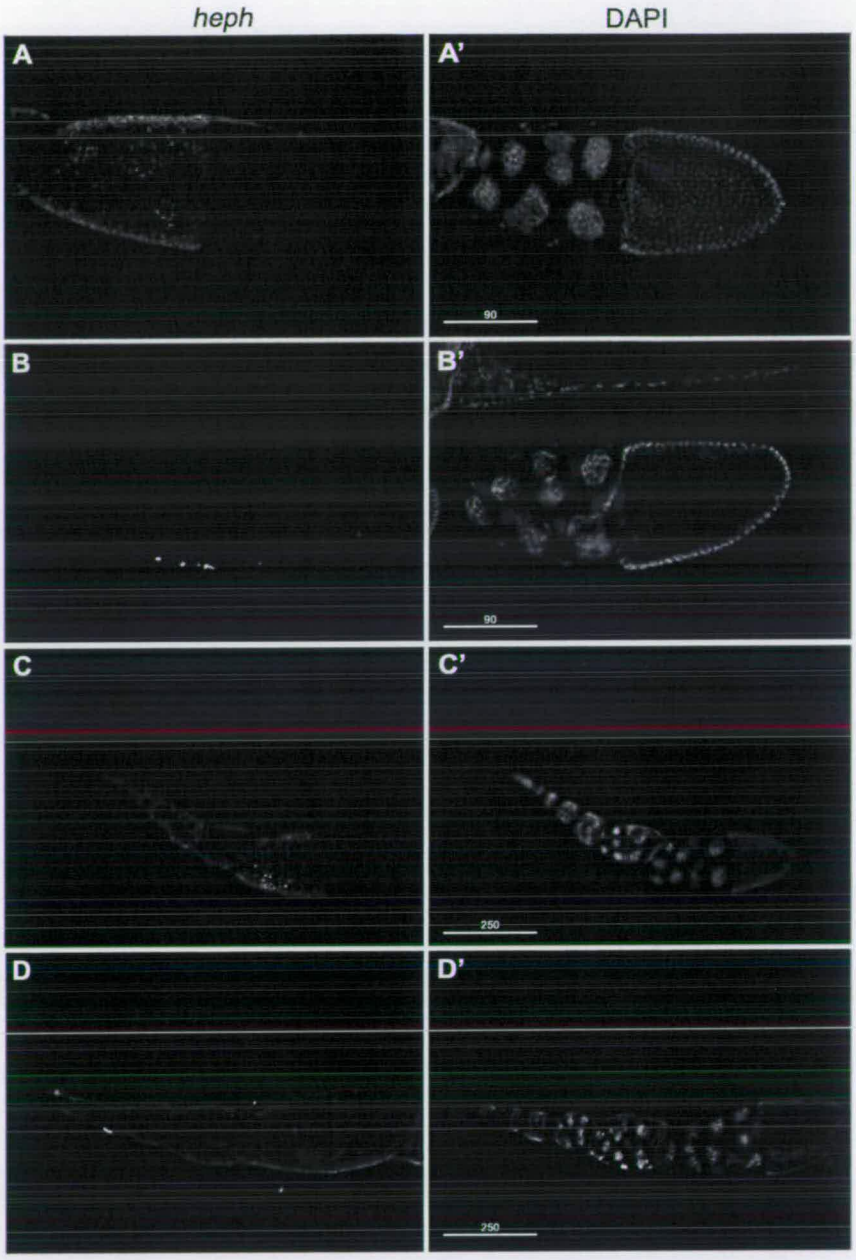

Figure 5.2 *heph* is strongly expressed in stage 10 egg chambers. (A-D) *heph* is detected in the nurse cell nuclei and cytoplasm of stage 10B egg chambers. **(A)** Distinct foci of *heph* are detected within nurse cell nuclei using an antisense *heph* RNA probe, but not with **(B)** a sense *heph* RNA probe control. **(C)** *heph* is more weakly expressed in younger egg chambers and is not detected in these stages using the **(D)** sense probe. Scale bars and associated numbers represent μm.

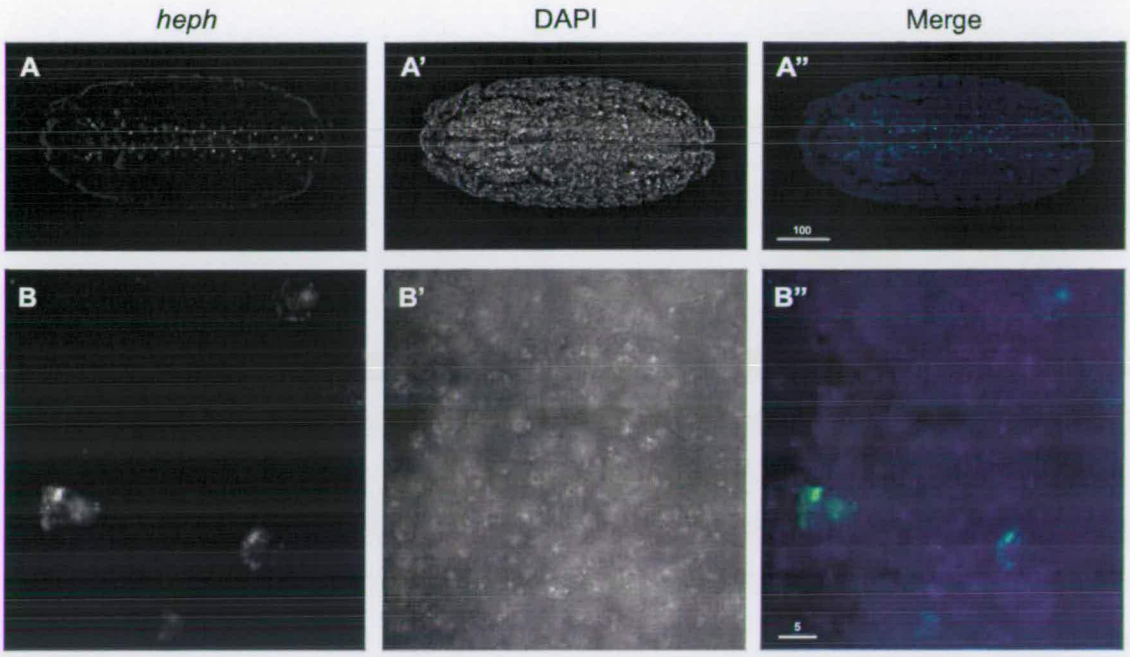

Figure 5.3 *heph* is expressed in the CNS of late stage embryos. (A) *heph* is expressed in a subset of cells of the CNS, and **(B)** *heph* mRNA is asymmetrically localized within these cells.

The expression pattern of Heph protein during oogenesis

Staining with anti-Heph antibodies revealed localization in the cytoplasm of the follicular epithelial cells throughout oogenesis (Fig. 5.4A-E). In the germline, Heph is present in the oocyte cytoplasm with an accumulation at the posterior pole of the oocyte from around stage 9 of oogenesis onward (Fig. 5.4C-E). The posterior localization of Heph is particularly strong in late stage 10 egg chambers (Fig. 5.4D-E). Heph therefore colocalizes with localized *osk* mRNA at later stages of oogenesis. No staining at the dorso-anterior cap coincident with *grk* RNA, or at the anterior with *bicoid* mRNA, was observed.

Heph specifically associates with *grk* and *osk* mRNAs

Given the *in vitro* association of Heph and *grk* (GLS) RNA, and the colocalization of Heph and *osk* mRNA, immunoprecipitation experiments were carried out to ask whether Heph is a component of localized RNPs in the germline. RT-PCR showed that *grk* and *osk* mRNAs are present in the fractions precipitated from GFP-Heph protein-trap ovaries and from SqdGFP control ovaries using anti-GFP antibodies, but not in anti-GFP immunoprecipitates from wild-type control females, or from control rabbit serum (Fig. 5.5). For explanation of anti-CG17838 immunoprecipitation see Chapter 6. No specific enrichment of mRNAs highly expressed in ovaries (*rp49*, *tubulin67C*), other mRNAs asymmetrically localized within the oocyte (*bicoid*, *nanos*) or the non-localized mRNA control from the initial *in vitro* experiments (*hunchback*) was observed in the GFP-Heph precipitated fractions. This was also the case for SqdGFP precipitated fractions, the only difference being that *bcd* was present in these fractions.

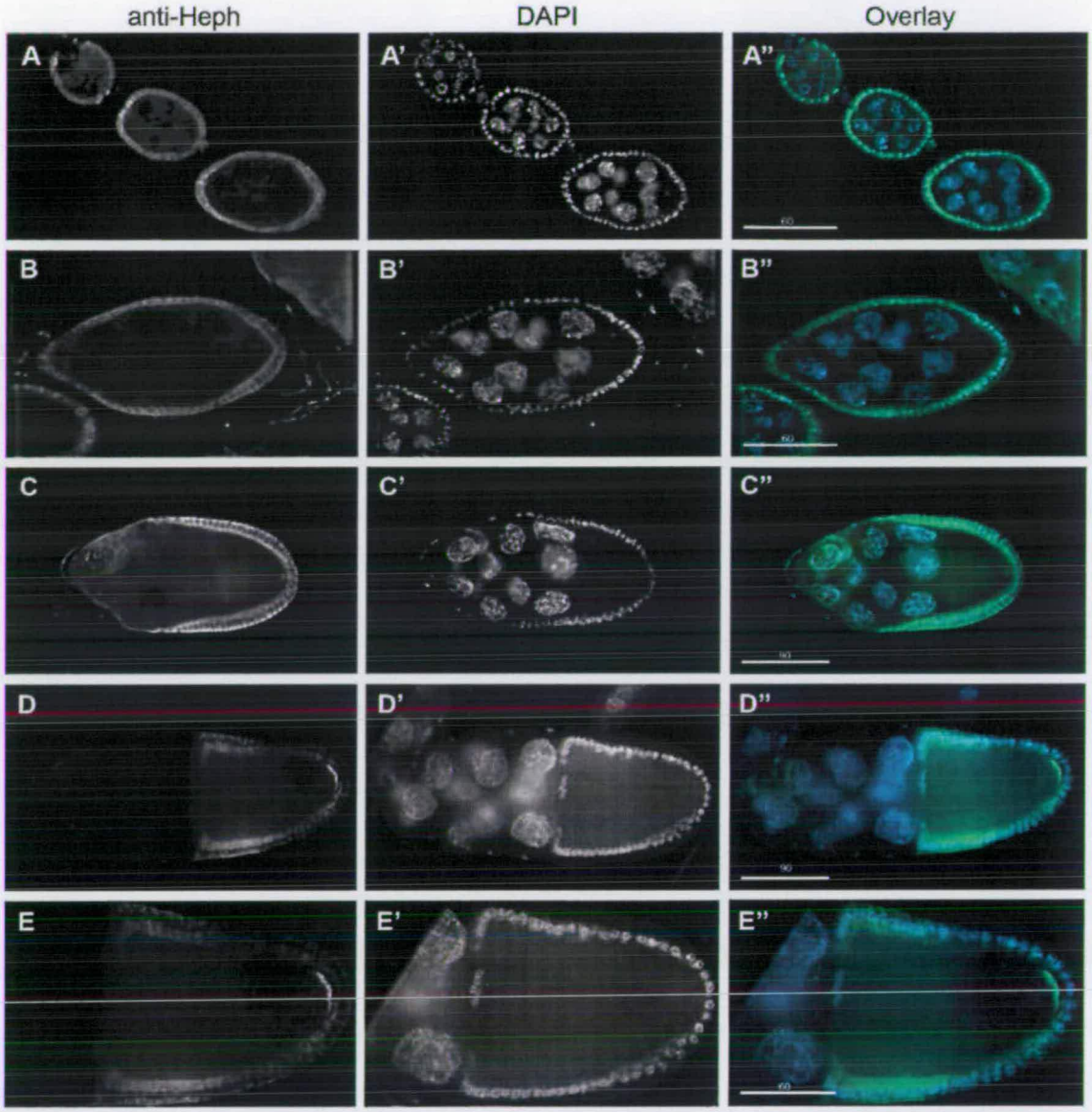

Figure 5.4 Distribution of Heph during *Drosophila* oogenesis. (A-E) Stages 4-6 **(A)**, stage 8 **(B)**, stage 9 **(C)** and stage 10B **(D and E)** stained with anti-Heph antibodies and DAPI. **(E)** is an enlargement of the oocyte shown in the egg chamber in **(D)**. Scale bars and associated numbers represent μm.

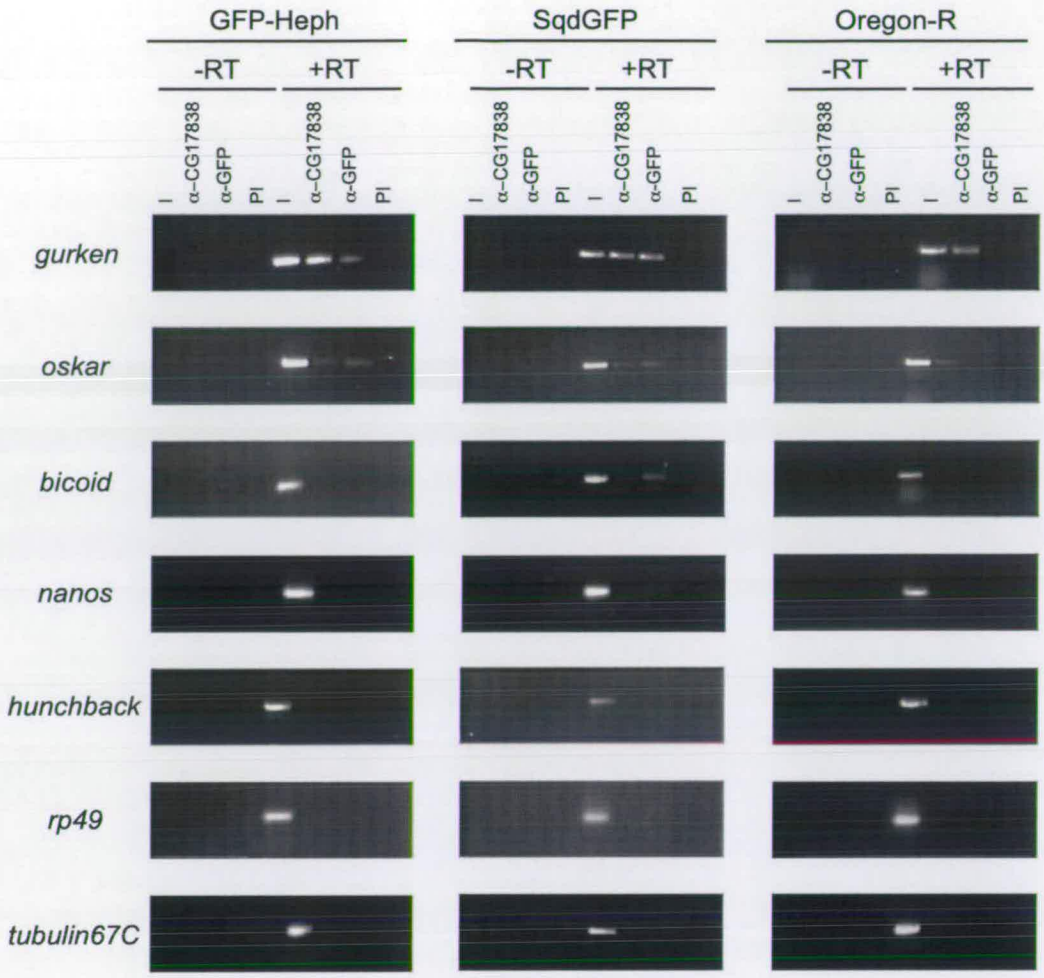

Figure 5.5 Heph associates with *grk* and *osk* mRNAs. RT-PCR amplification of mRNAs recovered in fractions immunoprecipitated from GFP-Heph protein trap, SqdGFP control or Oregon-R control ovarian extracts using anti-GFP, anti-CG17838 (see chapter 6) and control rabbit serum. I=Input RNA (10%); PI=control rabbit serum; -/+RT=minus/plus reverse transcriptase.

heph mutant alleles

The spatial and temporal distribution of *heph* RNA and protein, in addition to the ability to specifically bind *osk* mRNA suggests that Heph regulates *osk* mRNA localization and/or localized translation. The biochemical evidence, first the identification of Heph as a factor able to specifically bind GLS-containing RNA (Chapter 4), and second, the ability of Heph to bind specifically to *grk* mRNA in ovarian extracts, also indicates that Heph may regulate *grk* mRNA localization and/or translation. The function of Heph in *osk* mRNA regulation was studied and published (Besse *et al.*, 2009) during the preparation of this thesis. This study identified Heph as a key structural component of *osk* RNP complexes, required for efficient *osk* mRNA localization and also translational repression of *osk* mRNA during localization. Heph is required indirectly for *osk* localization through the properly timed organization of the oocyte microtubule cytoskeleton, but directly controls *osk* translation through the multimerization of individual *osk* mRNA molecules and the formation of high order translationally repressed *osk* RNP complexes. The remainder of this work therefore focussed on the regulation of *grk* mRNA.

To investigate the role of Heph in *grk* mRNA regulation, three different alleles, known to affect wing development, and belonging to the same lethal complementation group were used. These alleles also fail to complement the male sterility of the original P-element-induced allele $heph^{2}$ (known to map to an intron-Fig. 5.6A). $heph^{03429}$ is a P-element insertion that maps to a large intron (Fig. 5.6A). $heph^{e1}$ and $heph^{e2}$ are EMS-induced mutations. The first is a mis-sense mutation that substitutes a conserved glycine (G) residue to a glutamine (Q) residue in RRM 1, and the second corresponds to a deletion covering RRM 1, RRM 2 and part of RRM 3 (Dansereau *et al.*, 2002; Fig. 5.6A, B).

Due to the lethality of these alleles, it was necessary to make germline clones using the FLP-DFS technique (Chou and Perrimon 1993; Chou and Perrimon 1996; Fig. 5.7). *heph*^{e2} behaves as a null allele (Dansereau *et al.*, 2002), whilst *heph*^{e1} and *heph*^{03429} are hypomorphic mutants strongly affecting *heph* expression levels (Fig. 5.11). Germ cells homozygous for *heph*^{e2} fail to produce differentiated egg chambers.

heph mutant eggs have patterning defects

Analysis of patterning and dorsal appendage morphogenesis in the eggshell is a sensitive way in which to investigate Grk signalling within the egg chamber. A number of eggshell phenotypes were observed. None of the eggs laid were fully wild-type (class A) (Fig. 5.8A and table 5.1), and most were shorter and rounder than wild-type eggs (class B-D) (Fig. 5.8B-D, and table 5.1). There were a number of phenotypes seen in the dorsal appendages; wild-type length with smooth edges (class B) (Fig. 5.8B and table 5.1), broader than wild-type with ragged edges (class C) (Fig. 5.8C and table 5.1); shorter with ragged edges, resembling 'antlers', joined at the centre by additional dorsal appendage material (class D (Fig. 5.8D and table 5.1). Within class D, the operculum of a number of eggs was weak, and cytoplasm streamed from the anterior upon preparation, leaving a hole in the chorion (Fig. 5.8D). A small number of eggs were also fully open at the anterior (class E) (Fig. 5.8E and table 5.1), resembling eggs laid by *cup* mutants. The distribution of the numbers of eggs in the different classes varies for *heph*^{e1} and *heph*^{03429} eggs. The majority of *heph*^{e1} eggs were class D, whilst *heph*^{03429} eggs were class B or C.

The eggshells shown in Fig. 5.8B-D have characteristics of those that are slightly dorsalized. The eggs are short and round, and the dorsal appendages are broader than wild-type (Fig. 5.8C), or there is ectopic dorsal appendage material at the midline (Fig. 5.8D). The dorsal appendages of the eggs in Figure 5.8D resemble the 'moose antlers' seen in *bullwinkle* (*bwk*) mutants, where the follicle cell migrations that form the dorsal appendages are abnormal. The lack of wild-type *heph* function also results in a partial dumpless phenotype (due to incomplete transfer of nurse cell contents into the oocyte at stage 11), and the eggs resemble the dumpless eggs seen for

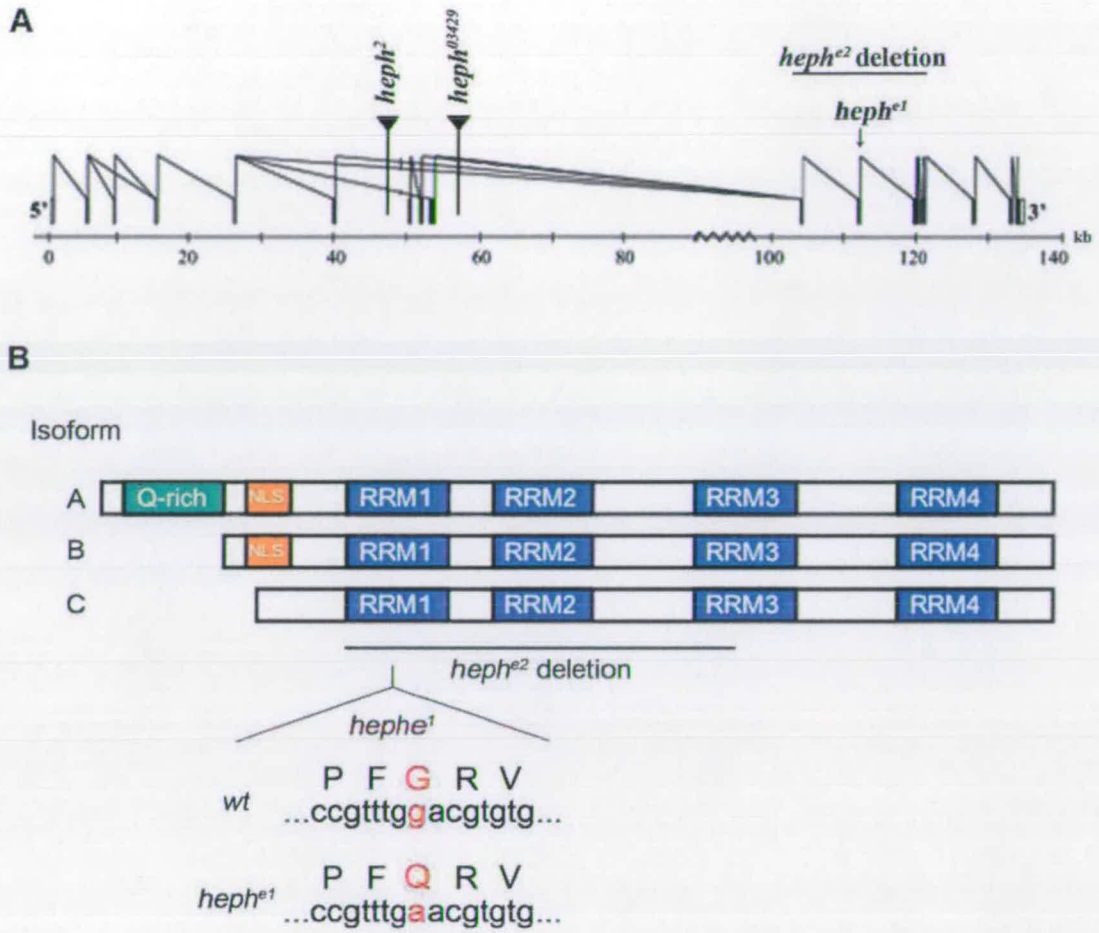

Figure 5.6 The *heph* locus and associated alleles. (A) A number of alleles map to the *heph* locus. Two P-element alleles, $heph^{2}$ (Castrillon *et al.*, 1993) and $heph^{03429}$ (Dansereau *et al.*, 2002) map to *heph* introns. **(A and B)** Two EMS-induced alleles, $heph^{e1}$ and $heph^{e2}$, alter RRM domains. $heph^{e2}$ is a deletion of several coding exons including the coding region for RRM1, RRM2 and part of RRM3. $heph^{e1}$ is a mis-sense mutation that changes a glycine (G) to a glutamine (Q) in RRM1.

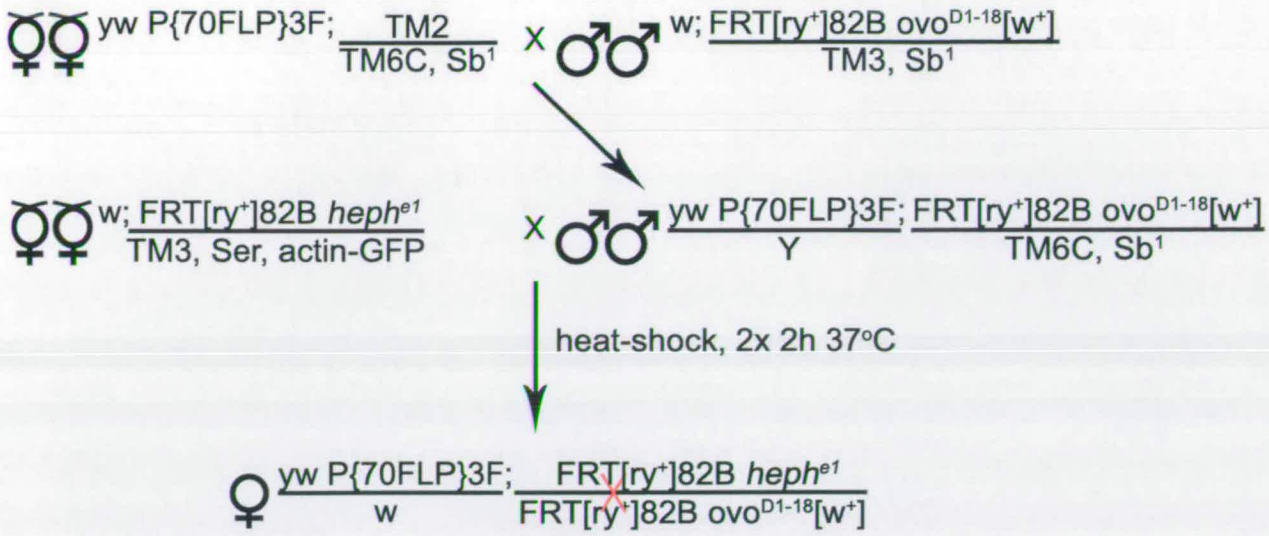

Figure 5.7 Genetic strategy for generation of *heph* germline clones using the FLP-DFS system (Chou and Perrimon, 1993; Chou and Perrimon 1996). Flies carrying heat-shock induced flippase (70FLP) and also $ovo^{D1\text{-}18}$ on an FRT82B chromosome were crossed to flies carrying the *heph* mutant allele also on an FRT82B chromosome. The red 'X' shows a mitotic recombination event between the two FRT sequences, which occurs after induction of FLP expression in response to heat-shock. $ovo^{D1\text{-}18}$ is a dominant female sterile (DFS) mutation that blocks oogenesis at early stages. Within a clonal ovary, the only egg chambers that develop to later stages are those that are homozygous for the *heph* mutant allele.

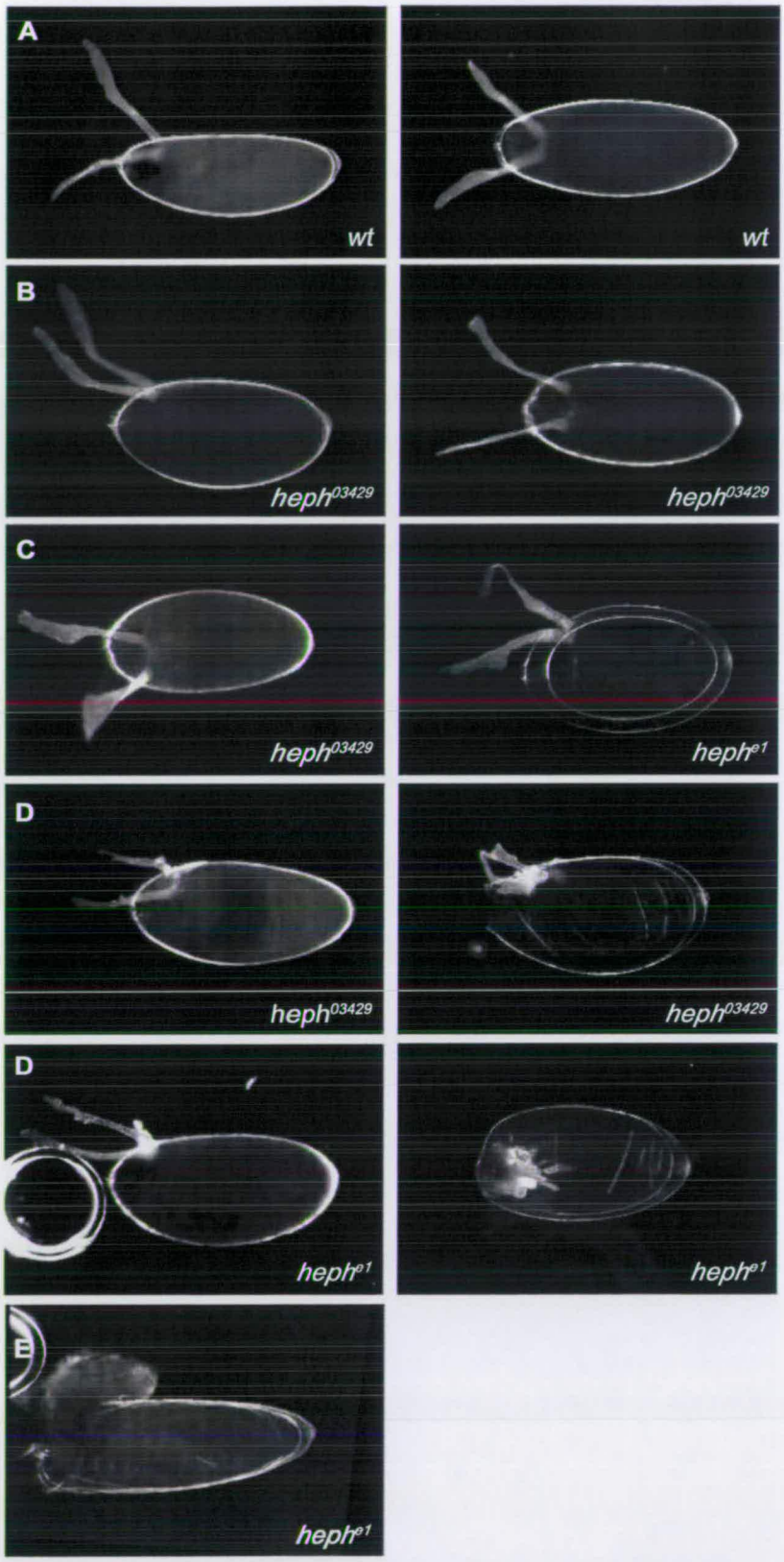

Figure 5.8 *heph* mutant eggs have patterning defects. (A) Wild-type egg with two dorsal appendages that mark the dorsal anterior surface. **(B-D)** Eggs are shorter and rounder in the *heph* mutant alleles and have a range of dorsal appendage defects from **(C)** broad with ragged edges to **(D)** shorter with 'antlers', joined by additional dorsal appendage material. **(E)** A small number of eggs are fully open at the anterior.

mutants where actin dynamics or regulation is perturbed. The eggshells shown in Fig. 5.8E are fully open at the anterior and resemble eggs laid by *cup* mutant females. Cup eggs result from defects in centripetal cell migration to close the eggshell (for review of eggshell patterning see Berg, 2005).

TABLE 5.1 Quantitation of eggshell phenotypes observed for *heph^{e1}* and *heph^{03429}* germline clones (shown in Fig. 5.8).

	% eggshell phenotype				
Genotype	**A wild-type**	**B**	**C**	**D**	**E**
w **(n=153)**	100	0	0	0	0
heph^{e1} **(n=111)**	0	24.3	10.8	56.8	8.1
heph^{03429} **(n=135)**	0	42.2	42.2	8.9	6.7

grk mRNA localization is not perturbed in *heph* mutant oocytes

Due to the dorso-ventral patterning defects seen in *heph* mutant eggs, the distribution of *grk* mRNA and Grk protein was examined in *heph* mutant egg chambers. In wild-type egg chambers, the pattern of *grk* mRNA localization changes during the progression of oogenesis. In early oogenesis (stages 1-7), *grk* is localized in a posterior crescent between the nucleus and the overlying follicle cells (Fig. 5.9A). During stages 7 and 8, *grk* begins to accumulate around the new dorso-anterior position of the nucleus as well as forming a transient ring at the anterior of the oocyte From stages 9 to 10B, *grk* is tightly localized in a dorso-anterior cap near the oocyte nucleus (Fig. 5.9C, E). *grk* mRNA localization in *heph^{e1}* and *heph^{03429}* oocytes was analysed by *in situ* hybridisation and found to be identical to the wild-type pattern of localization at all stages of oogenesis (shown for *heph^{e1}* oocytes Fig. 5.9B, D, F).

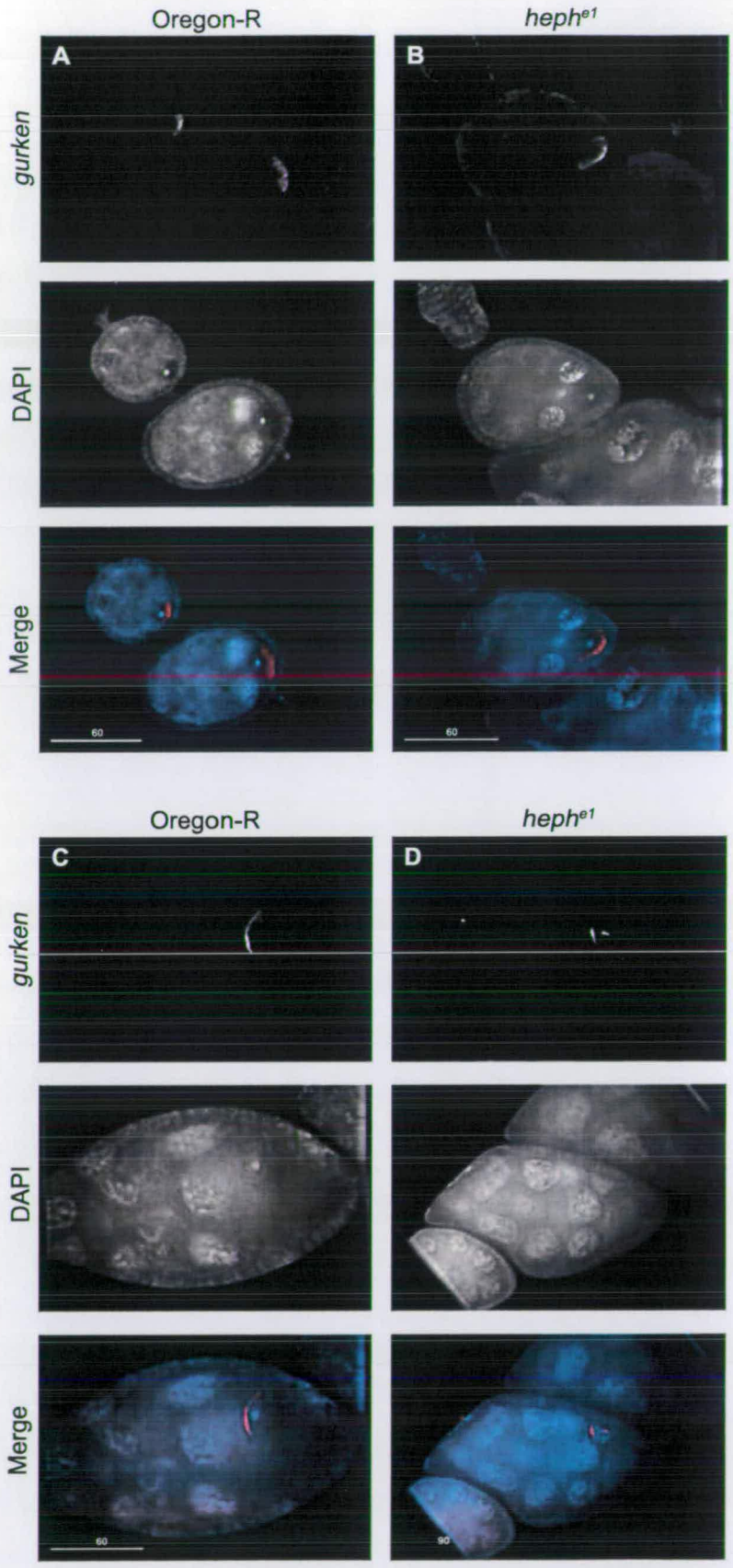

Figure 5.9 *grk* mRNA localization is not perturbed in *heph* mutant oocytes.

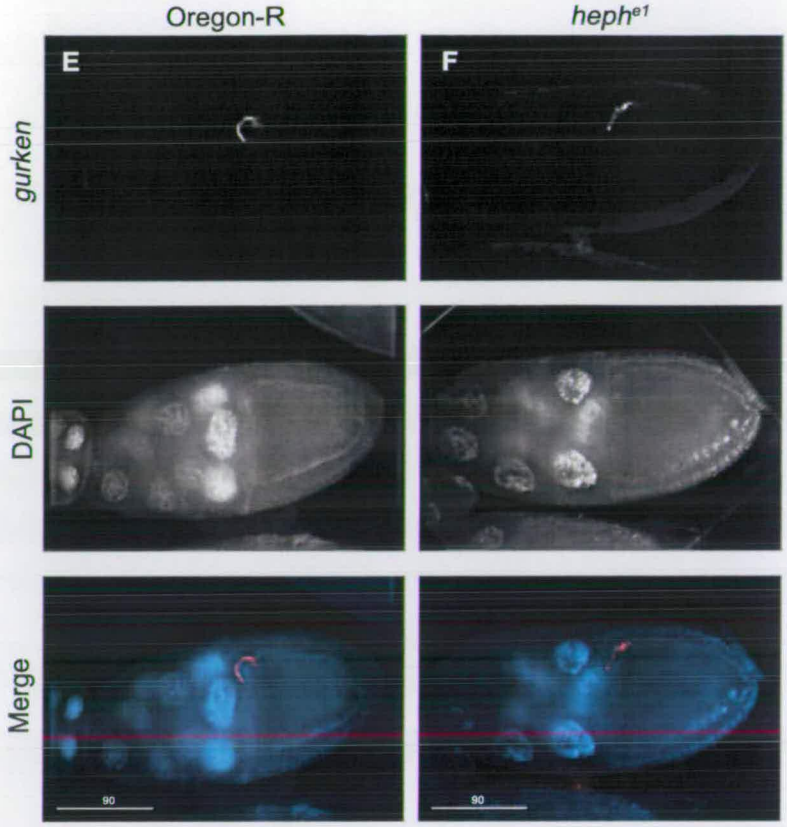

Figure 5.9 (continued) *grk* mRNA localization is not perturbed in *heph* mutant oocytes. (A, C, E) Oregon-R egg chambers at stages 6, 9 and 10 of oogenesis respectively showing *grk* mRNA localization. **(B, D, F)** *heph*^{e1} germline mutant egg chambers of the same respective stages show no difference in *grk* mRNA localization when compared to Oregon-R. Scale bars and associated numbers represent μm.

Grk protein is mislocalized in *heph* mutant oocytes

During early and mid-oogenesis the distribution of Grk protein mirrors that of *grk* mRNA, reflecting the two signalling events in which Grk acts to polarize both the follicular epithelium and the future embryo. At stage 6, Grk is enriched at the posterior of the oocyte (Fig. 5.10A), whilst by stage 9 Grk is at the dorso-anterior cap where it colocalizes with cortical actin (Fig 5.10D, G). At later stages of oogenesis (stages 10-12) the distribution of the Grk protein is different to that of the *grk* mRNA (Fig. 5.10J, M). While the *grk* mRNA is still tightly localized to the dorso-anterior cortex of the oocyte, the distribution of Grk protein extends over approximately half the length of the dorsal midline of the oocyte to form an elongated anterior to posterior stripe (Neuman-Silberberg and Schüpbach, 1996). Grk is present in the oocyte cytoplasm close to the nucleus, and in neighbouring follicle cells, but closer inspection reveals that at these stages the bulk of Grk lies in the extracellular space between the cortices of the oocyte and the follicular epithelium (Pizette *et al.*, 2009). Grk can diffuse within this space in a process regulated by glycosphingolipids (Pizette *et al.*, 2009).

Grk protein localization is wild-type up to stage 9 of oogenesis in *heph* mutant oocytes (Fig. 5.10B, C, E, F, H, I). However, in stage 10A and 10B *heph* mutant oocytes, Grk is mislocalized throughout the oocyte cytoplasm (Fig. 5.10K, L, N, O). In 42.9% $heph^{03429}$ stage 10A (n=35) oocytes and 66.7% of 10B (n=36) oocytes Grk was dispersed throughout the oocyte cytoplasm. The percentage of oocytes with this defect was higher in the $heph^{e1}$ mutant where 96.9% stage 10A (n=32) and 97.3% stage 10B (n=37) oocytes showed Grk throughout the oocyte cytoplasm. The total levels of Grk protein are unaffected in *heph* mutant ovaries (Fig. 5.11), indicating that the phenotype is due to mislocalization of translated protein, and not to overexpression of Grk. Stage 10 *heph* mutant egg chambers are also occasionally smaller than wild-type, but do not appear to have defects in actin organization.

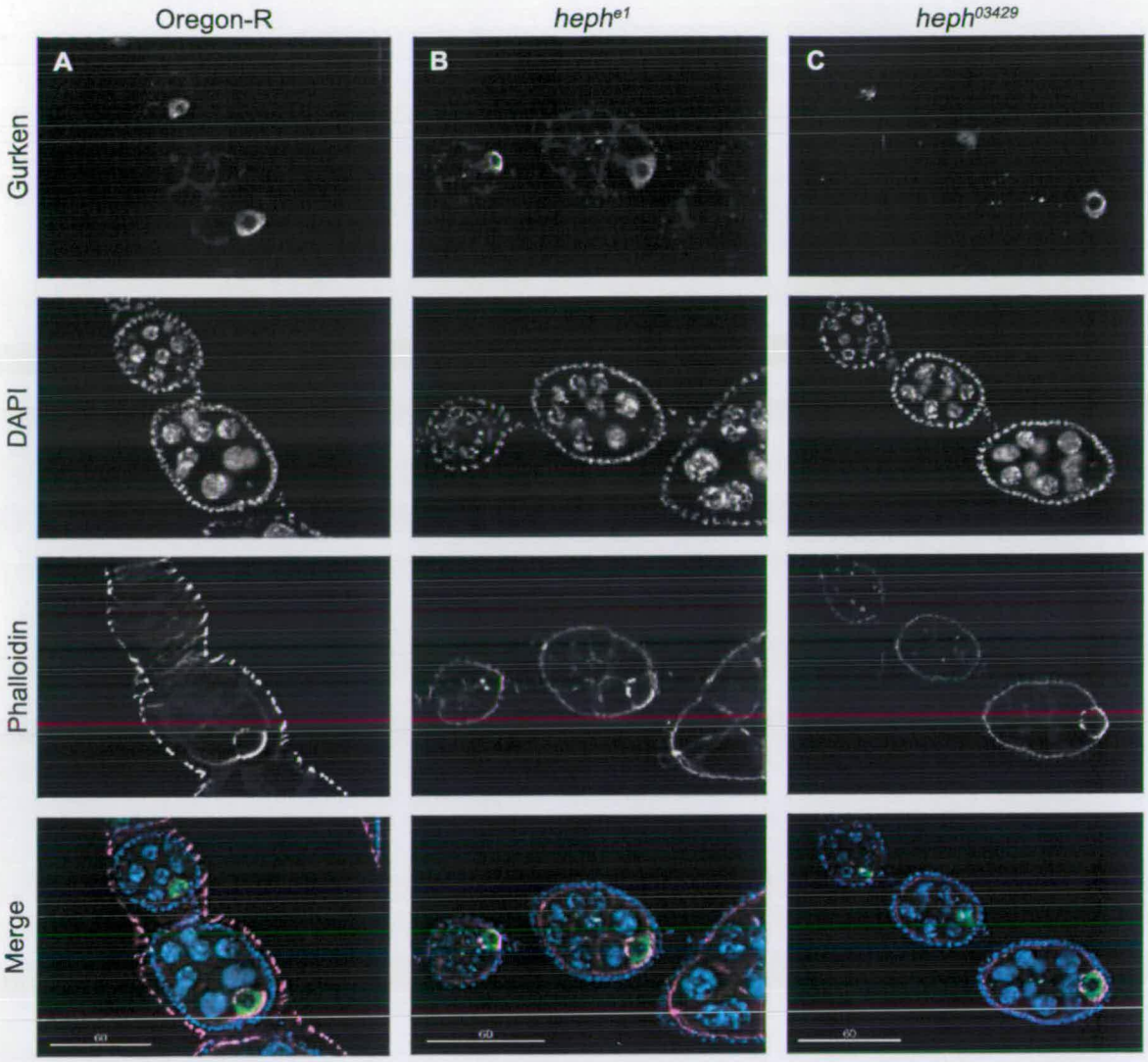

Figure 5.10 Grk protein is mislocalized in *heph* mutant stage 10 oocytes. (A) Oregon-R egg chambers at stage 6 of oogenesis. Egg chambers have been stained with anti-Gurken, DAPI and Phalloidin (labels F-actin), showing Grk localization throughout oogenesis. **(B)** $heph^{e1}$ germline mutant egg chambers at stage 6 show no difference in Grk distribution when compared to Oregon-R. **(C)** $heph^{03429}$ germline mutant egg chambers at stage 6 show no difference in Grk distribution when compared to Oregon-R. Scale bars and associated numbers represent μm.

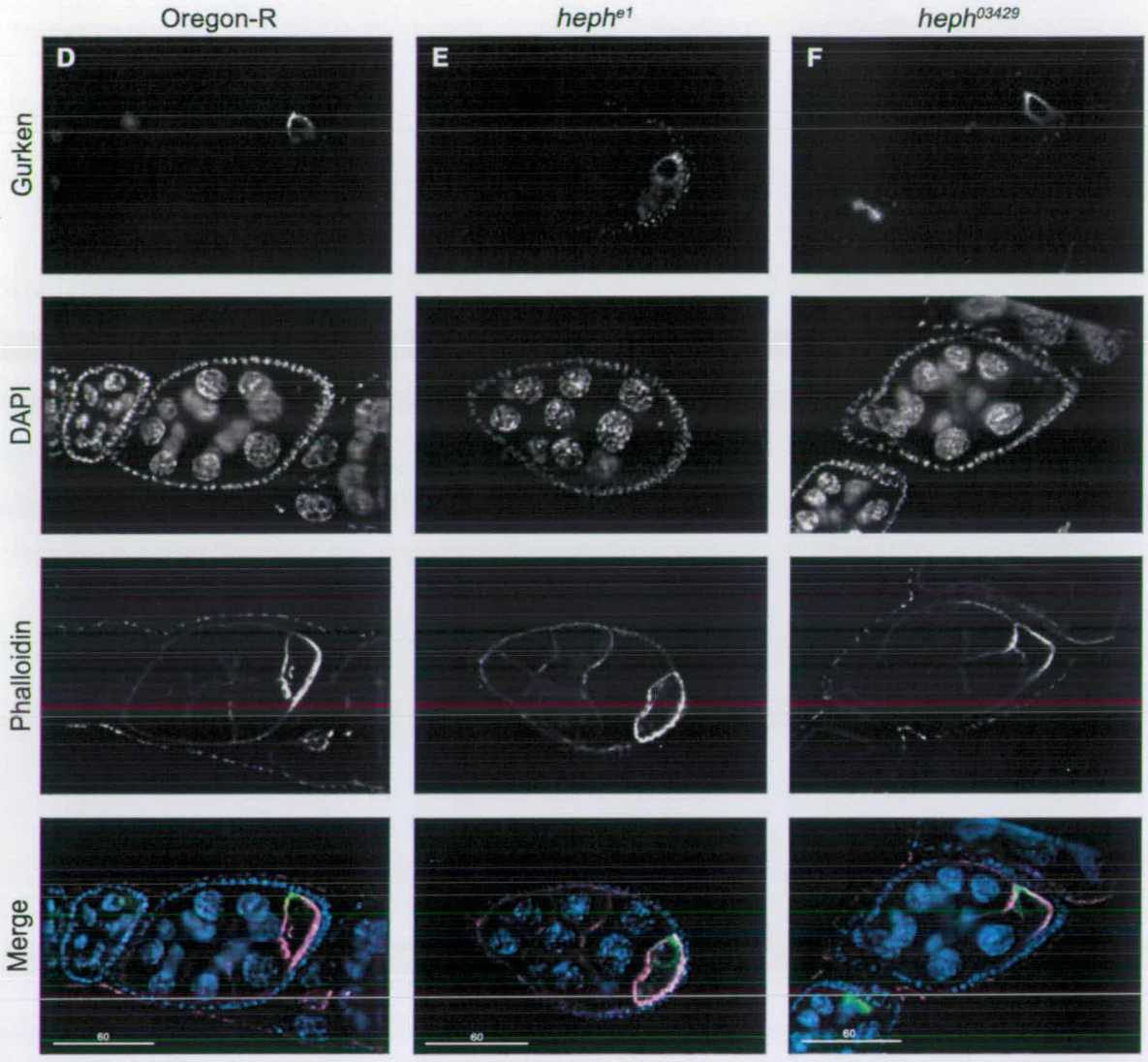

Figure 5.10 Grk protein is mislocalized in *heph* mutant stage 10 oocytes. (D) Oregon-R egg chambers at stage 8 of oogenesis. Egg chambers have been stained with anti-Gurken, DAPI and Phalloidin (labels F-actin), showing Grk localization throughout oogenesis. **(E)** *heph*^{e1} germline mutant egg chambers at stage 8 show no difference in Grk distribution when compared to Oregon-R. **(F)** *heph*^{03429} germline mutant egg chambers at stage 8 show no difference in Grk distribution when compared to Oregon-R. Scale bars and associated numbers represent μm.

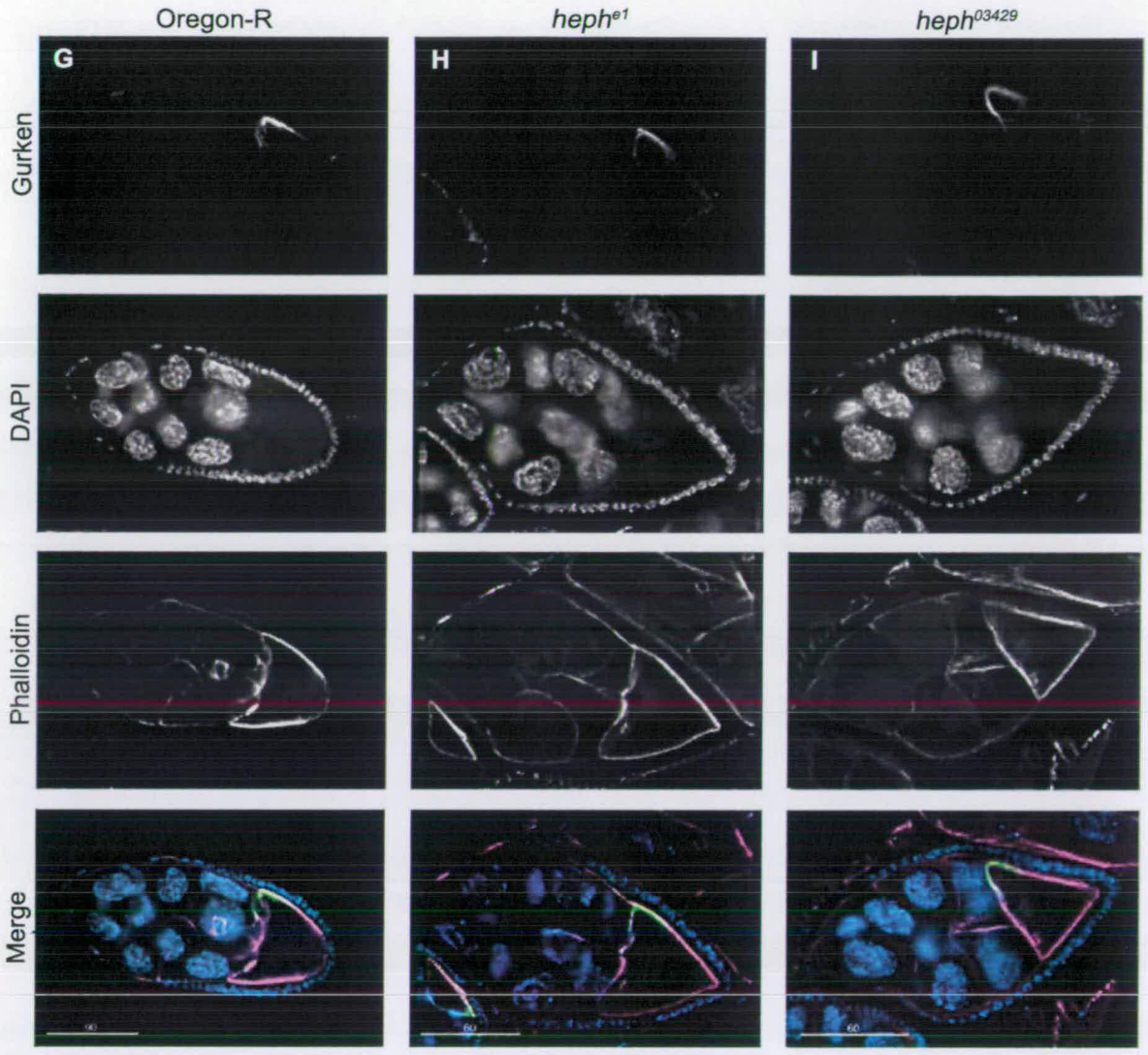

Figure 5.10 Grk protein is mislocalized in *heph* mutant stage 10 oocytes. (G) Oregon-R egg chambers at stage 9 of oogenesis. Egg chambers have been stained with anti-Gurken, DAPI and Phalloidin (labels F-actin), showing Grk localization throughout oogenesis. **(H)** *heph*^{e1} germline mutant egg chambers at stage 9 show no difference in Grk distribution when compared to Oregon-R. **(I)** *heph*^{03429} germline mutant egg chambers at stage 9 show no difference in Grk distribution when compared to Oregon-R. Scale bars and associated numbers represent μm.

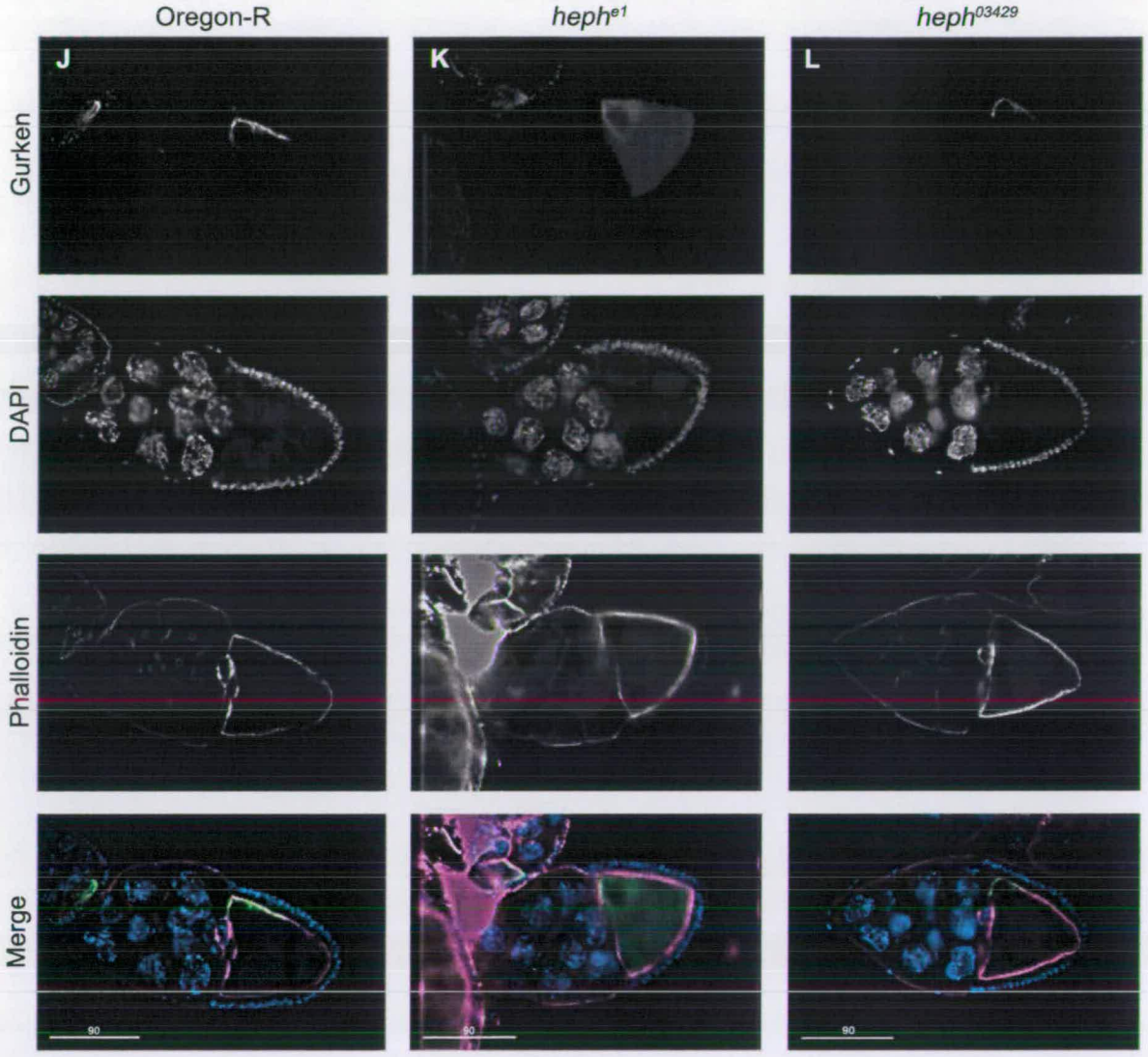

Figure 5.10 Grk protein is mislocalized in *heph* mutant stage 10 oocytes. (J, M) Oregon-R egg chambers at stages 10A and 10B of oogenesis respectively. Egg chambers have been stained with anti-Gurken, DAPI and Phalloidin (labels F-actin), showing Grk localization throughout oogenesis. **(K, N)** In $heph^{e1}$ germline mutant egg chambers at stages 10A (K) and 10B (N), Grk is evenly distributed throughout the oocyte. **(L)** The majority of $heph^{03429}$ stage 10A oocytes had a localized Grk distribution, although in 42.9% $heph^{03429}$ mutant oocytes Grk was evenly distributed throughout the oocyte. **(O)** In the majority of $heph^{03429}$ stage 10B oocytes Grk was dispersed throughout the oocyte cytoplasm. Scale bars and associated numbers represent μm.

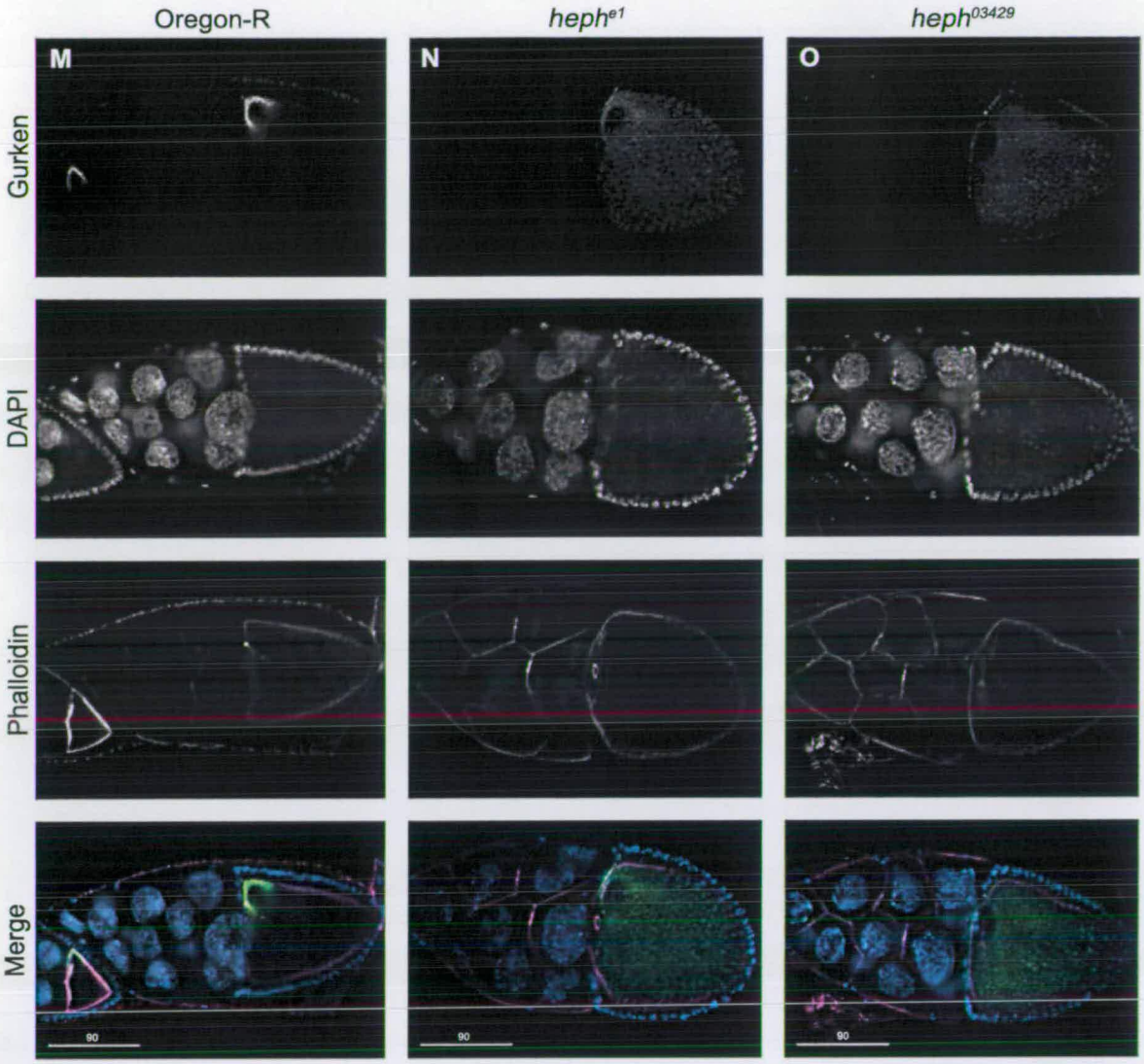

Figure 5.10 Grk protein is mislocalized in *heph* mutant stage 10 oocytes. (J, M) Oregon-R egg chambers at stages 10A and 10B of oogenesis respectively. Egg chambers have been stained with anti-Gurken, DAPI and Phalloidin (labels F-actin), showing Grk localization throughout oogenesis. **(K, N)** In $heph^{e1}$ germline mutant egg chambers at stages 10A (K) and 10B (N), Grk is evenly distributed throughout the oocyte. **(L)** The majority of $heph^{03429}$ stage 10A oocytes had a localized Grk distribution, although in 42.9% $heph^{03429}$ mutant oocytes Grk was evenly distributed throughout the oocyte. **(O)** In the majority of $heph^{03429}$ stage 10B oocytes Grk was dispersed throughout the oocyte cytoplasm. Scale bars and associated numbers represent μm.

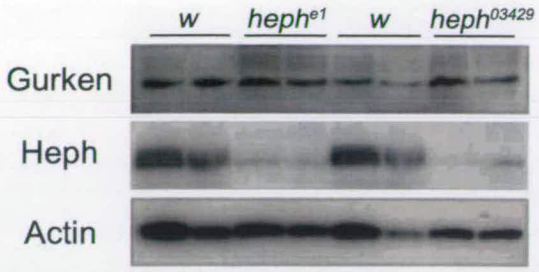

Figure 5.11 Levels of Grk protein are unaffected in *heph* mutant ovaries. Western-blot analysis comparing Heph and Grk levels in wild-type (*w*) ovarian extract with those in ovarian extracts derived from *heph* germline clones. Actin was used as a loading control.

Discussion

Heph colocalizes with *osk* mRNA during oogenesis

In agreement with studies by Davis *et al.* (2002), *heph* mRNA was detected by *in situ* hybridization in the ovaries, where it is most strongly expressed in the nurse cells of stage 10 egg chambers. Furthermore, it was also possible to detect distinct foci, perhaps nascent *heph* transcripts, within the nuclei of the nurse cells at this stage. Due to the large size of the gene, the possibility that these foci are nascent transcripts is not surprising. In the germline, Heph protein is present in the oocyte cytoplasm with an accumulation at the posterior pole of the oocyte from around stage 9 of oogenesis onward, and this posterior localization of Heph is particularly strong in late stage 10 egg chambers. This pattern of expression is consistent with a role in the regulation of localized *osk* mRNA. Heph has recently been shown to be required for correctly timed *osk* localization, possibly indirectly via a delay in focussing microtubule plus ends to the posterior pole of the oocyte (Besse *et al.*, 2009). Here, it was speculated that Heph regulates the splicing of genes involved in the establishment of microtubule polarity. However, the major function for Heph is in the multimerization of individual *osk* mRNA molecules and the formation of high order translationally repressed *osk* RNP complexes (Besse *et al.*, 2009). Heph is also localized in the cytoplasm of the follicular epithelial cells throughout oogenesis, indicating that Heph may function in the somatic as well as the germline cells of the egg chamber. No staining at the dorso-anterior cap coincident with *grk* RNA was observed, although interaction with *grk* mRNA may be transient at any of a number of stages of *grk* mRNA localization.

Besse *et al.* reported that Heph (both endogenous and GFP-Heph) colocalizes with *osk* and *osk*-associated Stau, throughout oogenesis. Additionally, Heph was shown to be present in the cytoplasm of the follicle cells only at late stages of oogenesis, and also to localize in the nuclei of both somatic and germline cells. The differences in expression pattern between the work in this thesis and in Besse *et al.* may be due to

the use of different antibodies (Besse *et al.* raised two antibodies against recombinant-PTB in rabbits and rats) or conditions for immunostaining.

Heph interacts specifically with *grk* and *osk* mRNAs

The results of RNA immunoprecipitation experiments indicate that Heph binds specifically to *grk* and *osk* mRNAs, whilst Sqd binds specifically to *grk*, *osk* and also *bcd* mRNAs. Neither protein interacted with *hb* or *nos* mRNAs. These results are consistent with GRNA experiments (Chapter 4) in which both proteins also specifically associated with ORF16 RNA, and therefore suggest that Heph is involved for the regulation of localized *grk* mRNA in addition to *osk* mRNA.

Heph has multiple functions in *Drosophila* oogenesis

Examination of *heph* germline clones reveals multiple roles for *heph* in the female germline. Germ cells homozygous for the null allele $heph^{e2}$ stop developing after the formation of 16-cell cysts (Besse *et al.*, 2009) and fail to produce differentiated egg chambers, suggesting that Heph function is required for early germ cell maintenance. The eggshell phenotypes of *heph* hypomorphic mutant eggs reveal further functions for *heph*. The eggs are short and round with a number of dorsal appendage defects. The dorsal appendages are broader than wild-type, or shorter with ectopic dorsal appendage material at the midline. The dorsal appendages of these eggs also resemble the 'moose antlers' seen in *bullwinkle* (*bwk*) mutants, suggestive of a defect in follicle cell migration and dorsal appendage morphogenesis. Moreover, a number of the eggs also displayed a dumpless phenotype, or were fully open at the anterior, indicative of defects in actin regulation and centripetal cell migration. Analysis of *grk* and Grk expression throughout oogenesis further shows that although *grk* mRNA localization is unaffected throughout oogenesis, Grk protein is dispersed throughout the cytoplasm of stage 10A and 10B oocytes. This phenotype is consistent with a defect in the processing of Grk protein following synthesis, and may explain the presence of ectopic dorsal appendage material at the midline of *heph* mutant eggs.

Therefore, from the analysis of *heph* mutant germline phenotypes it seems that *heph* may be required for germ cell maintenance, Grk processing, dorsal appendage morphogenesis, centripetal cell migration and nurse cell dumping, in addition to the characterized role of Heph in *osk* mRNA localization and translational repression (Besse *et al.*, 2009). Multiple functions for Heph in oogenesis is not surprising given that Heph orthologues are involved in many different processes. These different potential functions are now considered in greater detail.

Grk processing

Grk protein is synthesized as a 285-amino acid transmembrane protein precursor and is cleaved in the ER by a specific protease, Brother of Rhomboid (Bokel *et al.*, 2006; Ghiglione *et al.*, 2002; Guichard *et al.*, 2000; Urban *et al.*, 2002). Cleavage generates a lumenal fragment that is transported to the Golgi and released by exocytosis. The transmembrane protein Cornichon (Cni) is essential for Grk secretion and is thought to act as a specific cargo receptor for the cleaved lumenal Grk fragment in ER to Golgi transport (Bokel *et al.*, 2006; Roth *et al.*, 1995). At stage 8 Grk is concentrated within the oocyte at the dorso-anterior corner, and is present in the extracellular space between the cortices of the oocyte and the follicular epithelium above the oocyte nucleus (Herpers and Rabouille, 2004). A small fraction is also seen in the adjacent follicle cells due to uptake of secreted protein (Ghiglione *et al.*, 2002). From stage 10A onwards the bulk of Grk lies in the extracellular space (Pizette *et al.*, 2009). Grk diffuses within this space in a process regulated by glycosphingolipids (Pizette *et al.*, 2009) to form an elongated anterior to posterior stripe (Neuman-Silberberg and Schüpbach, 1996) that extends over approximately half the length of the dorsal midline of the oocyte. In the extracellular space, Grk can bind the epidermal growth factor receptor Torpedo in the plasma membrane of the follicle cells, inducing a signalling cascade that ultimately leads to the induction of dorsal fate in these cells.

The exocytic pathway in the stage 9-10 *Drosophila* oocyte comprises a continuous ER that pervades the entire oocyte (Bobinnec *et al.*, 2003; Herpers and Rabouille,

2004). Newly synthesized proteins exit the ER at specialized transitional ER sites (tER; ER exit sites). In *Drosophila* the Golgi apparatus does not always exhibit a typical morphology of stacked cisternae, but can form a clusters of vesicles and tubules that are positive for several Golgi markers and are dispersed throughout the cytoplasm. The Golgi apparatus are in proximity to tER sites, and the resulting membrane structure of one tER site and one Golgi complex is known as a tER-Golgi unit. In the *Drosophila* oocyte, multiple identical tER-Golgi units are evenly distributed throughout the cytoplasm (Herpers and Rabouille, 2004). Despite the continuity of the ER and the presence of numerous tER-Golgi units, only a subset at the dorso-anterior corner of the oocyte are involved in the transport, processing and secretion of Grk. Furthermore, mutants in which *grk* mRNA is mislocalized show that the localization of *grk* controls the choice of the tER-Golgi units used (Herpers and Rabouille, 2004).

When either Grk cleavage or ER to Golgi transport is compromised, Grk mislocalizes throughout the ER or in the oocyte cytoplasm. In *cni* mutants, Grk is retained intracellularly and is observed throughout the entire oocyte. In these mutants, Grk abnormally diffuses into the ER lumen throughout the oocyte and is not sorted at tER-Golgi units (Herpers and Rabouille, 2004; Bokel *et al.*, 2006). The same effect is also observed when ER exit is chemically blocked (Herpers and Rabouille, 2004). Furthermore, a form of Grk that cannot be cleaved accumulates in and is dispersed throughout the oocyte cytoplasm (Pizette *et al.*, 2009). The dispersal of Grk throughout the oocyte in *heph* mutants suggests that Heph could possibly function in the cleavage or in the regulation of secretion of Grk.

It is unclear as to how Heph bound to *grk* mRNA could regulate the secretion of Grk protein, and it is probable that the eggshell and Grk phenotypes observed for *heph* mutants and the ability of Heph to interact with *grk* mRNA and associate specifically with RNA containing the GLS (Chapter 4) are unrelated. Intriguingly however, Me31B and Cup are thought to be components of the *grk* transport RNP and *grk*-containing sponge bodies, but also exist in a complex (with Tral) that is associated with tER sites. This complex is thought to regulate tER site function and assembly

(Wilhelm *et al.*, 2005) by regulating the translation of tER components. Furthermore, BicC was also identified as binding specifically to GLS-containing RNA, and is also thought to regulate tER site function (Kugler *et al.*, 2009; Snee and Macdonald, 2009). *BicC* mutants interact genetically with *tral* and *cni* mutants, and both *BicC* and *tral* mutants lay ventralized eggs. The eggs are ventralized because Grk is sequestered into large 'actin cages' enriched in secretory proteins. Heph mutant eggs appear to be slightly dorsalized, but this could be due to diffusion of Grk within the ER, unrestricted use of all tER sites and therefore low level Grk signalling all over the oocyte. This could also give rise to ectopic dorsal appendage material at the midline, as very high Grk signalling is required here to properly specify follicle cell fate at the midline. It is possible then that Heph is required from stage 10 of oogenesis at tER sites in the dorso-anterior corner of the oocyte. At these sites Heph would then act to restrict the selection of tER-Golgi units, and therefore Grk protein trafficking to this region only. Together, Me31B, BicC, Cup and Heph, all known or potential components of the *grk* RNP, may also act to promote efficient and restricted local secretion of Grk protein.

A more detailed analysis of Grk localization and Grk signalling within *heph* mutant oocytes is therefore required in order to test this hypothesis. The colocalization of Grk with various ER, tER and Golgi markers, such as Sar1 (tER sites), Surf4 (ER membrane), Boca (ER resident protein) and Lava Lamp (Golgi), could be used to visualize where mislocalized Grk is in *heph* mutant oocytes. This could also be looked at closely using EM techniques. Grk signalling can be assessed using markers for Top activation, such as mirror, and for follicle cell fate, such as Broad, Rhomboid and the enhancer trap line PZ5650, that marks the follicle cells that will form the dorsal appendages. The presence of Grk in the extracellular space between the oocyte and the follicle cells should also be examined closely as should genetic interactions between *heph*, *cni*, *BicC* and *tral*.

Nurse cell dumping

The lack of wild-type *heph* function also results in a partial dumpless phenotype due to incomplete transfer of nurse cell contents into the oocyte at stage 11. *heph* mutant eggs resemble the dumpless eggs seen for mutants where actin dynamics or regulation is perturbed (for example, *quail* mutant eggs) (Robinson and Cooley, 1997). These eggs are also small with abnormal, paddleless dorsal appendages. However, initial examination of *heph* mutant egg chambers does not reveal any defects in actin organization up to stage 10B of oogenesis. It is possible that actin defects are only seen later in oogenesis, or were missed in this analysis, and so should be looked at in greater detail. *BicC* and *tral* mutants also have a dumpless phenotype, and either lack the actin organization required for dumping, or the actin cytoskeleton has an abnormal distribution and appearance. It is therefore possible that *heph* could be acting in concert again with BicC and Tral in the organization of the actin required for nurse cell dumping.

Follicle cell migration: dorsal appendage morphogenesis and centripetal cell migration

The dorsal appendages of *heph* mutant eggs resemble the 'moose antlers' seen in *bullwinkle* (*bwk*) mutants (Rittenhouse and Berg, 1995). Dorsal appendage formation involves the coordinated movement of roof and floor dorsal follicle cells progressing through three distinct phases of morphological change. Not only do the cells reorganize to form a tube, but the tube extends over the apoptosing nurse cells and then alters shape to create paddles. In *bwk* mutants, migration of the follicle cells that will form the dorsal appendages is abnormal. This is due to defects in the expression of signalling molecules that control the identity of the stretched cells, that in turn possibly produce guidance cues for the migration of the dorsal follicle cells (Tran and Berg, 2003). Mutations in 'dumpless' genes also result in abnormal dorsal appendages. It has been proposed that the residual nurse cell material in these mutants acts as a barrier that inhibits normal follicle cell migration (Schüpbach and Wieschaus, 1991). It is possible that the partially dumpless nature of *heph* mutants

therefore results in dorsal appendage defects. However, as exemplified by *bwk*, a number of signalling pathways are also required for dorsal follicle cell migration and correct dorsal appendage morphogenesis, including the Notch pathway (Ward *et al.*, 2006). As *heph* is a regulator of the Notch pathway in the *Drosophila* wing (Dansereau *et al.*, 2002), it is possible that *heph* is acting non-cell autonomously in the germline to influence Notch signalling in the dorsal follicle cells.

A small number of *heph* mutant eggshells are fully open at the anterior and resemble eggs laid by *cup* mutant females. *cup* eggshell defects result from the disruption of centripetal cell migration to close the egg (Berg, 2005). It is possible that the open anterior is an indirect effect of a defect in dumping in *heph* mutants. This can alter follicle cell function by disrupting the relative positions of, and coordination between, the germline and follicle cells. The small size of the oocyte can prevent the bulk of follicle cells from moving over the oocyte during the middle stages of oogenesis, and those cells competent to carry out centripetal migrations are too far anterior to migrate between nurse cells and oocyte, resulting in an open-ended eggshell. However, a number of signalling pathways can also regulate centripetal cell migration, including the Notch pathway. *Notch* mutant females lay *cup* eggs with an open anterior and short, wide dorsal appendages (Dobens *et al.*, 2005), and late Notch signalling in the centripetal cells is required for migration. Therefore, it may be that *heph* is also acting non-cell autonomously in the germline to influence Notch signalling in the centripetal follicle cells.

Heph may function in the *Drosophila* nervous system

heph expression becomes patterned in the developing CNS in late stage embryos, suggesting that *heph* may be required for the development of the nervous system. Consistent with this was the identification of *heph* in a screen designed to identify genes affecting neural development (Norga *et al.*, 2003). Interestingly, the same screen also identified a number of other RNA binding proteins implicated in mRNA localization/localized translation, including Imp and Smooth. An RNA localization function for *heph* in the developing nervous system also has a precedent in that PTB

is required for the localization of *β-actin* mRNA transcripts to neurite terminals (Ma *et al.*, 2007) and subsequently for neurite growth in rat PC12 cell lines. It is possible that Heph could be added to a growing list of proteins that regulate localized mRNAs in both the oocyte and the nervous system.

Intriguingly, *heph* transcripts appear to be asymmetrically localized in a crescent within cells of the CNS. Asymmetric localization of mRNA is well characterized in the CNS. The neural precursors of the nervous system, the neuroblasts, divide asymmetrically to produce an apical daughter that remains a neuroblast, and a smaller, basal daughter called a ganglion mother cell (GMC). The cell fate determinants, Numb and Prospero, become localized to the basal cortex of the neuroblast as it enters mitosis, and are subsequently segregated into the GMC (Hirata *et al.*, 1995; Knoblich *et al.*, 1995; Spana and Doe, 1995). Both Prospero protein and mRNA are localized to the basal cortex of the neuroblast (Jan and Jan, 1998). It is possible that local translation of Heph is required to maintain the asymmetrical localization of mRNAs within the neuroblast.

To determine whether Heph functions in the nervous system in regulating localized mRNAs, a more comprehensive study of the Heph expression pattern in the nervous system is required. Visualization of Heph in primary neuronal cultures or in the brain, in combination with localized mRNAs such as β-actin, *CamKIIα* and *chickadee* (Ashraf *et al.*, 2006; Estes *et al.*, 2008) will allow us to see whether Heph is a component of neuronal mRNA granules. Generation of *heph* mutant clones or overexpression of Heph in the nervous system will also reveal if *heph* has any function in the regulation of localized mRNAs in the nervous system. Within the embryonic CNS, identification of the specific cells in which *heph* is expressed is required. This is possible by double staining with markers for specific cell lineages within the CNS. It will be interesting to see where the protein, as well as the RNA, is expressed within the nervous system and whether the protein is also asymmetrically localized, as for Prospero.

In summary, *Drosophila* Heph is expressed during oogenesis in a pattern that supports a role in *osk* mRNA localization and can interact specifically with both *grk* and *osk* mRNAs. Mutant analysis has revealed that Heph has multiple functions during oogenesis and is involved in the direct translational regulation of *osk* mRNA (Besse *et al.*, 2009), can possibly act in the regulation of localized Grk secretion, and may be required in the germline for Notch signalling in the follicle cells. Heph is also required for germ cell maintenance during oogenesis, and for germ cell differentiation during spermatogenesis. If Heph is also required for the regulation mRNAs localized within neurons, then it will add to a growing list of proteins that function in maternal and neuronal transport RNPs.

The functions of mammalian and *Xenopus* orthologues of Heph, PTB and VgRBP60 respectively, indicate that Heph can potentially act in the nucleus and the cytoplasm as a direct translational regulator, as a splicing factor and as a regulator of mRNA stability. Heph can promote oligomerization of RNA molecules consistent with the ability of PTB to restructure RNA, and may also be able to remodel RNA-protein complexes. The challenge in future experiments will be to define exactly how and why Heph interacts with *grk* mRNA, and how this relates if at all to a possible role for Heph in Grk secretion, and also how Heph can also affect follicle cell migration and the organization of the cytoskeleton in the egg chamber. For example, Heph might be required directly to facilitate proper Grk secretion, but could also regulate the splicing of genes required for Notch signalling or for the establishment of the cytoskeletal network.

CG17838: A CONSERVED FACTOR REQUIRED FOR mRNA LOCALIZATION IN OOCYTES AND NEURONS?

Introduction

Drosophila CG17838 was identified in Chapter 4 as one of a number of proteins able to bind specifically to GLS-containing RNA. It was therefore hypothesized that CG17838 could be a component of a *grk* RNP at one or a number of stages of oogenesis and play a role in *grk,* and possibly other mRNAs, localization, localized translation or anchoring in the oocyte. This hypothesis is supported by functions for the mammalian orthologues, SYNaptotagmin-binding, Cytoplasmic, RNA-Interacting Protein (SYNCRIP) and hnRNP R, in neuronal mRNA localization and translational regulation.

CG17838 is the *Drosophila* orthologue of mammalian SYNCRIP and hnRNP R

This work has identified the hnRNP protein CG17838 as the *Drosophila* orthologue of mammalian SYNCRIP and hnRNP R. The name of SYNCRIP is derived from the ability of the protein to bind both ubiquitous Synaptotagmins (Syts) and RNA, and its cytoplasmic subcellular localization in transfected tissue culture cells, mouse cerebellar and rat hippocampal neurons (Bannai *et al.*, 2004; Mizutani *et al.*, 2000). In mouse there are two splice isoforms, 1 and 2. Both isoforms contain an N-terminal acidic domain, three RRM domains, nuclear localization signals and an RGG box (a region rich in arginine and glycine residues that can bind RNA and protein). Isoform 1 is also referred to as hnRNP Q3 and GRY-RBP and has a C-terminal extension that is not present in isoform 2. Isoform 2 is also known as hnRNP Q1 and NSAP1, and has a shorter, unique C-terminus. As isoform 2 was the isoform shown to bind Syts and RNA and localize in the cytoplasm, SYNCRIP, unless otherwise stated, refers to isoform 2. In human there is a third isoform referred to as hnRNP Q2 that lacks a region of the second RRM domain (Mourelatos *et al.*, 2001). SYNCRIP is also highly homologous (82% identical) to hnRNP R (Mizutani *et al.*, 2000). Both

SYNCRIP and hnRNP R are ubiquitously expressed across a number of different tissues in the mouse. However, at the subcellular level, hnRNP R is predominantly nuclear (Mizutani *et al.*, 2000), and it has been suggested that SYNCRIP is the cytoplasmic counterpart of hnRNP R.

SYNCRIP isoforms interact with the orthologues of many of the proteins isolated by GRNA, and are involved in multiple forms of mRNA regulation such as the regulation of stability, RNA editing, splicing and mRNA localization. This suggests that SYNCRIP, and CG17838, may be part of a core conserved protein complex that is required for a number of processes, including pre-mRNA splicing and mRNA localization. The functions of SYNCRIP and its interacting proteins and RNAs are now discussed.

RNA editing

Apolipoprotein (apo)B plays a central role in lipoprotein metabolism, and exists in two major isoforms, one of which is the result of editing of the transcript to introduce an alternative stop codon. GRY-RBP has been identified as part of a large multiprotein complex that mediates apoB mRNA editing (Blanc *et al.*, 2001; Lau *et al.*, 2001). This complex, known as the editosome, contains Apobec-1 as the catalytic component and Apobec-1 complementation factor (ACF). GRY-RBP binds Apobec-1, ACF and apoB mRNA. Furthermore, GRY-RBP binding to ACF competitively inhibits the binding of ACF to apoB (Blanc *et al.*, 2001; Chen *et al.*, 2007), thereby inhibiting and regulating the editing of mammalian apoB RNA during development (Chen *et al.*, 2007).

mRNA stability

Proto-oncogene *c-fos* is a member of a class of genes whose transient expression plays a crucial role in cell proliferation, differentiation, and apoptosis. Rapid turnover of *c-fos* mRNA is an important mechanism for controlling this transient expression. The stability of *c-fos* mRNA is controlled by the major protein coding

region determinant (mCRD) that facilitates deadenylation and decay of the transcript in a process that requires translation in order to occur (Schiavi *et al.* 1994). SYNCRIP was purified with PABP, PABP-interacting protein 1 (PAIP-1), the RNA binding protein Unr and hnRNP D as part of a complex that can form on the mCRD (Grosset *et al.*, 2000). These proteins are thought to form a bridging complex on the mRNA between the poly(A) tail and the mCRD that stabilizes the mRNA. Ribosome transit is thought to reorganize or disrupt this complex so that deadenylation and decay can occur. *c-myc* mRNA is also subject to translation-coupled decay by polysome-associated endonucleases (Bergstrom *et al.* 2006; Sparanese and Lee 2007). Rare codons in the CRD of the transcript are thought to slow down ribosome transit allowing cleavage to occur (Lemm and Ross, 2002). The mRNA is stabilized by a protein complex that contains SYNCRIP, IMP1, hnRNP U, Y-box protein YBX1, and the RNA helicase DHX9. This multi-protein SYNCRIP-containing complex prevents decay by sequestering the mRNA into nontranslating cytoplasmic RNPs (Weidensdorfer *et al.*, 2009).

Viral RNA regulation-translation and replication

SYNCRIP was first identified as NS-associated protein 1 (NSAP1) (Harris *et al.*, 1999). NS1 is the major nonstructural parvovirus protein and is responsible for multiple aspects of viral replication. A yeast two-hybrid screen for host protein interactors of NS1 identified NSAP1. SYNCRIP has since been shown to bind to the positive and negative strands of the 5'UTR of mouse hepatitis virus (MHV) with PTB, PABP, hnRNP A1 and several other unidentified proteins, and directly regulate MHV RNA synthesis (Choi *et al.*, 2004). In addition, SYNCRIP colocalizes with newly synthesized HCV RNA and knockdown of SYNCRIP suppresses HCV replication by directly inhibiting HCV RNA replication (Liu *et al.*, 2009).

In addition to viral replication, SYNCRIP is also required for HCV translation. PTB and a second protein, La also have this dual function in the HCV life cycle. Translational initiation of HCV occurs by internal entry of ribosomes into an IRES spanning the 5'UTR. Full activity of the IRES depends upon the presence of a

protein-coding sequence downstream of the initiating codon. SYNCRIP was found to bind this region and was shown to enhance HCV IRES-dependent translation. Knockdown experiments showed that SYNCRIP was also required for translation of HCV mRNA during HCV proliferation, suggesting that SYNCRIP plays an important role in the production of viral proteins during HCV infection (Kim *et al.*, 2004). SYNCRIP can also enhance IRES activity within cellular mRNAs. The IRES activity of *Bip* mRNA (*Bip* encodes a stress response protein) increases when cells are subject to heat stress and SYNCRIP is required for this response via direct binding to the *Bip* mRNA (Cho *et al.*, 2007).

RNA splicing

Drosophila CG17838 is the only fly hnRNP protein to be consistently isolated in the spliceosomal B complex (spliceosomal assembly intermediate) affinity purified using tagged pre-mRNA (Herold *et al.*, 2008), although its function in the spliceosome has not been characterized. A role for hnRNP Q in splicing was first suggested by the identification of hnRNPQ 3 (GRY-RBP) as a major spliceosome-associated protein (Neubauer *et al.*, 1998). In *in vitro* splicing assays, hnRNP Q proteins immunoprecipitate with pre-mRNA and intron-containing RNA intermediates. Immunodepletion of hnRNP Qs and the closely related hnRNP R also leads to an overall decrease in splicing efficiency (Mourelatos *et al.*, 2001). Moreover, the splicing activity of hnRNP Q has links to human disease. Spinal muscular atrophy (SMA) is a disorder characterised by muscle weakness and atrophy caused by progressive motor neuron degeneration. The disease is caused by mutations in the Survival Motor Neuron 1 (*SMN1*) gene (Lefebvre *et al.*, 1995), and motor neuron degeneration is observed when full-length SMN levels are reduced, or when SMN is truncated (Jablonka *et al.*, 2000). The human genome contains a duplication of the *SMN* gene, known as *SMN2*. The only coding region difference between the two is a single nucleotide substitution that results in skipping of exon 7 in most *SMN2* transcripts, resulting in a truncated protein that is unable to function fully (Lorson and Androphy, 2000). *SMN2* is unable to compensate for *SMN1* loss in SMA, and motor neuron degeneration is observed in mouse models when exon 7 is deleted

(Frugier *et al.*, 2000) or human *SMN2* is expressed at low levels in an *SMN* null background (Hsieh-Li *et al.*, 2000; Monani *et al.*, 2000). hnRNP Q can serve as a splicing regulator for alternative splicing of *SMN*. hnRNP Q1 (SYNCRIP) directly binds to *SMN* exon 7 and promotes inclusion of this exon, probably by activating use of its upstream 3'splice site. Furthermore, the hnRNP Q2 and Q3 splice isoforms antagonise this activity and promote exon 7 exclusion suggesting that differential expression of hnRNP Q isoforms can result in fine control of SMN precursor mRNA splicing (Chen *et al.*, 2008). This also raises the possibility that hnRNP Q is a potential therapeutic target for SMA and could act to increase exon 7 inclusion in *SMN2* transcripts in patients with SMA.

SMN itself is primarily involved in the assembly of spliceosomal U snRNPs and may also participate in pre-mRNA splicing (Meister *et al.*, 2002; Paushkin *et al.*, 2002; Pellizzoni *et al.*, 1998). SMN protein lacking exon 7 is unable to interact with U snRNP Sm proteins and fails to promote splicing *in vitro* (Pellizzoni *et al.*, 1998; Pellizzoni *et al.*, 1999). hnRNP Q proteins and hnRNP R have also been shown to interact *in vitro* and *in vivo* with SMN protein through the C-terminal RGG box, and the most common SMN mutant in SMA is deficient in its ability to interact with the hnRNP Q proteins (Mourelatos *et al.*, 2001; Rossoll *et al.*, 2002), suggesting that hnRNP Q and R also function with SMN protein itself in pre-mRNA splicing.

mRNA localization

SMN is also thought to have functions in addition to splicing in neurons, including the assembly and regulation of localized RNP complexes. SMN has been detected in the cytoplasm of neurites and axons of motor neurons (Rossoll *et al.*, 2002; Rossoll *et al.*, 2003), and has been observed in association with cytoskeletal elements in spinal dendrites and axons (Bechade *et al.*, 1999; Pagliardini *et al.*, 2000). In cultured primary neurons, endogenous SMN was localized in granules (that did not contain other snRNP assembly factors) that extended throughout processes and into growth cones (Zhang *et al.*, 2003). Furthermore, live cell imaging revealed that SMN granules displayed rapid, bidirectional and cytoskeletal-dependent movements

(Zhang *et al.*, 2003). Disruption of exon 7 impaired this trafficking and resulted in reduced neurite outgrowth. Deficiency of SMN has also been shown to result in reduced localization of *β-actin* mRNA to distal axons and growth cones in cultured motor neurons (Rossoll *et al.*, 2003) and subsequently reduced axon growth. In the same study, hnRNP R was also shown to modulate *β-actin* localization in axons and could associate with the *β-actin* 3'UTR in an interaction that required SMN. As hnRNP R also localizes with SMN in the axons of motor neurons, and binds SMN via a domain that is highly conserved in hnRNP Q, it is tempting to speculate that hnRNP Q and R are part of an SMN-containing complex that is required for axonal RNP localization, and that this is disrupted in SMA.

Interestingly, the ability of SYNCRIP to bind ubiquitous Syts and RNA led to the hypothesis that the Syts and SYNCRIP function together in the regulation of organelle-based mRNA transport. Syts are thought to regulate neuronal synaptic vesicle docking, fusion and neurotransmitter release and non-neuronal SNARE-based vesicle trafficking. It was therefore proposed that ubiquitous Syts and SYNCRIP could both regulate mRNA transport involving vesicles and membranes. This would not be the first example of the coupling of membrane and mRNA trafficking (Cohen, 2005). In *S. cerevisiae*, *ASH1* mRNA localization is coupled with ER segregation (Schmid *et al.*, 2006), whilst in *Xenopus* oocytes, *Vg1* mRNA is associated with a subcompartment of the ER during localization (Deshler *et al.*, 1997) and cortical ER is implicated in anchoring localized *Vg1* mRNA (Alarcon and Elinson, 2001).

Although SYNCRIP-dependent, membrane-coupled mRNA localization has yet to be shown, more direct evidence for SYNCRIP function in mRNA localization stems from its presence in the dendrites of rat hippocampal neurons. Proteomic analysis showed that SYNCRIP preferentially associates with protein complexes involved in mRNA processing and translation, including hnRNPs, DEAD-box helicases, PABP, IMP1-3, YBX-1, La and ribosomal proteins. Within dendrites, SYNCRIP has been shown to be a component of granules containing *IP$_3$R1* mRNA, Stau and Ef1α that are transported in a microtubule-dependent manner (Bannai *et al.*, 2004). SYNCRIP

has also been shown to interact directly with the noncoding BC200 RNA and to be part of the native BC200 RNP (already shown for La, FMRP and PABP; Kremerskothen *et al.*, 1998a; Muddashetty *et al.*, 2002; Zalfa *et al.*, 2005). The interaction between SYNCRIP and BC200 requires the conserved SYNCRIP RRMs 1 and 2 and a poly(A) domain within BC200 (Duning *et al.*, 2008). SYNCRIP has also been isolated as a component of neuronal RNA granules (Elvira *et al.*, 2006; Kanai *et al.*, 2004) including the large RNA granule purified using the tail of KIF5 from brain extract (Kanai *et al.*, 2004). This granule was shown to contain many proteins including FMRP, Stau, DEAD-box proteins, hnRNPs, Ef1α and the mRNAs *CamKIIα* and *Arc*. Functional analysis suggested that SYNCRIP does not play an essential role in dendritic RNA granule transport, but may play a role in the translational regulation of localized mRNAs, consistent with its interaction with BC200 and PABP.

SYNCRIP has also been shown to be a component of P bodies, the RNAi machinery, and potentially stress granules (Moser *et al.*, 2007; Quaresma *et al.*, 2009). This highlights again the shared components between neuronal localized RNA granules, P bodies and stress bodies, and also provides a further indication that small RNAs may act to regulate localized mRNAs. Given that these similarities extend to maternal RNA granules, it is a possibility that the *Drosophila* orthologue of SYNCRIP is involved in the regulation of localized mRNAs in the oocyte.

Aims of this chapter

It was the general aim of the work in this chapter to study the function of CG17838 in mRNA localization and localized translation in the oocyte (with particular regard to *grk* mRNA) and nervous system by asking the following questions:

- What is the expression pattern of CG17838 during oogenesis?
- Does CG17838 interact with localized mRNAs and *trans*-acting factors in the germline?
- Does the distribution/levels of localized transcripts and the proteins they encode change in *CG17838* mutants?
- Is the role of SYNCRIP in mammalian neuronal mRNA localization conserved in the *Drosophila* nervous system?

Results

CG17838 is the *Drosophila* orthologue of mammalian SYNCRIP and hnRNP R

Drosophila CG17838 was identified by mass spectrometry in Chapter 4 as one of a number of proteins able to bind specifically to GLS-containing RNA. *CG17838* is a complex gene contained within 50 kb of genomic sequence. Two genes, CG31195 (function unknown) and Tak1-like 1 (Takl1; predicted to have tyrosine kinase activity), also lie within the first intron of CG17838. Alternative splicing is predicted to result in a number of *CG17838* transcripts, and therefore protein isoforms (CG17838-A to -H) (Fig. 6.1). CG17838-F was identified in GRNA mass spectrometry. BLAST searches identified mammalian SYNCRIP and hnRNP R as potential orthologues of CG17838-F, with up to 47.1% amino acid identity and 59.6% similarity (table 6.1) between the proteins.

Mouse has two splice isoforms of the SYNCRIP protein. Isoform 1 (also referred to as hnRNP Q3 and GRY-RBP in human) is a 623 amino-acid protein composed of an N-terminal acidic domain followed by three consecutive RNA binding RRM domains, two putative nuclear localization signals (NLS), a 120 amino-acid region rich in arginine and glycine (RGG box) and tyrosine residues, and a C-terminal domain rich in glutamine (Q) and asparagines (N) residues. Isoform 2 (also referred to as hnRNP Q1 and NSAP1 in human) lacks the last 74 amino acids (that include one predicted bipartite NLS, and the Q/N-rich region) from the C-terminus of isoform 1, which have been replaced by 15 unique amino acids. In human, there is a third isoform known as hnRNP Q2 that lacks 34 amino acids of RRM 2 (Mourelatos *et al.* 2001). SYNCRIP is also highly homologous to (82% identical for isoform 1) to hnRNP R (Mizutani *et al.*, 2000; table 6.1). hnRNP R has the C-terminal Q/N-rich extension and second NLS seen in isoform 1/hnRNP Q3/GRY-RBP, and differs in amino acid sequence at the N-terminus to the SYNCRIP isoforms. A schematic of the domain organization and the differences between these proteins is shown in Figure 6.2.

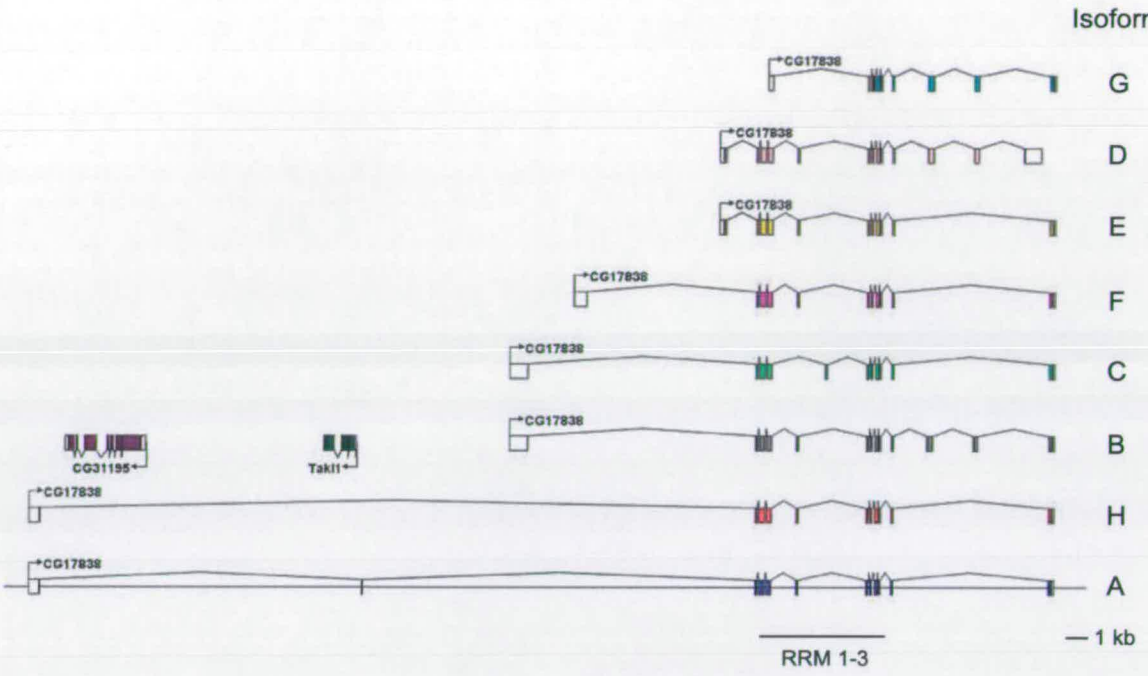

Figure 6.1 The genomic organization of *CG17838*. CG17838 is a complex gene, containing 19 exons within 50 kb of genomic sequence. Two genes, *Takl1* and *CG31195*, lie within introns, and alternative splicing is predicted to result in eight isoforms, CG17838-A-H. The exons encoding the conserved RRMs 1-3 are indicated.

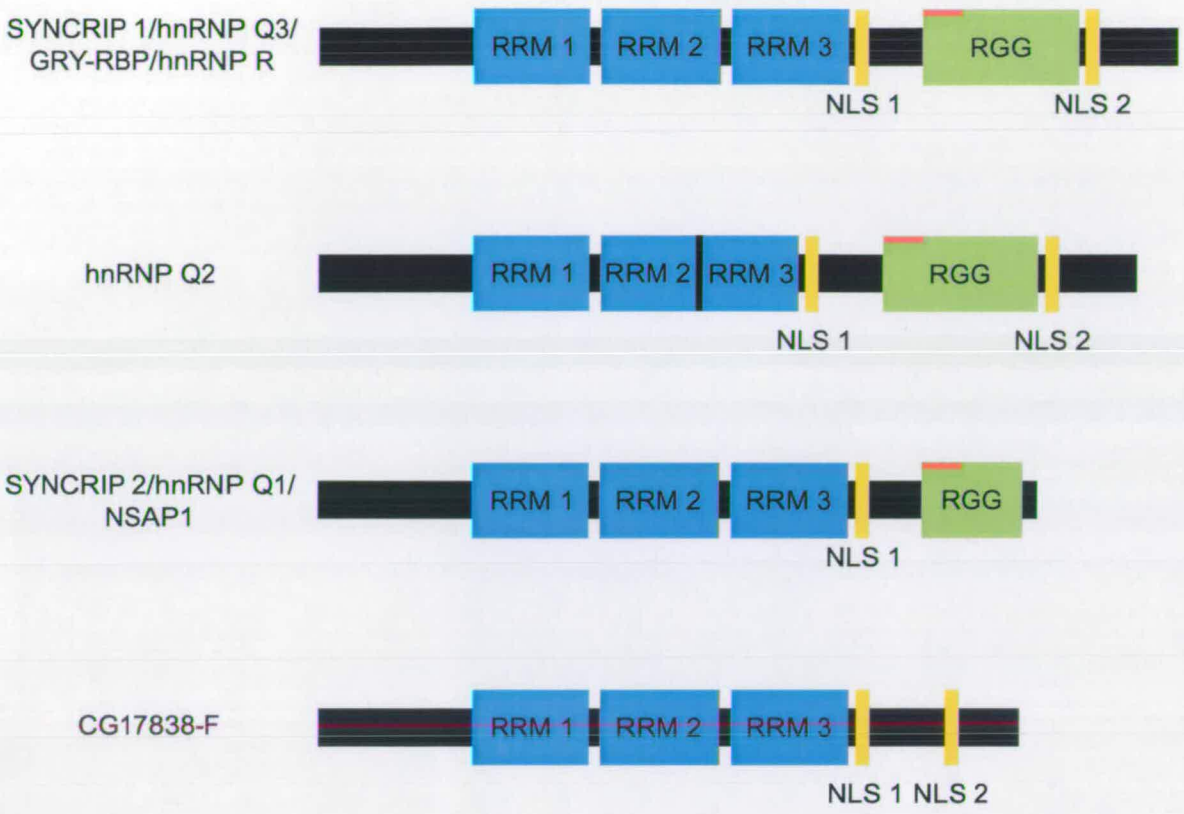

Figure 6.2 Schematic representation of the mouse and human SYNCRIP/hnRNP Q isoforms, hnRNP R and CG17838-F. RRM, RNA Recognition Motif; NLS, Nuclear Localization Signal; RGG, arginine-glycine-glycine-rich domain. Red line within RGG domain corresponds to a tyrosine-rich region.

Alignment of CG17838-F with all human and mouse SYNCRIP isoforms and hnRNP R reveals that the three RRM domains are highly conserved (percent amino acid identity increases up to 68% in the RRM domains; table 6.2), as is the N-terminal domain. All human and mouse isoforms have the RGG box and tyrosine-rich region. Both of these are absent in CG17838-F, but CG17838-F is predicted to contain the second bipartite NLS that is present in SYNCRIP isoform 1/hnRNP Q3/GRY-RBP, hnRNP Q2 and hnRNP R. CG17838-F also has a C-terminus that contains a number of glutamine and asparagine residues (Fig. 6.3).

Examination of other CG17838 isoforms reveals that most isoforms are also homologous to SYNCRIP and hnRNP R (Fig. 6.4; table 6.1). Most contain the three-conserved RRM domains found in isoform F (Fig. 6.4). Isoform C has a stretch of 20 amino acids that differ in sequence from F at the C-terminal end of RRM 1 (Fig. 6.4; table 6.2). Isoforms A, H, D and E have N-terminal extensions that are not conserved in SYNCRIP isoforms and hnRNP R. Isoforms B, D and G have a glycine-rich insertion at the C-terminus that contains multiple RG dipeptides and tyrosine residues. Isoform G is otherwise truncated, and consists of RRM 3 and the extended C-terminus only. Isoform D does not have the second predicted bipartite NLS or C-terminus that is present in isoform F and all other isoforms. These differences probably reflect different tissue/cellular compartment specific functions for the multiple isoforms, just as SYNCRIP isoforms have different functions, and SYNCRIP and hnRNP R differ in their subcellular localization. For example, similar to SYNCRIP 2/hnRNP Q1/NSAP, isoform D does not have the second predicted NLS that could reflect more cytoplasmic functions for this isoform. Isoform C differs within RRM1 and isoform G only has RRM 3 and this could reflect a difference in the RNA binding targets and ability for F, C and G. Different isoforms could also act to regulate the functions of others as hnRNP Q2 and 3 have been shown to act antagonistically to hnRNP Q1 in splicing (Chen *et al.*, 2008).

The specific identification of CG17838-F in mass spectrometry does not necessarily mean that CG17838-F was the isoform able to associate with ORF16 in GRNA experiments. The peptides isolated were all within CG17838-F, but as described above, most isoforms share the domains found in isoform F with additional extensions and insertions at the N- and C-termini. The absence of peptides corresponding to these extensions in mass spectrometry does not mean that they were not present. However, I chose to work with CG17838-F initially as preliminary RT-PCR analysis showed that it was expressed in the ovary and it contains domains that are found in all other isoforms.

Due to the conserved N-terminus and RRM domain structure, and the ability of CG17838-F to bind *Drosophila* Synaptotagmin and RNA (Fig. 6.6), I propose that CG17838 is a *Drosophila* orthologue of SYNCRIP. Multiple CG17838 isoforms could potentially reflect functions related to different SYNCRIP isoforms and hnRNP R.

Conserved residues linked to post-translational modification

SYNCRIP/hnRNP Q isoforms are phosphorylated at a number of residues. SYNCRIP was shown to be tyrosine (Y) phosphorylated in response to insulin stimulation in adipocytes, and this phosphorylation was increased by osmotic shock (Hresko and Mueckler, 2000). Furthermore, *in vitro* phosphorylation of SYNCRIP is only possible in the absence of RNA (Hresko and Mueckler, 2002). Further analysis of tyrosine residues that were phosphorylated in response to fibroblast growth factor receptor-1 (FGF-1) (Hinsby *et al.*, 2003) identified Y-373 as a phosphorylation site in SYNCRIP. This residue lies within RRM 2, and so is a good candidate for a residue whose phosphorylation can be regulated by RNA binding. This tyrosine is conserved in all SYNCRIP/hnRNP Q isoforms, hnRNP R, CG17838-F and all other CG17838 isoforms (Fig. 6.3 and 6.4), suggesting that CG17838 could also be phosphorylated at this site.

TABLE 6.1 CG17838 is homologous to SYNCRIP and hnRNP R. Percent amino acid identity is indicated and, in brackets, percent similarity. Percentages were calculated using the EMBOSS Blosum62 pairwise alignment algorithm.

	SYNCRIP 2/ hnRNP Q1/NSAP1	hnRNP Q2	SYNCRIP 1/ hnRNP Q3/GRY-RBP	hnRNP R
CG17838-F	47.1 (59.6)	42.7 (52.9)	45.9 (57.1)	46.0 (58.2)
CG17838-A	45.1 (57.0)	41.1 (52.9)	44.1 (54.9)	44.0 (55.5)
CG17838-B	41.8 (52.1)	42.4 (52.1)	45.1 (55.7)	44.4 (55.9)
CG17838-C	46.6 (59.6)	42.3 (52.9)	45.4 (57.1)	45.4 (57.9)
CG17838-D	42.2 (52.9)	38.3 (48.0)	40.9 (52.0)	41.3 (52.7)
CG17838-E	44.2 (56.3)	40.3 (50.2)	43.3 (54.2)	43.4 (55.0)
CG17838-G	14.0 (18.1)	18.3 (23.2)	17.7 (22.3)	17.2 (22.4)
CG17838-H	47.2 (59.7)	42.8 (53.0)	45.9 (57.2)	46.0 (58.0)
hnRNP R	72.5 (80.5)	76.9 (85.2)	82.1 (90.7)	

TABLE 6.2 The RRM domains are highly conserved between SYNCRIP, hnRNP R and CG17838. Percent amino acid identity is indicated and, in brackets, percent similarity. Percentages were calculated using the EMBOSS Blosum62 pairwise alignment algorithm. Amino acid identity increases up to 68% in the RRM domains.

	RRM 1	RRM 2	RRM 3
CG17838 all isoforms (G only RRM 3)	63.8 (78.8)	68.3 (82.9)	59.7 (80.6)
CG17838-C (Differs RRM 1)	66.2 (78.8)	As above	As above

Figure 6.3 Alignment of mouse SYNCRIP/human hnRNP Q isoforms, hnRNP R and *Drosophila* CG17838-F

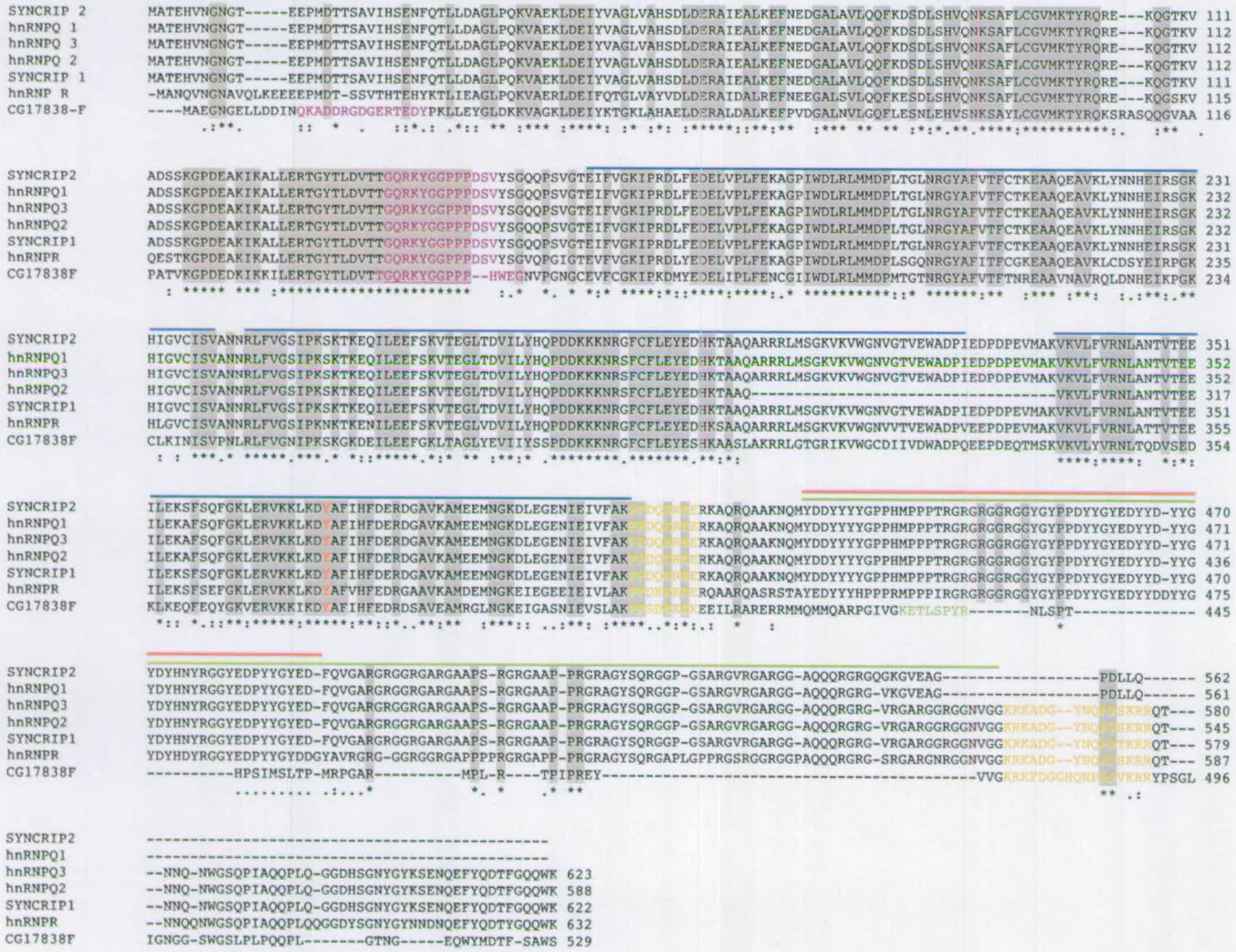

Figure 6.3 Alignment of mouse SYNCRIP/human hnRNP Q isoforms, hnRNP R and *Drosophila* CG17838-F. Blue line, RRM domains; green line, RGG domain; red line, tyrosine-rich region; orange residues, predicted NLS sequences; red residues, post-translationally modified in SYNCRIP; purple residues, peptide sequences used to raise anti-CG17838 polyclonal antibody (the partially conserved peptide against which the anti-SYNCRIP (mouse protein) antibody was raised is underlined); green residues, additional amino acids present in the CG17838-F sequence cloned from *Drosophila* ovary total RNA. The alignment was generated using ClustalW2.

Figure 6.4 Alignment of CG17838 protein isoforms

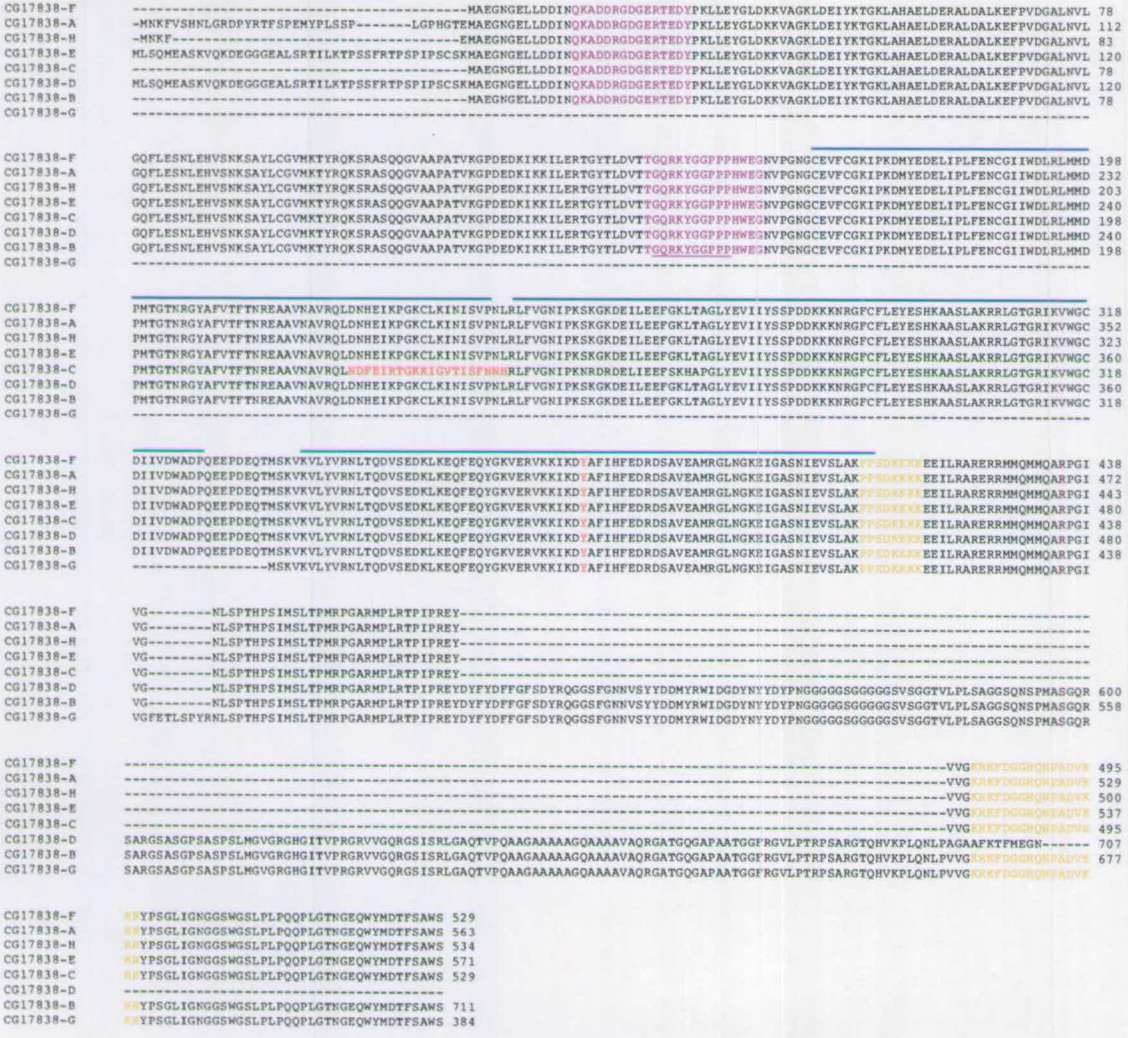

Figure 6.4 Alignment of CG17838 protein isoforms. Most isoforms contain the three-conserved RRM domains (blue line). Isoform C has a stretch of 20 amino acids highlighted in red that differ in sequence at the C-terminal end of RRM 1. Isoforms A, H, D and E have N-terminal extensions. Isoforms B, D and G have a glycine-rich insertion at the C-terminus that contains multiple RG dipeptides and tyrosine residues. Isoform G is otherwise truncated, and consists of RRM 3 and the extended C-terminus only. Isoform D does not have the second predicted bipartite NLS or C-terminus that is present in all other isoforms. Orange residues, predicted NLS sequences; red tyrosine residue, phosphorylated in SYNCRIP; purple residues, peptide sequences used to raise the anti-CG17838 polyclonal antibody. Underlined is the partially conserved peptide against which the anti-SYNCRIP (mouse protein) antibody was raised. The alignment was generated using ClustalW2.

Cloning of CG17838-F cDNA

Nested RT-PCR was used to isolate the entire protein coding cDNA sequence of *Drosophila* CG17838-F. cDNAs were reverse transcribed using total RNA isolated from *Drosophila* ovaries and oligo$(dT)_{20}$ primers. Comparison of the submitted sequence with the cloned sequence revealed that the cloned sequence contained an additional eight encoded amino acids in the nonconserved region between the end of the RRM domains and the second predicted NLS (Fig. 6.3). This probably has resulted from the prediction of a false positive splice site in the vicinity of the actual splice site. The cDNA was subcloned into a pGex bacterial expression vector for the production of an N-terminally tagged GST-fusion protein (Fig. 6.5A), and also into pUASP:GFP and pUAST:GFP for the generation of transgenic flies and overexpression of GFP-tagged CG17838-F. A polyclonal peptide antibody was also raised in rabbit using a double peptide strategy. Two peptides were designed using the CG17838-F amino acid sequence (Fig. 6.3 and 6.4), and both injected into the same rabbit (Eurogentec). On the basis of sequence and peptide position, the resulting antibody is predicted to recognize all CG17838 isoforms excluding CG17838-G.

The integrity of the purified recombinant CG17838-F was checked by SDS-PAGE, followed by coomassie staining (Fig. 6.5A') or Western blotting with an anti-GST antibody (Fig. 6.5B). The anti-CG17838 polyclonal antibody was tested first by Western blot on the recombinant protein and *in vitro* translated CG17838-F (Fig. 6.5B). In both cases, anti-CG17838 recognized a single band of the expected size.

An anti-SYNCRIP antibody shown to recognize mouse SYNCRIP in brain extracts was also obtained (Bannai *et al.*, 2004). This antibody was raised against a peptide within a conserved region of the N-terminal acidic domain (Fig. 6.3 and 6.4), and in Western blotting recognizes multiple proteins in mouse brain extracts corresponding to SYNCRIP isoforms and hnRNP R. However, despite the partial conservation of the peptide that the antibody was raised against, this antibody did not detect any proteins in *Drosophila* ovary extracts (Fig. 6.5C). In contrast, following peptide

affinity purification, the anti-CG17838 antibody recognized multiple proteins ranging between ~51-75 kDa in *Drosophila* ovary extracts that were not recognized by the pre-immune serum (not shown). CG17838-F is most likely the ~59 kDa band (which could also correspond to isoform C), whilst others represent other isoforms (for example, isoforms B and D are predicted to be 74-77 kDa). A maternal triple driver, MTD-GAL4 (Petrella *et al.*, 2007; Appendix A.3), containing three GAL4 or GAL4:VP16 transgenes under the control of the *nos* or *otu* promoters was used to induce strong expression of UAS-CG17838-F-GFP throughout oogenesis. Western blotting with anti-CG17838 on ovary extracts made from flies expressing UAS-CG17838-F-GFP during oogenesis also revealed a ~86 kDa band. This was also was also recognized by an anti-GFP antibody (Fig. 6.5C'), and corresponds to the expected size of CG17838-F-GFP. Western blots with extracts prepared from other tissues also show that CG17838 is highly expressed in testis, adult head and third-instar larval brain (C. Meignin, unpublished). However, it must also be stated that the peptide antibody does not reliably detect CG17838 isoforms in wild-type extracts, and so a new antibody is being raised against the recombinant protein.

CG17838 interacts with *Drosophila* Syt and RNA

The name of SYNCRIP results from the ability of the protein to bind both ubiquitous Syts and RNA (with a preference for poly(A) RNA), and its cytoplasmic subcellular localization (Bannai *et al.*, 2004; Mizutani *et al.*, 2000). The ability of CG17838 to bind *Drosophila* Syt was tested by anti-GFP immunoprecipitation from adult head extracts prepared with flies expressing UAS-CG17838-F-GFP in neuronal cells using the *elavC155*-GAL4 driver. Syt and CG17838-F-GFP were coimmunoprecipitated by the anti-CG17838 antibody, but not by control rabbit serum, indicating that CG17838 and Syt interact (Fig. 6.6A). At the synapse, calcium plays an important role in synaptic vesicle and Syt protein dynamics. In order to examine whether presence or absence of calcium has any role in the interaction of CG17838 and Syt, immunoprecipitation was done in the presence of calcium or EGTA. No differences were observed between the two conditions.

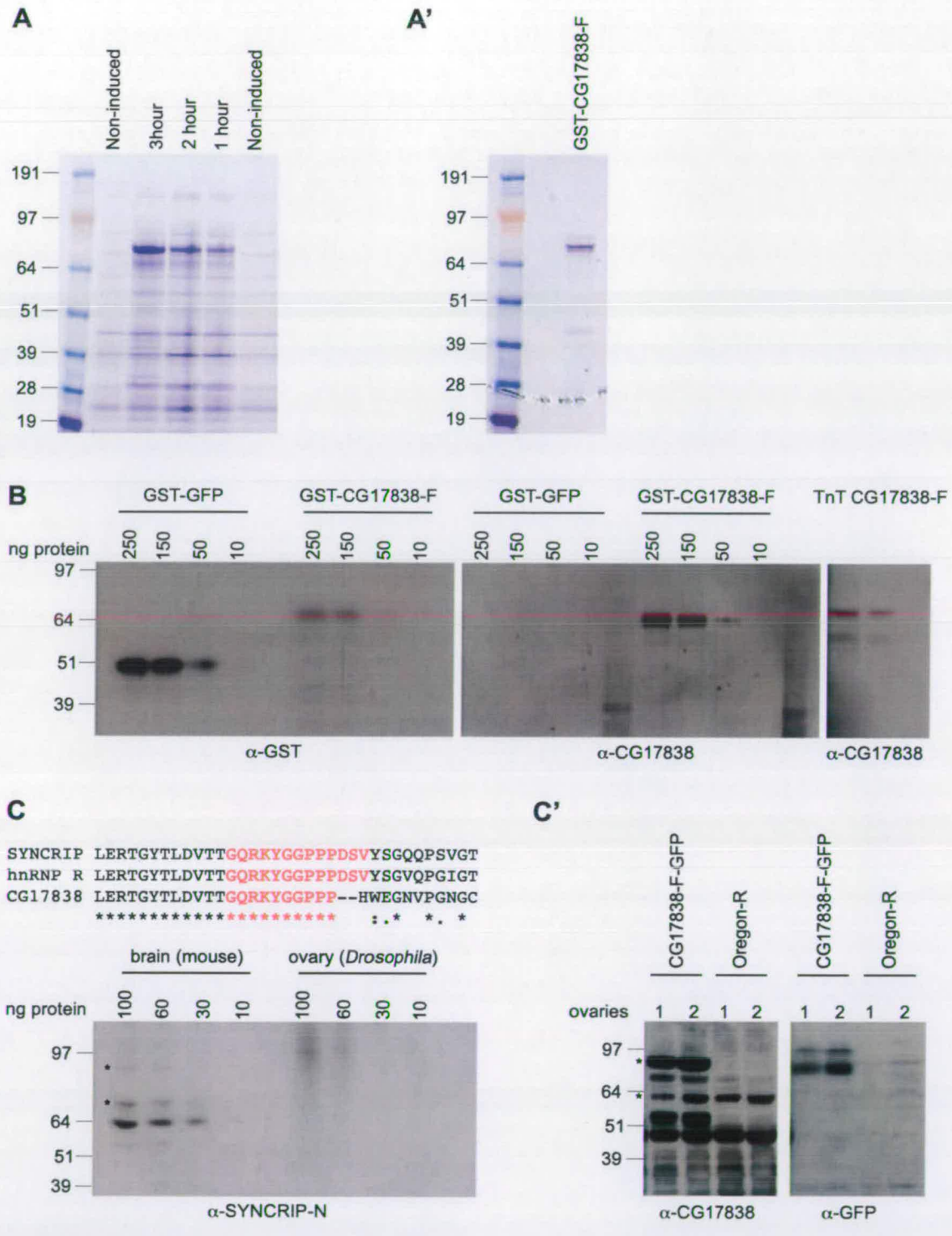

Figure 6.5 Purification of GST-CG17838-F and testing of an anti-CG17838 polyclonal antibody.

Figure 6.5 (continued) Purification of GST-CG17838-F and testing of an anti-CG17838 polyclonal antibody. (A) Induction of expression of N-terminally GST-tagged CG17838-F. **(A')** The integrity of purified GST-CG17838-F was checked by SDS-PAGE followed by coomassie staining and, **(B)** by Western blotting with an anti-GST antibody. **(B)** The polyclonal anti-CG17838 antibody was tested by Western blot on GST-CG17838-F and *in vitro* translated CG17838-F. **(C)** An antibody raised against a partially conserved peptide in mouse SYNCRIP recognizes multiple bands (asterisks correspond to SYNCRIP isoforms and hnRNP R) in mouse brain extract, but not in *Drosophila* ovary extract. **(C')** A Western blot of ovary extracts from Oregon-R and CG17838-F-GFP expressing flies, probed with anti-CG17838 and anti-GFP. Asterisks correspond to CG17838-F and CG17838-F-GFP.

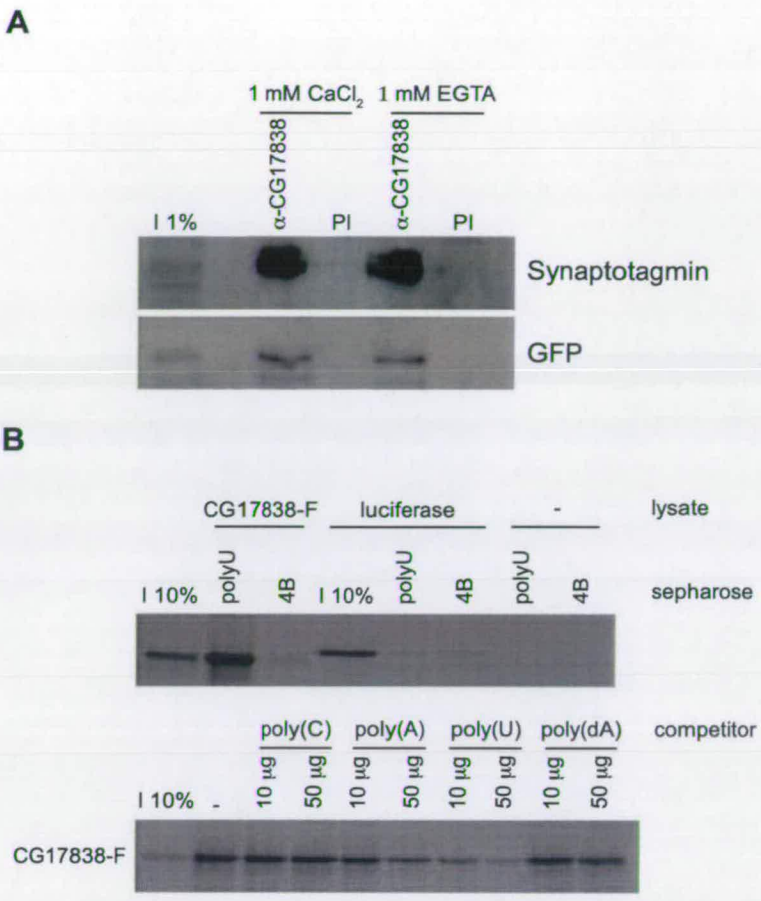

Figure 6.6 CG17838-F interacts with Synaptotagmin and RNA. (A) Western blot of immunoprecipitation (IP) from adult head extracts with anti-CG17838 antibodies or pre-immune serum (PI). Extracts were prepared using flies expressing UAS-CG17838-F-GFP in neuronal cells with the *elavC155*-GAL4 driver and the IP was carried out in the presence (1 mM $CaCl_2$) or absence (1 mM EGTA) of calcium. Proteins on the blot were detected with anti-Synaptotagmin and anti-GFP. An amount of head extract equal to 1% of that used for IP was loaded in the input lane (I 1%). **(B)** *In vitro* translated CG17838-F or luciferase labelled with [^{35}S]Met was incubated with poly(U)-sepharose or sepharose-4B. Poly(U)-sepharose binding assays were also carried out in the presence of the indicated amount of homopolymer (poly(C), poly(A) and poly(U) RNA, and poly(dA) DNA as a competitor.

The ability of *in vitro* translated CG17838-F to bind RNA *in vitro* was examined using poly(U)-sepharose binding assays. CG17838-F bound strongly to poly(U)-sepharose, but did not detectably bind to sepharose 4B. In contrast, *in vitro* translated luciferase, a protein not predicted to bind RNA, did not interact with poly(U)-sepharose or sepharose 4B (Fig. 6.6B). Poly(C) RNA did not compete binding to poly(U)-sepharose, whilst poly(U) RNA, and to a lesser extent, poly(A) RNA did compete effectively. Poly(A) DNA did not compete suggesting that CG17838-F preferentially binds poly(U) and poly(A) RNA, although binding to poly(A) RNA is weaker than that to poly(U). SYNCRIP preferentially bound poly(A) RNA *in vitro* (Mizutani *et al.*, 2000) indicating that there are differences in the *in vivo* target RNAs for SYNCRIP and CG17838-F.

The expression pattern of CG17838 during oogenesis

Staining of wild-type ovaries with anti-CG17838 antibodies (C. Meignin, unpublished) revealed that CG17838 is expressed in the germline. CG17838 protein is enriched in the oocyte from stage 7 onwards, and is present in an anterior-posterior gradient (Fig. 6.7A). Microtubules within the oocyte also form an anterior-posterior gradient. When visualized directly, microtubules appear to be nucleated from both the anterior and lateral cortex and extend in all directions (Cha *et al.*, 2001; MacDougall *et al.*, 2003). The density of microtubules is greatest at the anterior cortex and lowest at the posterior pole, and the intensity of CG17838 staining within the oocyte matches this pattern. CG17838 also accumulates at the posterior of the oocyte from stage 9 of oogenesis onwards (Fig. 6.7B), as seen for *osk* mRNA, factors required for *osk* localization (for example Stau, and Heph described in Chapter 5) and also for dynein (Li *et al.*, 1994). The pattern of staining is specific for the anti-CG17838 antibody and is not seen with the control pre-immune serum (Fig. 6.7C). This pattern of localization is consistent with a role for CG17838 in the transport or translational regulation of localized mRNAs within the oocyte.

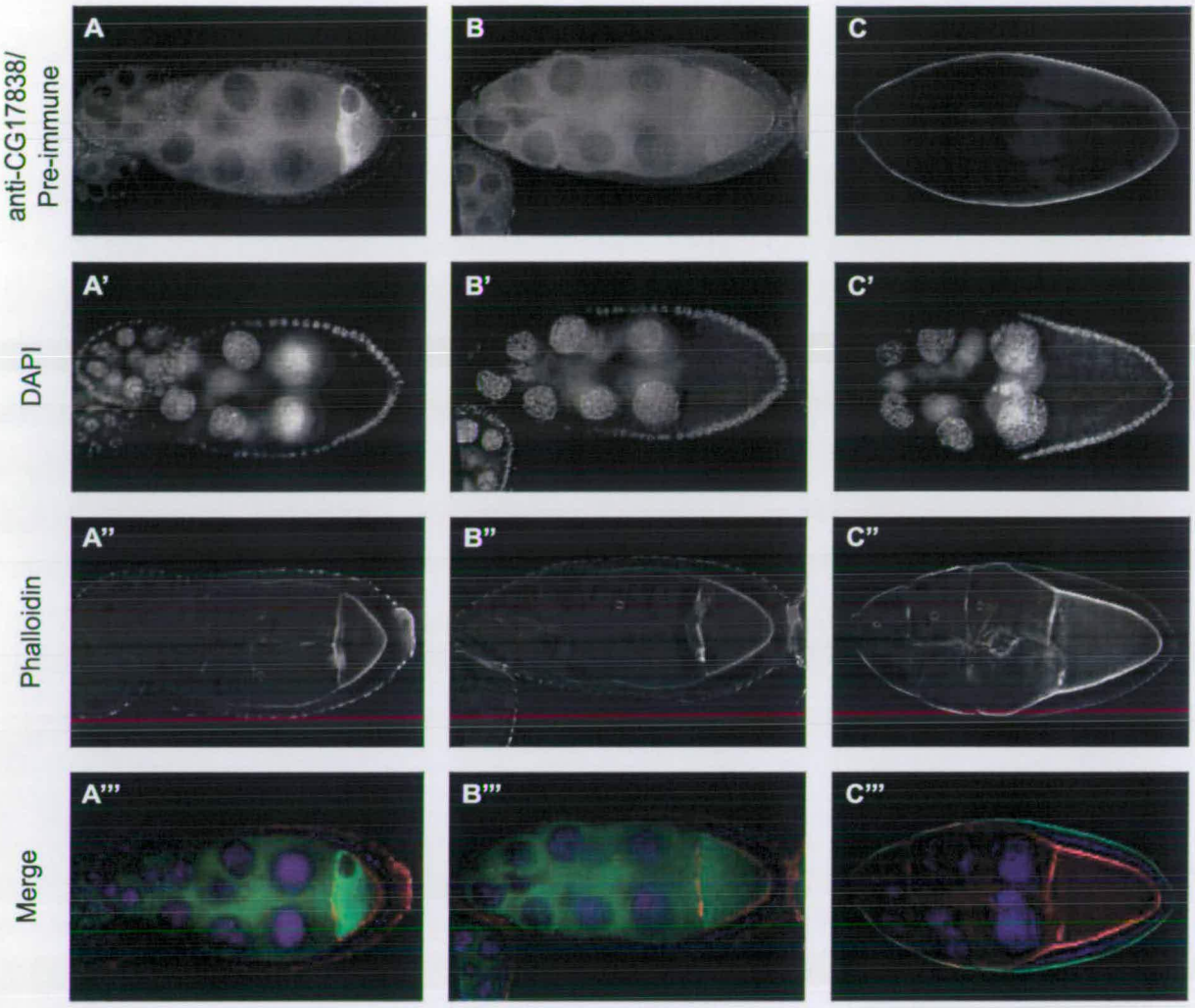

Figure 6.7 CG17838 is expressed in the germline. (A) CG17838 is present in an anterior-posterior gradient similar to microtubules. **(B)** CG17838 accumulates at the posterior of the oocyte from stage 9 onwards, similar to *osk* mRNA. **(C)** The pattern of staining is not observed using control pre-immune rabbit serum. Egg chambers were stained using anti-CG17838 or pre-immune serum, phalloidin to label F-actin and DAPI.

Visualization of GFP in UAS-CG17838-F-GFP expressing egg chambers (using *tubulin*-GAL4 and MTD-GAL4) shows high levels of expression in germline nuclei throughout all stages of oogenesis, and is reminiscent of GFP expression in SqdGFP protein-trap flies. The difference in localization of endogenous protein and overexpressed GFP protein could be an artefact of overexpressing a protein that is predicted to contain two NLSs.

CG17838 interacts directly with RNAs and *trans*-acting factors *in vitro*

Recombinant CG17838 and Sqd interact directly and non-specifically with ORF16 RNA

To confirm the specific GRNA (Chapter 4) association of CG17838 with ORF16 RNA, and to test if this interaction could be direct, the ability of recombinant GST-CG17838-F to bind to radiolabelled ORF16, ORF16ΔGLS, hb and nos RNAs was assessed using a UV cross-linking assay. As controls, the binding of GST-Sqd A (also specifically bound ORF16 in GRNA experiments) and GST-GFP to the same RNAs were also tested. GST-CG17838-F and GST-Sqd A both directly bound ORF16, but in contrast to the specificity observed in GRNA experiments, both proteins bound all RNAs tested (GST-Sqd S also bound all RNAs tested in the same manner as Sqd A, but this is not shown) (Fig. 6.8A). The difference in specificity observed for CG17838 and Sqd between GRNA and UV cross-linking is explained by the specific recognition of *grk* only by an intact protein complex (see discussion). Interestingly, multiple RNA-protein complexes were observed upon UV cross-linking of Sqd A to all probes, suggesting that Sqd A can form oligomers on RNA molecules.

CG17838 interacts directly with all Sqd isoforms *in vitro*

To test whether CG17838 can directly interact with *grk trans*-acting factors, the ability of *in vitro* translated CG17838-F or Sqd A to bind to GST-tagged Sqd isoforms, A, S and B or GST-CG17838-F was examined using a GST-pulldown assay (Fig. 6.8B). CG17838-F associates with all GST-Sqd isoforms, but not with control GST-GFP and GST only proteins, whilst Sqd A associates with GST-CG17838-F, but also not with control proteins. Interestingly, the *in vitro* translated CG17838-F protein that associated with GST-Sqd A and B migrated slightly slower than CG17838-F associated with GST-Sqd S. It was hypothesized that this could reflect phosphorylation of the CG17838-F associated with GST-Sqd A and B. To test this hypothesis, CG17838-F bound to the three isoforms was mock treated or treated with phosphatase following GST-pulldown (Fig. 6.8B'). Upon phosphatase treatment CG17838-F bound to GST-Sqd A migrated at the same speed as CG17838-F bound to GST-Sqd S, whilst CG17838-F binding to GST Sqd B was difficult to visualize following mock or phosphatase treatment. These experiments therefore indicate that CG17838-F can bind directly to all Sqd isoforms, and that phosphorylated and non-phosphorylated forms of CG17838-F bind preferentially to different Sqd isoforms.

CG17838 interacts with localized mRNAs and *trans*-acting factors in the germline

CG17838 specifically interacts with *grk* and *osk* mRNAs

Given the *in vitro* association of CG17838 and *grk* (GLS) RNA, and the localization of CG17838 at the posterior of the oocyte, immunoprecipitation experiments were carried out to ask whether CG17838 is a component of localized RNPs in the germline (Fig. 6.9). RT-PCR showed that *grk* and *osk* mRNAs are present in the fractions precipitated from ovaries taken from flies expressing UAS-CG17838-F-GFP with MTD-GAL4 or *tubulin*-GAL4, and from SqdGFP protein trap and Oregon-R (and GFP-Heph; see Chapter 5) control ovaries using anti-CG17838 antibodies, but not in immunoprecipitates from control rabbit serum (Fig. 5.5). *grk* and *osk*

mRNAs were also present in fractions precipitated from CG17838-F-GFP and SqdGFP (and GFP-Heph; see Chapter 5) ovary extracts using anti-GFP antibodies, but not in anti-GFP immunoprecipitates from Oregon-R control females. No specific enrichment of mRNAs highly expressed in ovaries (*rp49*, *tubulin67C*), other mRNAs asymmetrically localized within the oocyte (*bicoid*, *nanos*) or the non-localized mRNA control from the initial *in vitro* experiments (*hunchback*) was observed in the anti-CG17838 precipitated fractions from all extracts, or in the anti-GFP precipitated fractions from CG17838-F-GFP and SqdGFP extracts.

The results of RNA immunoprecipitation experiments therefore indicate that CG17838 binds specifically to *grk* and *osk* mRNAs, whilst Sqd binds specifically to *grk*, *osk* and also *bcd* mRNAs. Neither protein interacted with *hb* or *nos* mRNAs. This is consistent again with the specific recognition of localized mRNAs only by an intact protein complex, present in RNA immunoprecipitation and GRNA experiments, but not in UV cross-linking with recombinant protein or in poly(U)-sepharose binding assays (see discussion).

CG17838 interacts with Sqd and Hrb27C

The presence of CG17838 and two well-characterized *grk trans*-acting factors, Sqd and Hrb27C in the same protein complex in *Drosophila* ovaries was confirmed by coimmunoprecipitation experiments. The *in vivo* association of CG17838 and Sqd was tested by anti-CG17838 and anti-GFP immunoprecipitation from ovary extracts prepared with flies expressing UAS-CG17838-F-GFP in the germline (using MTD-GAL4) and SqdGFP flies. Sqd was coimmunoprecipitated with CG17838-F-GFP by the anti-CG17838 and anti-GFP antibodies, but not by control rabbit serum, indicating that CG17838 and Sqd interact (Fig. 6.10A).

Both CG17838 and Sqd are RNA binding proteins, and their association could involve only protein/protein contacts or could depend on RNA binding. Furthermore, the potential effect of CG17838-F phosphorylation on Sqd isoform binding *in vitro* could also indicate regulation of their association by phosphorylation *in vivo*.

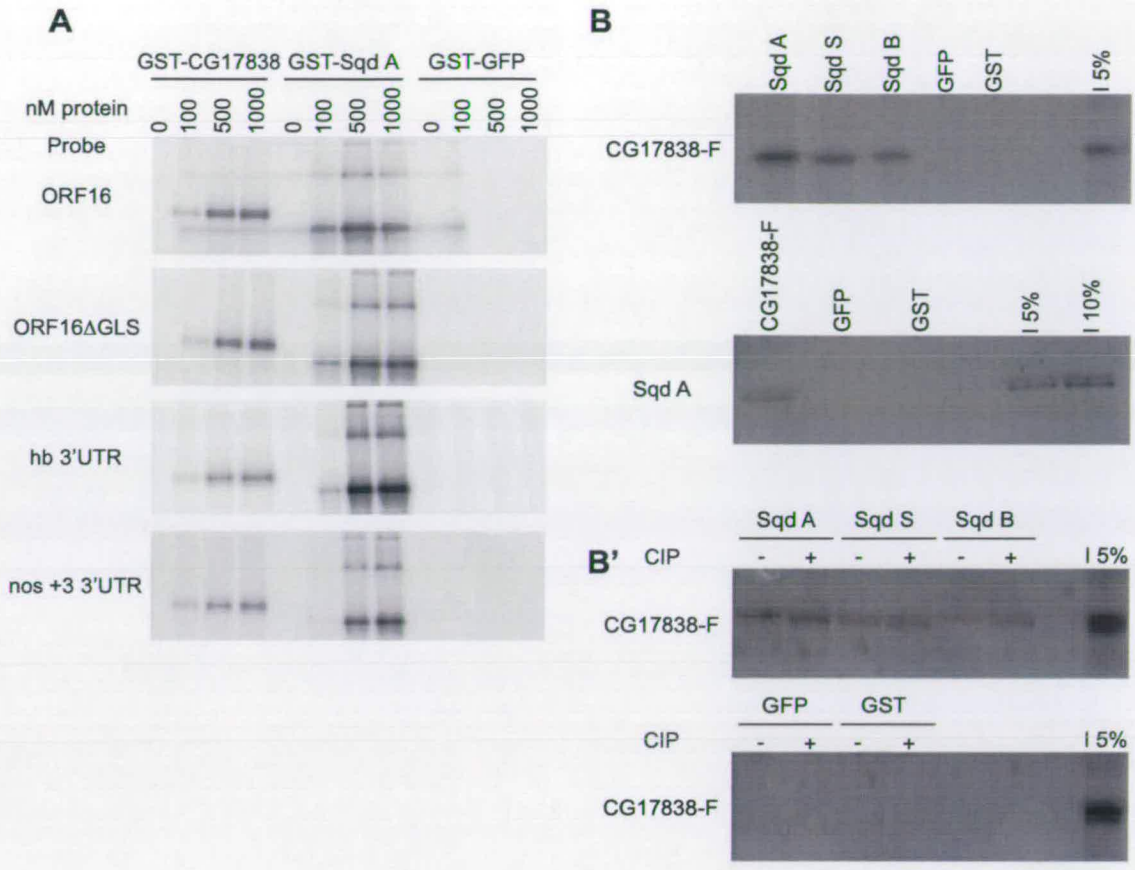

Figure 6.8 CG17838 and Squid interact directly with RNA and each other *in vitro*. **(A)** Recombinant GST-CG17838-F, GST-Sqd A and GST-GFP control at a concentration of 0, 500 or 1000 nM were incubated with ^{32}P-labelled RNA probe as indicated and the binding reaction subjected to UV cross-linking. ORF16 and ORF16ΔGLS are RNAs previously used for GRNA experiments described in Chapter 4. hb 3'UTR is a small region of the *hb* 3'UTR containing *nanos* response elements (NREs) required for translational repression of *hb* mRNA. nos +3 3'UTR is the region of the *nos* 3'UTR containing the *nos* +3 RNA localization element. **(B)** *In vitro* translated CG17838-F or Sqd A labelled with [^{35}S]Met were incubated with a series of GST tagged recombinant proteins, GST-Sqd isoforms A, S and B or GST-CG17838-F, GST-GFP and GST only. An amount of *in vitro* translated CG17838-F or Sqd A equal to 5% or 10% of that used for the GST-pulldown was loaded in the input lane (I 5%, I 10%). **(B')** The experiment described in (B) was carried out in the presence or absence of CIP (calf intestinal alkaline phosphatase).

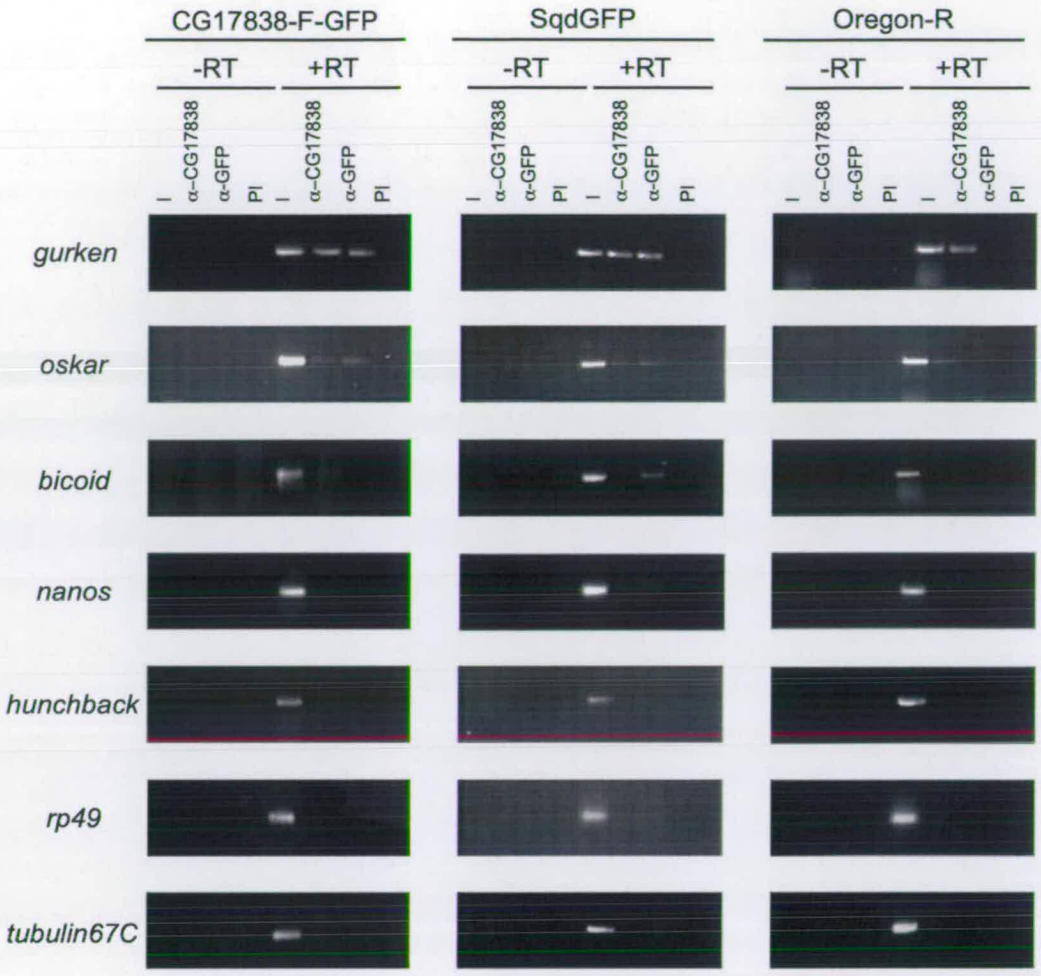

Figure 6.9 CG17838 associates with *grk* and *osk* mRNAs. RT-PCR amplification of mRNAs recovered in fractions immunoprecipitated from UAS-CG17838-F-GFP (expressed using MTD-GAL4), SqdGFP control or Oregon-R control ovarian extracts using anti-CG17838, anti-GFP and control rabbit serum. I=Input RNA (10%); PI=control rabbit serum; -/+RT=minus/plus reverse transcriptase.

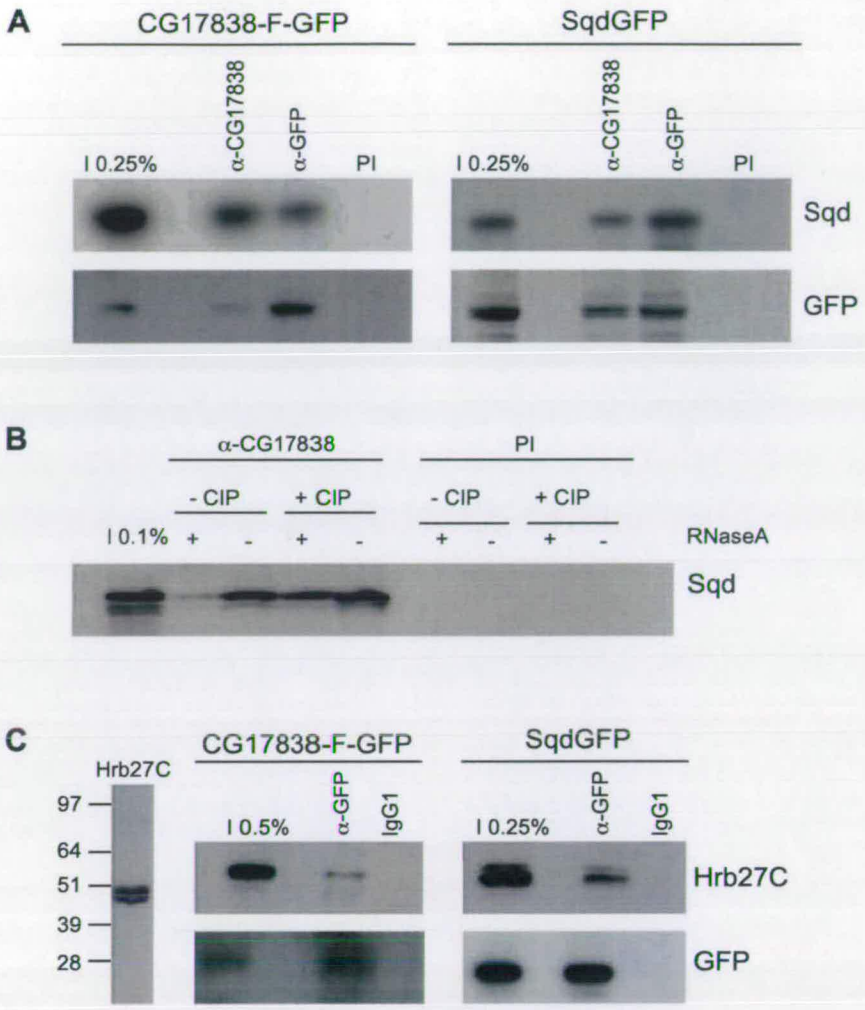

Figure 6.10 CG17838 interacts with Squid and Hrb27C. (A) Western blots of immunoprecipitation (IP) from ovary extracts with anti-CG17838, anti-GF or pre-immune serum (PI). Extracts were prepared using flies expressing UAS-CG17838-F-GFP in the germline with MTD-GAL4 or SqdGFP flies. Proteins on the blot were detected with anti-Sqd A and anti-GFP. An amount of ovary extract equal to 0.25% of that used for IP was loaded in the input lane (I 0.25%). **(B)** Western blot of IP from Oregon-R ovary extracts with anti-CG17838 or pre-immune serum (PI). IP was carried out in the presence or absence of RNase A and CIP (calf intestinal alkaline phosphatase) and proteins on the blot were detected with anti-Sqd A. An amount of ovary extract equal to 0.1% of that used for IP was loaded in the input lane (I 0.1%). **(C)** A Hrb27C peptide antibody was raised that recognizes a doublet of Hrb27C protein at 48–50 kD. anti-Hrb27C and anti-GFP were used to probe Western blots of IP from ovary extracts with monoclonal anti-GFP or an isotype control (IgG1). Extracts were prepared as in (A). An amount of ovary extract equal to 0.5% or 0.25% of that used for IP was loaded in the input lane (I 0.5%, I 0.25%).

Coimmunoprecipitation was carried out in the presence or absence of RNase A and/or phosphatase (Fig. 6.10B). RNase A treatment in the absence of phosphatase reduced Sqd binding to CG17838 when compared to an immunoprecipitation done in the absence of both phosphatase and RNase A. This suggests that RNA facilitates the association of CG17838 and Sqd *in vivo*. However, treatment with both RNase A and phosphatase does not result in a change in Sqd immunoprecipitation, suggesting that dephosphorylation of factors within the immunoprecipitated complex can also enhance the association of CG17838 and Sqd, even in the absence of RNA.

A polyclonal antibody against two peptides in the C-terminus of Hrb27C was raised as described in Huynh *et al.*, 2004. This antibody recognizes the expected protein doublet at 48-50 kDa on Western blots. The ability of CG17838 to bind Hrb27C was tested by anti-GFP immunoprecipitation from ovary extracts prepared using flies expressing UAS-CG17838-F-GFP in the germline (using MTD-GAL4) and SqdGFP flies. Hrb27C was coimmunoprecipitated with both SqdGFP and CG17838-F-GFP by the anti-GFP antibody, but not by an isotype control antibody, indicating that CG17838 and Hrb27C interact (Fig. 6.10C).

CG17838 mutants

A number of lines containing P-element or piggyBac insertions in the *CG17838* gene were available from the Bloomington and DGRC (*Drosophila* Genetic Resource Centre) Kyoto Stock Centres and the Exelixis Collection (Fig. 6.11). Two of these alleles, $CG17838^{e00286}$ and $CG17838^{f03775}$ showed highly reduced viability both in homozygotes and in combination with *Df(3R)BSC124* (table 6.3) and *Df(3R)BSC141* (deficiencies uncovering *CG17838*). It was not possible using the current stocks to determine when most homozygous individuals died, although a small number died at late pupal stages (these lines were balanced with TM6B carrying the dominant marker Tubby, allowing identification of heterozygous and homozygous pupae). Rebalancing the lines over appropriate GFP balancers will allow better characterization of the stage when death occurs. Each of the two alleles also fails to complement the lethality of the other, and viability is even more reduced when both

alleles are present. However, *CG17838*^{e00286} and *CG17838*^{f03775} are not null alleles because the percentage of lethality in *CG17838*^{e00286} or ^{f03775}/*Df* individuals is higher than in homozygotes. *CG17838*^{e00286} and *CG17838*^{f03775} homozygotes or combinations with deficiency that do eclose are unhealthy, do not crawl within the vial and are prone to getting stuck in the growth medium. These adults also die within one day of eclosure, meaning that egg chambers are not developed enough to assess RNA localization processes during oogenesis in these mutants.

The *CG17838*^{e00286} insertion lies within an exon coding for RRM 3 and is predicted to affect all CG17838 isoforms, suggesting that the RNA binding activity of CG17838 proteins is essential for viability. The *CG17838*^{f03775} insertion lies within an intron between exons that make up the C-terminal glycine-rich region (contains multiple RG dipeptides and tyrosine residues) in isoforms B, D and G. It is possible that the *f03775* insertion disrupts correct splicing in this region resulting in reduced viability. As *Df(3R)BSC124* does not uncover isoform G, this isoform alone must not be able to compensate for the disruption in *CG17838* function in *CG17838*^{e00286} and *CG17838*^{f03775} alleles. Other insertions do not have reduced viability in combination with *Df(3R)BSC124* (table 6.3) and *Df(3R)BSC141.* These insertions either lie within introns upstream of the first exon common to all isoforms or between exons coding for the N-terminal extension seen in isoforms A and H. Females homozygous for these alleles, or in combination with deficiency are not sterile, and *grk* mRNA is properly localized throughout oogenesis (table 6.3).

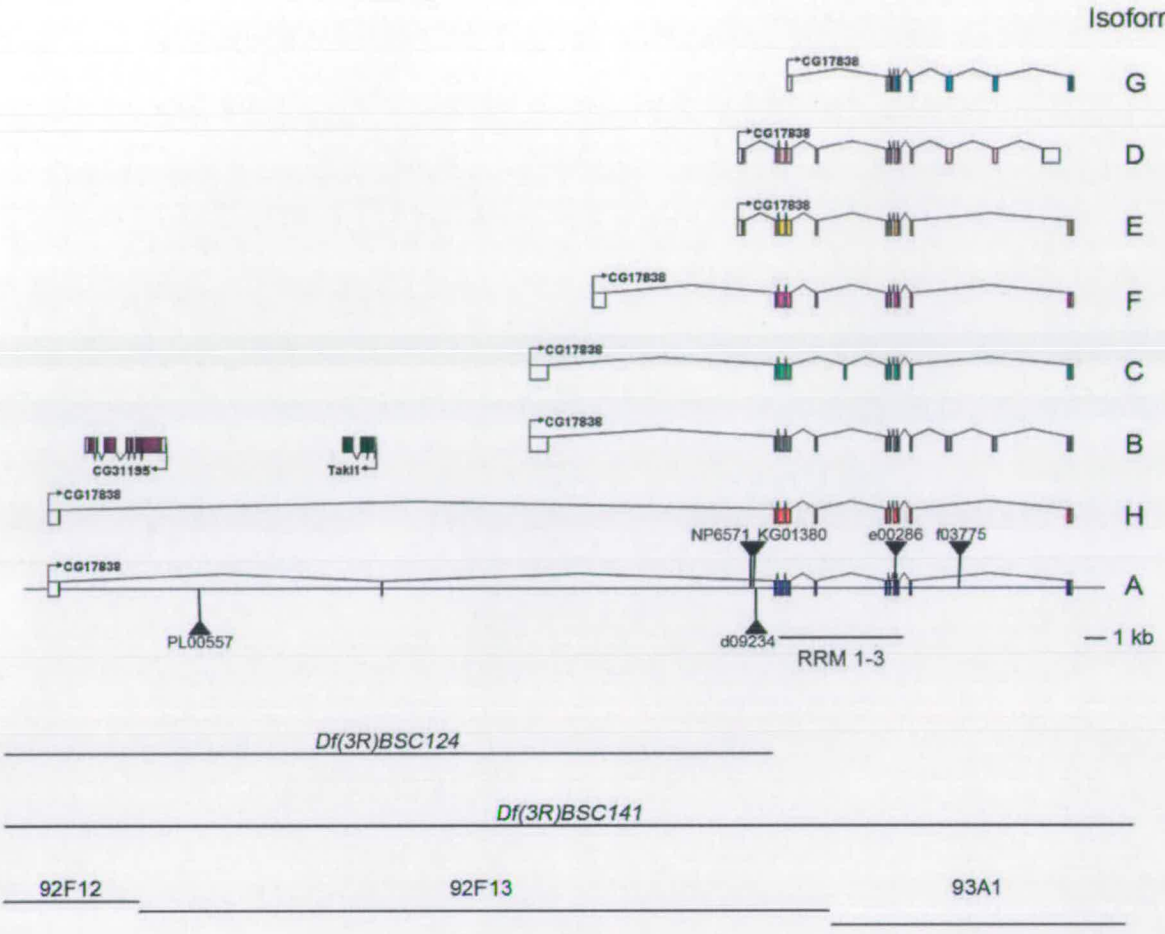

Figure 6.11 Insertions and deficiencies associated with *CG17838*. Insertions PL00557, d09234, NP6571, KG01380, e00286 and f03775 are shown across the gene, whilst deficiencies *Df(3R)BSC124* and *Df(3R)BSC141*, and the cytogenetic bands 92F12-93A1 are shown below.

TABLE 6.3 *CG17838*^{e00286} and *CG17838*^{f03775} alleles show highly reduced viability both in homozygotes and in combination with a deficiency. Percentage viability is the ratio of the number of flies with no balancer to half the number of adults with a balancer. ND, not done.

Genotype	n	% Viability	Female sterile	*grk* localized
PL00557/PL00557	463	51%	Yes	ND
PL00557/Df(3R)BSC124	404	95%	No	Yes
NP6571/NP6571	241	96%	No	Yes
NP6571/Df(3R)BSC124	202	72%	No	Yes
KG01380/KG01380	419	63%	No	Yes
KG01380/Df(3R)BSC124	893	83%	No	Yes
f03775/f03775	703	10%	ND	ND
f03775/Df(3R)BSC124	429	2%	ND	ND
e00286/e00286	730	12%	ND	ND
e00286/Df(3R)BSC124	400	2%	ND	ND
e00286/f03775	195	3%	ND	ND

The role of CG17838 in mRNA localization during oogenesis

The posterior localization of CG17838 in the stage 9 oocytes and the *in vitro* and *in vivo* association of CG17838 with Sqd, Hrb27C and *grk* and *osk* mRNAs suggests that CG17838 is a component of localized RNPs in the *Drosophila* germline. However, females homozygote, or in combination with a deficiency, for the two hypomorphic alleles, *CG17838*^{e00286} and *CG17838*^{f03775}die within one day of eclosure meaning that egg chambers are not developed enough to assess RNA localization processes during oogenesis in these mutants.

To generate additional *CG17838* mutations, the *NP6571* and *KG01380* P elements were mobilized (Adams and Sekelsky, 2002) (Fig. 6. 12). The original inserts lie within the first intron of most isoforms (Fig. 6.11) and are viable and fertile both in homozygotes and in combination with deficiency. 50 excision lines for each of the original insertions were generated. All lines produced by excision of *KG01380* were

homozygous lethal but viable over both deficiencies and laid wild-type eggs. From the lines generated by excision of *NP6571*, eight were homozygous female sterile. Females from these lines laid short, rounded eggs with paddleless dorsal appendages (Fig. 6.13A-C). Eggs with this phenotype are also laid by mutants in genes such as *quail* (Villin) and resemble typical phenotypes due to loss of actin regulatory components. Phalloidin staining revealed that in these excision lines the actin cytoskeleton was disorganized (Fig. 6.13D, E). Direct sequencing across the original insertion site of NP6571 revealed that these female sterile alleles carried insertions corresponding to a duplication of P element inverted repeats, or to a larger (up to 1.5 kb) region of NP6571. However, these same lines were fertile and laid wild-type eggs over both deficiencies indicating the generation of a secondary mutation during P element mobilization. Therefore these lines were not pursued further.

Another eight NP6571 excision lines were homozygous lethal, but all except one, $NP6571^{15}$, were also viable over both deficiencies. $NP6571^{15}$ was lethal over deficiency and $CG17838^{e00286}$. PCR analysis and sequencing across *CG17838* revealed that the $NP6571^{15}$ allele carries an approximately 8kb-long insert at the same genomic location as in the parental NP6571 line, corresponding to an internally deleted NP6571 P element (the parental element is 11.2 kb).

In order to study the $NP6571^{15}$ and $CG17838^{e00286}$ alleles during oogenesis, germline clones were generated using the FLP-DFS technique (C. Meignin, unpublished). $NP6571^{15}$ eggs were wild-type and oocytes showed no defects in *grk* and *osk* mRNA and Grk and Osk protein localization (C. Meignin, unpublished). It is possible that the $NP6571^{15}$ allele selectively affects the expression of certain CG17838 isoforms that are not required for mRNA localization in the oocyte. For example, it is possible that this allele disrupts the splicing of the first intron in isoforms D and E only, but further characterization of the expression pattern of different isoforms in wild-type and mutant is required to confirm this. Preliminary observations do show that $CG17838^{e00286}$ eggs are ventralized, consistent with a role for CG17838 in *grk* mRNA localization or translational regulation. Experiments are ongoing to determine

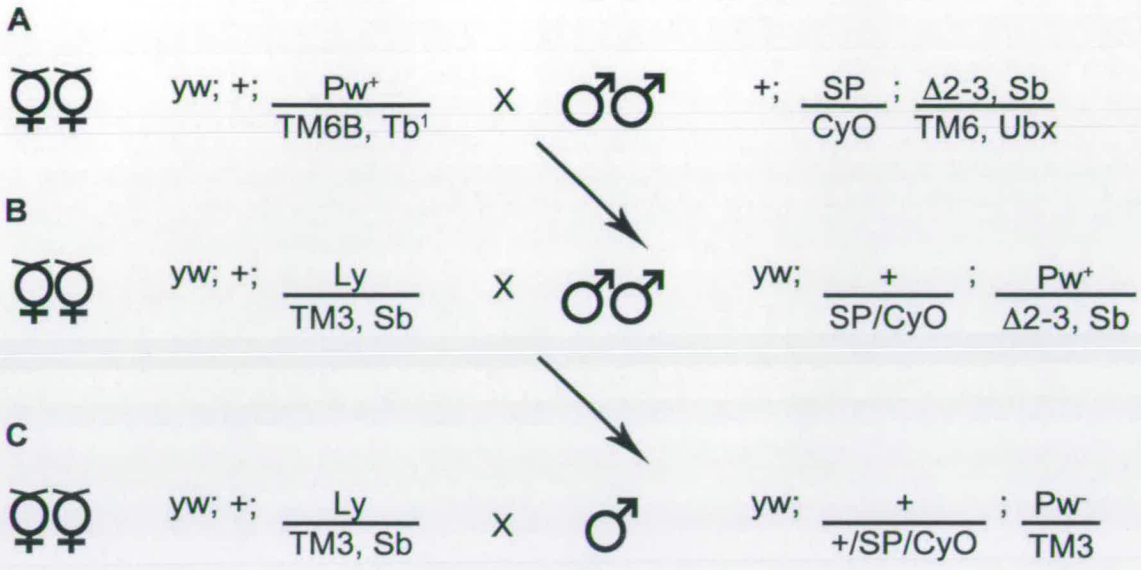

Figure 6.12 Genetic strategy for P-element mobilization on the 3rd chromosome. **(A)** Females of lines with P-element insertions in *CG17838* were crossed to males expressing the Δ2-3 transposase. **(B)** Males with the P-element insertion (coloured eyes) and the Δ2-3 transposase (so that the P-element is enabled to hop) were crossed to females with Ly and TM3 balancer in order to balance lines with an excised P element. **(C)** Single males with an excised P-element (white eyes) were crossed again to females with Ly and TM3 balancer in order to establish individual balanced lines. Males and females from each line were then self-crossed in order to expand the stock.

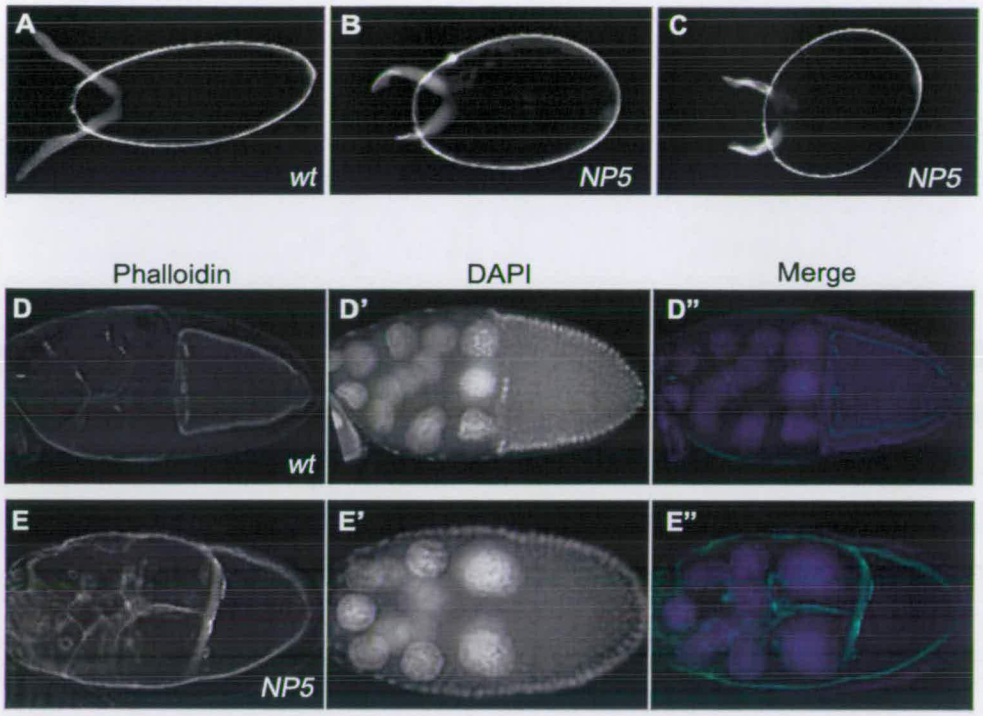

Figure 6.13 Homozygous *CG17838* excision mutants. (A-C) Comparison of eggs laid by wild-type (*wt*) flies and homozygous female sterile excision lines (*NP5*) reveals that these excision lines lay short, rounded eggs with paddleless dorsal appendages. **(D, E)** Phalloidin staining shows that oocytes taken from homozygous excision line females have a disorganized actin cytoskeleton.

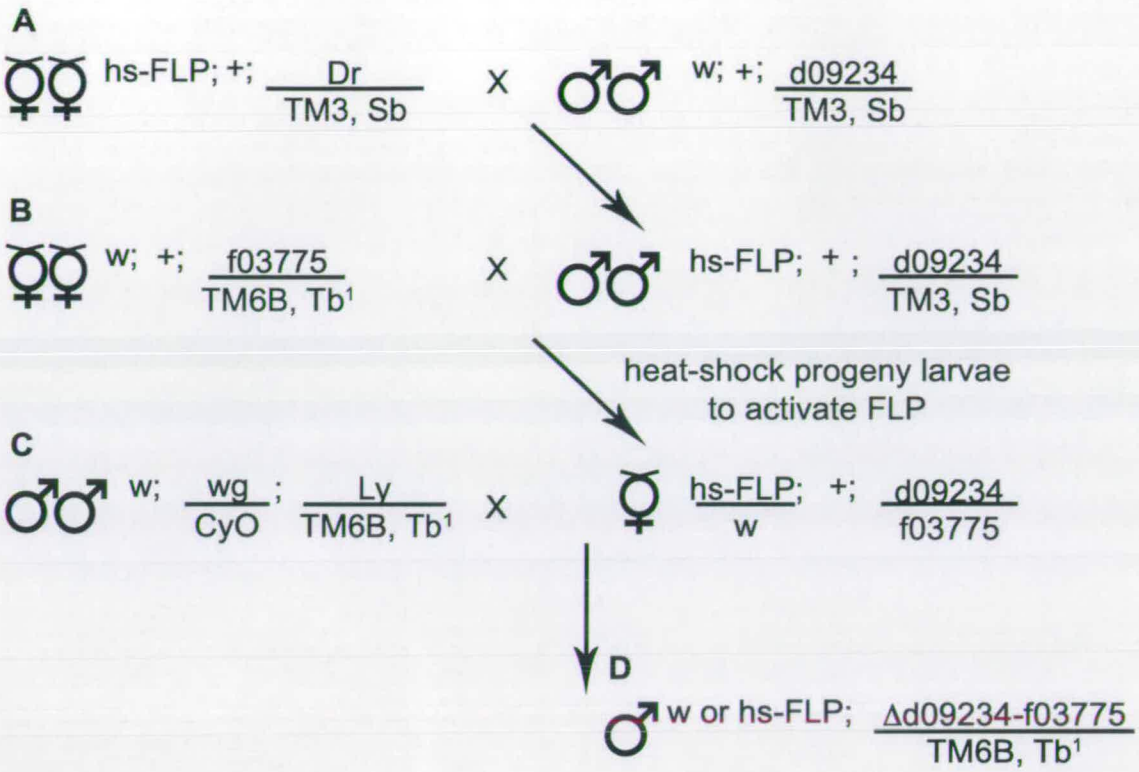

Figure 6.14 Genetic strategy used to generate a FLP-FRT-based deletion on the 3rd chromosome. (A, B) Crosses place two FRT-bearing transposon insertions, d09234 and f03775 in *trans* in the presence of heat shock-driven FLP recombinase (*hs-FLP*). **(A)** Males carrying one insertion were crossed to females carrying a FLP recombinase. **(B)** Progeny males carrying both the insertion and FLP recombinase were then crossed to females carrying the second insertion. Activation of FLP recombinase by heat shock results in the generation of deletion of intervening sequence between the two insertions. **(C)** Progeny females were then crossed to males with marked balancer chromosomes. **(D)** Single progeny males potentially carrying a deletion were then used to establish stocks with balancers that could also give additional progeny for deletion confirmation by PCR.

whether this is the case, and also to test whether CG17838 is involved in the regulation of *osk* mRNA.

Due to the complexity of the *CG17838*, existing insertions and P-element mobilization probably do not fully disrupt the function of all isoforms, resulting in phenotypes being obscured by redundancy. Efforts are also ongoing to produce a null mutation affecting all isoforms by generating a FLP-FRT-based deletion (Fig. 6.14) (Parks *et al.*, 2004) between the insertions *d09234* and *f03775* (Fig. 6.11). This is predicted to delete exons encoding the N-terminus and the RRMs of all isoforms, and also the glycine-rich C-terminal region in isoforms B, D and G.

The role of CG17838 in the nervous system

UAS-CG17838 RNAi (lines 33011/33012 obtained from the Vienna *Drosophila* RNAi Centre), expressed in all cell types under the control of *actin*-GAL4 fail to eclose and die at late pupal stages. In addition, preliminary results show that targeted expression of UAS-CG17838 RNAi using a variety of nervous system GAL4 drivers also results in lethality at late pupal stages (C. Meignin, unpublished). These were the pan-neuronal driver *elavC155*-GAL4, the pan-glial driver *repo*-GAL4, the mushroom body driver *eas[alaP]*-GAL4, and the all nerves driver *1407*-GAL4. Expression of the RNAi lines with a number of other nervous system GAL4 drivers did not result in lethality or any observable phenotype. These were the motoneuronal drivers *C164*-GAL4 and *D42*-GAL4, the cholinergic neuronal driver *Cha*-GAL4, the multidenditic (md) neuronal (a subset of sensory neurons of the PNS) driver *109(2)80*-GAL4, the mushroom body (expression directed specifically to the γ lobes) driver *1471*-GAL4, the dendritic arborization (da) neuronal (a subset of md neurons) driver *477*-GAL4, and the segment specific muscle and motoneuronal driver *A51*-GAL4. This preliminary data indicates that CG17838 expression is required in specific neurons and in glia for adult viability. Pharate adult lethality as seen for CG17838 RNAi, and in some cases $CG17838^{e00286}$ and $CG17838^{f03775}$ is observed in *Imp* mutants (adult *Imp* null mutant escapers, like *CG17838* mutant adults also remain on the food and exhibit little movement) (Boylan *et al.*, 2008), and also

commonly in mutants that are defective in synaptic transmission. For example, SNAP-25 is a plasma membrane t-SNARE that is a component of the neurotransmitter release machinery, and promotes the docking of synaptic vesicles with the plasma membrane. Like SYNCRIP, SNAP-25 can interact with the vesicle membrane protein Synaptotagmin. *SNAP-25* mutants also fail to eclose, and when manually freed from the puparium are capable only of slight twitching movements with the forelegs and palps (Vilinsky *et al.*, 2002). Interestingly, when UAS-CG17838 RNAi is expressed with the all nerves-Gal4 driver the few adults that do eclose also are only capable of twitching movements, and do not survive.

In the case of Imp, it was shown that the protein acts to modulate synaptic terminal growth, and when this is disrupted, locomotion, and hence neuromuscular defects are observed. It was hypothesized that Imp is involved in the transport and translational control of transcripts at synaptic termini that encode components of signalling pathways coordinating synaptic with muscle growth. It is possible that common phenotypes are observed for *CG17838* and *Imp* mutants because CG17838 acts with Imp in the nervous system to regulate mRNA localization and translation, and potentially synaptic growth. A further possibility is that CG17838 modulates synaptic transmission at the level of the neurotransmitter release machinery (as for SNAP-25) via its ability to bind Syt.

Expression of CG17838 in the nervous system

Preliminary immunostaining indicates that CG17838 is highly expressed in the third instar larval brain and ventral ganglion (C. Meignin, unpublished), although colocalization experiments with specific markers are required to define this expression in greater detail. CG17838 is also present in particles throughout cultured neurites, both proximal and distal to the neuronal cell body (C. Meignin, unpublished). It is possible that these particles represent vesicles or RNA granules, and again colocalization experiments are needed to confirm the identity of these particles.

Discussion

Drosophila CG17838 was identified in Chapter 4 as one of a number of proteins able to bind specifically to GLS-containing RNA. *CG17838* is the orthologue of mammalian SYNCRIP, and like SYNCRIP, CG17838 is able to associate with Synaptotagmin and interact directly with RNA, with a preference for poly(U) homoribopolymers. Western blotting and immunofluorescence confirm the expression of CG17838 in the *Drosophila* egg chamber in a pattern similar to microtubules and dynein, with an accumulation at the posterior pole of the oocyte from stage 9 onwards. Immunoprecipitation experiments confirm the results of the GRNA experiment in that CG17838 is a component of a complex that includes Sqd, Hrb27C and *grk* mRNA. The interaction of CG17838 with *osk* mRNA also adds to the list of proteins, consisting of Heph, CG17838, Me31B, Sqd, Hrb27C, Bruno, Cup and possibly Imp, that are able to associate with both *grk* and *osk*. Preliminary data suggests that an insertion in an RRM disrupts *grk* mRNA localization and/or translational regulation, and that this insertion and CG17838 RNAi also potentially result in synaptic transmission defects (C. Meignin, unpublished). As SYNCRIP interacts with dendritically localized mRNAs in mammalian neurons, it is possible that CG17838 is also required for the regulation of localized mRNAs in the *Drosophila* nervous system, and therefore that the protein has a conserved role in transport RNPs during oogenesis, and in neurons in different organisms. Furthermore, given the association of SYNCRIP with BC200 RNA, PABP (Duning *et al.*, 2008) and the RNAi machinery (Moser *et al.*, 2007), it is possible that SYNCRIP and CG17838 act as regulators of translation maternal and neuronal transport RNPs.

CG17838 is a complex gene

CG17838 is contained within 50 kb of genomic sequence and alternative splicing is predicted to result in a number of *CG17838* transcripts, and therefore protein isoforms (CG17838-A to -H). RT-PCR and Western blotting confirmation of the expression of different isoforms in different tissues and developmental stages is

required before the function of *CG17838* can be fully understood, and would also aid interpretation of the phenotypes of different mutants. It is possible that different isoforms act together, have different functions or even antagonize one another. Indeed, the hnRNP Q proteins (the human SYNCRIP orthologues) hnRNP Q2 and 3 have been shown to act antagonistically to hnRNP Q1 in splicing (Chen *et al.*, 2008).

CG17838 is expressed in the egg chamber in a pattern similar to microtubules and dynein

Staining of wild-type ovaries with anti-CG17838 antibodies revealed that CG17838 protein is present in an anterior-posterior gradient in the oocyte, much like the staining observed for microtubules. CG17838 also accumulates at the posterior of stage 9 oocytes, as seen for *osk* mRNA, factors required for *osk* localization (for example Stau, and Heph described in chapter 5) and also for dynein (Li *et al.*, 1994). This pattern of localization is consistent with a role for CG17838 in the transport or translational regulation of localized mRNAs within the oocyte. The *in vivo* association of CG17838 with localized mRNAs in the oocyte could be further studied by following the distribution of CG17838 in oocytes of various mutant backgrounds. For example, if CG17838 is associated with *osk* mRNA and this is responsible for the posterior localization of the protein, then CG17838 should not localize to the posterior in $stau^{D3}$ oocytes (Palacios and St Johnston, 2002; St Johnston *et al.*, 1991).

CG17838 interacts with *trans*-acting factors required for *grk* and *osk* localization

CG17838 coimmunoprecipitates with Sqd and Hrb27C, confirming the association of these proteins in GRNA experiments, and also indicating that CG17838 is a component of the *grk* and *osk* RNPs *in vivo*. The association of CG17838 with Sqd is sensitive to RNase, and is reduced in the absence of RNA. However, dephosphorylation events can compensate for the reduction in binding observed in the absence of RNA, suggesting that the Sqd-CG17838 interaction is regulated by

phosphorylation. It is possible that dephosphorylation stabilizes a complex containing Sqd and CG17838 that would otherwise dissociate in the absence of RNA. A regulatory role for phosphorylation was also suggested by *in vitro* GST-pulldowns between CG17838-F and the different Sqd isoforms. CG17838-F can bind directly to all Sqd isoforms, but phosphorylated CG17838-F seems to preferentially interact with Sqd A, whilst non-phosphorylated CG17838-F preferentially binds Sqd S. Given the different roles for Sqd A and S in *grk* mRNA regulation (A is required for translational regulation, whilst S is required for localization; Norvell *et al.*, 1999), it is possible that phosphorylation of CG17838 dictates the function of the protein in the *grk* RNP. SYNCRIP RRM 2 is phosphorylated at a tyrosine residue conserved in CG17838, suggesting that this residue is a good candidate for phosphorylation. Phosphorylation of *trans*-acting factors has previously been shown to regulate translation of localized *β-actin* mRNA (Hüttelmaier *et al.*, 2005), and given that there are multiple steps in mRNA localization, any one of these steps could be regulated by the phosphorylation of *trans*-acting factors.

CG17838 interacts specifically with *grk* and *osk* only when in an intact protein complex

The results of RNA immunoprecipitation experiments indicate that CG17838 binds specifically to *grk* and *osk* mRNAs, whilst Sqd binds specifically to *grk*, *osk* and also *bcd* mRNAs. Neither protein interacted with *hb* or *nos* mRNAs. In GRNA experiments (Chapter 4), both proteins also specifically associated with ORF16 RNA, and not with ORF16ΔGLS or hb RNAs. These results are not consistent with the poly(U)-sepharose binding assays in which in *in vitro* translated CG17838-F bound poly(U) and poly(A) RNA homoploymers, or with the UV cross-linking experiments described earlier in which recombinant CG17838 and Sqd proteins alone were shown to directly bind ORF16, ORF16ΔGLS, hb and nos RNAs without specificity. This can be explained if multiple factors form an RNA recognition complex (as would occur in GRNA and RNA immunoprecipitation experiments), and it is this complex that has binding specificity. The binding of recombinant Modulo to a *bcd* localization element was also previously shown to lack the

specificity observed for the binding of the intact recognition complex to the same element (Arn *et al.*, 2003). Together, these results suggest that the recognition of localized mRNAs by *trans*-acting factors is the sum of multiple interactions, none of which by themselves has the binding affinity and specificity of the whole complex.

Other RNA targets of CG17838

RNA immunoprecipitation followed by RT-PCR has been used here to assess the association of CG17838 with known RNAs. However, in order to fully understand the function of CG17838, a more comprehensive list of RNA targets is required. RNA immunoprecipitation can be combined with high-throughput sequencing in order to identify unknown RNA targets. Recently, *in vivo* UV cross-linking of RNA to protein followed by immunoprecipitation and partial digestion of RNA to form 'CLIP' RNA tags corresponding to protein binding sites (CLIP; Ule *et al.*, 2005), has also been used to understand the 'RNA maps' for a number of proteins (Guil and Caceres, 2007; Ule *et al.*, 2006; Yeo *et al.*, 2009). This has also been combined with high-throughput sequencing (Jensen and Darnell, 2008; Wang *et al.*, 2009). The CLIP method has the advantage that RNA-protein complexes formed in intact tissue can be purified under highly stringent conditions. Information about the position of protein-RNA interaction is obtained in addition to the full complement of RNA targets of a particular protein. It is hoped that such methods can be employed to study the RNA targets of CG17838 during oogenesis and in the nervous system.

The role of CG17838 in mRNA localization during oogenesis

Homozygotes, or in combination with a deficiency, for the two hypomorphic alleles, $CG17838^{e00286}$ and $CG17838^{f03775}$ die within one day of eclosure meaning that egg chambers of mutant females are not developed enough to assess RNA localization processes during oogenesis in these mutants. In order to study the $CG17838^{e00286}$ allele during oogenesis, germline clones were generated using the FLP-DFS technique (C. Meignin, unpublished). Preliminary observations suggest that $CG17838^{e00286}$ eggs are ventralized, consistent with a role for CG17838 in *grk*

mRNA localization or translational regulation. The predicted disruption of RNA binding activity in the *CG17838*^{e00286} allele is consistent with this. Mammalian SYNCRIP was hypothesized to be involved in membrane-dependent RNA transport (Banai *et al.*, 2004). As membranes are not found in *grk*-containing transport particles or sponge bodies (Delanoue *et al.*, 2007), this would not be the case for CG17838 in *grk* RNA transport. Experiments are ongoing to determine whether CG17838 is required for *grk* RNA localization or translation, and also to test whether CG17838 is involved in the regulation of *osk* mRNA. In addition to characterization of CG17838 mRNA and protein expression in the mutant, rescue of the mutant phenotype by overexpression of CG17838, or precise excision of the insertion is also needed to confirm that *CG17838* is responsible for this phenotype.

Efforts are also ongoing to produce a null mutation affecting all isoforms by generating a FLP-FRT-based deletion (Fig. 6.14) (Parks *et al.*, 2004) between the insertions *d09234* and *f03775* (Fig. 6.11). This is predicted to delete exons encoding the N-terminus and the RRMs of all isoforms, and also the glycine-rich C-terminal region in isoforms B, D and G. It is hoped that this deletion will be used to make germline clones. Homologous recombination could also be used as a more targeted approach to generate mutants.

The role of CG17838 in the nervous system

The presence of CG17838 particles in cultured neurites also suggests that, like SYNCRIP, CG17838 is a component of transport RNPs within neurons. This can be tested directly by the visualization of localized mRNAs in primary neuronal cultures or in the brain, such as *CamKIIα* and *chickadee*, using the MS2-MCP system (Ashraf *et al.*, 2006; Estes *et al.*, 2008) in conjunction with CG17838-GFP or anti-CG17838 immunostaining.

The defects observed in surviving *CG17838*^{e00286} and *CG17838*^{f03775} homozygotes and in preliminary RNAi experiments using *actin*-GAL4 and various nervous system drivers to knockdown CG17838 expression (although knockdown does need to be

confirmed) are consistent with defects also observed in mutants where synaptic transmission is disrupted, including mutants in the pre-synaptic membrane protein *SNAP-25* and also *Imp*. Further work is required to determine where and when CG17838 is acting in the nervous system, using colocalization experiments with different nervous system markers, and what isoforms are involved. Rescue of the mutant phenotype by overexpression of CG17838, or precise excision of the insertion is particularly needed to confirm that CG17838 is indeed responsible for the phenotype. The mutant and RNAi defects need to be characterized in greater detail to determine whether it is synaptic transmission that is affected. This can be achieved by comparing wild-type and mutant/RNAi flies in electrophysiological and behavioural assays, and by studying the morphology of the synapse in these flies. It is possible that CG17838 is acting in a similar manner as or with Imp in regulating the localization and/or translation of mRNAs at synaptic termini that influence synaptic morphology. As Imp and CG17838 have been isolated in the same protein complex on *grk* mRNA (Chapter 4) it is tempting to speculate that the proteins function together in both oogenesis and the nervous system. It is also possible that CG17838 is regulates directly neurotransmitter release through its interaction with Syt.

DISCUSSION AND FUTURE PERSPECTIVES

mRNA localization coupled to localized translation is a widespread strategy used by diverse cell types and systems to spatially restrict protein synthesis to specific regions of a cell (Bashirullah *et al.*, 1998; Martin and Ephrussi, 2009; Palacios and St. Johnston, 2001; St Johnston, 2005). Indeed, recent results suggest that mRNA localization and regulated translation may be a means of regulating the majority of cellular functions (Lécuyer *et al.*, 2007). Many of the best-characterized localized mRNAs are found in oocytes and early embryos, where they play an important role in axis determination. This has been extensively studied in *Drosophila*, where the localization of maternal mRNAs, such as *bcd*, *osk* and *grk* to specific regions of the oocyte is crucial for anterior-posterior (A-P) and dorso-ventral (D-V) patterning of the embryo (Lasko, 1999; Johnstone and Lasko, 2001; St Johnston and Nüsslein-Volhard, 1992). More recent studies have also shown that mRNA localization is a central regulator of neuronal development in axonal navigation, and is also required in mature neurons for the plastic changes at synapses that underlie memory and learning. In both cases, mRNA localization allows a rapid response to local environmental cues and stimuli. Axonally targeted mRNAs are translated in response to local guidance cues as they navigate toward their synaptic partners (Antar *et al.*, 2006; Leung *et al.*, 2006; Wu *et al.*, 2006; Zhang *et al.*, 2001), whilst the regulated translation of post-synaptically localized mRNAs allows each of the many synapses made by a particular neuron to alter its structure and function during synaptic plasticity (reviewed in Dahm *et al.*, 2007).

Transport of mRNA by molecular motors along cytoskeletal filaments has been implicated as the major localization mechanism in most cell types. This active transport of mRNA within the cell has been studied using genetic manipulation, biochemical techniques, pharmacological disruption, and techniques for the *in vivo* visualization of motile mRNA. Labelling of RNA with fluorescent dyes *in vitro* (Bullock *et al.*, 2006; Clark *et al.*, 2007; Ferrandon *et al.*, 1994; MacDougall *et al.*, 2003; Van De Bor *et al.*, 2005; Vendra *et al.*, 2007; Wilkie and Davis, 2001) and

with fluorescently tagged proteins that can recognise endogenous or inserted elements within mRNA *in vivo* (Jaramillo *et al.*, 2008; Weil *et al.*, 2006; Weil *et al.*, 2008; Zimyanin *et al.*, 2008) has been particularly instrumental in advancing our understanding of the mechanism of mRNA localization. These studies have revealed that cytoplasmic mRNA localization is a multi-step process that in a number of cases is initiated in the nucleus. Subcellular destination is partially specified by *cis*-acting 'localization elements' in the RNA that are recognized by *trans*-acting factors that can function in transcript localization, regulation of translation or anchoring of the RNA at the final destination. Complexes of localizing mRNAs and protein factors form large structures termed RNA transport granules. Major questions remain about the biochemical nature of RNA transport granules, the proteins and RNAs that are present in them, what jobs these factors do and how they are organized both spatially and temporally. However, it has been suggested that both neuronal and maternal RNA transport granules share a number of components with each other and with P bodies (Barbee *et al.*, 2006; Kiebler and Bassell, 2006; Snee and Macdonald, 2009). RNA transport granules are transported through the cytoplasm along microtubules or actin filaments by the motor proteins Dynein and Kinesin or Myosin respectively. At the final destination in the cell the RNA is anchored, and is either translated or stored in a translationally repressed state until translation is required.

A major question in the field of mRNA localization is that of specificity. In motor-dependent localization, it is thought that specific *trans*-acting factors, or a certain number or arrangement of factors can bind to and interpret localization elements within the RNA, and it is this interaction that drives the association of RNA with motors and also determines destination. Bioinformatic searches for RNA localization sequences and structures (Betley *et al.*, 2002; Hamilton *et al.*, 2009; Lewis *et al.*, 2004; Rabani *et al.*, 2008) have suggested that mRNAs localizing to the same subcellular regions share consensus localization elements, although more evidence is required to show this conclusively. Destination may be then be specified by the effects of *cis*-acting elements or *trans*-acting factors on the recruitment of motor proteins (Bullock *et al.*, 2006), conformation or processivity of motor proteins or the

choice of cytoskeletal tracks used within the cell (MacDougall *et al.*, 2003; Messitt *et al.*, 2008).

Given the central role of *cis*-acting sequences and *trans*-acting factors in the definition of specificity, the overall aim of this thesis was to study the nature of both of these using *grk* localization in the *Drosophila* oocyte as a model. *grk* localization is required for both A-P and D-V patterning within the *Drosophila* embryo. Translationally repressed *grk* (Caceres and Nilson, 2009; Clouse *et al.*, 2008; Norvell *et al.*, 2009) localizes to the dorso-anterior corner of the oocyte in a Dynein and microtubule-dependent manner within transport particles (Delanoue et al., 2007; MacDougall *et al.*, 2003). The RNA is then subsequently anchored at the dorso-anterior corner within sponge bodies in a mechanism that also requires the Dynein motor (Delanoue *et al.*, 2007). The *grk* localization signal, or GLS, is a 64-nucleotide RNA hairpin that is necessary and sufficient for localization (Van De Bor *et al.*, 2005). The *I* Factor retrotransposon RNA also localizes to the dorso-anterior corner of the *Drosophila* oocyte and requires Dynein and microtubules for this localization (Van De Bor *et al.*, 2005). The *I* Factor localization signal, or ILS, is predicted to contain similar secondary structural elements to the GLS, and it has been hypothesized that the GLS and ILS form a consensus element for dorso-anterior localization.

In order to test this hypothesis we took into consideration that the architecture of RNA is also shaped by specific tertiary interactions that can give rise to more complex RNA structures than the predicted secondary structures. In Chapter 3 of this thesis, GLS and ILS RNAs were prepared and studied by NMR spectroscopy. This revealed that the lower stem portions of the hairpins have slightly different structures. The stem of a truncated, functional form of the GLS forms an extended helical structure, whilst that of a truncated ILS is kinked. Despite these differences, both structures exhibit an exposed internal loop with the sequence UUC, and also a bulged U. Preliminary mutagenesis experiments (V. Van De Bor, unpublished) suggest that whilst the bulged U is not a key determinant of dorso-anterior localization, the UUC internal loop is. Furthermore, comparison of the GLS with the

same element from different species of *Drosophilid* and with the *G2* and *Jockey* retrotransposon localization elements suggests that the identity of the UUC nucleotides is not critically important. Instead, it appears that it is the structure formed by these nucleotides that is required for localization. This internal loop may therefore represent a key feature shared by dorso-anterior localizing *grk* and the *I*, *G2* and *Jockey* retrotransposons.

The combination of RNA mutagenesis experiments and the study of RNA structure is a powerful way by which to define the key features of an RNA structure that are required for localization. This is exemplified in this work by replacement of the hairpin loops of the GLS and ILS with an ultrastable tetraloop. This was done initially to aid folding and reduce mutlimerization of the GLS through the hairpin loop, but also revealed that this loop is essential for GLS localization. In comparison, tetraloop ILS does localize, but preliminary mutagenesis experiments (V. Van De Bor, unpublished) have suggested that a loop of any sequence, but with a certain level of stability is required for ILS localization. Structural studies of the hairpin loops and the full-length elements and further mutagenesis experiments are therefore required to test shared and unique features in the GLS and ILS for effects on localization. Only then will we be able to fully address the question as to whether these signals are consensus localization elements. Structural information can also be used to refine and improve genome-wide sequence and structural searches for new localization elements, further testing the concept of consensus localization elements that target mRNAs to common subcellular destinations.

Structural and mutagenesis experiments can also be combined with biochemistry in order to fully understand how localized mRNAs interact with *trans*-acting factors within RNA transport granules. A number of *trans*-acting factors required for *grk* localization have been identified by genetic approaches (Kelley, 1993; Manseau and Schüpbach, 1989; Schüpbach, 1987; Schüpbach and Wieschaus, 1991; Wieschaus, 1978). However, genetic studies for the identification of *trans*-acting factors have been hampered by redundancy among factors, lethal phenotypes and indirect effects of genes on mRNA localization. In Chapter 4 of this thesis, I took an alternative and

complementary biochemical approach in order to identify *trans*-acting factors able to interact with the GLS.

An affinity chromatography approach known as GRNA chromatography (Czaplinski *et al.*, 2005), was adapted for use with *Drosophila* ovarian extract. The isolation of factors shown previously to be required for *grk* mRNA localization and translational regulation, including Sqd (Caceres and Nilson, 2009; Delanoue *et al.*, 2007; Jaramillo *et al.*, 2008; Kelley *et al.*, 1993; Norvell *et al.*, 1999), Hrb27C (Goodrich *et al.*, 2004), Imp (Geng and Macdonald, 2006), UAP56 (Meignin and Davis, 2008) and PABP (Clouse *et al.*, 2008), showed that this approach could successfully identify components of the *grk* transport and anchoring granule. Additional proteins that could specifically interact with GLS-containing RNA included Me31B, Dp1, BicC, Ef1α, Dhd, Exu, CG5205, Rig, Fib, CG6745, CG17838, Heph and a small number of ribosomal proteins. A repeat of the experiment did isolate a number of proteins identified in the initial experiment, but also produced additional candidates including Upf1, Ago2, NXF1, UAP56, TRA1 and Piwi. The purification of different sets of proteins could be due to non-specific binding of some proteins in the GRNA experiment. Indeed, given what is already known it is difficult to envisage how a number of these proteins could function in the regulation of the localiztion or localized translation of *grk* mRNA. Such proteins include Piwi, TRA1, Rig and Fib.

The candidate *trans*-acting factors identified by GRNA add to the list of factors that can potentially be involved in the regulation of both *grk* and *osk* mRNAs (this list now includes Sqd, Hrb27C, Imp, Bruno, Cup, Orb, Otu, Glo, UAP56, Exu, Heph and Me31B). A number of factors, or orthologues of the factors, have also been shown to interact with, or be required for localization of other mRNAs both in *Drosophila* and other organisms. This is especially true of factors involved in neuronal RNA localization, adding to the similarities between maternal and neuronal RNA granules. Many are also P body components, further illustrating the similarities in components of transport RNA granules and P bodies. Several of the protein candidates have also been shown to be members of the same complexes functioning in multiple forms of RNA regulation. Therefore, the GRNA results suggest that core conserved

complexes of proteins are involved in the regulation of localized mRNAs in different tissues and different organisms. Furthermore, these results also more specifically indicate that previously unstudied mechanisms are acting to regulate *grk* mRNA within the *grk* transport RNP. For example, the isolation of Ago2 and the presence of miRNA target sites in the *grk* 3'UTR indicates the *grk* might be subject to miRNA-mediated translational repression during localization.

The GRNA experiment does not reveal any information regarding the organization of the proteins on the RNA, and further experiments are required to identify which proteins directly contact the RNA, and which proteins are members of the complex through protein-protein interactions. The ultimate aim of such experiments would be to understand the necessary factors and their organization to an extent that mRNA localization could be reconstituted *in vitro*, and the basis of specificity identified. The roles and interactions of two specific factors, Heph and CG17838, in *grk* mRNA localization and translational regulation were studied further in Chapters 5 and 6 of this thesis. These factors were chosen due to the roles of their orthologues, PTB/VgRBP60 and SYNCRIP respectively, in mRNA localization and translational regulation in *Xenopus* oogenesis (Cote *et al.*, 1999; Lewis *et al.*, 2008) and in neurons (Bannai *et al.*, 2004; Duning *et al.*, 2008; Elvira *et al.*, 2006; Kanai *et al.*, 2004; Ma *et al.*, 2007).

Heph and CG17838 are expressed in the oocyte in a pattern that supports a role for each of these proteins in mRNA localization during oogenesis. Both proteins accumulate at the posterior from stage 9 of oogenesis onwards, mirroring the localization of *osk* mRNA at this stage, whilst CG17838 is also expressed in a pattern similar to that of the oocyte microtubule cytoskeleton and Dynein (Cha *et al.*, 2001; Li *et al.*, 1994; MacDougall *et al.*, 2003). Furthermore, Heph and CG17838 associate specifically with *grk* and *osk* mRNAs in RNA immunoprecipitation experiments. CG17838 can associate directly with *grk*, but this interaction is specific only when CG17838 is part of an intact protein complex. This has been observed for other *trans*-acting factors and localization elements (Arn *et al.*, 2003) and suggests that recognition of localized mRNAs by *trans*-acting factors is the sum of multiple

interactions, none of which by themselves has the binding affinity and specificity of the whole complex. Initial experiments indicate that CG17838 can function in the regulation of *grk* mRNA localization and/or translation. Roles for Heph in *osk* mRNA localization and translational repression have recently been described (Besse *et al.*, 2009). The role of Heph in *osk* mRNA localization appears to be indirect through regulation of the establishment of microtubule polarity in the oocyte, perhaps in the potential capacity of Heph to regulate splicing. However, Heph directly represses Osk translation by binding *osk* and facilitating the oligomerization of the mRNA. In the case of *grk*, it appears that Heph acts to regulate Grk secretion rather than *grk* mRNA localization. This may be as part of a complex, with other proteins thought to be part of the *grk* transport granule (Kugler *et al.*, 2009; Snee and Macdonald, 2009; Wilhelm *et al.*, 2005), but it is still unclear how Heph might be required for proper Grk processing, and how this relates, if at all, to the ability of Heph to interact with *grk* mRNA.

The mammalian orthologues of Heph and CG17838, PTB and SYNCRIP, are multifunctional proteins shown to have roles in alternative splicing, mRNA stability, regulation of translation and mRNA localization. Indeed, both of these proteins may be part of the *grk* RNP due to earlier mRNA regulation events, such as splicing, in the nucleus. In neurons, PTB is thought to be required for the localization of *β-actin* mRNA to neurite terminals (Ma *et al.*, 2007), whilst SYNCRIP can interact with RNA and with the synaptic vesicle component Syt (Mizutani *et al.*, 2000), as can CG17838, and has been shown to be a component of dendritically localized mRNA granules (Bannai *et al.*, 2004; Duning *et al.*, 2008; Kanai et al., 2004). *heph* mRNA is also expressed in the CNS of late stage embryos, and is required for neural development (Norga *et al.*, 2003), and mutants in *CG17838* and preliminary CG17838 RNAi experiments indicate that CG17838 is required for synaptic transmission. It is therefore tempting to speculate that Heph and CG17838 are required for regulation of mRNAs localized within neurons, and that CG17838 is required for synaptic transmission either through regulation of localized mRNAs at the synapse and/or via its interaction with Syt.

The potential roles of Heph and CG17838 in mRNA localization in oogenesis and in the nervous system are consistent with the concept that core conserved complexes of proteins are involved in the regulation of localized mRNAs. Moreover, this also indicates that the same complex of *trans*-acting factors can associate with mRNAs localizing to different subcellular destinations, and is consistent with previous studies showing that the same machinery can drive localization within *Drosophila* oocytes and embryos (Bullock and Ish-Horowicz, 2001; Lall *et al.*, 1999), and the growing lists of proteins common to *grk* and *osk* mRNAs in the Drosophila oocyte and to maternal and neuronal RNA granules (Barbee *et al.*, 2006; Kiebler and Bassell, 2006). Specificity of mRNA localization must therefore arise through the elaboration of these complexes with additional RNA-specific factors, different numbers of the same factors in these complexes (Bullock *et al.*, 2006), or different arrangements of the same factors on the RNA. Signals within transcripts that localize to the same subcellular destination may also contain consensus features that determine the specific destination. The challenge for future work is to pinpoint the similarities and the differences between these core complexes, how the complexes interact with different consensus mRNA localization elements, and how the interactions between localized mRNA and protein relate to motor activity and choice of cytoskeletal tracks to result in transport to a specific subcellular destination.

At a general level, understanding the molecular details of specificity in mRNA localization will add to current understanding of the regulation of all forms of intracellular trafficking, an increasing number of cellular processes and also more specific events including pattern formation in polarized cells, oocytes and embryos and the development of the nervous system. The conservation of the *trans*-acting factors required for mRNA localization and localized translation in *Drosophila* and other model systems also means that the study of these factors during *Drosophila* oogenesis and in the *Drosophila* nervous system can lead to a greater understanding of how this process can go awry in human disease. This may be particularly important for understanding certain disorders of the nervous system such as Fragile X syndrome and SMA.

REFERENCES

Abramochkin, G., and Shrader, T.E. (1995). The leucyl/phenylalanyl-tRNA-protein transferase. Overexpression and characterization of substrate recognition, domain structure, and secondary structure. J. Biol. Chem. *270*, 20621-20628.

Adams, M.D., Celniker, S.E., Holt, R.A., Evans, C.A., Gocayne, J.D., Amanatides, P.G., Scherer, S.E., Li, P.W., Hoskins, R.A., Galle, R.F., *et al.* (2000). The genome sequence of *Drosophila melanogaster*. Science *287*, 2185-2195.

Adams, M.D., and Sekelsky, J.J. (2002). From sequence to phenotype: reverse genetics in *Drosophila melanogaster*. Nat. Rev. Genet. *3*, 189-198.

Adams, P.L., Stahley, M.R., Gill, M.L., Kosek, A.B., Wang, J., and Strobel, S.A. (2004a). Crystal structure of a group I intron splicing intermediate. RNA *10*, 1867-1887.

Adams, P.L., Stahley, M.R., Kosek, A.B., Wang, J., and Strobel, S.A. (2004b). Crystal structure of a self-splicing group I intron with both exons. Nature *430*, 45-50.

Ainger, K., Avossa, D., Diana, A.S., Barry, C., Barbarese, E., and Carson, J.H. (1997). Transport and localization elements in myelin basic protein mRNA. J. Cell Biol. *138*, 1077-1087.

Ainger, K., Avossa, D., Morgan, F., Hill, S.J., Barry, C., Barbarese, E., and Carson, J.H. (1993). Transport and localization of exogenous myelin basic protein mRNA microinjected into oligodendrocytes. J. Cell Biol. *123*, 431-441.

Aizaki, H., Choi, K.S., Liu, M.Y., Li, Y.J. and Lai, M.M.C. (2006). Polypyrimidine-tract-binding protein is a component of the HCV RNA replication complex and necessary for RNA synthesis. J. Biomed. Sci. *13*, 469–480.

Alarcon, V.B., and Elinson, R.P. (2001). RNA anchoring in the vegetal cortex of the Xenopus oocyte. J. Cell Sci. *114*, 1731-1741.

Allain, F.H., and Varani, G. (1995). Structure of the P1 helix from group I self-splicing introns. J. Mol. Biol *250*, 333-353.

Ali, N., and Siddiqui, A. (1995). Interaction of polypyrimidine tract-binding protein with the 5' noncoding region of the hepatitis C virus RNA genome and its functional requirement in internal initiation of translation. J. Virol. *69*, 6367-6375.

Allison, R., Czaplinski, K., Git, A., Adegbenro, E., Stennard, F., Houliston, E., and Standart, N. (2004). Two distinct Staufen isoforms in Xenopus are vegetally localized during oogenesis. RNA *10*, 1751-1763.

Anderson, A.C., Scaringe, S.A., Earp, B.E., and Frederick, C.A. (1996). HPLC purification of RNA for crystallography and NMR. RNA *2*, 110-117.

Anderson, P., and Kedersha, N. (2006). RNA granules. J. Cell Biol. *172*, 803-808.

Antao, V.P., Lai, S.Y., and Tinoco, I., Jr. (1991). A thermodynamic study of unusually stable RNA and DNA hairpins. Nucleic Acids Res. *19*, 5901-5905.

Antar, L.N., Li, C., Zhang, H., Carroll, R.C., and Bassell, G.J. (2006). Local functions for FMRP in axon growth cone motility and activity-dependent regulation of filopodia and spine synapses. Mol. Cell. Neurosci. *32*, 37-48.

Anwar, A., Ali, N., Tanveer, R., and Siddiqui, A. (2000). Demonstration of functional requirement of polypyrimidine tract-binding protein by SELEX RNA during hepatitis C virus internal ribosome entry site-mediated translation initiation. J. Biol. Chem. *275*, 34231-34235.

Arn, E.A., Cha, B.J., Theurkauf, W.E., and Macdonald, P.M. (2003). Recognition of a bicoid mRNA localization signal by a protein complex containing Swallow, Nod, and RNA binding proteins. Dev. Cell *4*, 41-51.

Aronov, S., Aranda, G., Behar, L., and Ginzburg, I. (2001). Axonal tau mRNA localization coincides with tau protein in living neuronal cells and depends on axonal targeting signal. J. Neurosci. *21*, 6577-6587.

Ashiya, M., and Grabowski, P.J. (1997). A neuron-specific splicing switch mediated by an array of pre-mRNA repressor sites: evidence of a regulatory role for the polypyrimidine tract binding protein and a brain-specific PTB counterpart. RNA *3*, 996-1015.

Ashraf, S.I., McLoon, A.L., Sclarsic, S.M., and Kunes, S. (2006). Synaptic protein synthesis associated with memory is regulated by the RISC pathway in Drosophila. Cell *124*, 191-205.

Aspengren, S., Hedberg, D., Skold, H.N., and Wallin, M. (2009). New insights into melanosome transport in vertebrate pigment cells. Int. Rev. Cell Mol. Biol. *272*, 245-302.

Auweter, S.D., Oberstrass, F.C., and Allain, F.H. (2007). Solving the structure of PTB in complex with pyrimidine tracts: an NMR study of protein-RNA complexes of weak affinities. J. Mol. Biol. *367*, 174-186.

Bachler, M., Schroeder, R., and von Ahsen, U. (1999). StreptoTag: a novel method for the isolation of RNA-binding proteins. RNA *5*, 1509-1516.

Bannai, H., Fukatsu, K., Mizutani, A., Natsume, T., Iemura, S., Ikegami, T., Inoue, T., and Mikoshiba, K. (2004). An RNA-interacting protein, SYNCRIP (heterogeneous nuclear ribonuclear protein Q1/NSAP1) is a component of mRNA granule transported with inositol 1,4,5-trisphosphate receptor type 1 mRNA in neuronal dendrites. J. Biol. Chem. *279*, 53427-53434.

Barbarese, E., Koppel, D.E., Deutscher, M.P., Smith, C.L., Ainger, K., Morgan, F., and Carson, J.H. (1995). Protein translation components are colocalized in granules in oligodendrocytes. J. Cell Sci. *108*, 2781-2790.

Barbee, S.A., Estes, P.S., Cziko, A.M., Hillebrand, J., Luedeman, R.A., Coller, J.M., Johnson, N., Howlett, I.C., Geng, C., Ueda, R., *et al.* (2006). Staufen- and FMRP-containing neuronal RNPs are structurally and functionally related to somatic P bodies. Neuron *52*, 997-1009.

Bashirullah, A., Cooperstock, R.L., and Lipshitz, H.D. (1998). RNA localization in development. Ann. Rev. Bioc. *67*, 335-394.

Bashirullah, A., Halsell, S.R., Cooperstock, R.L., Kloc, M., Karaiskakis, A., Fisher, W.W., Fu, W., Hamilton, J.K., Etkin, L.D., and Lipshitz, H.D. (1999). Joint action of two RNA degradation pathways controls the timing of maternal transcript elimination at the midblastula transition in *Drosophila melanogaster*. EMBO J. *18*, 2610-2620.

Bassell, G.J., and Warren, S.T. (2008). Fragile X syndrome: loss of local mRNA regulation alters synaptic development and function. Neuron *60*, 201-214.

Bassell, G.J., Zhang, H., Byrd, A.L., Femino, A.M., Singer, R.H., Taneja, K.L., Lifshitz, L.M., Herman, I.M., and Kosik, K.S. (1998). Sorting of beta-actin mRNA and protein to neurites and growth cones in culture. J. Neurosci. *18*, 251-265.

Batey, R.T., Gilbert, S.D., and Montange, R.K. (2004). Structure of a natural guanine-responsive riboswitch complexed with the metabolite hypoxanthine. Nature *432*, 411-415.

Beach, D.L., Salmon, E.D., and Bloom, K. (1999). Localization and anchoring of mRNA in budding yeast. Curr. Biol. *9*, 569-578.

Bechade, C., Rostaing, P., Cisterni, C., Kalisch, R., La Bella, V., Pettmann, B., and Triller, A. (1999). Subcellular distribution of survival motor neuron (SMN) protein: possible involvement in nucleocytoplasmic and dendritic transport. Eur. J. Neurosci. *11*, 293-304.

Belsham, G. J., and Jackson, R. J. (2000). Translation initiation on picornavirus RNA. Translational Control of Gene Expression (Sonenberg, N., Hershey, J.W.B. and Mathews, M.B., eds.), pp. 869–900, Cold Spring Harbor Laboratory Press, Cold Spring Harbor, NY.

Berg, C.A. (2005). The *Drosophila* shell game: patterning genes and morphological change. Trends Genet. *21*, 346-355.

Bergstrom, K., Urquhart, J.C., Tafech, A., Doyle, E., and Lee, C.H. (2006). Purification and characterization of a novel mammalian endoribonuclease. J. Cell. Biochemistry *98*, 519-537.

Berleth, T., Burri, M., Thoma, G., Bopp, D., Richstein, S., Frigerio, G., Noll, M., and Nusslein-Volhard, C. (1988). The role of localization of bicoid RNA in organizing the anterior pattern of the *Drosophila* embryo. EMBO J. *7*, 1749-1756.

Besse, F., Lopez de Quinto, S., Marchand, V., Trucco, A., and Ephrussi, A. (2009). *Drosophila* PTB promotes formation of high-order RNP particles and represses oskar translation. Genes Dev. *23*, 195-207.

Betley, J.N., Frith, M.C., Graber, J.H., Choo, S., and Deshler, J.O. (2002). A ubiquitous and conserved signal for RNA localization in chordates. Curr. Biol. *12*, 1756-1761.

Blanc, V., Navaratnam, N., Henderson, J.O., Anant, S., Kennedy, S., Jarmuz, A., Scott, J., and Davidson, N.O. (2001). Identification of GRY-RBP as an apolipoprotein B RNA-binding protein that interacts with both apobec-1 and apobec-1 complementation factor to modulate C to U editing. J. Biol. Chem. *276*, 10272-10283.

Bobinnec, Y., Marcaillou, C., Morin, X., and Debec, A. (2003). Dynamics of the endoplasmic reticulum during early development of *Drosophila melanogaster*. Cell Motil. Cytoskeleton *54*, 217-225.

Bobola, N., Jansen, R.P., Shin, T.H., and Nasmyth, K. (1996). Asymmetric accumulation of Ash1p in postanaphase nuclei depends on a myosin and restricts yeast mating-type switching to mother cells. Cell *84*, 699-709.

Bohl, F., Kruse, C., Frank, A., Ferring, D., and Jansen, R.P. (2000). She2p, a novel RNA-binding protein tethers ASH1 mRNA to the Myo4p myosin motor via She3p. EMBO J. *19*, 5514-5524.

Bokel, C., Dass, S., Wilsch-Brauninger, M., and Roth, S. (2006). *Drosophila* Cornichon acts as cargo receptor for ER export of the TGFalpha-like growth factor Gurken. Development *133*, 459-470.

Bolivar, J., Huynh, J.R., Lopez-Schier, H., González, C., St Johnston, D., and González-Reyes, A. (2001). Centrosome migration into the *Drosophila* oocyte is independent of *BicD*, *egl* and of the organization of the microtubule cytoskeleton. Development *128*, 1889-1897.

Boswell, R.E., Prout, M.E., and Steichen, J.C. (1991). Mutations in a newly identified *Drosophila melanogaster* gene, mago nashi, disrupt germ cell formation and result in the formation of mirror-image symmetrical double abdomen embryos. Development *113*, 373-384.

Boylan, K.L., Mische, S., Li, M., Marques, G., Morin, X., Chia, W., and Hays, T.S. (2008). Motility screen identifies *Drosophila* IGF-II mRNA-binding protein--zipcode-binding protein acting in oogenesis and synaptogenesis. PLoS Genetics *4*, e36.

Bramham, C.R., and Wells, D.G. (2007). Dendritic mRNA: transport, translation and function. Nat. Rev. Neurosci. *8*, 776-789.

Brendza, R.P., Serbus, L.R., Duffy, J.B., and Saxton, W.M. (2000). A function for kinesin I in the posterior transport of oskar mRNA and Staufen protein. Science *289*, 2120-2122.

Brenner, H.R., Witzemann, V., and Sakmann, B. (1990). Imprinting of acetylcholine receptor messenger RNA accumulation in mammalian neuromuscular synapses. Nature *344*, 544-547.

Broadus, J., Fuerstenberg, S., and Doe, C.Q. (1998). Staufen-dependent localization of prospero mRNA contributes to neuroblast daughter-cell fate. Nature *391*, 792-795.

Brogna, S., and Wen, J. (2009). Nonsense-mediated mRNA decay (NMD) mechanisms. Nat. Struct. Mol. Biol. *16*, 107-113.

Bucheton, A. (1990). I transposable elements and I-R hybrid dysgenesis in Drosophila. Trends Genet. *6*, 16-21.

Bullock, S.L., and Ish-Horowicz, D. (2001). Conserved signals and machinery for RNA transport in *Drosophila* oogenesis and embryogenesis. Nature *414*, 611-616.

Bullock, S.L., Nicol, A., Gross, S.P., and Zicha, D. (2006). Guidance of bidirectional motor complexes by mRNA cargoes through control of dynein number and activity. Curr. Biol. *16*, 1447-1452.

Burgess, S.A., and Knight, P.J. (2004). Is the dynein motor a winch? Curr. Opin. Struct. Biol. *14*, 138-146.

Burkhardt, J.K., Echeverri, C.J., Nilsson, T., and Vallee, R.B. (1997). Overexpression of the dynamitin (p50) subunit of the dynactin complex disrupts dynein-dependent maintenance of membrane organelle distribution. J. Cell Biol. *139*, 469-484.

Caceres, L., and Nilson, L.A. (2009). Translational repression of gurken mRNA in the *Drosophila* oocyte requires the hnRNP Squid in the nurse cells. Dev. Biol. *326*, 327-334.

Carpenter, A.T.C. (1975). Electron microscopy of meiosis in *Drosophila melanogaster* females I. Structure, arrangement, and temporal change of the synaptonemal complex in wild-type. Chromosoma *51*, 157-182.

Carpenter, A. (1994). egalitarian and the choice of cell fates in *Drosophila melanogaster* oogenesis. Germline development (Marsh, J., and Goode, J. eds.), pp223-246. John Wiley and Sons, Chichester.

Carson, J.H., Worboys, K., Ainger, K., and Barbarese, E. (1997). Translocation of myelin basic protein mRNA in oligodendrocytes requires microtubules and kinesin. Cell Motil. Cytoskeleton *38*, 318-328.

Carter, A.P., Garbarino, J.E., Wilson-Kubalek, E.M., Shipley, W.E., Cho, C., Milligan, R.A., Vale, R.D., and Gibbons, I.R. (2008). Structure and functional role of dynein's microtubule-binding domain. Science *322*, 1691-1695.

Castagnetti, S., Hentze, M.W., Ephrussi, A., and Gebauer, F. (2000). Control of oskar mRNA translation by Bruno in a novel cell-free system from *Drosophila* ovaries. Development *127*, 1063-1068.

Castelo-Branco, P., Furger, A., Wollerton, M., Smith, C., Moreira, A., and Proudfoot, N. (2004). Polypyrimidine tract binding protein modulates efficiency of polyadenylation. Mol. Cell. Biol. *24*, 4174-4183.

Castrillon, D.H., Gonczy, P., Alexander, S., Rawson, R., Eberhart, C.G., Viswanathan, S., DiNardo, S., and Wasserman, S.A. (1993). Toward a molecular genetic analysis of spermatogenesis in *Drosophila melanogaster*: characterization of male-sterile mutants generated by single P element mutagenesis. Genetics *135*, 489-505.

Caviston, J.P., and Holzbaur, E.L. (2006). Microtubule motors at the intersection of trafficking and transport. Trends Cell Biol. *16*, 530-537.

Cha, B.J., Koppetsch, B.S., and Theurkauf, W.E. (2001). In vivo analysis of *Drosophila* bicoid mRNA localization reveals a novel microtubule-dependent axis specification pathway. Cell *106*, 35-46.

Cha, B.J., Serbus, L.R., Koppetsch, B.S., and Theurkauf, W.E. (2002). Kinesin I-dependent cortical exclusion restricts pole plasm to the oocyte posterior. Nat. Cell Biol. *4*, 592-598.

Chakkalakal, J.V., and Jasmin, B.J. (2003). Localizing synaptic mRNAs at the neuromuscular junction: it takes more than transcription. Bioessays *25*, 25-31.

Chang, J.S., Tan, L., Wolf, M.R., and Schedl, P. (2001). Functioning of the *Drosophila* orb gene in gurken mRNA localization and translation. Development *128*, 3169-3177.

Chang, K. S., and Luo, G. (2006). The polypyrimidine tract-binding protein (PTB) is required for efficient replication of hepatitis C virus (HCV) RNA. Virus Res. *115*, 1-8.

Chartrand, P., Meng, X.H., Singer, R.H., and Long, R.M. (1999). Structural elements required for the localization of ASH1 mRNA and of a green fluorescent protein reporter particle in vivo. Curr. Biol. *9*, 333-336.

Chekulaeva, M., Hentze, M.W., and Ephrussi, A. (2006). Bruno acts as a dual repressor of oskar translation, promoting mRNA oligomerization and formation of silencing particles. Cell *124*, 521-533.

Chen, C.Y., and Shyu, A.B. (2003). Rapid deadenylation triggered by a nonsense codon precedes decay of the RNA body in a mammalian cytoplasmic nonsense-mediated decay pathway. Mol. Cell. Biol. *23*, 4805-4813.

Chen, H.H., Chang, J.G., Lu, R.M., Peng, T.Y., and Tarn, W.Y. (2008). The RNA binding protein hnRNP Q modulates the utilization of exon 7 in the survival motor neuron 2 (SMN2) gene. Mol. Cell. Biol. *28*, 6929-6938.

Chen, Z., Eggerman, T.L., and Patterson, A.P. (2007). ApoB mRNA editing is mediated by a coordinated modulation of multiple apoB mRNA editing enzyme components. Am. J. Physiol. *292*, G53-65.

Cheng, J.G., Tiedge, H., and Brosius, J. (1996). Identification and characterization of BC1 RNP particles. DNA Cell Biol. *15*, 549-559.

Cheong, C., Varani, G., and Tinoco, I., Jr. (1990). Solution structure of an unusually stable RNA hairpin, 5'GGAC(UUCG)GUCC. Nature *346*, 680-682.

Cheong, H.K., Hwang, E., Lee, C., Choi, B.S., and Cheong, C. (2004). Rapid preparation of RNA samples for NMR spectroscopy and X-ray crystallography. Nucleic Acids Res. *32*, e84.

Cheung, H.K., Serano, T.L., and Cohen, R.S. (1992). Evidence for a highly selective RNA transport system and its role in establishing the dorsoventral axis of the *Drosophila* egg. Development *114*, 653-661.

Chicoine, J., Benoit, P., Gamberi, C., Paliouras, M., Simonelig, M., and Lasko, P. (2007). Bicaudal-C recruits CCR4-NOT deadenylase to target mRNAs and regulates oogenesis, cytoskeletal organization, and its own expression. Dev. Cell *13*, 691-704.

Cho, S., Park, S.M., Kim, T.D., Kim, J.H., Kim, K.T., and Jang, S.K. (2007). BiP internal ribosomal entry site activity is controlled by heat-induced interaction of NSAP1. Mol. Cell. Biol. *27*, 368-383.

Choi, K.S., Mizutani, A., and Lai, M.M. (2004). SYNCRIP, a member of the heterogeneous nuclear ribonucleoprotein family, is involved in mouse hepatitis virus RNA synthesis. J. Virol. *78*, 13153-13162.

Chou, T.B., Noll, E., and Perrimon, N. (1993). Autosomal P[ovoD1] dominant female-sterile insertions in *Drosophila* and their use in generating germ-line chimeras. Development *119*, 1359-1369.

Chou, T.B., and Perrimon, N. (1996). The autosomal FLP-DFS technique for generating germline mosaics in *Drosophila melanogaster*. Genetics *144*, 1673-1679.

Christerson, L.B., and McKearin, D.M. (1994). orb is required for anteroposterior and dorsoventral patterning during *Drosophila* oogenesis. Genes Dev. *8*, 614-628.

Cilley, C.D., and Williamson, J.R. (1997). Analysis of bacteriophage N protein and peptide binding to boxB RNA using polyacrylamide gel coelectrophoresis (PACE). RNA *3*, 57-67.

Clark, A., Meignin, C., and Davis, I. (2007). A Dynein-dependent shortcut rapidly delivers axis determination transcripts into the *Drosophila* oocyte. Development *134*, 1955-1965.

Clark, I., Giniger, E., Ruohola-Baker, H., Jan, L.Y., and Jan, Y.N. (1994). Transient posterior localization of a kinesin fusion protein reflects anteroposterior polarity of the *Drosophila* oocyte. Curr. Biol. *4*, 289-300.

Clark, I.E., Jan, L.Y., and Jan, Y.N. (1997). Reciprocal localization of Nod and kinesin fusion proteins indicates microtubule polarity in the *Drosophila* oocyte, epithelium, neuron and muscle. Development *124*, 461-470.

Clarke, E.J., and Allan, V. (2002). Intermediate filaments: vimentin moves in. Curr Biol *12*, R596-598.

Clouse, K.N., Ferguson, S.B., and Schüpbach, T. (2008). Squid, Cup, and PABP55B function together to regulate gurken translation in Drosophila. Dev. Biol. *313*, 713-724.

Cohen, R.S. (2005). The role of membranes and membrane trafficking in RNA localization. Biol. Cell *97*, 5-18.

Colegrove-Otero, L.J., Minshall, N., and Standart, N. (2005). RNA-binding proteins in early development. Crit. Rev. Biochem. Mol. Biol. *40*, 21-73.

Conte, M.R., Grune, T., Ghuman, J., Kelly, G., Ladas, A., Matthews, S., and Curry, S. (2000). Structure of tandem RNA recognition motifs from polypyrimidine tract binding protein reveals novel features of the RRM fold. EMBO J. *19*, 3132-3141.

Corbin, V., Michelson, A.M., Abmayr, S.M., Neel, V., Alcamo, E., Maniatis, T., and Young, M.W. (1991). A role for the *Drosophila* neurogenic genes in mesoderm differentiation. Cell *67*, 311-323.

Cote, C.A., Gautreau, D., Denegre, J.M., Kress, T.L., Terry, N.A., and Mowry, K.L. (1999). A Xenopus protein related to hnRNP I has a role in cytoplasmic RNA localization. Mol. Cell *4*, 431-437.

Cox, D.N., Lu, B., Sun, T.Q., Williams, L.T., and Jan, Y.N. (2001). *Drosophila* par-1 is required for oocyte differentiation and microtubule organization. Curr. Biol. *11*, 75-87.

Cox, R.T., and Spradling, A.C. (2003). Balbiani body and the fusome mediate mitochondrial inheritance during *Drosophila* oogenesis. Development *130*, 1579-1590.

Cristofanilli, M., Iacoangeli, A., Muslimov, I.A., and Tiedge, H. (2006). Neuronal BC1 RNA: microtubule-dependent dendritic delivery. J. Mol. Biol. *356*, 1118-1123.

Czaplinski, K., Kocher, T., Schelder, M., Segref, A., Wilm, M., and Mattaj, I.W. (2005). Identification of 40LoVe, a Xenopus hnRNP D family protein involved in localizing a TGF-beta-related mRNA during oogenesis. Dev. Cell *8*, 505-515.

Czaplinski, K., and Singer, R.H. (2006). Pathways for mRNA localization in the cytoplasm. Trends Biochem. Sci. *31*, 687-693.

D'Souza, V., Dey, A., Habib, D., and Summers, M.F. (2004). NMR structure of the 101-nucleotide core encapsidation signal of the Moloney murine leukemia virus. J. Mol. Biol. *337*, 427-442.

Dahanukar, A., and Wharton, R.P. (1996). The Nanos gradient in *Drosophila* embryos is generated by translational regulation. Genes Dev. *10*, 2610-2620.

Dahlgaard, K., Raposo, A.A., Niccoli, T., and St Johnston, D. (2007). Capu and Spire assemble a cytoplasmic actin mesh that maintains microtubule organization in the *Drosophila* oocyte. Dev. Cell *13*, 539-553.

Dahm, R., Kiebler, M., and Macchi, P. (2007). RNA localisation in the nervous system. Semin. Cell Dev. Biol. *18*, 216-223.

Dale, L., Matthews, G., and Colman, A. (1993). Secretion and mesoderm-inducing activity of the TGF-beta-related domain of Xenopus Vg1. EMBO J. *12*, 4471-4480.

Dansereau, D.A., Lunke, M.D., Finkielsztein, A., Russell, M.A., and Brook, W.J. (2002). Hephaestus encodes a polypyrimidine tract binding protein that regulates Notch signalling during wing development in *Drosophila melanogaster*. Development *129*, 5553-5566.

Davis, I. (2000). Imaging fluorescence in thick *Drosophila* specimens. Chapter 5, p133 'Protein localization using fluorescence microscopy: a practical approach'. Editor: Allan, V. OUP.

Davis, I., and Ish-Horowicz, D. (1991). Apical localization of pair-rule transcripts requires 3' sequences and limits protein diffusion in the *Drosophila* blastoderm embryo. Cell *67*, 927-940.

Davis, J.H., Tonelli, M., Scott, L.G., Jaeger, L., Williamson, J.R., and Butcher, S.E. (2005). RNA helical packing in solution: NMR structure of a 30 kDa GAAA tetraloop-receptor complex. J. Mol. Biol. *351*, 371-382.

Davis, M.B., Sun, W., and Standiford, D.M. (2002). Lineage-specific expression of polypyrimidine tract binding protein (PTB) in *Drosophila* embryos. Mech. Dev. *111*, 143-147.

Dawson, A., Hartswood, E., Paterson, T., and Finnegan, D.J. (1997). A LINE-like transposable element in Drosophila, the *I* Factor, encodes a protein with properties similar to those of retroviral nucleocapsids. EMBO J. *16*, 4448-4455.

de Cuevas, M., and Spradling, A.C. (1998). Morphogenesis of the *Drosophila* fusome and its implications for oocyte specification. Development *125*, 2781-2789.

de Cuevas, M., Lee, J.L., and Spradling, A.C. (1996). α-spectrin is required for germline cell division and differentiation in the *Drosophila* ovary. Development *124*, 3959-3968.

Delanoue, R., and Davis, I. (2005). Dynein anchors its mRNA cargo after apical transport in the *Drosophila* blastoderm embryo. Cell *122*, 97-106.

Delanoue, R., Herpers, B., Soetaert, J., Davis, I., and Rabouille, C. (2007). *Drosophila* Squid/hnRNP helps Dynein switch from a gurken mRNA transport motor to an ultrastructural static anchor in sponge bodies. Dev. Cell *13*, 523-538.

Deshler, J.O., Highett, M.I., Abramson, T., and Schnapp, B.J. (1998). A highly conserved RNA-binding protein for cytoplasmic mRNA localization in vertebrates. Curr. Biol. *8*, 489-496.

Deshler, J.O., Highett, M.I., and Schnapp, B.J. (1997). Localization of Xenopus Vg1 mRNA by Vera protein and the endoplasmic reticulum. Science *276*, 1128-1131.

Ding, D., Parkhurst, S.M., Halsell, S.R., and Lipshitz, H.D. (1993). Dynamic Hsp83 RNA localization during *Drosophila* oogenesis and embryogenesis. Mol. Cell. Biol. *13*, 3773-3781.

Dobens, L., Jaeger, A., Peterson, J.S., and Raftery, L.A. (2005). Bunched sets a boundary for Notch signaling to pattern anterior eggshell structures during *Drosophila* oogenesis. Dev. Biol. *287*, 425-437.

Dohner, K., Wolfstein, A., Prank, U., Echeverri, C., Dujardin, D., Vallee, R., and Sodeik, B. (2002). Function of dynein and dynactin in herpes simplex virus capsid transport. Mol. Biol. Cell *13*, 2795-2809.

Dreyfuss, G., Kim, V.N., and Kataoka, N. (2002). Messenger-RNA-binding proteins and the messages they carry. Nat. Rev. Mol. Cell Biol. *3*, 195-205.

Driever, W., and Nusslein-Volhard, C. (1988). A gradient of bicoid protein in *Drosophila* embryos. Cell *54*, 83-93.

Dubowy, J., and Macdonald, P.M. (1998). Localization of mRNAs to the oocyte is common in *Drosophila* ovaries. Mech. Dev. *70*, 193-195.

Duchaine, T.F., Hemraj, I., Furic, L., Deitinghoff, A., Kiebler, M.A., and DesGroseillers, L. (2002). Staufen2 isoforms localize to the somatodendritic domain of neurons and interact with different organelles. J. Cell Sci. *115*, 3285-3295.

Duncan, J.E., and Warrior, R. (2002). The cytoplasmic dynein and kinesin motors have interdependent roles in patterning the *Drosophila* oocyte. Curr. Biol. *12*, 1982-1991.

Duning, K., Buck, F., Barnekow, A., and Kremerskothen, J. (2008). SYNCRIP, a component of dendritically localized mRNPs, binds to the translation regulator BC200 RNA. J. Neurochem. *105*, 351-359.

Dunn, S., Morrison, E.E., Liverpool, T.B., Molina-Paris, C., Cross, R.A., Alonso, M.C., and Peckham, M. (2008). Differential trafficking of Kif5c on tyrosinated and detyrosinated microtubules in live cells. J. Cell Sci. *121*, 1085-1095.

Eberwine, J., Belt, B., Kacharmina, J.E., and Miyashiro, K. (2002). Analysis of subcellularly localized mRNAs using in situ hybridization, mRNA amplification, and expression profiling. Neurochem. Res. *27*, 1065-1077.

Eckley, D.M., Gill, S.R., Melkonian, K.A., Bingham, J.B., Goodson, H.V., Heuser, J.E., and Schroer, T.A. (1999). Analysis of dynactin subcomplexes reveals a novel actin-related protein associated with the arp1 minifilament pointed end. J. Cell Biol. *147*, 307-320.

Elvira, G., Wasiak, S., Blandford, V., Tong, X.K., Serrano, A., Fan, X., del Rayo Sanchez-Carbente, M., Servant, F., Bell, A.W., Boismenu, D., *et al.* (2006). Characterization of an RNA granule from developing brain. Mol. Cell. Proteomics *5*, 635-651.

Ennifar, E., Nikulin, A., Tishchenko, S., Serganov, A., Nevskaya, N., Garber, M., Ehresmann, B., Ehresmann, C., Nikonov, S., and Dumas, P. (2000). The crystal structure of UUCG tetraloop. J. Mol. Biol. *304*, 35-42.

Ephrussi, A., Dickinson, L.K., and Lehmann, R. (1991). Oskar organizes the germ plasm and directs localization of the posterior determinant nanos. Cell *66*, 37-50.

Ephrussi, A., and Lehmann, R. (1992). Induction of germ cell formation by oskar. Nature *358*, 387-392.

Erdelyi, M., Michon, A.M., Guichet, A., Glotzer, J.B., and Ephrussi, A. (1995). Requirement for *Drosophila* cytoplasmic tropomyosin in oskar mRNA localization. Nature *377*, 524-527.

Estes, P.S., O'Shea, M., Clasen, S., and Zarnescu, D.C. (2008). Fragile X protein controls the efficacy of mRNA transport in *Drosophila* neurons. Mol. Cell. Neurosci. *39*, 170-179.

Eulalio, A., Behm-Ansmant, I., and Izaurralde, E. (2007). P bodies: at the crossroads of post-transcriptional pathways. Nat. Rev. Mol. Cell Biol. *8*, 9-22.

Farina, K.L., Huttelmaier, S., Musunuru, K., Darnell, R., and Singer, R.H. (2003). Two ZBP1 KH domains facilitate beta-actin mRNA localization, granule formation, and cytoskeletal attachment. J. Cell Biol. *160*, 77-87.

Fawcett, D.H., Lister, C.K., Kellett, E., and Finnegan, D.J. (1986). Transposable elements controlling I-R hybrid dysgenesis in D. melanogaster are similar to mammalian LINEs. Cell *47*, 1007-1015.

Ferrandon, D., Elphick, L., Nusslein-Volhard, C., and St Johnston, D. (1994). Staufen protein associates with the 3'UTR of bicoid mRNA to form particles that move in a microtubule-dependent manner. Cell *79*, 1221-1232.

Ferrandon, D., Koch, I., Westhof, E., and Nusslein-Volhard, C. (1997). RNA-RNA interaction is required for the formation of specific bicoid mRNA 3' UTR-STAUFEN ribonucleoprotein particles. EMBO J. *16*, 1751-1758.

Filardo, P., and Ephrussi, A. (2003). Bruno regulates gurken during *Drosophila* oogenesis. Mech. Dev. *120*, 289-297.

Forrest, K.M., and Gavis, E.R. (2003). Live imaging of endogenous RNA reveals a diffusion and entrapment mechanism for nanos mRNA localization in Drosophila. Curr. Biol. *13*, 1159-1168.

Fred, R.G., Tillmar, L., and Welsh, N. (2006). The role of PTB in insulin stability control. Curr. Diabetes Rev. *2*, 363-366.

Frohnhöfer, H. G., and Nüsslein-Volhard, C. (1987). Maternal genes required for the anterior localization of *bicoid* activity in the embryo of *Drosophila*. Genes Dev. *1*, 880-890.

Frugier, T., Tiziano, F.D., Cifuentes-Diaz, C., Miniou, P., Roblot, N., Dierich, A., Le Meur, M., and Melki, J. (2000). Nuclear targeting defect of SMN lacking the C-terminus in a mouse model of spinal muscular atrophy. Hum. Mol. Genet. *9*, 849-858.

Furic, L., Maher-Laporte, M., and DesGroseillers, L. (2008). A genome-wide approach identifies distinct but overlapping subsets of cellular mRNAs associated with Staufen1- and Staufen2-containing ribonucleoprotein complexes. RNA *14*, 324-335.

Furtig, B., Richter, C., Wohnert, J., and Schwalbe, H. (2003). NMR spectroscopy of RNA. Chembiochem *4*, 936-962.

Fusco, D., Accornero, N., Lavoie, B., Shenoy, S.M., Blanchard, J.M., Singer, R.H., and Bertrand, E. (2003). Single mRNA molecules demonstrate probabilistic movement in living mammalian cells. Curr. Biol. *13*, 161-167.

Gao, Y., Tatavarty, V., Korza, G., Levin, M.K., and Carson, J.H. (2008). Multiplexed dendritic targeting of alpha calcium calmodulin-dependent protein kinase II, neurogranin, and activity-regulated cytoskeleton-associated protein RNAs by the A2 pathway. Mol. Biol. Cell *19*, 2311-2327.

Garcia-Blanco, M.A., Jamison, S.F., and Sharp, P.A. (1989). Identification and purification of a 62,000-dalton protein that binds specifically to the polypyrimidine tract of introns. Genes Dev. *3*, 1874-1886.

Gates, J., Lam, G., Ortiz, J.A., Losson, R., and Thummel, C.S. (2004). *rigor mortis* encodes a novel nuclear receptor interacting protein required for ecdysone signaling during *Drosophila* larval development. Development *131*, 25-36.

Gatfield, D., and Izaurralde, E. (2002). REF1/Aly and the additional exon junction complex proteins are dispensable for nuclear mRNA export. J. Cell Biol. *159*, 579-588.

Gatfield, D., Le Hir, H., Schmitt, C., Braun, I.C., Kocher, T., Wilm, M., and Izaurralde, E. (2001). The DExH/D box protein HEL/UAP56 is essential for mRNA nuclear export in Drosophila. Curr. Biol. *11*, 1716-1721.

Gautier, T., Berges, T., Tollervey, D., and Hurt, E. (1997). Nucleolar KKE/D repeat proteins Nop56p and Nop58p interact with Nop1p and are required for ribosome biogenesis. Mol. Cell. Biol. *17*, 7088-7098.

Gavis, E.R., Lunsford, L., Bergsten, S.E., and Lehmann, R. (1996). A conserved 90 nucleotide element mediates translational repression of nanos RNA. Development *122*, 2791-2800.

Geng, C., and Macdonald, P.M. (2006). Imp associates with squid and Hrp48 and contributes to localized expression of gurken in the oocyte. Mol. Cell. Biol. *26*, 9508-9516.

Gennerich, A., and Vale, R.D. (2009). Walking the walk: how kinesin and dynein coordinate their steps. Curr. Opin. Cell Biol. *21*, 59-67.

Ghetti, A., Pinol-Roma, S., Michael, W.M., Morandi, C., and Dreyfuss, G. (1992). hnRNP I, the polypyrimidine tract-binding protein: distinct nuclear localization and association with hnRNAs. Nucleic Acids Res. *20*, 3671-3678.

Ghiglione, C., Bach, E.A., Paraiso, Y., Carraway, K.L., 3rd, Noselli, S., and Perrimon, N. (2002). Mechanism of activation of the *Drosophila* EGF Receptor by the TGFalpha ligand Gurken during oogenesis. Development *129*, 175-186.

Gibbons, I.R. (1981). Cilia and flagella of eukaryotes. J. Cell Biol. *91*, 107s-124s.

Gibbons, I.R., Garbarino, J.E., Tan, C.E., Reck-Peterson, S.L., Vale, R.D., and Carter, A.P. (2005). The affinity of the dynein microtubule-binding domain is modulated by the conformation of its coiled-coil stalk. J. Biol. Chem. *280*, 23960-23965.

Gil, A., Sharp, P.A., Jamison, S.F., and Garcia-Blanco, M.A. (1991). Characterization of cDNAs encoding the polypyrimidine tract-binding protein. Genes Dev. *5*, 1224-1236.

Giorgi, C., Yeo, G.W., Stone, M.E., Katz, D.B., Burge, C., Turrigiano, G., and Moore, M.J. (2007). The EJC factor eIF4AIII modulates synaptic strength and neuronal protein expression. Cell *130*, 179-191.

Glanzer, J., Miyashiro, K.Y., Sul, J.Y., Barrett, L., Belt, B., Haydon, P., and Eberwine, J. (2005). RNA splicing capability of live neuronal dendrites. Proc. Natl. Acad. Sci. USA *102*, 16859-16864.

Golden, B.L., Kim, H., and Chase, E. (2005). Crystal structure of a phage Twort group I ribozyme-product complex. Nat. Struct. Mol. Biol. *12*, 82-89.

Gonsalvez, G.B., Urbinati, C.R., and Long, R.M. (2005). RNA localization in yeast: moving towards a mechanism. Biol. Cell *97*, 75-86.

Gonzalez-Reyes, A., Elliott, H., and St Johnston, D. (1995). Polarization of both major body axes in *Drosophila* by gurken-torpedo signalling. Nature *375*, 654-658.

Gonzalez-Reyes, A., and St Johnston, D. (1998). Patterning of the follicle cell epithelium along the anterior-posterior axis during *Drosophila* oogenesis. Development *125*, 2837-2846.

Gooding, C., Kemp, P., and Smith, C.W. (2003). A novel polypyrimidine tract-binding protein paralog expressed in smooth muscle cells. J. Biol. Chem. *278*, 15201-15207.

Goodrich, J.S., Clouse, K.N., and Schüpbach, T. (2004). Hrb27C, Sqd and Otu cooperatively regulate gurken RNA localization and mediate nurse cell chromosome dispersion in *Drosophila* oogenesis. Development *131*, 1949-1958.

Grieder, N.C., de Cuevas, M., and Spradling, A.C. (2000). The fusome organizes the microtubule network during oocyte differentiation in *Drosophila*. Development *127*, 4253-4264.

Groebe, D.R., and Uhlenbeck, O.C. (1988). Characterization of RNA hairpin loop stability. Nucleic Acids Res. *16*, 11725-11735.

Gross, S.P., Tuma, M.C., Deacon, S.W., Serpinskaya, A.S., Reilein, A.R., and Gelfand, V.I. (2002). Interactions and regulation of molecular motors in Xenopus melanophores. J. Cell Biol. *156*, 855-865.

Gross, S.P., Welte, M.A., Block, S.M., and Wieschaus, E.F. (2000). Dynein-mediated cargo transport in vivo. A switch controls travel distance. J. Cell Biol. *148*, 945-956.

Grosset, C., Chen, C.Y., Xu, N., Sonenberg, N., Jacquemin-Sablon, H., and Shyu, A.B. (2000). A mechanism for translationally coupled mRNA turnover: interaction between the poly(A) tail and a c-fos RNA coding determinant via a protein complex. Cell *103*, 29-40.

Gu, W., Deng, Y., Zenklusen, D., and Singer, R.H. (2004). A new yeast PUF family protein, Puf6p, represses ASH1 mRNA translation and is required for its localization. Genes Dev. *18*, 1452-1465.

Gu, W., Pan, F., Zhang, H., Bassell, G.J., and Singer, R.H. (2002). A predominantly nuclear protein affecting cytoplasmic localization of beta-actin mRNA in fibroblasts and neurons. J. Cell Biol. *156*, 41-51.

Guichard, A., Roark, M., Ronshaugen, M., and Bier, E. (2000). brother of rhomboid, a rhomboid-related gene expressed during early *Drosophila* oogenesis, promotes EGF-R/MAPK signaling. Dev. Biol. *226*, 255-266.

Guil, S., and Caceres, J.F. (2007). The multifunctional RNA-binding protein hnRNP A1 is required for processing of miR-18a. Nat. Struct. Mol. Biol. *14*, 591-596.

Guo, F., Gooding, A.R., and Cech, T.R. (2004). Structure of the Tetrahymena ribozyme: base triple sandwich and metal ion at the active site. Mol. Cell *16*, 351-362.

Hachet, O., and Ephrussi, A. (2004). Splicing of oskar RNA in the nucleus is coupled to its cytoplasmic localization. Nature *428*, 959-963.

Hall, D.H., and Hedgecock, E.M. (1991). Kinesin-related gene unc-104 is required for axonal transport of synaptic vesicles in C. elegans. Cell *65*, 837-847.

Hamilton, B.J., Genin, A., Cron, R.Q., and Rigby, W.F. (2003). Delineation of a novel pathway that regulates CD154 (CD40 ligand) expression. Mol. Cell. Biol. *23*, 510-525.

Hamilton, R.S., Hartswood, E., Vendra, G., Jones, C., Van De Bor, V., Finnegan, D., and Davis, I. (2009). A bioinformatics search pipeline, RNA2DSearch, identifies RNA localization elements in *Drosophila* retrotransposons. RNA *15*, 200-207.

Harris, C.E., Boden, R.A., and Astell, C.R. (1999). A novel heterogeneous nuclear ribonucleoprotein-like protein interacts with NS1 of the minute virus of mice. J. Virol. *73*, 72-80.

Hawkins, N.C., Van Buskirk, C., Grossniklaus, U., and Schüpbach, T. (1997). Post-transcriptional regulation of gurken by encore is required for axis determination in Drosophila. Development *124*, 4801-4810.

Herold, N., Will, C.L., Wolf, E., Kastner, B., Urlaub, H., and Luhrmann, R. (2009). Conservation of the protein composition and electron microscopy structure of *Drosophila melanogaster* and human spliceosomal complexes. Mol. Cell. Biol. *29*, 281-301.

Herpers, B., and Rabouille, C. (2004). mRNA localization and ER-based protein sorting mechanisms dictate the use of transitional endoplasmic reticulum-golgi units involved in gurken transport in *Drosophila* oocytes. Mol. Biol. Cell *15*, 5306-5317.

Hirata, J., Nakagoshi, H., Nabeshima, Y., and Matsuzaki, F. (1995). Asymmetric segregation of the homeodomain protein Prospero during *Drosophila* development. Nature *377*, 627-630.

Hirokawa, N., Noda, Y., and Okada, Y. (1998). Kinesin and dynein superfamily proteins in organelle transport and cell division. Curr. Opin. Cell Biol. *10*, 60-73.

Hirokawa, N., and Takemura, R. (2005). Molecular motors and mechanisms of directional transport in neurons. Nat. Rev. Neurosci. *6*, 201-214.

Hoek, K.S., Kidd, G.J., Carson, J.H., and Smith, R. (1998). hnRNP A2 selectively binds the cytoplasmic transport sequence of myelin basic protein mRNA. Biochemistry *37*, 7021-7029.

Holleran, E.A., Karki, S., and Holzbaur, E.L. (1998). The role of the dynactin complex in intracellular motility. Int. Rev. Cytol. *182*, 69-109.

Holleran, E.A., Tokito, M.K., Karki, S., and Holzbaur, E.L. (1996). Centractin (ARP1) associates with spectrin revealing a potential mechanism to link dynactin to intracellular organelles. J. Cell Biol. *135*, 1815-1829.

Hong, A., Lee-Kong, S., Iida, T., Sugimura, I., and Lilly, M.A. (2003). The p27 (cip/kip) ortholog dacapo maintains the *Drosophila* oocyte in prophase of meiosis I. Development *130*, 1235-1242.

Hoogenraad, C.C., Akhmanova, A., Howell, S.A., Dortland, B.R., De Zeeuw, C.I., Willemsen, R., Visser, P., Grosveld, F., and Galjart, N. (2001). Mammalian Golgi-associated Bicaudal-D2 functions in the dynein-dynactin pathway by interacting with these complexes. EMBO J. *20*, 4041-4054.

Hook, P., and Vallee, R.B. (2006). The dynein family at a glance. J. Cell Sci. *119*, 4369-4371.

Horne-Badovinac, S., and Bilder, D. (2005). Mass transit: epithelial morphogenesis in the *Drosophila* egg chamber. Dev. Dyn. *232*, 559-574.

Horne-Badovinac, S., and Bilder, D. (2008). Dynein regulates epithelial polarity and the apical localization of stardust A mRNA. PLoS Genet. *4*, e8.

Hsieh-Li, H.M., Chang, J.G., Jong, Y.J., Wu, M.H., Wang, N.M., Tsai, C.H., and Li, H. (2000). A mouse model for spinal muscular atrophy. Nat. Genet. *24*, 66-70.

Huang, F., Chotiner, J.K., and Steward, O. (2007). Actin polymerization and ERK phosphorylation are required for Arc/Arg3.1 mRNA targeting to activated synaptic sites on dendrites. J. Neurosci. *27*, 9054-9067.

Huang, Y.S., Jung, M.Y., Sarkissian, M., and Richter, J.D. (2002). N-methyl-D-aspartate receptor signaling results in Aurora kinase-catalyzed CPEB phosphorylation and alpha CaMKII mRNA polyadenylation at synapses. EMBO J. *21*, 2139-2148.

Huber, K.M., Gallagher, S.M., Warren, S.T., and Bear, M.F. (2002). Altered synaptic plasticity in a mouse model of fragile X mental retardation. Proc. Natl. Acad. Sci. USA *99*, 7746-7750.

Huertas, D., Cortes, A., Casanova, J., and Azorin, F. (2004). *Drosophila* DDP1, a multi-KH-domain protein, contributes to centromeric silencing and chromosome segregation. Curr. Biol. *14*, 1611-1620.

Hughes, J.R., Bullock, S.L., and Ish-Horowicz, D. (2004). Inscuteable mRNA localization is dynein-dependent and regulates apicobasal polarity and spindle length in *Drosophila* neuroblasts. Curr. Biol. *14*, 1950-1956.

Huttelmaier, S., Zenklusen, D., Lederer, M., Dictenberg, J., Lorenz, M., Meng, X., Bassell, G.J., Condeelis, J., and Singer, R.H. (2005). Spatial regulation of beta-actin translation by Src-dependent phosphorylation of ZBP1. Nature *438*, 512-515.

Huynh, J.R., Munro, T.P., Smith-Litiere, K., Lepesant, J.A., and St Johnston, D. (2004). The *Drosophila* hnRNPA/B homolog, Hrp48, is specifically required for a distinct step in osk mRNA localization. Dev. Cell *6*, 625-635.

Huynh, J.R., Petronczki, M., Knoblich, J.A., and St Johnston, D. (2001). Bazooka and PAR-6 are required with PAR-1 for the maintenance of oocyte fate in Drosophila. Curr. Biol. *11*, 901-906.

Huynh, J.R., and St Johnston, D. (2000). The role of BicD, Egl, Orb and the microtubules in the restriction of meiosis to the *Drosophila* oocyte. Development *127*, 2785-2794.

Huynh, J.R., and St Johnston, D. (2004). The origin of asymmetry: early polarisation of the *Drosophila* germline cyst and oocyte. Curr. Biol. *14*, R438-449.

Ichetovkin, I.E., Abramochkin, G., and Shrader, T.E. (1997). Substrate recognition by the leucyl/phenylalanyl-tRNA-protein transferase. Conservation within the enzyme family and localization to the trypsin-resistant domain. J. Biol. Chem. *272*, 33009-33014.

Irie, K., Tadauchi, T., Takizawa, P.A., Vale, R.D., Matsumoto, K., and Herskowitz, I. (2002). The Khd1 protein, which has three KH RNA-binding motifs, is required for proper localization of ASH1 mRNA in yeast. EMBO J. *21*, 1158-1167.

Irion, U., and St Johnston, D. (2007). bicoid RNA localization requires specific binding of an endosomal sorting complex. Nature *445*, 554-558.

Ishizuka, A., Siomi, M.C., and Siomi, H. (2002). A *Drosophila* fragile X protein interacts with components of RNAi and ribosomal proteins. Genes Dev. *16*, 2497-2508.

Iwasaki, S., Kawamata, T., and Tomari, Y. (2009). *Drosophila* Argonaute1 and Argonaute2 Employ Distinct Mechanisms for Translational Repression. Mol. Cell. *34*, 58-67.

Jablonka, S., Schrank, B., Kralewski, M., Rossoll, W., and Sendtner, M. (2000). Reduced survival motor neuron (Smn) gene dose in mice leads to motor neuron degeneration: an animal model for spinal muscular atrophy type III. Hum. Mol. Genet. *9*, 341-346.

Jain, R.A., and Gavis, E.R. (2008). The *Drosophila* hnRNP M homolog Rumpelstiltskin regulates nanos mRNA localization. Development *135*, 973-982.

Jan, Y.N., and Jan, L.Y. (1998). Asymmetric cell division. Nature *392*, 775-778.

Jankovics, F., Sinka, R., Lukacsovich, T., and Erdelyi, M. (2002). MOESIN crosslinks actin and cell membrane in *Drosophila* oocytes and is required for OSKAR anchoring. Curr. Biol. *12*, 2060-2065.

Januschke, J., Gervais, L., Dass, S., Kaltschmidt, J.A., Lopez-Schier, H., St Johnston, D., Brand, A.H., Roth, S., and Guichet, A. (2002). Polar transport in the *Drosophila* oocyte requires Dynein and Kinesin I cooperation. Curr. Biol. *12*, 1971-1981.

Jaramillo, A.M., Weil, T.T., Goodhouse, J., Gavis, E.R., and Schüpbach, T. (2008). The dynamics of fluorescently labeled endogenous gurken mRNA in Drosophila. J. Cell Sci. *121*, 887-894.

Jeffery, W.R., Tomlinson, C.R., and Brodeur, R.D. (1983). Localization of actin messenger RNA during early ascidian development. Dev. Biol. *99*, 408-417.

Jenny, A., Hachet, O., Zavorszky, P., Cyrklaff, A., Weston, M.D., Johnston, D.S., Erdelyi, M., and Ephrussi, A. (2006). A translation-independent role of *oskar* RNA in early *Drosophila* oogenesis. Development *133*, 2827-2833.

Jensen, K.B., and Darnell, R.B. (2008). CLIP: crosslinking and immunoprecipitation of in vivo RNA targets of RNA-binding proteins. Methods Mol. Biol. *488*, 85-98.

Jimbo, T., Kawasaki, Y., Koyama, R., Sato, R., Takada, S., Haraguchi, K., and Akiyama, T. (2002). Identification of a link between the tumour suppressor APC and the kinesin superfamily. Nat. Cell Biol. *4*, 323-327.

Jin, P., Zarnescu, D.C., Ceman, S., Nakamoto, M., Mowrey, J., Jongens, T.A., Nelson, D.L., Moses, K., and Warren, S.T. (2004). Biochemical and genetic interaction between the fragile X mental retardation protein and the microRNA pathway. Nat. Neurosci. *7*, 113-117.

Johnstone, O., and Lasko, P. (2001). Translational regulation and RNA localization in *Drosophila* oocytes and embryos. Annu. Rev. of Genet. *35*, 365-406.

Johnstone, O., and Lasko, P. (2004). Interaction with eIF5B is essential for Vasa function during development. Development *131*, 4167-4178.

Jongens, T.A., Hay, B., Jan, L.Y., and Jan, Y.N. (1992). The germ cell-less gene product: a posteriorly localized component necessary for germ cell development in Drosophila. Cell *70*, 569-584.

Jovine, L., Oubridge, C., Avis, J.M., and Nagai, K. (1996). Two structurally different RNA molecules are bound by the spliceosomal protein U1A using the same recognition strategy. Structure *4*, 621-631.

Kalifa, Y., Armenti, S.T., and Gavis, E.R. (2009). Glorund interactions in the regulation of gurken and oskar mRNAs. Dev. Biol. *326*, 68-74.

Kalifa, Y., Huang, T., Rosen, L.N., Chatterjee, S., and Gavis, E.R. (2006). Glorund, a *Drosophila* hnRNP F/H homolog, is an ovarian repressor of nanos translation. Dev. Cell *10*, 291-301.

Kanai, Y., Dohmae, N., and Hirokawa, N. (2004). Kinesin transports RNA: isolation and characterization of an RNA-transporting granule. Neuron *43*, 513-525.

Karki, S., and Holzbaur, E.L. (1995). Affinity chromatography demonstrates a direct binding between cytoplasmic dynein and the dynactin complex. J. Biol. Chem. *270*, 28806-28811.

Kawamura, Y., Saito, K., Kin, T., Ono, Y., Asai, K., Sunohara, T., Okada, T.N., Siomi, M.C., and Siomi, H. (2008). *Drosophila* endogenous small RNAs bind to Argonaute 2 in somatic cells. Nature *453*, 793-797.

Kelley, R.L. (1993). Initial organization of the *Drosophila* dorsoventral axis depends on an RNA-binding protein encoded by the squid gene. Genes Dev. *7*, 948-960.

Keyes, L.N., and Spradling, A.C. (1997). The *Drosophila* gene *fs(2)cup* interacts with *otu* to define a cytoplasmic pathway required for the structure and function of germline chromosomes. Development *124*, 1419-1431.

Kiebler, M.A., and Bassell, G.J. (2006). Neuronal RNA granules: movers and makers. Neuron *51*, 685-690.

Kim YK, Hahm B, Jang SK. (2000). Polypyrimidine tract-binding protein inhibits translation of bip mRNA. J. Mol. Biol. *304*, 119-33.

Kim, I., Lukavsky, P.J., and Puglisi, J.D. (2002). NMR study of 100 kDa HCV IRES RNA using segmental isotope labeling. J. Am. Chem. Soc. *124*, 9338-9339.

Kim, J.H., Paek, K.Y., Ha, S.H., Cho, S., Choi, K., Kim, C.S., Ryu, S.H., and Jang, S.K. (2004). A cellular RNA-binding protein enhances internal ribosomal entry site-dependent translation through an interaction downstream of the hepatitis C virus polyprotein initiation codon. Mol. Cell. Biol. *24*, 7878-7890.

Kim, Y.K., Furic, L., Desgroseillers, L., and Maquat, L.E. (2005). Mammalian Staufen1 recruits Upf1 to specific mRNA 3'UTRs so as to elicit mRNA decay. Cell *120*, 195-208.

Kim-Ha, J., Smith, J.L., and Macdonald, P.M. (1991). oskar mRNA is localized to the posterior pole of the *Drosophila* oocyte. Cell *66*, 23-35.

King, R.C. (1970). Ovarian Development in *Drosophila melanogaster*. Academic Press, New York.

King, S.J., and Schroer, T.A. (2000). Dynactin increases the processivity of the cytoplasmic dynein motor. Nature Cell biology *2*, 20-24.

King, S.M. (2000). The dynein microtubule motor. Biochimica et biophysica acta *1496*, 60-75.

Kislauskis, E.H., Zhu, X., and Singer, R.H. (1997). β-actin messenger RNA localization and protein synthesis augment cell motility. J. Cell Biol. *136*, 1263-1270.

Klann, E., and Dever, T.E. (2004). Biochemical mechanisms for translational regulation in synaptic plasticity. Nat. Rev. Neurosci. *5*, 931-942.

Klattenhoff, C., Bratu, D.P., McGinnis-Schultz, N., Koppetsch, B.S., Cook, H.A., and Theurkauf, W.E. (2007). *Drosophila* rasiRNA pathway mutations disrupt embryonic axis specification through activation of an ATR/Chk2 DNA damage response. Dev. Cell *12*, 45-55.

Kloc, M., Spohr, G., and Etkin, L.D. (1993). Translocation of repetitive RNA sequences with the germ plasm in Xenopus oocytes. Science *262*, 1712-1714.

Kloc, M., Wilk, K., Vargas, D., Shirato, Y., Bilinski, S., and Etkin, L.D. (2005). Potential structural role of non-coding and coding RNAs in the organization of the cytoskeleton at the vegetal cortex of Xenopus oocytes. Development *132*, 3445-3457.

Kloc, M., Zearfoss, N.R., and Etkin, L.D. (2002). Mechanisms of subcellular mRNA localization. Cell *108*, 533-544.

Knoblich, J.A., Jan, L.Y., and Jan, Y.N. (1995). Asymmetric segregation of Numb and Prospero during cell division. Nature *377*, 624-627.

Knoblich, J.A., Jan, L.Y., and Jan, Y.N. (1999). Deletion analysis of the *Drosophila* Inscuteable protein reveals domains for cortical localization and asymmetric localization. Curr. Biol. *9*, 155-158.

Knowles, R.B., Sabry, J.H., Martone, M.E., Deerinck, T.J., Ellisman, M.H., Bassell, G.J., and Kosik, K.S. (1996). Translocation of RNA granules in living neurons. J. Neurosci. *16*, 7812-7820.

Kolev, N.G., and Huber, P.W. (2003). VgRBP71 stimulates cleavage at a polyadenylation signal in Vg1 mRNA, resulting in the removal of a cis-acting element that represses translation. Mol. Cell *11*, 745-755.

Kon, T., Nishiura, M., Ohkura, R., Toyoshima, Y.Y., and Sutoh, K. (2004). Distinct functions of nucleotide-binding/hydrolysis sites in the four AAA modules of cytoplasmic dynein. Biochemistry *43*, 11266-11274.

Kondrashov, A.V., Kiefmann, M., Ebnet, K., Khanam, T., Muddashetty, R.S., and Brosius, J. (2005). Inhibitory effect of naked neural BC1 RNA or BC200 RNA on eukaryotic in vitro translation systems is reversed by poly(A)-binding protein (PABP). J. Mol. Biol. *353*, 88-103.

Koplin, J., Mu, Y., Richter, C., Schwalbe, H., and Stock, G. (2005). Structure and dynamics of an RNA tetraloop: a joint molecular dynamics and NMR study. Structure *13*, 1255-1267.

Korostelev, A., Trakhanov, S., Laurberg, M., and Noller, H.F. (2006). Crystal structure of a 70S ribosome-tRNA complex reveals functional interactions and rearrangements. Cell *126*, 1065-1077.

Krecic, A.M., and Swanson, M.S. (1999). hnRNP complexes: composition, structure, and function. Curr. Opin. Cell Biol. *11*, 363-371.

Kremerskothen, J., Nettermann, M., op de Bekke, A., Bachmann, M., and Brosius, J. (1998). Identification of human autoantigen La/SS-B as BC1/BC200 RNA-binding protein. DNA Cell Biol. *17*, 751-759.

Kress, T.L., Yoon, Y.J., and Mowry, K.L. (2004). Nuclear RNP complex assembly initiates cytoplasmic RNA localization. J. Cell Biol. *165*, 203-211.

Krichevsky, A.M., and Kosik, K.S. (2001). Neuronal RNA granules: a link between RNA localization and stimulation-dependent translation. Neuron *32*, 683-696.

Kroll, T.T., Zhao, W.M., Jiang, C., and Huber, P.W. (2002). A homolog of FBP2/KSRP binds to localized mRNAs in Xenopus oocytes. Development *129*, 5609-5619.

Kural, C., Kim, H., Syed, S., Goshima, G., Gelfand, V.I., and Selvin, P.R. (2005). Kinesin and dynein move a peroxisome in vivo: a tug-of-war or coordinated movement? Science *308*, 1469-1472.

Kusch, T., Florens, L., Hayes MacDonald, W., Swanson, S.K., Glaser, R.L., Yates, J.R., Abmayr, S.M., Washburn, M.P., and Workman, J.L. (2004). Acetylation by Tip60 is required for selective histone variant exchange at DNA lesions. Science *306*, 2084-2087.

Kwon, S., Abramson, T., Munro, T.P., John, C.M., Kohrmann, M., and Schnapp, B.J. (2002). UUCAC- and vera-dependent localization of VegT RNA in Xenopus oocytes. Curr. Biol. *12*, 558-564.

Lall, S., Francis-Lang, H., Flament, A., Norvell, A., Schüpbach, T., and Ish-Horowicz, D. (1999). Squid hnRNP protein promotes apical cytoplasmic transport and localization of *Drosophila* pair-rule transcripts. Cell *98*, 171-180.

Lantz, V., Chang, J., Horabin, J., Bopp, D., and Schedl, P. (1994). The *Drosophila* orb RNA-binding protein is required for the formation of the egg chamber and the establishment of polarity. Genes Dev. *8*, 598-613.

Lasko, P. (1999). RNA sorting in *Drosophila* oocytes and embryos. FASEB J. *13*, 421-433.

Lasko, P. (2000). The *Drosophila melanogaster* genome: translation factors and RNA binding proteins. J. Cell Biol. *150*, F51-56.

Lau, P.P., Chang, B.H., and Chan, L. (2001). Two-hybrid cloning identifies an RNA-binding protein, GRY-RBP, as a component of apobec-1 editosome. Biochem. Biophys. Res. Commun. *282*, 977-983.

Lecuyer, E., Yoshida, H., Parthasarathy, N., Alm, C., Babak, T., Cerovina, T., Hughes, T.R., Tomancak, P., and Krause, H.M. (2007). Global analysis of mRNA localization reveals a prominent role in organizing cellular architecture and function. Cell *131*, 174-187.

Lefebvre, S., Burglen, L., Reboullet, S., Clermont, O., Burlet, P., Viollet, L., Benichou, B., Cruaud, C., Millasseau, P., Zeviani, M., and et al. (1995). Identification and characterization of a spinal muscular atrophy-determining gene. Cell *80*, 155-165.

Lehmann, M., Milev, M., Abrahamyan, L., Yao, X.J., Pante, N., and Mouland, A.J. (2009). Intracellular transport of human immunodeficiency virus type 1 genomic RNA and viral production are dependent on dynein motor function and late endosome positioning. J. Biol. Chem. Epub.

Lemm, I., and Ross, J. (2002). Regulation of c-myc mRNA decay by translational pausing in a coding region instability determinant. Mol. Cell. Biol.*22*, 3959-3969.

Leung, K.M., van Horck, F.P., Lin, A.C., Allison, R., Standart, N., and Holt, C.E. (2006). Asymmetrical beta-actin mRNA translation in growth cones mediates attractive turning to netrin-1. Nat. Neurosci. *9*, 1247-1256.

Lewis, R.A., Gagnon, J.A., and Mowry, K.L. (2008). PTB/hnRNP I is required for RNP remodeling during RNA localization in Xenopus oocytes. Mol. Cell. Biol.*28*, 678-686.

Lewis, R.A., Kress, T.L., Cote, C.A., Gautreau, D., Rokop, M.E., and Mowry, K.L. (2004). Conserved and clustered RNA recognition sequences are a critical feature of signals directing RNA localization in Xenopus oocytes. Mech. Dev. *121*, 101-109.

Li, B., and Yen, T.S. (2002). Characterization of the nuclear export signal of polypyrimidine tract-binding protein. J. Biol. Chem. *277*, 10306-10314.

Li, M., McGrail, M., Serr, M., and Hays, T.S. (1994). *Drosophila* cytoplasmic dynein, a microtubule motor that is asymmetrically localized in the oocyte. J. Cell Biol. *126*, 1475-1494.

Li, P., Yang, X., Wasser, M., Cai, Y., and Chia, W. (1997). Inscuteable and Staufen mediate asymmetric localization and segregation of prospero RNA during *Drosophila* neuroblast cell divisions. Cell *90*, 437-447.

Li, Z., Wang, L., Hays, T.S., and Cai, Y. (2008). Dynein-mediated apical localization of crumbs transcripts is required for Crumbs activity in epithelial polarity. J. Cell Biol. *180*, 31-38.

Lin, D., Pestova, T.V., Hellen, C.U., and Tiedge, H. (2008). Translational control by a small RNA: dendritic BC1 RNA targets the eukaryotic initiation factor 4A helicase mechanism. Mol. Cell. Biol. *28*, 3008-3019.

Lin, M.D., Fan, S.J., Hsu, W.S., and Chou, T.B. (2006). *Drosophila* decapping protein 1, dDcp1, is a component of the oskar mRNP complex and directs its posterior localization in the oocyte. Dev. Cell *10*, 601-613.

Lin, M.D., Jiao, X., Grima, D., Newbury, S.F., Kiledjian, M., and Chou, T.B. (2008). *Drosophila* processing bodies in oogenesis. Dev. Biol. *322*, 276-288.

Lin, H., Yue, L., and Spradling, A.C. (1994). The *Drosophila* fusome, a germline-specific organelle, contains membrane skeletal proteins and functions in cyst formation. Development *120*, 947-956.

Ling, S.C., Fahrner, P.S., Greenough, W.T., and Gelfand, V.I. (2004). Transport of *Drosophila* fragile X mental retardation protein-containing ribonucleoprotein granules by kinesin-1 and cytoplasmic dynein. Proc. Natl. Acad. Sci. USA *101*, 17428-17433.

Liu, G., Edmonds, B.T., and Condeelis, J. (1996). pH, EF-1alpha and the cytoskeleton. Trends Cell Biol. *6*, 168-171.

Liu, G., Grant, W.M., Persky, D., Latham, V.M., Jr., Singer, R.H., and Condeelis, J. (2002). Interactions of elongation factor 1alpha with F-actin and beta-actin mRNA: implications for anchoring mRNA in cell protrusions. Mol. Biol. Cell *13*, 579-592.

Liu, H., Zhang, W., Reed, R.B., Liu, W., and Grabowski, P.J. (2002). Mutations in RRM4 uncouple the splicing repression and RNA-binding activities of polypyrimidine tract binding protein. RNA *8*, 137-149.

Liu, H.M., Aizaki, H., Choi, K.S., Machida, K., Ou, J.J., and Lai, M.M. (2009). SYNCRIP (synaptotagmin-binding, cytoplasmic RNA-interacting protein) is a host factor involved in hepatitis C virus RNA replication. Virology *386*, 249-256.

Liu, J., Valencia-Sanchez, M.A., Hannon, G.J., and Parker, R. (2005). MicroRNA-dependent localization of targeted mRNAs to mammalian P-bodies. Nat. Cell Biol. *7*, 719-723.

Long, R.M., Gu, W., Lorimer, E., Singer, R.H., and Chartrand, P. (2000). She2p is a novel RNA-binding protein that recruits the Myo4p-She3p complex to ASH1 mRNA. EMBO J. *19*, 6592-6601.

Lorson, C.L., and Androphy, E.J. (2000). An exonic enhancer is required for inclusion of an essential exon in the SMA-determining gene SMN. Hum. Mol. Genet. *9*, 259-265.

Lou, H., Helfman, D.M., Gagel, R.F., and Berget, S.M. (1999). Polypyrimidine tract-binding protein positively regulates inclusion of an alternative 3'-terminal exon. Mol. Cell. Biol. *19*, 78-85.

Lukavsky, P.J., Kim, I., Otto, G.A., and Puglisi, J.D. (2003). Structure of HCV IRES domain II determined by NMR. Nat. Struct. Biol. *10*, 1033-1038.

Lukavsky, P.J., and Puglisi, J.D. (2004). Large-scale preparation and purification of polyacrylamide-free RNA oligonucleotides. RNA *10*, 889-893.

Lukavsky, P.J., and Puglisi, J.D. (2005). Structure determination of large biological RNAs. Methods Enzymol. *394*, 399-416.

Ma, S., Liu, G., Sun, Y., and Xie, J. (2007). Relocalization of the polypyrimidine tract-binding protein during PKA-induced neurite growth. Biochimica et biophysica acta *1773*, 912-923.

Macchi, P., Kroening, S., Palacios, I.M., Baldassa, S., Grunewald, B., Ambrosino, C., Goetze, B., Lupas, A., St Johnston, D., and Kiebler, M. (2003). Barentsz, a new component of the Staufen-containing ribonucleoprotein particles in mammalian cells, interacts with Staufen in an RNA-dependent manner. J. Neurosci. *23*, 5778-5788.

Macdonald, P.M., and Kerr, K. (1997). Redundant RNA recognition events in bicoid mRNA localization. RNA *3*, 1413-1420.

Macdonald, P.M., and Kerr, K. (1998). Mutational analysis of an RNA recognition element that mediates localization of bicoid mRNA. Mol. Cell. Biol. *18*, 3788-3795.

Macdonald, P.M., Kerr, K., Smith, J.L., and Leask, A. (1993). RNA regulatory element BLE1 directs the early steps of bicoid mRNA localization. Development *118*, 1233-1243.

Macdonald, P.M., Leask, A., and Kerr, K. (1995). exl protein specifically binds BLE1, a bicoid mRNA localization element, and is required for one phase of its activity. Proc. Natl. Acad. Sci. USA *92*, 10787-10791.

MacDougall, N., Clark, A., MacDougall, E., and Davis, I. (2003). *Drosophila* gurken (TGFalpha) mRNA localizes as particles that move within the oocyte in two dynein-dependent steps. Dev. Cell *4*, 307-319.

MacDougall, N., Lad, Y., Wilkie, G.S., Francis-Lang, H., Sullivan, W., and Davis, I. (2001). Merlin, the *Drosophila* homologue of neurofibromatosis-2, is specifically required in posterior follicle cells for axis formation in the oocyte. Development *128*, 665-673.

Mach, J.M., and Lehmann, R. (1997). An Egalitarian-BicaudalD complex is essential for oocyte specification and axis determination in Drosophila. Genes Dev. *11*, 423-435.

Mallik, R., Petrov, D., Lex, S.A., King, S.J., and Gross, S.P. (2005). Building complexity: an in vitro study of cytoplasmic dynein with in vivo implications. Curr. Biol. *15*, 2075-2085.

Mancebo, R., Zhou, X., Shillinglaw, W., Henzel, W., and Macdonald, P.M. (2001). BSF binds specifically to the bicoid mRNA 3' untranslated region and contributes to stabilization of bicoid mRNA. Mol. Cell. Biol. *21*, 3462-3471.

Maney, T., Ginkel, L.M., Hunter, A.W., and Wordeman, L. (2000). The kinetochore of higher eucaryotes: a molecular view. Int. Rev. Cytol. *194*, 67-131.

Manseau, L.J., and Schüpbach, T. (1989). cappuccino and spire: two unique maternal-effect loci required for both the anteroposterior and dorsoventral patterns of the *Drosophila* embryo. Genes Dev. *3*, 1437-1452.

Markovtsov, V., Nikolic, J.M., Goldman, J.A., Turck, C.W., Chou, M.Y., and Black, D.L. (2000). Cooperative assembly of an hnRNP complex induced by a tissue-specific homolog of polypyrimidine tract binding protein. Mol. Cell. Biol. *20*, 7463-7479.

Martin, K.C., and Ephrussi, A. (2009). mRNA localization: gene expression in the spatial dimension. Cell *136*, 719-730.

Martin, K.C., and Zukin, R.S. (2006). RNA trafficking and local protein synthesis in dendrites: an overview. J. Neurosci. *26*, 7131-7134.

Martin, M., Iyadurai, S.J., Gassman, A., Gindhart, J.G., Jr., Hays, T.S., and Saxton, W.M. (1999). Cytoplasmic dynein, the dynactin complex, and kinesin are interdependent and essential for fast axonal transport. Mol. Biol. Cell *10*, 3717-3728.

Martin, S.G., Leclerc, V., Smith-Litiere, K., and St Johnston, D. (2003). The identification of novel genes required for *Drosophila* anteroposterior axis formation in a germline clone screen using GFP-Staufen. Development *130*, 4201-4215.

Mathews, D.H., and Turner, D.H. (2006). Prediction of RNA secondary structure by free energy minimization. Curr. Opin. Struct. Biol. *16*, 270-278.

Matunis, E.L., Kelley, R., and Dreyfuss, G. (1994a). Essential role for a heterogeneous nuclear ribonucleoprotein (hnRNP) in oogenesis: hrp40 is absent from the germ line in the dorsoventral mutant squid. Proc. Natl. Acad. Sci. USA *91*, 2781-2784.

Matunis, E.L., Matunis, M.J., and Dreyfuss, G. (1992b). Characterization of the major hnRNP proteins from *Drosophila melanogaster*. J. Cell Biol. *116*, 257-269.

Matunis, M.J., Matunis, E.L., and Dreyfuss, G. (1992). Isolation of hnRNP complexes from *Drosophila melanogaster*. J. Cell Biol. *116*, 245-255.

McGrail, M., and Hays, T.S. (1997). The microtubule motor cytoplasmic dynein is required for spindle orientation during germline cell divisions and oocyte differentiation in *Drosophila*. Development *124*, 2409-2419.

Meignin, C., Alvarez-Garcia, I., Davis, I., and Palacios, I.M. (2007). The salvador-warts-hippo pathway is required for epithelial proliferation and axis specification in Drosophila. Curr. Biol. *17*, 1871-1878.

Meignin, C., and Davis, I. (2008). UAP56 RNA helicase is required for axis specification and cytoplasmic mRNA localization in Drosophila. Dev. Biol. *315*, 89-98.

Meister, G., Eggert, C., and Fischer, U. (2002). SMN-mediated assembly of RNPs: a complex story. Trends Cell Biol. *12*, 472-478.

Melton, D.A. (1987). Translocation of a localized maternal mRNA to the vegetal pole of Xenopus oocytes. Nature *328*, 80-82.

Messitt, T.J., Gagnon, J.A., Kreiling, J.A., Pratt, C.A., Yoon, Y.J., and Mowry, K.L. (2008). Multiple kinesin motors coordinate cytoplasmic RNA transport on a subpopulation of microtubules in Xenopus oocytes. Dev. Cell *15*, 426-436.

Meyer, W.J., Schreiber, S., Guo, Y., Volkmann, T., Welte, M.A., and Muller, H.A. (2006). Overlapping functions of argonaute proteins in patterning and morphogenesis of *Drosophila* embryos. PLoS Genet. *2*, e134.

Micklem, D.R., Adams, J., Grunert, S., and St Johnston, D. (2000). Distinct roles of two conserved Staufen domains in oskar mRNA localization and translation. EMBO J. *19*, 1366-1377.

Miki, H., Okada, Y., and Hirokawa, N. (2005). Analysis of the kinesin superfamily: insights into structure and function. Trends Cell Biol. *15*, 467-476.

Milligan, J.F., Groebe, D.R., Witherell, G.W., and Uhlenbeck, O.C. (1987). Oligoribonucleotide synthesis using T7 RNA polymerase and synthetic DNA templates. Nucleic Acids Res. *15*, 8783-8798.

Mitchell, S.A., Spriggs, K.A., Coldwell, M.J., Jackson, R.J., and Willis, A.E. (2003). The Apaf-1 internal ribosome entry segment attains the correct structural conformation for function via interactions with PTB and unr. Mol. Cell *11*, 757-771.

Mizutani, A., Fukuda, M., Ibata, K., Shiraishi, Y., and Mikoshiba, K. (2000). SYNCRIP, a cytoplasmic counterpart of heterogeneous nuclear ribonucleoprotein R, interacts with ubiquitous synaptotagmin isoforms. J. Biol. Chem. *275*, 9823-9831.

Mohr, E., Fuhrmann, C., and Richter, D. (2001a). VP-RBP, a protein enriched in brain tissue, specifically interacts with the dendritic localizer sequence of rat vasopressin mRNA. Eur. J. Neurosci. *13*, 1107-1112.

Mohr, E., Prakash, N., Vieluf, K., Fuhrmann, C., Buck, F., and Richter, D. (2001b). Vasopressin mRNA localization in nerve cells: characterization of cis-acting elements and trans-acting factors. Proc. Natl. Acad. Sci. USA *98*, 7072-7079.

Mohr, S.E., Dillon, S.T., and Boswell, R.E. (2001). The RNA-binding protein Tsunagi interacts with Mago Nashi to establish polarity and localize oskar mRNA during *Drosophila* oogenesis. Genes Dev. *15*, 2886-2899.

Monani, U.R., Sendtner, M., Coovert, D.D., Parsons, D.W., Andreassi, C., Le, T.T., Jablonka, S., Schrank, B., Rossoll, W., Prior, T.W., *et al.* (2000). The human centromeric survival motor neuron gene (SMN2) rescues embryonic lethality in Smn(-/-) mice and results in a mouse with spinal muscular atrophy. Hum. Mol. Genet. *9*, 333-339.

Monshausen, M., Gehring, N.H., and Kosik, K.S. (2004). The mammalian RNA-binding protein Staufen2 links nuclear and cytoplasmic RNA processing pathways in neurons. Neuromolecular Med. *6*, 127-144.

Montange, R.K., and Batey, R.T. (2006). Structure of the S-adenosylmethionine riboswitch regulatory mRNA element. Nature *441*, 1172-1175.

Moser, J.J., Eystathioy, T., Chan, E.K., and Fritzler, M.J. (2007). Markers of mRNA stabilization and degradation, and RNAi within astrocytoma GW bodies. J. Neurosci. Res. *85*, 3619-3631.

Mourelatos, Z., Abel, L., Yong, J., Kataoka, N., and Dreyfuss, G. (2001). SMN interacts with a novel family of hnRNP and spliceosomal proteins. EMBO J. *20*, 5443-5452.

Mowry, K.L. (1996). Complex formation between stage-specific oocyte factors and a Xenopus mRNA localization element. Proc. Natl. Acad. Sci. USA *93*, 14608-14613.

Muddashetty, R., Khanam, T., Kondrashov, A., Bundman, M., Iacoangeli, A., Kremerskothen, J., Duning, K., Barnekow, A., Huttenhofer, A., Tiedge, H., and Brosius, J. (2002). Poly(A)-binding protein is associated with neuronal BC1 and BC200 ribonucleoprotein particles. J. Mol. Biol. *321*, 433-445.

Muhlrad, D., and Parker, R. (1999). Recognition of yeast mRNAs as "nonsense containing" leads to both inhibition of mRNA translation and mRNA degradation: implications for the control of mRNA decapping. Mol. Biol. Cell *10*, 3971-3978.

Muller, M., Heuck, A., and Niessing, D. (2007). Directional mRNA transport in eukaryotes: lessons from yeast. Cell. Mol. Life Sci. *64*, 171-180.

Munro, T.P., Kwon, S., Schnapp, B.J., and St Johnston, D. (2006). A repeated IMP-binding motif controls oskar mRNA translation and anchoring independently of *Drosophila melanogaster* IMP. J. Cell Biol. *172*, 577-588.

Murray, J.W., Edmonds, B.T., Liu, G., and Condeelis, J. (1996). Bundling of actin filaments by elongation factor 1 alpha inhibits polymerization at filament ends. J. Cell Biol. *135*, 1309-1321.

Muslimov, I.A., Iacoangeli, A., Brosius, J., and Tiedge, H. (2006). Spatial codes in dendritic BC1 RNA. J. Cell Biol. *175*, 427-439.

Muslimov, I.A., Santi, E., Homel, P., Perini, S., Higgins, D., and Tiedge, H. (1997). RNA transport in dendrites: a cis-acting targeting element is contained within neuronal BC1 RNA. J. Neurosci. *17*, 4722-4733.

Nakamura, A., Amikura, R., Hanyu, K., and Kobayashi, S. (2001). Me31B silences translation of oocyte-localizing RNAs through the formation of cytoplasmic RNP complex during *Drosophila* oogenesis. Development *128*, 3233-3242.

Nakamura, A., Amikura, R., Mukai, M., Kobayashi, S., and Lasko, P.F. (1996). Requirement for a noncoding RNA in *Drosophila* polar granules for germ cell establishment. Science *274*, 2075-2079.

Nakamura, A., Sato, K., and Hanyu-Nakamura, K. (2004). *Drosophila* cup is an eIF4E binding protein that associates with Bruno and regulates oskar mRNA translation in oogenesis. Dev. Cell *6*, 69-78.

Navarro, C., Puthalakath, H., Adams, J.M., Strasser, A., and Lehmann, R. (2004). Egalitarian binds dynein light chain to establish oocyte polarity and maintain oocyte fate. Nature Cell Biology *6*, 427-435.

Nelson, M.R., Luo, H., Vari, H.K., Cox, B.J., Simmonds, A.J., Krause, H.M., Lipshitz, H.D., and Smibert, C.A. (2007). A multiprotein complex that mediates translational enhancement in *Drosophila*. J. Biol. Chem. *282*, 34031-34038.

Neubauer, G., King, A., Rappsilber, J., Calvio, C., Watson, M., Ajuh, P., Sleeman, J., Lamond, A., and Mann, M. (1998). Mass spectrometry and EST-database searching allows characterization of the multi-protein spliceosome complex. Nat. Genet. *20*, 46-50.

Neuman-Silberberg, F.S., and Schüpbach, T. (1993). The *Drosophila* dorsoventral patterning gene gurken produces a dorsally localized RNA and encodes a TGF alpha-like protein. Cell *75*, 165-174.

Neuman-Silberberg, F.S., and Schüpbach, T. (1996). The *Drosophila* TGF-alpha-like protein Gurken: expression and cellular localization during *Drosophila* oogenesis. Mech. Dev. *59*, 105-113.

Newmark, P.A., and Boswell, R.E. (1994). The mago nashi locus encodes an essential product required for germ plasm assembly in Drosophila. Development *120*, 1303-1313.

Nishiura, M., Kon, T., Shiroguchi, K., Ohkura, R., Shima, T., Toyoshima, Y.Y., and Sutoh, K. (2004). A single-headed recombinant fragment of Dictyostelium cytoplasmic dynein can drive the robust sliding of microtubules. J. Biol. Chem. *279*, 22799-22802.

Norga, K.K., Gurganus, M.C., Dilda, C.L., Yamamoto, A., Lyman, R.F., Patel, P.H., Rubin, G.M., Hoskins, R.A., Mackay, T.F., and Bellen, H.J. (2003). Quantitative analysis of bristle number in *Drosophila* mutants identifies genes involved in neural development. Curr. Biol. *13*, 1388-1396.

Norvell, A., Debec, A., Finch, D., Gibson, L., and Thoma, B. (2005). Squid is required for efficient posterior localization of oskar mRNA during *Drosophila* oogenesis. Dev. Genes Evol. *215*, 340-349.

Norvell, A., Kelley, R.L., Wehr, K., and Schüpbach, T. (1999). Specific isoforms of Squid, a *Drosophila* hnRNP, perform distinct roles in Gurken localization during oogenesis. Genes Dev. *13*, 864-876.

Nosyreva, E.D., and Huber, K.M. (2006). Metabotropic receptor-dependent long-term depression persists in the absence of protein synthesis in the mouse model of fragile X syndrome. J. Neurophysiol. *95*, 3291-3295.

Numata, N., Kon, T., Shima, T., Imamula, K., Mogami, T., Ohkura, R., Sutoh, K., and Sutoh, K. (2008). Molecular mechanism of force generation by dynein, a molecular motor belonging to the AAA+ family. Biochem. Soc. Trans. *36*, 131-135.

Obbard, D.J., and Finnegan, D.J. (2008). RNA interference: endogenous siRNAs derived from transposable elements. Curr. Biol. *18*, R561-563.

Oberstrass, F.C., Auweter, S.D., Erat, M., Hargous, Y., Henning, A., Wenter, P., Reymond, L., Amir-Ahmady, B., Pitsch, S., Black, D.L., and Allain, F.H. (2005). Structure of PTB bound to RNA: specific binding and implications for splicing regulation. Science *309*, 2054-2057.

Oh, Y.L., Hahm, B., Kim, Y.K., Lee, H.K., Lee, J.W., Song, O., Tsukiyama-Kohara, K., Kohara, M., Nomoto, A., and Jang, S.K. (1998). Determination of functional domains in polypyrimidine-tract-binding protein. Biochem. J. *331*, 169-175.

Okada, Y., Yamazaki, H., Sekine-Aizawa, Y., and Hirokawa, N. (1995). The neuron-specific kinesin superfamily protein KIF1A is a unique monomeric motor for anterograde axonal transport of synaptic vesicle precursors. Cell *81*, 769-780.

Okamura, K., Ishizuka, A., Siomi, H., and Siomi, M.C. (2004). Distinct roles for Argonaute proteins in small RNA-directed RNA cleavage pathways. Genes Dev. *18*, 1655-1666.

Olivier, C., Poirier, G., Gendron, P., Boisgontier, A., Major, F., and Chartrand, P. (2005). Identification of a conserved RNA motif essential for She2p recognition and mRNA localization to the yeast bud. Mol. Cell. Biol. *25*, 4752-4766.

Page, S.L., and Hawley, R.S. (2001). c(3)G encodes a *Drosophila* synaptonemal complex protein. Genes Dev. *15*, 3130-3143.

Pagliardini, S., Giavazzi, A., Setola, V., Lizier, C., Di Luca, M., DeBiasi, S., and Battaglia, G. (2000). Subcellular localization and axonal transport of the survival motor neuron (SMN) protein in the developing rat spinal cord. Hum. Mol. Genet. *9*, 47-56.

Palacios, I.M., Gatfield, D., St Johnston, D., and Izaurralde, E. (2004). An eIF4AIII-containing complex required for mRNA localization and nonsense-mediated mRNA decay. Nature *427*, 753-757.

Palacios, I.M., and St Johnston, D. (2001). Getting the message across: the intracellular localization of mRNAs in higher eukaryotes. Annu. Rev. Cell Dev. Biol. *17*, 569-614.

Palacios, I.M., and St Johnston, D. (2002). Kinesin light chain-independent function of the Kinesin heavy chain in cytoplasmic streaming and posterior localisation in the *Drosophila* oocyte. Development *129*, 5473-5485.

Pan, F., Huttelmaier, S., Singer, R.H., and Gu, W. (2007). ZBP2 facilitates binding of ZBP1 to beta-actin mRNA during transcription. Mol. Cell. Biol.*27*, 8340-8351.

Pane, A., Wehr, K., and Schüpbach, T. (2007). zucchini and squash encode two putative nucleases required for rasiRNA production in the *Drosophila* germline. Dev. Cell *12*, 851-862.

Paquin, N., and Chartrand, P. (2008). Local regulation of mRNA translation: new insights from the bud. Trends Cell Biol. *18*, 105-111.

Parisien, M., and Major, F. (2008). The MC-Fold and MC-Sym pipeline infers RNA structure from sequence data. Nature *452*, 51-55.

Parks, A.L., Cook, K.R., Belvin, M., Dompe, N.A., Fawcett, R., Huppert, K., Tan, L.R., Winter, C.G., Bogart, K.P., Deal, J.E., *et al.* (2004). Systematic generation of high-resolution deletion coverage of the *Drosophila melanogaster* genome. Nat. Genet. *36*, 288-292.

Parton, R., Davis, I. Lifting the fog: Image restoration by deconvolution. In: Celis J.E., editor. *Cell biology*. Academic Press; New York: 2006. pp. 187–200.

Patel, G.P., Ma, S., and Bag, J. (2005). The autoregulatory translational control element of poly(A)-binding protein mRNA forms a heteromeric ribonucleoprotein complex. Nucleic Acids Res. *33*, 7074-7089.

Paushkin, S., Gubitz, A.K., Massenet, S., and Dreyfuss, G. (2002). The SMN complex, an assemblyosome of ribonucleoproteins. Curr. Opin. Cell Biol. *14*, 305-312.

Pellizzoni, L., Charroux, B., and Dreyfuss, G. (1999). SMN mutants of spinal muscular atrophy patients are defective in binding to snRNP proteins. Proc. Natl. Acad. Sci. USA *96*, 11167-11172.

Pellizzoni, L., Kataoka, N., Charroux, B., and Dreyfuss, G. (1998). A novel function for SMN, the spinal muscular atrophy disease gene product, in pre-mRNA splicing. Cell *95*, 615-624.

Perez, I., McAfee, J.G., and Patton, J.G. (1997a). Multiple RRMs contribute to RNA binding specificity and affinity for polypyrimidine tract binding protein. Biochemistry *36*, 11881-11890.

Perez, I., Lin, C.H., McAfee, J.G., and Patton, J.G. (1997b). Mutation of PTB binding sites causes misregulation of alternative 3' splice site selection in vivo. RNA *3*, 764-778.

Petoukhov, M.V., Monie, T.P., Allain, F.H., Matthews, S., Curry, S., and Svergun, D.I. (2006). Conformation of polypyrimidine tract binding protein in solution. Structure *14*, 1021-1027.

Petrella, L.N., Smith-Leiker, T., and Cooley, L. (2007). The Ovhts polyprotein is cleaved to produce fusome and ring canal proteins required for *Drosophila* oogenesis. Development *134*, 703-712.

Pfister, K.K., Shah, P.R., Hummerich, H., Russ, A., Cotton, J., Annuar, A.A., King, S.M., and Fisher, E.M. (2006). Genetic analysis of the cytoplasmic dynein subunit families. PLoS Genet. *2*, e1.

Pickering, B.M., Mitchell, S.A., Spriggs, K.A., Stoneley, M. and Willis, A.E. (2004). BAG-1 internal ribosome entry segment activity is promoted by structural changes mediated by poly(rC) binding protein 1 and recruitment of polypyrimidine tract binding protein 1. Mol. Cell. Biol. *24*, 5595–5604.

Pilling, A.D., Horiuchi, D., Lively, C.M., and Saxton, W.M. (2006). Kinesin-1 and Dynein are the primary motors for fast transport of mitochondria in *Drosophila* motor axons. Mol. Biol. Cell *17*, 2057-2068.

Piper, M., and Holt, C. (2004). RNA translation in axons. Annu. Rev. Cell Dev. Biol. *20*, 505-523.

Pizette, S., Rabouille, C., Cohen, S.M., and Therond, P. (2009). Glycosphingolipids control the extracellular gradient of the *Drosophila* EGFR ligand Gurken. Development *136*, 551-561.

Polesello, C., and Tapon, N. (2007). Salvador-warts-hippo signaling promotes *Drosophila* posterior follicle cell maturation downstream of notch. Curr. Biol. *17*, 1864-1870.

Polydorides, A.D., Okano, H.J., Yang, Y.Y., Stefani, G., and Darnell, R.B. (2000). A brain-enriched polypyrimidine tract-binding protein antagonizes the ability of Nova to regulate neuron-specific alternative splicing. Proc. Natl. Acad. Sci. USA *97*, 6350-6355.

Porter, M.E. (1996). Axonemal dyneins: assembly, organization, and regulation. Curr. Opin. Cell Biol. *8*, 10-17.

Prasad, M., Jang, A.C., Starz-Gaiano, M., Melani, M., and Montell, D.J. (2007). A protocol for culturing *Drosophila melanogaster* stage 9 egg chambers for live imaging. Nat. Protoc. *2*, 2467-2473.

Prost, E., Deryckere, F., Roos, C., Haenlin, M., Pantesco, V., and Mohier, E. (1988). Role of the oocyte nucleus in determination of the dorsoventral polarity of *Drosophila* as revealed by molecular analysis of the K10 gene. Genes Dev. *2*, 891-900.

Puglisi, J.D., and Wyatt, J.R. (1995). Biochemical and NMR studies of RNA conformation with an emphasis on RNA pseudoknots. Methods Enzymol. *261*, 323-350.

Quaresma, A.J., Bressan, G.C., Gava, L.M., Lanza, D.C., Ramos, C.H., and Kobarg, J. (2009). Human HnRNP Q re-localizes to cytoplasmic granules upon PMA, thapsigargin, Arsenite and heat-shock treatments. Exp Cell Res.

Rabani, M., Kertesz, M., and Segal, E. (2008). Computational prediction of RNA structural motifs involved in posttranscriptional regulatory processes. Proc. Natl. Acad. Sci. USA *105*, 14885-14890.

Raff, J.W., Whitfield, W.G., and Glover, D.M. (1990). Two distinct mechanisms localise cyclin B transcripts in syncytial *Drosophila* embryos. Development *110*, 1249-1261.

Ran, B., Bopp, R., and Suter, B. (1994). Null alleles reveal novel requirements for *Bic-D* during *Drosophila* oogenesis. Development *120*, 1233-1242.

Ray, K., Perez, S.E., Yang, Z., Xu, J., Ritchings, B.W., Steller, H., and Goldstein, L.S. (1999). Kinesin-II is required for axonal transport of choline acetyltransferase in Drosophila. J. Cell Biol. *147*, 507-518.

Reck-Peterson, S.L., Provance, D.W., Jr., Mooseker, M.S., and Mercer, J.A. (2000). Class V myosins. Biochimica et biophysica acta *1496*, 36-51.

Reck-Peterson, S.L., Yildiz, A., Carter, A.P., Gennerich, A., Zhang, N., and Vale, R.D. (2006). Single-molecule analysis of dynein processivity and stepping behavior. Cell *126*, 335-348.

Rehbein, M., Kindler, S., Horke, S., and Richter, D. (2000). Two trans-acting rat-brain proteins, MARTA1 and MARTA2, interact specifically with the dendritic targeting element in MAP2 mRNAs. Brain Res. *79*, 192-201.

Reich, J., Snee, M.J., and Macdonald, P.M. (2009). miRNA-dependent translational repression in the *Drosophila* ovary. PLoS ONE *4*, e4669.

Richter, J.D., and Sonenberg, N. (2005). Regulation of cap-dependent translation by eIF4E inhibitory proteins. Nature *433*, 477-480.

Rietdorf, J., Ploubidou, A., Reckmann, I., Holmstrom, A., Frischknecht, F., Zettl, M., Zimmermann, T., and Way, M. (2001). Kinesin-dependent movement on microtubules precedes actin-based motility of Vaccinia virus. Nat. Cell Biol. *3*, 992-1000.

Rittenhouse, K.R., and Berg, C.A. (1995). Mutations in the *Drosophila* gene bullwinkle cause the formation of abnormal eggshell structures and bicaudal embryos. Development *121*, 3023-3033.

Roberts, A.J., Numata, N., Walker, M.L., Kato, Y.S., Malkova, B., Kon, T., Ohkura, R., Arisaka, F., Knight, P.J., Sutoh, K., and Burgess, S.A. (2009). AAA+ Ring and linker swing mechanism in the dynein motor. Cell *136*, 485-495.

Robida, M.D., and Singh, R. (2003). *Drosophila* polypyrimidine-tract binding protein (PTB) functions specifically in the male germline. EMBO J. *22*, 2924-2933.

Robinson, D.N., and Cooley, L. (1997). Genetic analysis of the actin cytoskeleton in the *Drosophila* ovary. Annu. Rev. Cell Dev. Biol. *13*, 147-170.

Rom, I., Faicevici, A., Almog, O., and Neuman-Silberberg, F.S. (2007). *Drosophila* Dynein light chain (DDLC1) binds to gurken mRNA and is required for its localization. Biochimica et biophysica acta *1773*, 1526-1533.

Romanelli, M.G., Weighardt, F., Biamonti, G., Riva, S., and Morandi, C. (1997). Sequence determinants for hnRNP I protein nuclear localization. Exp. Cell Res. *235*, 300-304.

Roper, K., and Brown, N.H.A. (2004). Spectraplakin is enriched on the fusome and organizes microtubules during oocyte specification in *Drosophila*. Curr. Biol. *14*, 99-110.

Ross, A.F., Oleynikov, Y., Kislauskis, E.H., Taneja, K.L., and Singer, R.H. (1997). Characterization of a β-actin mRNA zipcode-binding protein. Mol. Cell. Biol.*17*, 2158-2165.

Ross, J.L., Wallace, K., Shuman, H., Goldman, Y.E., and Holzbaur, E.L. (2006). Processive bidirectional motion of dynein-dynactin complexes in vitro. Nat. Cell Biol. *8*, 562-570.

Rossoll, W., Jablonka, S., Andreassi, C., Kroning, A.K., Karle, K., Monani, U.R., and Sendtner, M. (2003). Smn, the spinal muscular atrophy-determining gene product, modulates axon growth and localization of beta-actin mRNA in growth cones of motoneurons. J. Cell Biol. *163*, 801-812.

Rossoll, W., Kroning, A.K., Ohndorf, U.M., Steegborn, C., Jablonka, S., and Sendtner, M. (2002). Specific interaction of Smn, the spinal muscular atrophy determining gene product, with hnRNP-R and gry-rbp/hnRNP-Q: a role for Smn in RNA processing in motor axons? Hum. Mol. Genet. *11*, 93-105.

Roth, S., Neuman-Silberberg, F.S., Barcelo, G., and Schüpbach, T. (1995). cornichon and the EGF receptor signaling process are necessary for both anterior-posterior and dorsal-ventral pattern formation in Drosophila. Cell *81*, 967-978.

Rustighi, A., Tessari, M.A., Vascotto, F., Sgarra, R., Giancotti, V., and Manfioletti, G. (2002). A polypyrimidine/polypurine tract within the Hmga2 minimal promoter: a common feature of many growth-related genes. Biochemistry *41*, 1229-1240.

Saffery, R., Irvine, D.V., Griffiths, B., Kalitsis, P., Wordeman, L., and Choo, K.H. (2000). Human centromeres and neocentromeres show identical distribution patterns of >20 functionally important kinetochore-associated proteins. Hum. Mol. Genet. *9*, 175-185.

Saffman, E.E., Styhler, S., Rother, K., Li, W., Richard, S., and Lasko, P. (1998). Premature translation of oskar in oocytes lacking the RNA-binding protein Bicaudal-C. Mol. Cell. Biol.*18*, 4855-4862.

Sakato, M., and King, S.M. (2004). Design and regulation of the AAA+ microtubule motor dynein. J. Struct. Biol. *146*, 58-71.

Salles, F.J., Lieberfarb, M.E., Wreden, C., Gergen, J.P., and Strickland, S. (1994). Coordinate initiation of *Drosophila* development by regulated polyadenylation of maternal messenger RNAs. Science *266*, 1996-1999.

Sambrook, J., Fritsch, E. F., Maniatis, T. (1989). Molecular cloning: a laboratory manual. Cold Spring Harbour Laboratory Press, Cold Spring Harbour, NY.

Samso, M., Radermacher, M., Frank, J., and Koonce, M.P. (1998). Structural characterization of a dynein motor domain. J. Mol. Biol. *276*, 927-937.

Sanchez-Carbente Mdel, R., and Desgroseillers, L. (2008). Understanding the importance of mRNA transport in memory. Prog. Brain Res. *169*, 41-58.

Saunders, C., and Cohen, R.S. (1999). The role of oocyte transcription, the 5'UTR, and translation repression and derepression in *Drosophila* gurken mRNA and protein localization. Mol. Cell *3*, 43-54.

Schaeffer, L., de Kerchove d'Exaerde, A., and Changeux, J.P. (2001). Targeting transcription to the neuromuscular synapse. Neuron *31*, 15-22.

Schiavi, S.C., Wellington, C.L., Shyu, A.B., Chen, C.Y., Greenberg, M.E., and Belasco, J.G. (1994). Multiple elements in the c-fos protein-coding region facilitate mRNA deadenylation and decay by a mechanism coupled to translation. J. Biol. Chem. *269*, 3441-3448.

Schmid, M., Jaedicke, A., Du, T.G., and Jansen, R.P. (2006). Coordination of endoplasmic reticulum and mRNA localization to the yeast bud. Curr. Biol. *16*, 1538-1543.

Schratt, G.M., Nigh, E.A., Chen, W.G., Hu, L., and Greenberg, M.E. (2004). BDNF regulates the translation of a select group of mRNAs by a mammalian target of rapamycin-phosphatidylinositol 3-kinase-dependent pathway during neuronal development. J. Neurosci. *24*, 7366-7377.

Schratt, G.M., Tuebing, F., Nigh, E.A., Kane, C.G., Sabatini, M.E., Kiebler, M., and Greenberg, M.E. (2006). A brain-specific microRNA regulates dendritic spine development. Nature *439*, 283-289.

Schroer, T.A. (2004). Dynactin. Annu. Rev. Cell Dev. Biol. *20*, 759-779.

Schuldt, A.J., Adams, J.H., Davidson, C.M., Micklem, D.R., Haseloff, J., St Johnston, D., and Brand, A.H. (1998). Miranda mediates asymmetric protein and RNA localization in the developing nervous system. Genes Dev. *12*, 1847-1857.

Schulz, C., Kiger, A.A., Tazuke, S.I., Yamashita, Y.M., Pantalena-Filho, L.C., Jones, D.L., Wood, C.G., and Fuller, M.T. (2004). A misexpression screen reveals effects of bag-of-marbles and TGF beta class signaling on the *Drosophila* male germ-line stem cell lineage. Genetics *167*, 707-723.

Schüpbach, T. (1987). Germ line and soma cooperate during oogenesis to establish the dorsoventral pattern of egg shell and embryo in *Drosophila melanogaster*. Cell *49*, 699-707.

Schüpbach, T., and Wieschaus, E. (1989). Female sterile mutations on the second chromosome of *Drosophila melanogaster*. I. Maternal effect mutations. Genetics *121*, 101-117.

Schüpbach, T., and Wieschaus, E. (1991). Female sterile mutations on the second chromosome of *Drosophila melanogaster*. II. Mutations blocking oogenesis or altering egg morphology. Genetics *129*, 1119-1136.

Schurer, H., Lang, K., Schuster, J., and Morl, M. (2002). A universal method to produce in vitro transcripts with homogeneous 3' ends. Nucleic Acids Res. *30*, e56.

Searfoss, A., Dever, T.E., and Wickner, R. (2001). Linking the 3' poly(A) tail to the subunit joining step of translation initiation: relations of Pab1p, eukaryotic translation initiation factor 5b (Fun12p), and Ski2p-Slh1p. Mol. Cell. Biol.*21*, 4900-4908.

Seleme, M.C., Busseau, I., Malinsky, S., Bucheton, A., and Teninges, D. (1999). High-frequency retrotransposition of a marked I factor in *Drosophila melanogaster* correlates with a dynamic expression pattern of the ORF1 protein in the cytoplasm of oocytes. Genetics *151*, 761-771.

Seleme, M.C., Disson, O., Robin, S., Brun, C., Teninges, D., and Bucheton, A. (2005). In vivo RNA localization of I factor, a non-LTR retrotransposon, requires a cis-acting signal in ORF2 and ORF1 protein. Nucleic Acids Res. *33*, 776-785.

Selmer, M., Dunham, C.M., Murphy, F.V.t., Weixlbaumer, A., Petry, S., Kelley, A.C., Weir, J.R., and Ramakrishnan, V. (2006). Structure of the 70S ribosome complexed with mRNA and tRNA. Science *313*, 1935-1942.

Semotok, J.L., Cooperstock, R.L., Pinder, B.D., Vari, H.K., Lipshitz, H.D., and Smibert, C.A. (2005). Smaug recruits the CCR4/POP2/NOT deadenylase complex to trigger maternal transcript localization in the early *Drosophila* embryo. Curr. Biol. *15*, 284-294.

Semotok, J.L., Luo, H., Cooperstock, R.L., Karaiskakis, A., Vari, H.K., Smibert, C.A., and Lipshitz, H.D. (2008). *Drosophila* maternal Hsp83 mRNA destabilization is directed by multiple SMAUG recognition elements in the open reading frame. Mol. Cell. Biol. *28*, 6757-6772.

Sen, G.L., and Blau, H.M. (2005). Argonaute 2/RISC resides in sites of mammalian mRNA decay known as cytoplasmic bodies. Nat. Cell Biol. *7*, 633-636.

Serano, J., and Rubin, G.M. (2003). The *Drosophila* synaptotagmin-like protein bitesize is required for growth and has mRNA localization sequences within its open reading frame. Proc. Natl. Acad. Sci. *100*, 13368-13373.

Serano, T.L., Karlin-McGinness, M., and Cohen, R.S. (1995). The role of fs(1)K10 in the localization of the mRNA of the TGF alpha homolog gurken within the *Drosophila* oocyte. Mech. Dev. *51*, 183-192.

Shan, J., Munro, T.P., Barbarese, E., Carson, J.H., and Smith, R. (2003). A molecular mechanism for mRNA trafficking in neuronal dendrites. J. Neurosci. *23*, 8859-8866.

Shepard, K.A., Gerber, A.P., Jambhekar, A., Takizawa, P.A., Brown, P.O., Herschlag, D., DeRisi, J.L., and Vale, R.D. (2003). Widespread cytoplasmic mRNA transport in yeast: identification of 22 bud-localized transcripts using DNA microarray analysis. Proc. Natl. Acad. Sci. *100*, 11429-11434.

Sheth, U., and Parker, R. (2006). Targeting of aberrant mRNAs to cytoplasmic processing bodies. Cell *125*, 1095-1109.

Shields, T.P., Mollova, E., Ste Marie, L., Hansen, M.R., and Pardi, A. (1999). High-performance liquid chromatography purification of homogenous-length RNA produced by trans cleavage with a hammerhead ribozyme. RNA *5*, 1259-1267.

Short, B., Preisinger, C., Schaletzky, J., Kopajtich, R., and Barr, F.A. (2002). The Rab6 GTPase regulates recruitment of the dynactin complex to Golgi membranes. Curr. Biol. *12*, 1792-1795.

Shubeita, G.T., Tran, S.L., Xu, J., Vershinin, M., Cermelli, S., Cotton, S.L., Welte, M.A., and Gross, S.P. (2008). Consequences of motor copy number on the intracellular transport of kinesin-1-driven lipid droplets. Cell *135*, 1098-1107.

Silvanovich, A., Li, M.G., Serr, M., Mische, S., and Hays, T.S. (2003). The third P-loop domain in cytoplasmic dynein heavy chain is essential for dynein motor function and ATP-sensitive microtubule binding. Mol. Biol. Cell *14*, 1355-1365.

Simmonds, A.J., dos Santos, G., Livne-Bar, I., and Krause, H.M. (2001). Apical localization of wingless transcripts is required for wingless signaling. Cell *105*, 197-207.

Simon, A.M., Hoppe, P., and Burden, S.J. (1992). Spatial restriction of AChR gene expression to subsynaptic nuclei. Development *114*, 545-553.

Simpson, P.J., Monie, T.P., Szendroi, A., Davydova, N., Tyzack, J.K., Conte, M.R., Read, C.M., Cary, P.D., Svergun, D.I., Konarev, P.V., *et al.* (2004). Structure and RNA interactions of the N-terminal RRM domains of PTB. Structure *12*, 1631-1643.

Smibert, C.A., Wilson, J.E., Kerr, K., and Macdonald, P.M. (1996). Smaug protein represses translation of unlocalized nanos mRNA in the *Drosophila* embryo. Genes Dev. *10*, 2600-2609.

Snee, M.J., and Macdonald, P.M. (2009). Dynamic organization and plasticity of sponge bodies. Dev. Dyn. *238*, 918-930.

Snee, M.J., and Macdonald, P.M. (2009). Bicaudal C and trailer hitch have similar roles in gurken mRNA localization and cytoskeletal organization. Dev. Biol. *328*, 434-444.

Sossin, W.S., and DesGroseillers, L. (2006). Intracellular trafficking of RNA in neurons. Traffic *7*, 1581-1589.

Southby, J., Gooding, C., and Smith, C.W. (1999). Polypyrimidine tract binding protein functions as a repressor to regulate alternative splicing of alpha-actinin mutally exclusive exons. Mol. Cell. Biol.*19*, 2699-2711.

Spana, E.P., and Doe, C.Q. (1995). The prospero transcription factor is asymmetrically localized to the cell cortex during neuroblast mitosis in Drosophila. Development *121*, 3187-3195.

Sparanese, D., and Lee, C.H. (2007). CRD-BP shields c-myc and MDR-1 RNA from endonucleolytic attack by a mammalian endoribonuclease. Nucleic Acids Res. *35*, 1209-1221.

Spradling, A. C., 1993. Developmental genetics of oogenesis, pp. 1–70 *The Development of Drosophila melanogaster*, edited by M. Bate and A. Martinez Arias. Cold Spring Harbor Laboratory Press, Cold Spring Harbor, NY.

Spriggs, K.A., Stoneley, M., Bushell, M. and Willis, A.E. (2008). Re-programming of translation following cell stress allows IRES-mediated translation to predominate. Biol. Cell *100*, 27–38.

Spriggs, K.A., Bushell, M., Mitchell, S.A. and Willis, A.E. (2005). Internal ribosome entry segments-mediated translation during apoptosis; the role of IRES-*trans*-acting factors. Cell Death Differ. *12*, 585–591.

Song, Y.T., Tzima, E., Ochs, K., Bassili, G., Trusheim, H., Linder, M., Preissner, K.T. and Niepmann, M. (2005). Evidence for an RNA chaperone function of polypyrimidine tract-binding protein in picornavirus translation. RNA *11*, 1809–1824.

St Johnston, D. (2005). Moving messages: the intracellular localization of mRNAs. Nat. Rev. Mol. Cell Biol. *6*, 363-375.

St Johnston, D., Beuchle, D., and Nusslein-Volhard, C. (1991). Staufen, a gene required to localize maternal RNAs in the *Drosophila* egg. Cell *66*, 51-63.

St Johnston, D., and Nusslein-Volhard, C. (1992). The origin of pattern and polarity in the *Drosophila* embryo. Cell *68*, 201-219.

Stebbins-Boaz, B., Cao, Q., de Moor, C.H., Mendez, R., and Richter, J.D. (1999). Maskin is a CPEB-associated factor that transiently interacts with elF-4E. Mol. Cell *4*, 1017-1027.

Steward, O., and Schuman, E.M. (2001). Protein synthesis at synaptic sites on dendrites. Annu. Rev. Neurosci. *24*, 299-325.

Styhler, S., Nakamura, A., Swan, A., Suter, B., and Lasko, P. (1998). vasa is required for GURKEN accumulation in the oocyte, and is involved in oocyte differentiation and germline cyst development. Development *125*, 1569-1578.

Sundell, C.L., and Singer, R.H. (1990). Actin mRNA localizes in the absence of protein synthesis. J. Cell Biol. *111*, 2397-2403.

Surdej, P., and Jacobs-Lorena, M. (1998). Developmental regulation of bicoid mRNA stability is mediated by the first 43 nucleotides of the 3' untranslated region. Mol. Cell. Biol.*18*, 2892-2900.

Suter, B., Romberg, L.M., and Steward, R. (1989). *Bicaudal-D*, a *Drosophila* gene involved in developmental asymmetry: localized transcript accumulation in ovaries and sequence similarity to myosin heavy chain tail domains. Genes Dev. *3*, 1957-1968.

Swan, A., and Suter, B. (1999). Role of *Bicaudal-D* in patterning the *Drosophila* egg chamber in mid-oogenesis. Development *122*, 3577-3586.

Takahashi, Y., Edamatsu, M., and Toyoshima, Y.Y. (2004). Multiple ATP-hydrolyzing sites that potentially function in cytoplasmic dynein. Proc. Natl. Acad. Sci. USA *101*, 12865-12869.

Takizawa, P.A., and Vale, R.D. (2000). The myosin motor, Myo4p, binds Ash1 mRNA via the adapter protein, She3p. Proc. Natl. Acad. Sci. *97*, 5273-5278.

Tang, Y., and Nilsson, L. (1999). Molecular dynamics simulations of the complex between human U1A protein and hairpin II of U1 small nuclear RNA and of free RNA in solution. Biophys. J. *77*, 1284-1305.

Tautz, D., and Pfeifle, C. (1989). A non-radioactive in situ hybridization method for the localization of specific RNAs in *Drosophila* embryos reveals translational control of the segmentation gene hunchback. Chromosoma *98*, 81-85.

Tekotte, H., and Davis, I. (2002). Intracellular mRNA localization: motors move messages. Trends Genet. *18*, 636-642.

Teng, J., Rai, T., Tanaka, Y., Takei, Y., Nakata, T., Hirasawa, M., Kulkarni, A.B., and Hirokawa, N. (2005). The KIF3 motor transports N-cadherin and organizes the developing neuroepithelium. Nat. Cell Biol. *7*, 474-482.

Theurkauf, W., Alberts, M., Jan, Y., and Jongens, T.A. (1993). A central role for microtubules in the differentiation of *Drosophila* oocytes. Development *118*, 1169-1180.

Thio, G.L., Ray, R.P., Barcelo, G., and Schüpbach, T. (2000). Localization of gurken RNA in *Drosophila* oogenesis requires elements in the 5' and 3' regions of the transcript. Dev. Biol. *221*, 435-446.

Thomsen, G.H., and Melton, D.A. (1993). Processed Vg1 protein is an axial mesoderm inducer in Xenopus. Cell *74*, 433-441.

Tiedge, H., Fremeau, R.T., Jr., Weinstock, P.H., Arancio, O., and Brosius, J. (1991). Dendritic location of neural BC1 RNA. Proc. Natl. Acad. Sci. USA *88*, 2093-2097.

Tinker, R., Silver, D., and Montell, D.J. (1998). Requirement for the vasa RNA helicase in gurken mRNA localization. Dev. Biol. *199*, 1-10.

Tirronen, M., Lahti, V.P., Heino, T.I., and Roos, C. (1995). Two otu transcripts are selectively localised in *Drosophila* oogenesis by a mechanism that requires a function of the otu protein. Mech. Dev. *52*, 65-75.

Tomancak, P., Beaton, A., Weiszmann, R., Kwan, E., Shu, S., Lewis, S.E., Richards, S., Ashburner, M., Hartenstein, V., Celniker, S.E., and Rubin, G.M. (2002). Systematic determination of patterns of gene expression during *Drosophila* embryogenesis. Genome Biol. *3*, RESEARCH0088.

Tomancak, P., Guichet, A., Zavorszky, P., and Ephrussi, A. (1998). Oocyte polarity depends on regulation of gurken by Vasa. Development *125*, 1723-1732.

Tomishige, M., Klopfenstein, D.R., and Vale, R.D. (2002). Conversion of Unc104/KIF1A kinesin into a processive motor after dimerization. Science *297*, 2263-2267.

Tran, D.H., and Berg, C.A. (2003). bullwinkle and shark regulate dorsal-appendage morphogenesis in *Drosophila* oogenesis. Development *130*, 6273-6282.

Trapp, B.D., Nishiyama, A., Cheng, D., and Macklin, W. (1997). Differentiation and death of premyelinating oligodendrocytes in developing rodent brain. J. Cell Biol. *137*, 459-468.

Tuerk, C., Gauss, P., Thermes, C., Groebe, D.R., Gayle, M., Guild, N., Stormo, G., d'Aubenton-Carafa, Y., Uhlenbeck, O.C., Tinoco, I., Jr., and et al. (1988). CUUCGG hairpins: extraordinarily stable RNA secondary structures associated with various biochemical processes. Proc. Natl. Acad. Sci. USA *85*, 1364-1368.

Tzakos, A.G., Easton, L.E., and Lukavsky, P.J. (2006). Complementary segmental labeling of large RNAs: economic preparation and simplified NMR spectra for measurement of more RDCs. J. Am. Chem. Soc. *128*, 13344-13345.

Tzakos, A.G., Grace, C.R., Lukavsky, P.J., and Riek, R. (2006). NMR techniques for very large proteins and rnas in solution. Annu. Rev. Biophys. Biomol. Struct. *35*, 319-342.

Uhlenbeck, O.C. (1990). Tetraloops and RNA folding. Nature *346*, 613-614.

Ule, J., Jensen, K., Mele, A., and Darnell, R.B. (2005). CLIP: a method for identifying protein-RNA interaction sites in living cells. Methods *37*, 376-386.

Ule, J., Stefani, G., Mele, A., Ruggiu, M., Wang, X., Taneri, B., Gaasterland, T., Blencowe, B.J., and Darnell, R.B. (2006). An RNA map predicting Nova-dependent splicing regulation. Nature *444*, 580-586.

Urban, S., Lee, J.R., and Freeman, M. (2002). A family of Rhomboid intramembrane proteases activates all *Drosophila* membrane-tethered EGF ligands. EMBO J. *21*, 4277-4286.

Vale, R.D. (2003). The molecular motor toolbox for intracellular transport. Cell *112*, 467-480.

Vallee, R.B., Shpetner, H.S., and Paschal, B.M. (1989). The role of dynein in retrograde axonal transport. Trends Neurosci. *12*, 66-70.

Van Buskirk, C., Hawkins, N.C., and Schüpbach, T. (2000). Encore is a member of a novel family of proteins and affects multiple processes in *Drosophila* oogenesis. Development *127*, 4753-4762.

Van De Bor, V., Hartswood, E., Jones, C., Finnegan, D., and Davis, I. (2005). gurken and the I factor retrotransposon RNAs share common localization signals and machinery. Dev. Cell *9*, 51-62.

Van Eeden, F.J., Palacios, I.M., Petronczki, M., Weston, M.J., and St Johnston, D. (2001). Barentsz is essential for the posterior localization of oskar mRNA and colocalizes with it to the posterior pole. J. Cell Biol. *154*, 511-523.

Vendra, G., Hamilton, R.S., and Davis, I. (2007). Dynactin suppresses the retrograde movement of apically localized mRNA in *Drosophila* blastoderm embryos. RNA *13*, 1860-1867.

Vershinin, M., Carter, B.C., Razafsky, D.S., King, S.J., and Gross, S.P. (2007). Multiple-motor based transport and its regulation by Tau. Proc. Natl. Acad. Sci. *104*, 87-92.

Vilinsky, I., Stewart, B.A., Drummond, J., Robinson, I., and Deitcher, D.L. (2002). A *Drosophila* SNAP-25 null mutant reveals context-dependent redundancy with SNAP-24 in neurotransmission. Genetics *162*, 259-271.

Wagner, E.J., and Garcia-Blanco, M.A. (2002). RNAi-mediated PTB depletion leads to enhanced exon definition. Mol. Cell *10*, 943-949.

Wang, C., Dickinson, L.K., and Lehmann, R. (1994). Genetics of nanos localization in Drosophila. Dev. Dyn. *199*, 103-115.

Wang, H., Iacoangeli, A., Popp, S., Muslimov, I.A., Imataka, H., Sonenberg, N., Lomakin, I.B., and Tiedge, H. (2002). Dendritic BC1 RNA: functional role in regulation of translation initiation. J Neurosci. *22*, 10232-10241.

Wang, Z., Tollervey, J., Briese, M., Turner, D., and Ule, J. (2009). CLIP: Construction of cDNA libraries for high-throughput sequencing from RNAs cross-linked to proteins in vivo. Methods Epub.

Ward, B.M., and Moss, B. (2004). Vaccinia virus A36R membrane protein provides a direct link between intracellular enveloped virions and the microtubule motor kinesin. J. Virol. *78*, 2486-2493.

Ward, E.J., Zhou, X., Riddiford, L.M., Berg, C.A., and Ruohola-Baker, H. (2006). Border of Notch activity establishes a boundary between the two dorsal appendage tube cell types. Dev. Biol. *297*, 461-470.

Webster, P.J., Liang, L., Berg, C.A., Lasko, P., and Macdonald, P.M. (1997). Translational repressor bruno plays multiple roles in development and is widely conserved. Genes Dev. *11*, 2510-2521.

Weidensdorfer, D., Stohr, N., Baude, A., Lederer, M., Kohn, M., Schierhorn, A., Buchmeier, S., Wahle, E., and Huttelmaier, S. (2009). Control of c-myc mRNA stability by IGF2BP1-associated cytoplasmic RNPs. RNA *15*, 104-115.

Weil, T.T., Forrest, K.M., and Gavis, E.R. (2006). Localization of bicoid mRNA in late oocytes is maintained by continual active transport. Dev. Cell *11*, 251-262.

Weil, T.T., Parton, R., Davis, I., and Gavis, E.R. (2008). Changes in bicoid mRNA anchoring highlight conserved mechanisms during the oocyte-to-embryo transition. Curr. Biol. *18*, 1055-1061.

Wells, D.G., Dong, X., Quinlan, E.M., Huang, Y.S., Bear, M.F., Richter, J.D., and Fallon, J.R. (2001). A role for the cytoplasmic polyadenylation element in NMDA receptor-regulated mRNA translation in neurons. J. Neurosci. *21*, 9541-9548.

Welte, M.A. (2004). Bidirectional transport along microtubules. Curr. Biol. *14*, R525-537.

Wharton, R.P., and Struhl, G. (1989). Structure of the *Drosophila Bicaudal-D* protein and its role in localizing the posterior determinant *nanos*. Cell 59, 881-892.

Wieschaus, E., Marsh, J. L., and Gehring, W. J. (1978). fs(1)K10, a germline-dependent female sterile mutation causing abnormal chorion morphology in *Drosophila melanogaster*. Rouxs Arch. Dev. Biol. *184*, 75-82.

Wilhelm, J.E., Buszczak, M., and Sayles, S. (2005). Efficient protein trafficking requires trailer hitch, a component of a ribonucleoprotein complex localized to the ER in Drosophila. Dev. Cell *9*, 675-685.

Wilhelm, J.E., Hilton, M., Amos, Q., and Henzel, W.J. (2003). Cup is an eIF4E binding protein required for both the translational repression of oskar and the recruitment of Barentsz. J. Cell Biol. *163*, 1197-1204.

Wilhelm, J.E., Mansfield, J., Hom-Booher, N., Wang, S., Turck, C.W., Hazelrigg, T., and Vale, R.D. (2000). Isolation of a ribonucleoprotein complex involved in mRNA localization in *Drosophila* oocytes. J. Cell Biol. *148*, 427-440.

Wilkie, G. S., and Davis, I. (1998). Visualizing mRNA by in situ hybridization using 'high resolution' and sensitive tyramide signal amplification. BioMedNet Tchnical Tips Online.

Wilkie, G.S., and Davis, I. (2001). *Drosophila* wingless and pair-rule transcripts localize apically by dynein-mediated transport of RNA particles. Cell *105*, 209-219.

Wilkie, G.S., Shermoen, A.W., O'Farrell, P.H., and Davis, I. (1999). Transcribed genes are localized according to chromosomal position within polarized *Drosophila* embryonic nuclei. Curr. Biol. *9*, 1263-1266.

Wilsch-Brauninger, M., Schwarz, H., and Nusslein-Volhard, C. (1997). A sponge-like structure involved in the association and transport of maternal products during *Drosophila* oogenesis. J. Cell Biol. *139*, 817-829.

Wincott, F., DiRenzo, A., Shaffer, C., Grimm, S., Tracz, D., Workman, C., Sweedler, D., Gonzalez, C., Scaringe, S., and Usman, N. (1995). Synthesis, deprotection, analysis and purification of RNA and ribozymes. Nucleic Acids Res. *23*, 2677-2684.

Wittmann, T., Hyman, A., and Desai, A. (2001). The spindle: a dynamic assembly of microtubules and motors. Nat. Cell Biol. *3*, E28-34.

Woese, C.R., Winker, S., and Gutell, R.R. (1990). Architecture of ribosomal RNA: constraints on the sequence of "tetra-loops". Proc. Natl. Acad. Sci. USA *87*, 8467-8471.

Wollerton, M.C., Gooding, C., Robinson, F., Brown, E.C., Jackson, R.J., and Smith, C.W. (2001). Differential alternative splicing activity of isoforms of polypyrimidine tract binding protein (PTB). RNA *7*, 819-832.

Woolley, D. (2000). The molecular motors of cilia and eukaryotic flagella. Essays Biochem. *35*, 103-115.

Wu, K.Y., Hengst, U., Cox, L.J., Macosko, E.Z., Jeromin, A., Urquhart, E.R., and Jaffrey, S.R. (2005). Local translation of RhoA regulates growth cone collapse. Nature *436*, 1020-1024.

Wu, L., Wells, D., Tay, J., Mendis, D., Abbott, M.A., Barnitt, A., Quinlan, E., Heynen, A., Fallon, J.R., and Richter, J.D. (1998). CPEB-mediated cytoplasmic polyadenylation and the regulation of experience-dependent translation of alpha-CaMKII mRNA at synapses. Neuron *21*, 1129-1139.

Wyatt, J.R., Chastain, M., and Puglisi, J.D. (1991). Synthesis and purification of large amounts of RNA oligonucleotides. BioTechniques *11*, 764-769.

Yamamoto, H., Tsukahara, K., Kanaoka, Y., Jinno, S., and Okayama, H. (1999). Isolation of a mammalian homologue of a fission yeast differentiation regulator. Mol. Cell. Biol.*19*, 3829-3841.

Yano, T., Lopez de Quinto, S., Matsui, Y., Shevchenko, A., Shevchenko, A., and Ephrussi, A. (2004). Hrp48, a *Drosophila* hnRNPA/B homolog, binds and regulates translation of oskar mRNA. Dev. Cell *6*, 637-648.

Yeo, G.W., Coufal, N.G., Liang, T.Y., Peng, G.E., Fu, X.D., and Gage, F.H. (2009). An RNA code for the FOX2 splicing regulator revealed by mapping RNA-protein interactions in stem cells. Nat. Struct. Mol. Biol. *16*, 130-137.

Yisraeli, J.K., and Melton, D.A. (1988). The material mRNA Vg1 is correctly localized following injection into Xenopus oocytes. Nature *336*, 592-595.

Yisraeli, J.K., Sokol, S., and Melton, D.A. (1990). A two-step model for the localization of maternal mRNA in Xenopus oocytes: involvement of microtubules and microfilaments in the translocation and anchoring of Vg1 mRNA. Development *108*, 289-298.

Yonekawa, Y., Harada, A., Okada, Y., Funakoshi, T., Kanai, Y., Takei, Y., Terada, S., Noda, T., and Hirokawa, N. (1998). Defect in synaptic vesicle precursor transport and neuronal cell death in KIF1A motor protein-deficient mice. J. Cell Biol. *141*, 431-441.

Yoon, Y.J., and Mowry, K.L. (2004). Xenopus Staufen is a component of a ribonucleoprotein complex containing Vg1 RNA and kinesin. Development *131*, 3035-3045.

Yusupov, M.M., Yusupova, G.Z., Baucom, A., Lieberman, K., Earnest, T.N., Cate, J.H., and Noller, H.F. (2001). Crystal structure of the ribosome at 5.5 A resolution. Science *292*, 883-896.

Yusupova, G.Z., Yusupov, M.M., Cate, J.H., and Noller, H.F. (2001). The path of messenger RNA through the ribosome. Cell *106*, 233-241.

Zaessinger, S., Busseau, I., and Simonelig, M. (2006). Oskar allows nanos mRNA translation in *Drosophila* embryos by preventing its deadenylation by Smaug/CCR4. Development *133*, 4573-4583.

Zalfa, F., Adinolfi, S., Napoli, I., Kuhn-Holsken, E., Urlaub, H., Achsel, T., Pastore, A., and Bagni, C. (2005). Fragile X mental retardation protein (FMRP) binds specifically to the brain cytoplasmic RNAs BC1/BC200 via a novel RNA-binding motif. J. Biol. Chem. *280*, 33403-33410.

Zeitelhofer, M., Karra, D., Macchi, P., Tolino, M., Thomas, S., Schwarz, M., Kiebler, M., and Dahm, R. (2008). Dynamic interaction between P-bodies and transport ribonucleoprotein particles in dendrites of mature hippocampal neurons. J. Neurosci. *28*, 7555-7562.

Zhang, H.L., Eom, T., Oleynikov, Y., Shenoy, S.M., Liebelt, D.A., Dictenberg, J.B., Singer, R.H., and Bassell, G.J. (2001). Neurotrophin-induced transport of a beta-actin mRNP complex increases beta-actin levels and stimulates growth cone motility. Neuron *31*, 261-275.

Zhang, H.L., Pan, F., Hong, D., Shenoy, S.M., Singer, R.H., and Bassell, G.J. (2003). Active transport of the survival motor neuron protein and the role of exon-7 in cytoplasmic localization. J. Neurosci. *23*, 6627-6637.

Zhong, J., Zhang, T., and Bloch, L.M. (2006). Dendritic mRNAs encode diversified functionalities in hippocampal pyramidal neurons. BMC Neurosci. *7*, 17.

Zimyanin, V.L., Belaya, K., Pecreaux, J., Gilchrist, M.J., Clark, A., Davis, I., and St Johnston, D. (2008). In vivo imaging of oskar mRNA transport reveals the mechanism of posterior localization. Cell *134*, 843-853.

Zuker, M. (2003). Mfold web server for nucleic acid folding and hybridization prediction. Nucleic Acids Res. *31*, 3406-3415.

APPENDIX

A.1 Antibody stocks and dilutions (WB, Western blotting; IF, immunofluorescence; IS, *in situ* hybridization)

Name	Raised in	Application	Dilution	Supplier	Reference
anti-CG17838	Rabbit	WB	1/1000	Eurogentec	This work
		IF	1/100		
		IP	1/50		
anti-SYNCRIP-N	Rabbit	WB	1/1000	A. Mizutani	J. Biol. Chem. 275, 9823-9831
anti-Squid A 2G9	Mouse	WB	1/1000	T. Schüpbach	
anti-Squid S 1B11	Mouse	WB	1/1000	T. Schüpbach	
anti-Hrb27C	Rabbit	WB	1/10000	Eurogentec	This work; Dev. Cell 5, 625-635
anti-GFP, rabbit IgG fraction (polyclonal)	Rabbit	WB	1/1000-1/5000	Invitrogen	
		IP	1/100		
anti-GFP mouse monoclonal, clone GFP-20	Mouse	WB	1/1000	Sigma Aldrich	
		IP	1/150	Sigma Aldrich	
anti-GST mouse monoclonal B-14	Mouse	WB	1/200	Santa Cruz Biotechnology	
anti-Gurken 1D12, concentrate	Mouse	IF	1/300	Developmental Studies Hybridoma Bank (DSHB)	Mech. Dev. 89, 35-42
anti-Oskar	Rabbit	IF	1/500	P. Macdonald	

A.1 (continued) Antibody stocks and dilutions (WB, Western blotting; IF, immunofluorescence; IS, *in situ* hybridization)

anti-PTB/Heph	Rabbit	IF	1/500	A. Ephrussi	Genes Dev. 23, 195-207
anti-PTB/Heph	Rat	WB	1/2000	A. Ephrussi	Genes Dev. 23, 195-207
anti-actin, A-2066	Rabbit	WB	1/2000	Sigma Aldrich	
anti-Synaptotagmin, 3H2 2D7, concentrate	Mouse	WB	1/500	DSHB	
ECL Mouse IgG HRP-linked	Sheep	WB	1/5000	GE Healthcare Life Sciences	
ECL Rabbit IgG HRP-linked	Donkey	WB	1/5000	GE Healthcare Life Sciences	
Alexa Fluor 488 goat anti-rabbit IgG	Goat	IF	1/500	Molecular Probes	
Alexa Fluor 647 goat anti-rabbit IgG	Goat	IF	1/500	Molecular Probes	
Alexa Fluor 568 goat anti-rabbit IgG	Goat	IF	1/500	Molecular Probes	
Alexa Fluor 488 goat anti-mouse IgG	Goat	IF	1/500	Molecular Probes	
Alexa Fluor 568 goat anti-mouse IgG	Goat	IF	1/500	Molecular Probes	
Anti-Digoxigenin-POD Fab fragments	Sheep	IS	1/500	Roche	
Control pre-immune sera	Rabbit	WB, IP		Eurogentec (for use with corresponding anti-CG17838 or anti-Hrb27C antibodies	
Mouse IgG1 monoclonal antibody-isotype control,	Mouse	WB, IP		Abcam AB27479	

A.2 Primers

A.2.1 Oligonucleotide primers used for the cloning of sequences for NMR into pUC18. Restriction endonuclease (RE) sites are underlined, where a *Bbs*I site is present, this is highlighted in red.

Name	Sequence	RE site
NMRM1F	5' GAGCAAGCTTAATACGACTCACTATAGGCTTCGTGCTCTCAACAATTG 3'	*Hind*III
NMRM1R	5' GCTCGAATTCGAAGACAAGGCTTCGGCTCGAACAACAATC 3'	*Eco*RI; *Bbs*I
NMRI3F	5' GAGCAAGCTTAATACGACTCACTATAGGCCTCGTCACTCTTGATTTTTCAAGAGCCT TC 3'	*Hind*III
NMRI3R	5' GCTCGAATTCGAAGACAAGGCCTCGATCGAAGGCTCTTGAAAAATCAA 3'	*Eco*RI; *Bbs*I
GLSuucgF	5' GAGCAAGCTTAATACGACTCACTATAGGCAGTAATTTTCGTGCTCTCAACAATTCTTC GGGATTGTTG 3'	*Hind*III
GLSuucgR	5' GCTCGAATTCGAAGACAAGGCAGTAAGATTCGGCTCGAACAACAATCCCGAAGAAT GTTGAGAGCAC 3'	*Eco*RI; *Bbs*I
M1uucgF	5' GAGCAAGCTTAATACGACTCACTATAGGCTTCGTGCTCTCAACAATTCTTCGGGATT GTTG 3'	*Hind*III
M1uucgR	5' GCTCGAATTCGAAGACAAGGCTTCGGCTCGAACAACAATCCCGAAGAATTGTTGAGA GCAC 3'	*Eco*RI; *Bbs*I
ILSuucgF	5' GAGCAAGCTTAATACGACTCACTATAGGCTGCACACCTCCCTCGTCACTCTTGATTCGTCAAGAGCCTTC 3'	*Hind*III
ILSuucgR	5' GCTCGAATTCGAAGACAAGGCTGCACACCTACTCGATCGAAGGCTCTTGACGAATCAA 3'	*Eco*RI; *Bbs*I
I3uucgF	5' GAGCAAGCTTAATACGACTCACTATAGGCCTCGTCACTCTTGATTCGTCAAGAGCCTTC 3'	*Hind*III
I3uucgR	5' GCTCGAATTCGAAGACAAGGCCTCGATCGAAGGCTCTTGACGAATCAA 3'	*Eco*RI; *Bbs*I
ampF	5' GAGCAAGCTTAATACGACTC 3'	*Hind*III
ampR	5' GCTCGAATTCGAAGACAAG 3'	*Eco*RI; *Bbs*I
GLStetpGEM	5' AGTAATTTTCGTGCTCTC 3'	NA

A.2.1 (continued) Oligonucleotide primers used for the cloning of sequences for NMR into pUC18. Restriction endonuclease (RE) sites are underlined, where a *Bbs*I site is present, this is highlighted in red.

GLStetpGEMR	5' AGTAAGATTCGGCTCGAAC 3'	NA
M1tetpGEM	5' TTCGTGCTCTCAACAATTC 3'	NA
M1tetpGEMR	5' TTCGGCTCGAACAAC 3'	NA
ILStetpGEM	5' TGCACACCTCCCTCGTCACTC 3'	NA
ILStetpGEMR	5' TGCACACCTACTCGATCGAAG 3'	NA
I3tetpGEM	5' CTCGTCACTCTTGATTCGTC 3'	NA
I3tetpGEMR	5' CTCGATCGAAGGCTC 3'	NA
M1 stem F	5' GAGCAAGCTTAATACGACTCACTATAGGCTTCGTGCTCTCAACTTCGGTTGTTC 3'	*Hind*III
M1 stem R	5' GCTCGAATTCGAAGACAAGGCTTCGGCTCGAACAACCGAAGTTGAGAG 3'	*Eco*RI; *Bbs*I
M1 loop F	5' GAGCAAGCTTAATACGACTCACTATAGGCCAATTGTCGCCGTCACAGAT 3'	*Hind*III
M1 loop R	5' GCTCGAATTCGAAGACAAGGCCAATCTGTGACGGCGACA 3'	*Eco*RI; *Bbs*I
I3 stem F	5' GAGCAAGCTTAATACGACTCACTATAGGCCTCGTCACTCTTCGGAGCCTTCGATC 3'	*Hind*III
I3 stem R	5' GCTCGAATTCGAAGACAAGGCCTCGATCGAAGGCTCCGAAGAGTG 3'	*Eco*RI; *Bbs*I
I3 loop F	5' GAGCAAGCTTAATACGACTCACTATAGGCCTTGATTTTTCAAGGC 3'	*Hind*III
I3 loop R	5' GCTCGAATTCGAAGACAAGGCCTTGAAAAATCAAGGC 3'	*Eco*RI; *Bbs*I
M13 F	5' GTAAAACGACGGCCAG 3' (Sequencing primer)	NA
M13 R	5' CAGGAAACAGCTATGAC 3' (Sequencing primer)	NA

A.2.2 Oligonucleotide primers used for the cloning of ORF16, ORF16ΔGLS and A and ILS sequences into p6xE2 for GRNA chromatography. Restriction sites are underlined.

Name	Sequence	Description	RE site
SM13F	5' GGATAAGCTTCGATCGTTTAGACCCCTTCATTG 3'	Forward primer for ORF16/ORF16ΔGLS cloning into p6xE2	*Hind*III
SM14R	5' CCATACTAGTGCTGCAGCTCGTGCGCATGCTCG 3'	Reverse primer for ORF16/ORF16ΔGLS cloning into p6xE2	*Spe*I
ILS GRNA F	5' GGATAAGCTTTGCACACCTCCCTCGTCAC 3'	Forward primer for ILS cloning into p6xE2	*Hind*III
ILS GRNA R	5' CCATACTAGTTGCACACCTACTCGATCGAAG 3'	Reverse primer for ILS cloning into p6xE2	*Spe*I
AILS GRNA F	5' GGATAAGCTTTAACGACAAACAATTCGGGTTC 3'	Forward primer for A+ILS, A+ILS$_{mut}$, and AΔILS cloning into p6xE2	*Hind*III
AILS GRNA R	5' CCATACTAGTGATTATGGAGTGCAC 3'	Reverse primer for A+ILS and ILS$_{mut}$ cloning into p6xE2	*Spe*I
AILSΔILS GRNA R	5' CCATACTAGTTCCATTCCTGCAATTGCTG 3'	Reverse primer for AΔILS cloning into p6xE2	*Spe*I

A.2.3 Oligonucleotide primers used for the cloning of CG17838-F cDNA and for cloning for protein expression. Restriction sites are underlined.

Name	Sequence	Description	RE site
CG17838 F	5' ATGGCGGAAGGTAATGGCGAAC 3'	Forward primer for amplification of CG17838-F	NA
CG17838 R	5' TTAACTCCATGCCGAAAACGTATC 3'	Reverse primer for amplification of CG17838-F and for generation of TnT template	NA
CG17838pGexF	5' GGATGGATCCATGGCGGAAGGTAATGGCGA 3'	Forward primer for amplification of CG17838-F to be subcloned into pGex3	*Bam*HI
CG17838pGexR	5' GCTCGAATTCTTAACTCCATGCCGAAAACG 3'	Reverse primer for amplification of CG17838-F to be subcloned into pGex3	*Eco*RI
TnTCG17838F	5'CCGCGGGGCCCTAATACGACTCACTATAGGGAGAACCATG GCGGAAGGTAATGGCGAAC 3'	Forward primer for generation of CG17838-F template for TnT	T7 promoter and Kozak sequences highlighted in red
seqmidCG17838F	5' CTGCGGCAAGATACCCAAG 3'	Sequencing primer from middle of CG17838-F	NA
5' pGex sequencing primer	5' GGGCTGGCAAGCCACGTTTGGTG 3'	From GE Healthcare Life Sciences	NA
3' pGex sequencing primer	5' CCGGGAGCTGCATGTGTCAGAGG 3'	From GE Healthcare Life Sciences	NA

A.2.4 Oligonucleotide primers used for RT-PCR analysis following immunoprecipitation

Name	Sequence	Description	RE site
gurken F	5' GTCACAGATTGTTGTTCGAGCCGAATC 3'	Amplifies 256 bases of *grk* coding region	NA
gurken R	5' CAATGGAGTCGTCTGCGTTTGGCAGTTG 3'	As above	NA
oskar F	5' CACGATATCGAGCATCAAGAGTGAATATC 3'	Amplifies 441 bases of *osk* coding region	NA
oskar R	5' GTAGAAATTGTTGAGATGCTTCCAATTATC 3'	As above	NA
bicoid F	5' GACGACGCTACAGATCTTGGAGCCTTTG 3'	Amplifies 810 bases of *bcd* coding region	NA
bicoid R	5' CTAATTGAAGCAGTAGGCAAACTGCGAG 3'	As above	NA
hunchback F	5' CCAGAATTGTATATATTCGTAGCATAAG 3'	Amplifies 436 bases of *hb* 3'UTR	NA
hunchback R	5' TACTGAGAGAATAATATCAGAGAAAG 3'	As above	NA
nanos F	5'ATTAACCCTCACTAAAGGGAAGAGGGCGAATCCAG 3'	Amplifies +1 and +2' segments of the *nos* 3'UTR	NA
nanos R	5' AGATCTATAGGCACGGGATAACGCTC 3'	As above	NA
rp49 F	5' GCTAAGCTGTCGCACAAA 3'	Amplifies 135 bases of *rp49* coding region	NA
rp49 R	5' TCCGGTGGGCAGCATGTG 3'	As above	NA
tubulin67C F	5' GGCAGCCTGAAGACCAAGGAGGAG 3'	Amplifies 320 bases of *tub67C* coding region	NA
tubulin67C R	5' CACTGCTCTGCGATCTTCTGC 3'	As above	NA

A.2.5 Oligonucleotide primers used to create templates for *in vitro* transcription of UV cross-linking probes

Name	Sequence	Description	RE sites
T3 hb 3'UTR NRE F	5' ATTAACCCTCACTAAAGGGATCATATAATCGTTGTCCAG 3'	Forward primer for NRE region of *hb* 3'UTR	NA
hb 3'UTR NRE R	5' TTGGCTTATGTACAATTTTCG 3'	Reverse primer for NRE region of *hb* 3'UTR	NA
T3 hb 3'UTR F	5' ATTAACCCTCACTAAAGGGAGTTCCCCATCACCATC 3'	Forward primer for larger region of *hb* 3'UTR	NA
Hb 3'UTR R	5' ACCGTTTTCAGGGTTTTTAGTCG 3'	Reverse primer for larger region of *hb* 3'UTR	NA
T3 nos 3 F	5' ATTAACCCTCACTAAAGGGATATAGTATAGACAACG 3'	Forward primer for +3 segment of *nos* 3'UTR	NA
nos 3 R	5' AGCGAACATTTTACGAAATGAAG 3'	Reverse primer for +3 segment of *nos* 3'UTR	NA
T3 nos 1-2 F	5'ATTAACCCTCACTAAAGGGAAGAGGGCGAATCCAG 3'	Forward primer for +1 and +2' segments of the *nos* 3'UTR	NA
nos 1-2 R	5' AGATCTATAGGCACGGGATAACGCTC 3'	Reverse primer for +1 and +2' segments of the *nos* 3'UTR	NA

A.3 Fly strains used in this work

Genotype	Source	Description
Oregon-R (OrR)		Wild-type stock
w[1118]	Bloomington (stock 6326)	Control stock
w[*]; P{ry[+t7.2]=neoFRT}82B P{w[+mC]=ovoD1-18}3R/st[1] betaTub85D[D] ss[1] e[s]/TM3, Sb[1]	Bloomington (stock 2149)	For germline clone generation
y[1] w[1118] P{ry[+t7.2]=70FLP}3F/Dp(1;Y)y[+]; TM2/TM6C, Sb[1]	Bloomington (stock 6419)	For germline clone generation
w; FRT82Bheph^{e1}/TM3, Ser	W. Brook	*heph* mutant allele for germline clone generation
w; FRT82Bheph^{e2}/TM3, Ser	W. Brook	*heph* mutant allele for germline clone generation
w; FRT82Bheph^{03429}/TM6B	A. Ephrussi	*heph* mutant allele for germline clone generation
P{GawB}elav^{C155}	Bloomington (stock 458)	Pan-neuronal driver
P{GawB}elav^{C155}, P{UAS-syt.eGFP}1, w*	A. Valles; Also available Bloomington (stock 6923)	Pan-neuronal expression of Synaptotagmin fused to eGFP
MTD-GAL4 Maternal Triple Driver w; P{*COG*-GAL4:VP16}; P{GAL4-*nos.NGT*}40; P{*nos*-GAL4:VP16}	L. Cooley	Germline specific driver
***tubulin*-GAL4**	J. Raff	Ubiquitous expression driver
w; p[UASp-CG17838-F-GFP] I/CyO	This work, C. Meignin	For overexpression of CG17838-F-GFP in the germline
w; p[UASt-CG17838-F-GFP] I/TM3, Sb	This work, C. Meignin	For overexpression of CG17838-F-GFP in somatic tissue
w[1118]; Df(3R)BSC124/TM6B, Tb[1]	Bloomington (stock 9289)	Deficiency uncovering CG17838
w[1118]; Df(3R)BSC141/TM6B, Tb[+]	Bloomington (stock 9501)	Deficiency uncovering CG17838
w[1118]; e00286/TM6B, Tb[1]	Exelixis collection	CG17838 insertion
w[1118]; f03775/TM6B, Tb[1]	Exelixis collection	CG17838 insertion
y[*] w[*]; P{GawB}NP6571 / TM6	DGRC Kyoto stock centre (stock 105236)	CG17838 insertion
y[1] w[67c23]; ry[506] P{y[+mDint2] w[BR.E.BR]=SUPor-P}KG01380	Bloomington (stock 13431)	CG17838 insertion
w*; P{FRT(w^{hs})}2A P{neoFRT}82B PBac{GAL4D,EYFP}CG17838^{PL00557}	Bloomington (stock 19547)	CG17838 insertion
w[1118]; d09234/TM6B, Tb[1]	Exelixis collection	CG17838 insertion

A.3 (continued) Fly strains used in this work

SqdGFP	A. Debec; Delanoue *et al.*, 2007	Squid protein-trap line containing an intronic GFP insertion
GFP-PTB pBac[dsRed+]/TM3, Ser	Besse *et al.*, 2009	PTB/Heph protein-trap line
SP/CyO; Δ2-3/TM6, Ubx		For P-element mobilization
yw; Ly/TM3		Balancer stock
P{ry[+t7.2]=hsFLP}1, y[1] w[1118]; Dr[Mio]/TM3, ry[*] Sb[1]	Bloomington (stock 7)	For deletion generation
w[1118]; wg[Sp-1]/CyO; sens[Ly-1]/TM6B, Tb[1]	Bloomington (stock 8136)	Balancer stock

A.4 GRNA results

GRNAexperiment1.xls and GRNAexperiment2.xls

These excel files, provided on the accompanying CD, list the proteins isolated using the ORF16, ORF16ΔGLS, GLS and hb GRNA in experiment 1 and experiment 2 respectively.